

A PARAMETRIC STUDY FOR THE CHARACTERIZATION OF SITE
AMPLIFICATION

by

Nazife Özge Fercan

B.S., Geological Engineering, Istanbul University, 2009

M.S., Civil Engineering, Istanbul University, 2013

Submitted to Kandilli Observatory and Earthquake Research Institute
in partial fulfillment of the requirements for the degree of
Doctor of Philosophy

Graduate Program in Earthquake Engineering

Boğaziçi University

2020

A PARAMETRIC STUDY FOR THE CHARACTERIZATION OF SITE
AMPLIFICATION

ACKNOWLEDGEMENTS

I feel great honour and appreciation for the guidance of my thesis supervisor Prof. Dr. Erdal Şafak. He has always supported and encouraged me during my thesis stage. I would like to thank him for sharing his deep knowledge of science and extensive research experience with me. His unique style of thinking and practising the science has been a great inspiration for me.

My co-advisor Prof. Dr. Atilla Ansal has been a great teacher, father and friend for me, since I met him at the first class of PhD programme. When we met for the first time, I was very impressed by his soul filled with energy. His worldview, energetic style, communication with people and sense of humour have always inspired me. He has been a role model for me with his great character, deep scientific knowledge and experience. I feel very appreciated for meeting him in my lifetime.

I would like to thank to my thesis progress committee members Assoc. Prof. Aslı Kurtuluş and Assoc. Prof. Gülüm Tanırcan for their guidance and contributions to my thesis and also for their patience and good intentions during my PhD qualification exam.

There is one more person whom I would like to present my deep appreciations. Asst. Prof. Can Zülfikar is the one who guided me for my post graduate education from the beginning of my master degree. The projects that I involved in with the coordination of him have provided a great aspect to me in earthquake engineering field. I would like to thank to him for his guidance.

During my whole education life, I always felt the support of my family intimately. In the very difficult times that I have experienced, they helped me with all their effort; moreover, they made so many sacrifices for me and for my education. I want to express my deep gratitude for their ongoing support. Finally, Ahmet has been a great husband and friend; he has been always by my side during my PhD education, thanks for being my life partner.

ABSTRACT

A PARAMETRIC STUDY FOR THE CHARACTERIZATION OF SITE AMPLIFICATION

In earthquake engineering, the approximation of site amplification by using practical ways has been an important issue. Various site parameters were proposed and applied in the engineering practice. Among these, time averaged shear wave velocity for the top 30 m, V_{s30} , and fundamental frequency, f_0 , have been used widely. In this study, we investigated the reliability of V_{s30} parameter, and the performance of alternative time averaged shear wave velocities (e.g., V_{s40} , V_{s50} , etc.) and shear wave travel times (T_{tz}) at various depths for the estimation of site amplification.

For the same bedrock depth, we considered 17 shear wave velocity profiles, changing from convex (i.e., the velocities changing faster near the surface and slower near the bedrock) to concave (i.e., the velocities changing slower near the surface and faster near the bedrock). We divided the soil media, first into layers with equal thickness, and then into layers with equal wave travel times. For each layering type and soil profile, we calculated the site amplification factors and fundamental frequencies, and studied their correlations with time averaged shear wave velocities (V_{sz}) and wave travel times (T_{tz}) for different depths, z . We have also investigated the correlation of site amplification factors, surface *PGAs* (Peak Ground Accelerations), and fundamental soil frequencies (f_0) for each case. We have identified the optimal averaging depths for the averaged shear wave velocity and the wave travel time to characterize site amplification. The study showed that there is a sharp change in the correlations when switching from convex to concave profiles.

By gradually increasing the bedrock acceleration levels, we have also studied the nonlinear soil response and its correlations with linear soil response. We presented guidelines to estimate nonlinear soil amplification factors and fundamental frequency from

the linear ones. Considering that the linear fundamental frequency and amplification can easily be calculated from field tests (e.g., ambient noise measurements for f_0 detection), these guidelines provide a useful tool to estimate nonlinear ones.

ÖZET

ZEMİN BÜYÜTMESİNİN KARAKTERİZE EDİLMESİ İÇİN PARAMETRİK BİR ÇALIŞMA

Deprem mühendisliğinde, zemin büyütmesinin pratik bir şekilde tahmin edilmesi önemli bir olgu haline gelmiştir. Çeşitli zemin parametreleri önerilmiş ve mühendislik uygulamalarında kullanılmıştır. Bunlar arasında, ilk 30 m'nin zamana göre ortalaması alınmış kayma dalga hızı, V_{s30} , ve zemin temel frekansı f_0 , sıklıkla kullanılmaktadır. Bu çalışmada, V_{s30} parametresinin güvenilirliğini ve zemin büyütmesinin tahmin edilmesinde kullanılacak çeşitli derinliklerdeki zaman ortalamalı kayma dalga hızlarının (örn. V_{s40} , V_{s50} vb.) ve kayma dalgası varış sürelerinin (T_{tz}) performansı incelenmiştir.

Aynı anakaya derinliği için, konveksden (kayma dalga hızlarının yüzey yakınında daha hızlı ve anakaya yakınında daha yavaş değiştiği) konkava (hızların yüzey yakınında daha yavaş ve anakaya yakınında daha hızlı değiştiği) doğru değişen 17 kayma dalgası hızı profili oluşturduk. Zemin ortamını önce eşit kalınlıktaki tabakalara ve sonra eşit dalga varış sürelerine böldük. Her tabakalama tipi ve zemin profili için zemin büyütme faktörü ve temel frekansını hesapladık ve bunların farklı derinlikler, z , için zaman ortalamalı kayma dalga hızı (V_{sz}) ve dalga varış süresi (T_{tz}) ile olan korelasyonlarını çalıştık. Ayrıca her bir durum için zemin büyütme faktörleri, yüzey *PGA*'leri (Peak Ground Accelerations) ve zemin temel frekanslarının (f_0) korelasyonlarını araştırdık. Zemin büyütmesini karakterize etmek için kullanılan ortalama kayma dalga hızı ve dalga varış süresi için optimum ortalama derinlikleri tanımladık. Çalışma ayrıca konveksten konkava doğru değişen profillerdeki korelasyonlarda keskin bir farklılık olduğunu göstermiştir.

Ayrıca giderek artan anakaya ivme seviyesi ile doğrusal olmayan zemin tepkisi ve onun doğrusal zemin tepkisi ile korelasyonlarını çalıştık. Doğrusal olmayan zemin büyütme faktörünü ve temel frekansını, doğrusal değerleri kullanarak tahmin etmek için bir kılavuz sunduk. Doğrusal zemin temel frekansının ve büyütmesinin arazi testleri (örn. f_0

belirlenmesi için çevre gürültüsü ölçümleri) ile kolaylıkla hesaplanabileceği göz önüne alındığında, bu kılavuz doğrusal olmayan değerlerin tahmin edilmesinde yararlı bir yöntem sunmaktadır.

TABLE OF CONTENTS

ACKNOWLEDGEMENTS.....	iii
ABSTRACT.....	iv
ÖZET	vi
TABLE OF CONTENTS.....	viii
LIST OF FIGURES	xi
LIST OF TABLES	xxvii
LIST OF SYMBOLS	xxix
LIST OF ABBREVIATIONS.....	xxxix
1. INTRODUCTION.....	1
1.1. General	1
1.2. Problem Statement and Objective of the Thesis	1
1.3. Organisation of the Thesis	2
2. LITERATURE SURVEY ON PARAMETERS SUGGESTED FOR SITE AMPLIFICATION	3
2.1. V_{s30}	3
2.2. Determination Methods of f_0	5
2.3. Proposed Alternative and Complimentary Parameters to V_{s30}	6
3. SITE RESPONSE ANALYSIS METHOD.....	8
3.1. Cyclic Behavior of Soil.....	8
3.2. Equivalent-Linear Method	9
4. SOIL MODELS.....	12
4.1. Validation of DEEPSOIL.....	12
4.2. Soil Models of Equal Thickness and Equal Travel Time for Each Layer	15
4.3. Impulsive and White-Noise Bedrock Motions.....	21
4.4. Soil Properties for Site Response Analysis.....	23
4.5. Site Amplification Characterization Parameters	24
5. INVESTIGATION OF SITE AMPLIFICATION CHARACTERIZATION PARAMETERS.....	28
5.1. Linear Analyses.....	28

5.1.1. Evaluation of Site Amplification and Fundamental Frequency Characterization Parameters.....	34
5.2. Equivalent-Linear Analyses.....	43
5.2.1. Analyses of Equal Thickness Model Under Impulsive Bedrock Motion.....	43
5.2.1.1. Site Amplification Characterization by Surface PGA.....	58
5.2.1.2. Site Amplification Characterization by Fundamental Soil Frequency, f_0	60
5.2.1.3. Site Amplification Characterization by V_{sz}	62
5.2.1.4. Site Amplification Characterization by T_{tz}	66
5.2.1.5. Fundamental Frequency Characterization by V_{sz}	71
5.2.1.6. Fundamental Frequency Characterization by T_{tz}	75
5.2.2. Analyses of Equal Thickness Model Under White-Noise Bedrock Motion.....	80
5.2.2.1. Site Amplification Characterization by Surface PGA.....	85
5.2.2.2. Site Amplification Characterization by Fundamental Soil Frequency, f_0	87
5.2.2.3. Site Amplification Characterization by V_{sz}	88
5.2.2.4. Site Amplification Characterization by T_{tz}	93
5.2.2.5. Fundamental Frequency Characterization by V_{sz}	97
5.2.2.6. Fundamental Frequency Characterization by T_{tz}	102
5.2.3. Analyses of Equal Wave Travel Time Model Under Impulsive Bedrock Motions.....	106
5.2.3.1. Site Amplification Characterization by Surface PGA.....	114
5.2.3.2. Site Amplification Characterization by Fundamental Soil Frequency, f_0	116
5.2.3.3. Site Amplification Characterization by V_{sz}	118
5.2.3.4. Site Amplification Characterization by T_{tz}	122
5.2.3.5. Fundamental Frequency Characterization by V_{sz}	126
5.2.3.6. Fundamental Frequency Characterization by T_{tz}	131
5.2.4. The Best Performing Parameters for Site Amplification and Fundamental Frequency Characterization.....	135
5.2.5. Correlation of Linear and Nonlinear Site Amplification Factors and Fundamental Frequencies.....	139
6. CONCLUSIONS.....	145

REFERENCES 148

LIST OF FIGURES

Figure 3.1. Graphical representation of cyclic shear strain, γ_c , and G/G_{\max} relation by modulus reduction curve.	9
Figure 3.2. Iterative procedure for the selection of G corresponding to effective shear strain through the modulus reduction curve.	10
Figure 4.1. Uniform 100 m deep soil profile with $V_s=100$ m/sec for each layer with an elastic bedrock at the base, $V_{s\text{bedrock}}=1524$ m/sec.	13
Figure 4.2. Acceleration-time history of the impulse displaying a peak at 0.005 sec.	13
Figure 4.3. Fourier amplitude spectrum of the impulse.	14
Figure 4.4. For the uniform soil profile: a) Response spectra of surface motions, b) Surface to bedrock spectral ratio that reveals the fundamental frequency at 0.25 Hz.	14
Figure 4.5. Soil profiles with the same V_{s30} (i.e., 133.3 m/sec) reveal different soil amplification factors.	15
Figure 4.6. Generalized soil profile for concave, convex and linear types; $V_s=50$ m/sec for the top and $V_s=1000$ m/sec for the 50 th layer.	16
Figure 4.7. Geometric shapes of concave, linear and convex type shear wave velocity profiles.	17
Figure 4.8. Shear wave velocity profiles changing from concave to convex (i.e., from left to right).	18
Figure 4.9. Generalized soil profile with equal wave travel time for each layer.	19

Figure 4.10. Incremental shear wave travel times for the velocity profiles of equal layer thickness model.	20
Figure 4.11. Soil profiles with equal shear wave travel time (0.04 sec) for each soil layer.	21
Figure 4.12. Bedrock impulsive accelerations with different amplitudes (gradually increasing PGAs: 0.005g, 0.05g, 0.1g, 0.2g, 0.4g, 0.6g, and 1.0g): a) Acceleration-time history, b) Fourier amplitude spectra, c) Response spectra.	22
Figure 4.13. White-noise motions with gradually increasing PGAs: a) Acceleration-time history, b) Fourier amplitude spectrum, c) Response spectra.....	23
Figure 4.14. Modulus reduction, G/G_{\max} , and damping ratio, ξ , curves defined by Seed and Idriss (1970) with respect to shear strains, γ_c	24
Figure 5.1. Transfer functions of all velocity profiles; red dots are representing the soil amplification factors and the corresponding fundamental frequencies.	30
Figure 5.2. Transfer functions of concave and linear type velocity profiles.	30
Figure 5.3. Transfer functions of linear and convex type velocity profiles.....	30
Figure 5.4. Surface PGAs for each velocity profile with respect to bedrock acceleration levels.	33
Figure 5.5. The linearity of the analysis by the same rate of increase for all profiles.	33
Figure 5.6. Maximum shear strains (γ -%) for each velocity profile with respect to bedrock accelerations.....	34
Figure 5.7. AF/V_{sz} data set and the mean of the data set as the best fitting straight line. ...	35

Figure 5.8. Correlation between soil amplification factors and surface PGAs with gradually increasing bedrock PGAs.....	35
Figure 5.9. Normalized relation between soil amplification factors and surface PGAs for the profiles.	35
Figure 5.10. Relation between the soil amplification factors and maximum shear strains with respect to gradually increasing bedrock PGAs.....	36
Figure 5.11. Normalized relation between the soil amplification factor and maximum shear strain for the profiles.....	36
Figure 5.12. Correlation between soil amplification factor and fundamental frequency with respect to profiles.....	37
Figure 5.13. Correlation between soil amplification factors and V_{sz} at various depths for all bedrock acceleration levels.....	38
Figure 5.14. AF/V_{sz} values and the means (gray dashed lines) for linear/concave profiles.	38
Figure 5.15. AF/V_{sz} values and the means (gray dashed lines) for convex profiles.....	38
Figure 5.16. AE values for AF/V_{sz} at various depths for each convex type profile.	39
Figure 5.17. Correlation of soil amplification factors with T_{tz} for various depths.	39
Figure 5.18. AE values for AF/T_{tz} at various depths for linear and concave type profiles.	40
Figure 5.19. Correlation of fundamental frequency with T_{tz} at various depths.....	40
Figure 5.20. AE values of $f_0 \times T_{tz}$ for convex type profiles.....	41

Figure 5.21. AE values of $f_0 \times T_{tz}$ for linear and concave type profiles.	41
Figure 5.22. Correlation of fundamental frequency with V_{sz} at various depths.	42
Figure 5.23. AE values of f_0/V_{sz} for convex type profiles.	42
Figure 5.24. AE values of f_0/V_{sz} for linear and concave type profiles.....	42
Figure 5.25. Modulus reductions for each layer at 0.005g bedrock acceleration level.	46
Figure 5.26. Damping ratios for each layer at 0.005g bedrock acceleration level.	46
Figure 5.27. Shear strains for each layer at 0.005g bedrock acceleration level.....	47
Figure 5.28. Modulus reductions for each layer at 1.0g bedrock acceleration level.	47
Figure 5.29. Damping ratios for each layer at 1.0g bedrock acceleration level.	48
Figure 5.30. Shear strains for each layer at 1.0g bedrock acceleration level.....	48
Figure 5.31. Surface PGAs with respect to gradually increasing bedrock PGAs.....	50
Figure 5.32. PGAs along the velocity profiles for 0.005g bedrock acceleration level.	51
Figure 5.33. PGAs along the velocity profiles for 0.05g bedrock acceleration level.	51
Figure 5.34. PGAs along the velocity profiles for 0.2g bedrock acceleration level.	52
Figure 5.35. PGAs along the velocity profiles for 0.6g bedrock acceleration level.	52
Figure 5.36. Transfer functions at 0.005g impulsive acceleration level.....	53
Figure 5.37. Transfer functions at 0.05g impulsive acceleration level.....	53

Figure 5.38. Transfer functions at 0.1g impulsive acceleration level.....	53
Figure 5.39. Transfer functions at 0.2g impulsive acceleration level.....	54
Figure 5.40. Transfer functions at 0.4g impulsive acceleration level.....	54
Figure 5.41. Transfer functions at 0.6g impulsive acceleration level.....	54
Figure 5.42. Transfer functions at 1.0g impulsive acceleration level.....	55
Figure 5.43. Maximum amplitude of transfer functions and corresponding fundamental frequencies for impulsive bedrock accelerations.....	56
Figure 5.44. Amplification and de-amplification of surface PGAs for each profile.	59
Figure 5.45. The correlation of soil amplification factors with surface PGAs with respect to velocity profiles.	59
Figure 5.46. The correlation of soil amplification factors with surface PGAs with respect to convex profiles.	60
Figure 5.47. Fundamental frequencies with respect to bedrock PGAs for each profile.	60
Figure 5.48. Fundamental frequencies with respect to profile numbers.....	61
Figure 5.49. The correlation of soil amplification factor with f_0 with respect to profile number.....	61
Figure 5.50. The correlation of AF with V_{sz} for 0.005g impulsive bedrock acceleration. ..	62
Figure 5.51. The correlation of AF with V_{sz} for 0.05g impulsive bedrock acceleration.	62
Figure 5.52. The correlation of AF with V_{sz} for 0.1g impulsive bedrock acceleration.	63

Figure 5.53. The correlation of AF with V_{sz} for 0.2g impulsive bedrock acceleration.	63
Figure 5.54. The correlation of AF with V_{sz} for 0.4g impulsive bedrock acceleration.	64
Figure 5.55. The correlation of AF with V_{sz} for 0.6g impulsive bedrock acceleration.	64
Figure 5.56. The correlation of AF with V_{sz} for 1.0g impulsive bedrock acceleration.	64
Figure 5.57. The variation of AE for AF/V_{sz} with increasing impulsive bedrock accelerations for convex profiles.....	65
Figure 5.58. The variation of AE for AF/V_{sz} with increasing impulsive bedrock accelerations for linear/concave profiles.	66
Figure 5.59. The correlation of AF with T_{tz} for 0.005g impulsive bedrock acceleration.	67
Figure 5.60. The correlation of AF with T_{tz} for 0.05g impulsive bedrock acceleration.	67
Figure 5.61. The correlation of AF with T_{tz} for 0.1g impulsive bedrock acceleration.	68
Figure 5.62. The correlation of AF with T_{tz} for 0.2g impulsive bedrock acceleration.	68
Figure 5.63. The correlation of AF with T_{tz} for 0.4g impulsive bedrock acceleration.	68
Figure 5.64. The correlation of AF with T_{tz} for 0.6g impulsive bedrock acceleration.	69
Figure 5.65. The correlation of AF with T_{tz} for 1.0g impulsive bedrock acceleration.	69
Figure 5.66. The variation of AE for AF/T_{tz} with increasing impulsive bedrock accelerations for convex profiles.....	70
Figure 5.67. The variation of AE for AF/T_{tz} with increasing impulsive bedrock accelerations for linear/concave profiles.	70

Figure 5.68. The correlation of f_0 with V_{sz} for 0.005g impulsive bedrock acceleration.....	72
Figure 5.69. The correlation of f_0 with V_{sz} for 0.05g impulsive bedrock acceleration.....	72
Figure 5.70. The correlation of f_0 with V_{sz} for 0.1g impulsive bedrock acceleration.....	72
Figure 5.71. The correlation of f_0 with V_{sz} for 0.2g impulsive bedrock acceleration.....	73
Figure 5.72. The correlation of f_0 with V_{sz} for 0.4g impulsive bedrock acceleration.....	73
Figure 5.73. The correlation of f_0 with V_{sz} for 0.6g impulsive bedrock acceleration.....	73
Figure 5.74. The correlation of f_0 with V_{sz} for 1.0g impulsive bedrock acceleration.....	74
Figure 5.75. The variation of AE for f_0/V_{sz} with increasing impulsive bedrock accelerations for convex profiles.....	74
Figure 5.76. The variation of AE for f_0/V_{sz} with increasing impulsive bedrock accelerations for linear/concave profiles.....	75
Figure 5.77. The correlation of f_0 with T_{tz} for 0.005g impulsive bedrock acceleration.	76
Figure 5.78. The correlation of f_0 with T_{tz} for 0.05g impulsive bedrock acceleration.	76
Figure 5.79. The correlation of f_0 with T_{tz} for 0.1g impulsive bedrock acceleration.	77
Figure 5.80. The correlation of f_0 with T_{tz} for 0.2g impulsive bedrock acceleration.	77
Figure 5.81. The correlation of f_0 with T_{tz} for 0.4g impulsive bedrock acceleration.	77
Figure 5.82. The correlation of f_0 with T_{tz} for 0.6g impulsive bedrock acceleration.	78
Figure 5.83. The correlation of f_0 with T_{tz} for 1.0g impulsive bedrock acceleration.	78

Figure 5.84. The variation of AE for $f_0 \times T_{tz}$ with increasing impulsive bedrock accelerations for convex profiles.....	79
Figure 5.85. The variation of AE for $f_0 \times T_{tz}$ with increasing impulsive bedrock accelerations for linear/concave profiles.	79
Figure 5.86. Surface PGAs with respect to gradually increasing white-noise accelerations.	81
Figure 5.87. Transfer functions at 0.005g white-noise acceleration level.....	82
Figure 5.88. Transfer functions at 0.05g white-noise acceleration level.....	82
Figure 5.89. Transfer functions at 0.1g white-noise acceleration level.....	82
Figure 5.90. Transfer functions at 0.2g white-noise acceleration level.....	83
Figure 5.91. Transfer functions at 0.4g white-noise acceleration level.....	83
Figure 5.92. Transfer functions at 0.6g white-noise acceleration level.....	83
Figure 5.93. Transfer functions at 1.0g white-noise acceleration level.....	84
Figure 5.94. Maximum amplitude of transfer functions and corresponding fundamental frequencies for white-noise bedrock accelerations.....	85
Figure 5.95. Amplification and de-amplification of surface PGAs for each profile.	86
Figure 5.96. The correlation of soil amplification factors with surface PGAs with respect to profiles.	86
Figure 5.97. The correlation of soil amplification factors with surface PGAs for convex profiles.	87

Figure 5.98. Fundamental soil frequencies with respect to bedrock PGAs for each profile.
87

Figure 5.99. Fundamental soil frequencies with respect to profile numbers.....88

Figure 5.100. The correlation of soil amplification factor with f_0 with respect to profile no.
88

Figure 5.101. The correlation of AF with V_{sz} for 0.005g white-noise bedrock acceleration.
89

Figure 5.102. The correlation of AF with V_{sz} for 0.05g white-noise bedrock acceleration.90

Figure 5.103. The correlation of AF with V_{sz} for 0.1g white-noise bedrock acceleration...90

Figure 5.104. The correlation of AF with V_{sz} for 0.2g white-noise bedrock acceleration...90

Figure 5.105. The correlation of AF with V_{sz} for 0.4g white-noise bedrock acceleration...91

Figure 5.106. The correlation of AF with V_{sz} for 0.6g white-noise bedrock acceleration...91

Figure 5.107. The correlation of AF with V_{sz} for 1.0g white-noise bedrock acceleration...91

Figure 5.108. The variation of AE for AF/V_{sz} with increasing white-noise bedrock
 accelerations for convex profiles.92

Figure 5.109. The variation of AE for AF/V_{sz} with increasing white-noise bedrock
 accelerations for linear/concave profiles.....93

Figure 5.110. The correlation of AF with T_{tz} for 0.005g white-noise bedrock acceleration.
93

Figure 5.111. The correlation of AF with T_{tz} for 0.05g white-noise bedrock acceleration. 94

Figure 5.112. The correlation of AF with T_{tz} for 0.1g white-noise bedrock acceleration. .	94
Figure 5.113. The correlation of AF with T_{tz} for 0.2g white-noise bedrock acceleration. .	94
Figure 5.114. The correlation of AF with T_{tz} for 0.4g white-noise bedrock acceleration. .	95
Figure 5.115. The correlation of AF with T_{tz} for 0.6g white-noise bedrock acceleration. .	95
Figure 5.116. The correlation of AF with T_{tz} for 1.0g white-noise bedrock acceleration. .	95
Figure 5.117. The variation of AE for AF/ T_{tz} with increasing white-noise bedrock accelerations for convex profiles.	96
Figure 5.118. The variation of AE for AF/ T_{tz} with increasing white-noise bedrock accelerations for linear/concave profiles.....	97
Figure 5.119. The correlation of f_0 with V_{sz} for 0.005g white-noise bedrock acceleration.	98
Figure 5.120. The correlation of f_0 with V_{sz} for 0.05g white-noise bedrock acceleration. .	98
Figure 5.121. The correlation of f_0 with V_{sz} for 0.1g white-noise bedrock acceleration.	99
Figure 5.122. The correlation of f_0 with V_{sz} for 0.2g white-noise bedrock acceleration.	99
Figure 5.123. The correlation of f_0 with V_{sz} for 0.4g white-noise bedrock acceleration.	99
Figure 5.124. The correlation of f_0 with V_{sz} for 0.6g white-noise bedrock acceleration. .	100
Figure 5.125. The correlation of f_0 with V_{sz} for 1.0g white-noise bedrock acceleration. .	100
Figure 5.126. The variation of AE for f_0/V_{sz} with increasing white-noise bedrock accelerations for convex profiles.	101

Figure 5.127. The variation of AE for f_0/V_{sz} with increasing white-noise bedrock accelerations for linear/concave profiles.....	101
Figure 5.128. The correlation of f_0 with T_{tz} for 0.005g white-noise bedrock acceleration.	102
Figure 5.129. The correlation of f_0 with T_{tz} for 0.05g white-noise bedrock acceleration.	102
Figure 5.130. The correlation of f_0 with T_{tz} for 0.1g white-noise bedrock acceleration.	103
Figure 5.131. The correlation of f_0 with T_{tz} for 0.2g white-noise bedrock acceleration.	103
Figure 5.132. The correlation of f_0 with T_{tz} for 0.4g white-noise bedrock acceleration.	103
Figure 5.133. The correlation of f_0 with T_{tz} for 0.6g white-noise bedrock acceleration.	104
Figure 5.134. The correlation of f_0 with T_{tz} for 1.0g white-noise bedrock acceleration.	104
Figure 5.135. The variation of AE for $f_0 \times T_{tz}$ with increasing white-noise bedrock accelerations for convex profiles.	105
Figure 5.136. The variation of AE for $f_0 \times T_{tz}$ with increasing white-noise bedrock accelerations for linear/concave profiles.....	105
Figure 5.137. Surface PGAs with respect to gradually increasing bedrock PGAs.....	109
Figure 5.138. Transfer functions at 0.005g impulsive acceleration level.....	110
Figure 5.139. Transfer functions at 0.05g impulsive acceleration level.....	110
Figure 5.140. Transfer functions at 0.1g impulsive acceleration level.....	110
Figure 5.141. Transfer functions at 0.2g impulsive acceleration level.....	111

Figure 5.142. Transfer functions at 0.4g impulsive acceleration level.....	111
Figure 5.143. Transfer functions at 0.6g impulsive acceleration level.....	111
Figure 5.144. Transfer functions at 1.0g impulsive acceleration level.....	112
Figure 5.145. Maximum amplitudes of transfer functions and corresponding fundamental frequencies for impulsive bedrock accelerations.	113
Figure 5.146. Amplification and de-amplification of surface PGAs for each profile.	114
Figure 5.147. The correlation of soil amplification factors with surface PGAs with respect to velocity profiles.....	115
Figure 5.148. The correlation of soil amplification factors with surface PGAs with respect to convex profiles.....	116
Figure 5.149. Fundamental frequencies with respect to bedrock PGAs for each profile. .	116
Figure 5.150. Fundamental frequencies with respect to profile numbers.....	117
Figure 5.151. The correlation of soil amplification factor with f_0 with respect to profile number.....	117
Figure 5.152. The correlation of AF with V_{sz} for 0.005g impulsive bedrock acceleration.	118
Figure 5.153. The correlation of AF with V_{sz} for 0.05g impulsive bedrock acceleration. .	119
Figure 5.154. The correlation of AF with V_{sz} for 0.1g impulsive bedrock acceleration. ..	119
Figure 5.155. The correlation of AF with V_{sz} for 0.2g impulsive bedrock acceleration. ..	119

Figure 5.156. The correlation of AF with V_{sz} for 0.4g impulsive bedrock acceleration. ..	120
Figure 5.157. The correlation of AF with V_{sz} for 0.6g impulsive bedrock acceleration. ..	120
Figure 5.158. The correlation of AF with V_{sz} for 1.0g impulsive bedrock acceleration. ..	120
Figure 5.159. The variation of AE for AF/V_{sz} with increasing impulsive bedrock accelerations for convex profiles.	121
Figure 5.160. The variation of AE for AF/V_{sz} with increasing impulsive bedrock accelerations for linear/concave profiles.....	122
Figure 5.161. The correlation of AF with T_{tz} for 0.005g impulsive bedrock acceleration.	123
Figure 5.162. The correlation of AF with T_{tz} for 0.05g impulsive bedrock acceleration. .	123
Figure 5.163. The correlation of AF with T_{tz} for 0.1g impulsive bedrock acceleration.	123
Figure 5.164. The correlation of AF with T_{tz} for 0.2g impulsive bedrock acceleration.	124
Figure 5.165. The correlation of AF with T_{tz} for 0.4g impulsive bedrock acceleration.	124
Figure 5.166. The correlation of AF with T_{tz} for 0.6g impulsive bedrock acceleration.	124
Figure 5.167. The correlation of AF with T_{tz} for 1.0g impulsive bedrock acceleration.	125
Figure 5.168. The variation of AE for AF/T_{tz} with increasing impulsive bedrock accelerations for convex profiles.	125
Figure 5.169. The variation of AE for AF/T_{tz} with increasing impulsive bedrock accelerations for linear/concave profiles.....	126

- Figure 5.170. The correlation of f_0 with V_{sz} for 0.005g impulsive bedrock acceleration..127
- Figure 5.171. The correlation of f_0 with V_{sz} for 0.05g impulsive bedrock acceleration...127
- Figure 5.172. The correlation of f_0 with V_{sz} for 0.1g impulsive bedrock acceleration.....128
- Figure 5.173. The correlation of f_0 with V_{sz} for 0.2g impulsive bedrock acceleration.....128
- Figure 5.174. The correlation of f_0 with V_{sz} for 0.4g impulsive bedrock acceleration.....128
- Figure 5.175. The correlation of f_0 with V_{sz} for 0.6g impulsive bedrock acceleration.....129
- Figure 5.176. The correlation of f_0 with V_{sz} for 1.0g impulsive bedrock acceleration.....129
- Figure 5.177. The variation of AE for f_0/V_{sz} with increasing impulsive bedrock accelerations for convex profiles. 130
- Figure 5.178. The variation of AE for f_0/V_{sz} with increasing impulsive bedrock accelerations for linear/concave profiles..... 130
- Figure 5.179. The correlation of f_0 with T_{tz} for 0.005g impulsive bedrock acceleration...131
- Figure 5.180. The correlation of f_0 with T_{tz} for 0.05g impulsive bedrock acceleration...131
- Figure 5.181. The correlation of f_0 with T_{tz} for 0.1g impulsive bedrock acceleration.....132
- Figure 5.182. The correlation of f_0 with T_{tz} for 0.2g impulsive bedrock acceleration. 132
- Figure 5.183. The correlation of f_0 with T_{tz} for 0.4g impulsive bedrock acceleration.....132
- Figure 5.184. The correlation of f_0 with T_{tz} for 0.6g impulsive bedrock acceleration.....133
- Figure 5.185. The correlation of f_0 with T_{tz} for 1.0g impulsive bedrock acceleration.....133

- Figure 5.186. The variation of AE for $f_0 \times T_{tz}$ with increasing impulsive bedrock accelerations for convex profiles. 134
- Figure 5.187. The variation of AE for $f_0 \times T_{tz}$ with increasing impulsive bedrock accelerations for linear/concave profiles..... 134
- Figure 5.188. Relation between linear and nonlinear f_0 with increasing impulsive accelerations for linear and concave profiles of equal thickness model. 140
- Figure 5.189. Relation between linear and nonlinear f_0 with increasing impulsive accelerations for convex profiles of equal thickness model..... 140
- Figure 5.190. Relation between linear and nonlinear f_0 with increasing white-noise accelerations for linear and concave profiles of equal thickness model. 141
- Figure 5.191. Relation between linear and nonlinear f_0 with increasing white-noise accelerations for convex profiles of equal thickness model..... 141
- Figure 5.192. Relation between linear and nonlinear f_0 with increasing impulsive accelerations for linear and concave profiles of equal travel time model...141
- Figure 5.193. Relation between linear and nonlinear f_0 with increasing impulsive accelerations for convex profiles of equal travel time model. 142
- Figure 5.194. Relation between linear and nonlinear soil amplification with increasing impulsive accelerations for linear and concave profiles of equal thickness model..... 142
- Figure 5.195. Relation between linear and nonlinear soil amplification with increasing impulsive accelerations for convex profiles of equal thickness model..... 143

- Figure 5.196. Relation between linear and nonlinear soil amplification with increasing white-noise accelerations for linear and concave profiles of equal thickness model..... 143
- Figure 5.197. Relation between linear and nonlinear soil amplification with increasing white-noise accelerations for convex profiles of equal thickness model. ... 143
- Figure 5.198. Relation between linear and nonlinear soil amplification with increasing impulsive accelerations for linear and concave profiles of equal travel time model..... 144
- Figure 5.199. Relation between linear and nonlinear soil amplification with increasing impulsive accelerations for convex profiles of equal travel time model. ... 144

LIST OF TABLES

Table 4.1. Properties and site response results of the soil profiles.	15
Table 4.2. Coefficients and constants of general equation for concave, linear and convex type soil profiles.....	18
Table 4.3. V_{sz} of the soil profiles with equal layer thickness.	25
Table 4.4. T_{tz} of the soil profiles with equal layer thickness.	26
Table 4.5. V_{sz} of the soil profiles with equal wave travel time for each layer.....	26
Table 4.6. T_{tz} of the soil profiles with equal wave travel time for each layer.	27
Table 5.1. Soil amplification factors (AF) and fundamental frequencies (f_0) for each velocity profile calculated by linear analysis.....	29
Table 5.2. Surface PGAs for each bedrock acceleration level.....	32
Table 5.3. Maximum shear strains for each bedrock acceleration level.....	32
Table 5.4. Fundamental frequencies (f_0) for gradually increasing bedrock accelerations...	44
Table 5.5. Soil amplification factors (AF) for gradually increasing bedrock accelerations.	44
Table 5.6. V_s and αz for Concave-10, Linear and Convex-6 profiles.	49
Table 5.7. The order of maximum peaks at transfer functions for f_0	71

Table 5.8. Fundamental frequencies (f_0) for gradually increasing bedrock accelerations...	80
Table 5.9. Soil amplification factors (AF) for gradually increasing bedrock accelerations.	81
Table 5.10. The order of maximum peaks at transfer functions for f_0	97
Table 5.11. Layer properties of convex profiles with equal wave travel time.	106
Table 5.12. Layer properties of linear/concave profiles with equal wave travel time.....	107
Table 5.13. Fundamental frequencies (f_0) for gradually increasing bedrock accelerations.	107
Table 5.14. Soil amplification factors (AF) for gradually increasing bedrock accelerations.	108
Table 5.15. V_s and α_z for Concave-10, Linear and Convex-6 profiles.	108
Table 5.16. The order of maximum peaks at transfer functions for f_0	126
Table 5.17. The characterization of soil amplification by surface PGAs.	136
Table 5.18. The characterization of soil amplification by f_0	136
Table 5.19. The best performing V_{sz} parameters for soil amplification characterization..	137
Table 5.20. The best performing T_{tz} parameters for soil amplification characterization. .	138
Table 5.21. The best performing V_{sz} parameters for f_0 characterization.	138
Table 5.22. The best performing T_{tz} parameters for f_0 characterization.	139

LIST OF SYMBOLS

f_0	Fundamental soil frequency
g	Acceleration of gravity
G	Shear modulus
G_d	Dynamic shear modulus
G_{max}	Maximum shear modulus
G_{sec}	Secant shear modulus
H or h	Thickness of soil layer
Hz	Hertz
T	Period of vibration
T_0	Fundamental site period
T_{tz}	Wave travel time at z m
T_{t05}	Wave travel time at 5 m
T_{t10}	Wave travel time at 10 m
T_{t20}	Wave travel time at 20 m
T_{t30}	Wave travel time at 30 m
T_{t40}	Wave travel time at 40 m
T_{t50}	Wave travel time at 50 m
T_{t100}	Wave travel time at 100 m
V_s	Shear wave velocity
V_{s05}	Time averaged shear wave velocity for the top 5 m
V_{s10}	Time averaged shear wave velocity for the top 10 m
V_{s20}	Time averaged shear wave velocity for the top 20 m
V_{s30}	Time averaged shear wave velocity for the top 30 m
V_{s40}	Time averaged shear wave velocity for the top 40 m
V_{s50}	Time averaged shear wave velocity for the top 50 m
V_{s100}	Time averaged shear wave velocity for the top 100 m
V_{sz}	Time averaged shear wave velocity for the top z m
z	Depth
α_z	Impedance ratio

γ	Unit weight of soil
$\gamma(\%)$	Shear strain
$\gamma_c(\%)$	Cyclic shear strain
$\gamma_{\text{eff}}(\%)$	Effective shear strain
κ_0	Kappa, high-frequency attenuation
ξ	Damping ratio
ρ	Density
τ	Shear stress

LIST OF ABBREVIATIONS

AE	Absolute error
AF	Amplification factor (Max. amplitude of transfer function)
FAS	Fourier amplitude spectrum
PGA	Peak ground acceleration
PI	Plasticity index
SSR	Standard spectral ratio
1D	One-dimensional

1. INTRODUCTION

1.1. General

The seismic regulations on geotechnical and structural design require the consideration of site effects and soil amplification. Defining simple parameters to characterize soil amplification is important. Since the engineering practice needs fast and useful methods, time averaged shear wave velocity for the top 30 m, V_{s30} , has been the most commonly used and practical method for this purpose. In this study, we investigate the validity of V_{s30} parameter and propose alternative parameters for the characterization of soil amplification.

1.2. Problem Statement and Objective of the Thesis

In earthquake regulations, the site classification method is based on V_{s30} (Borcherdt and Glassmoyer, 1992) due to its cost effectiveness and simplicity. This method evaluates the top 30 m of the soil profile for the determination of soil type and soil amplification factor. This approach was assessed as a practical and economical way of determining the soil amplification. Many researchers, however, stated that V_{s30} alone is not enough to reflect the properties of soil layers (Mucciarelli and Gallipoli, 2006; Castellaro et al., 2008), and proposed alternative parameters.

If we take two different soil profiles with the same V_{s30} values, but with different geologic units, number of horizontal soil layers, and depth to bedrock, we mostly find that they do not alter the ground motion in the same way. Therefore, it is justified to further investigate the validity of V_{s30} for site amplification characterization. In this study, we perform a parametric investigation of alternative parameters, mainly averaged velocities and travel times at different depths (i.e., V_{sz} and T_{tz}) for site amplification and fundamental frequency characterization.

Moreover, since the estimation of nonlinear soil amplification has been always a difficult issue, we investigate the possibility of predicting nonlinear soil amplification factor and nonlinear fundamental frequency from the linear ones, which can easily be identified from ambient ground noise measurements.

1.3. Organisation of the Thesis

In this study, we consider 17 shear wave velocity profiles for the same bedrock depth, changing from convex (i.e. the velocities changing faster near the surface and slower near the bedrock) to concave (i.e. the velocities changing slower near the surface and faster near the bedrock). The soil profiles were divided into layers, first with equal layer thicknesses, and next with equal wave travel times. One-dimensional site response analyses were carried out by using impulsive and white-noise type bedrock motions with gradually increasing acceleration levels. Both linear and equivalent-linear approaches were used to calculate the surface motions by assuming the same nonlinear soil model for the layers. Soil response, in terms of the relations between surface PGAs, shear strains, soil amplification factors, and fundamental frequencies were presented graphically. The performances of the commonly used V_{s30} parameter, and the alternative parameters that were considered for site amplification and fundamental site frequency characterization are compared. The correlations between linear and nonlinear site amplification factors and fundamental frequencies are investigated for different levels of bedrock motions.

2. LITERATURE SURVEY ON PARAMETERS SUGGESTED FOR SITE AMPLIFICATION

In this chapter, the previous studies on the characterization of site amplification are presented. The two most widely used parameters have been the time averaged shear wave velocity for the top 30 m, the V_{s30} , and the fundamental frequency, f_0 .

2.1. V_{s30}

In seismic design codes and ground motion prediction equations, the site effects are accounted for by a single parameter, the time averaged shear wave velocity for the top 30 m, the V_{s30} . It is defined as,

$$V_{s30} = \frac{30}{\sum(\frac{h_i}{V_{si}})} \quad (2.1)$$

where h_i is the thickness and V_{si} is the shear wave velocity of the i 'th soil layer within the top 30 m. Note that the denominator term in the equation corresponds to the total shear wave travel time for the top 30 m.

Site classification by V_{s30} was suggested by Borchardt and Glassmoyer (1992) after analyzing a large number of seismic records from different soil units. The soil units with similar seismic amplification levels were grouped based on their mean shear wave velocities. Three different site categories were introduced as “soil”, “soft rock” and “hard rock”, depending on the mean shear wave velocity bands. Borchardt (1994) also defined the same categories based on the level of site amplification. Site effects in seismic design codes are mostly based on the V_{s30} values, such as the NEHRP Provisions (BSSC, 1997), Uniform Building Code (ICBO, 1997), Eurocode 8 (CEN, 1998) and Turkish Earthquake Code (TEC, 1998).

Many researchers studied the performance of V_{s30} for site amplification characterization. Steidl (2000) investigated the relation between V_{s30} and site amplification factors. He showed that, at low bedrock motions (PGA smaller than 0.1g), lower V_{s30} values correspond to higher site response factors, especially for long periods. He emphasized the importance of depth-to-basement value, since the deeper sites showed higher site amplification factors.

Stewart et al. (2003) investigated the correlation of V_{s30} with amplification of spectral accelerations and classified the sites according to V_{s30} . He mentioned that in long periods, neither V_{s30} nor detailed surface geology can correlate well with site amplification.

Park and Hashash (2004) studied the nonlinear site coefficients and stated that site coefficients are highly dependent on the sediment thickness pointing out the insufficiency of V_{s30} for site classification.

Mucciarelli and Gallipoli (2006) worked on the validity of V_{s30} for the characterization of site amplification. They mentioned that V_{s30} is not a good proxy of site amplification and the fundamental frequency, if the velocity profile is not increasing with depth linearly and if there is not a strong impedance contrast in the velocity profile. Mucciarelli and Gallipoli (2009) stated that a reliable soil classification should be based on both V_s profile and fundamental frequency. Also, V_{s10} can be used instead of V_{s30} since it gives similar results.

Castellaro et al. (2008) investigated the reliability of V_{s30} as a proxy for site amplification and he mentioned that site amplification is too complex to be defined with a single parameter.

Lee and Trifunac (2010) stated that time averaged shear wave velocity is a weak proxy for site amplification. Regnier et al. (2011) suggested that V_{s30} alone does not represent soil stiffness accurately.

2.2. Determination Methods of f_0

According to the theory on the response of a uniform, undamped soil layer over an elastic rock, the largest amplification occurs at the lowest natural frequency, which is termed as the *fundamental frequency*, f_0 , (Kramer, 1996). Different approaches are available in the literature for the determination of f_0 , grouped as reference site and non-reference site techniques (Parolai, 2012).

Reference site technique, proposed by Borchardt (1970), states that the seismic site amplification at a soil site can be determined in terms of the ratio of the Fourier amplitude spectrum of the seismic record at that site to that of the record at a nearby rock site. This approach assumes that the effects of source, travel path and the recording instrument are identical at both locations, and therefore the ratio just represents the effects of site conditions.

Alternative to reference site technique, Nogoshi and Igarashi (1971) proposed to use the spectral ratio of horizontal to vertical records, the so-called H/V method, from a single station. It was further improved by Nakamura (1989) by working on microtremor measurements. The technique assumes that the ratio of horizontal to vertical spectra reveals the transfer function of the soil, and the fundamental frequency can be detected as the resonant frequency of the ratio. Lermo and Chavez (1993) proposed H/V Spectral Ratio, which can be applicable to earthquake records.

The performance of both reference site and non-reference site techniques were investigated by many researchers; the accuracy of the fundamental frequency detection by SSR and H/V methods was approved, however estimate of soil amplification factor by H/V method was stated as unreliable (Lachet and Bard, 1994, Field and Jacob, 1995 and Atakan, 1995). Safak (1997) investigated various methods to characterize site amplification factor by using a pair of records and approved to use standard spectral ratios and cross spectral ratios (even more reliable than SSR).

2.3. Proposed Alternative and Complimentary Parameters to V_{s30}

Many researchers proposed alternative and complimentary parameters for a more accurate soil amplification characterization.

Kokusho and Sato (2008) proposed the average S-wave velocity, \bar{V}_s as an alternative to V_{s30} . A good correlation was detected between the amplification factor and S-wave velocity ratio (i.e., the ratio of the bedrock shear wave velocity to average S-wave velocity, \bar{V}_s).

Cadet et al. (2008) revealed that site parameters and site amplification factors are correlated well with f_0 and V_{s30} couple. They proposed a site classification method based on the V_{s30} , f_0 , couple.

Luzi et al. (2011) proposed to use f_0 as alternative or complimentary to V_{s30} and they presented a soil classification method based on f_0 by using Italian strong motion data.

Cadet et al. (2012) studied the site characterization based on two parameters. They investigated the relation between site amplification and the V_{sz} , f_0 couple as alternative to V_{s30} . It was suggested that f_0 shows a better correlation than V_{s30} as a single proxy.

Laurendeau et al. (2013) studied the dependency of rock and stiff-soil (V_{s30} ranging from 500 m/sec to 1500 m/sec) site amplification on the parameters of V_{s30} and Kappa, the high-frequency attenuation (κ_0). They stated that site amplification depends on both V_{s30} and site κ_0 .

Regnier et al. (2014), proposed a complimentary parameter to V_{s30} , which is defined as the slope of V_s profile-depth curve, B_{30} . They mentioned that B_{30} may help for the evaluation of site response, since it is well correlated with site specific PGA level.

Hassani and Atkinson (2016) correlated V_{s30} of the recording stations with f_0 to obtain a predictive relationship. Then, they suggested replacing V_{s30} with f_0 in the ground-motion prediction equations.

Derras et al. (2017) investigated the performance of various site proxies; V_{s30} , topographical slope, f_0 , and the depth value (H_{800} ; where V_s is higher than 800 m/sec). The best proxy was defined as V_{s30} at short periods ($T < 0.6$ sec), while f_0 and H_{800} showed better performance at longer periods.

Zhu et al. (2020) searched for alternative and complimentary parameters to V_{s30} for site amplification characterization by using Kik-net database. They proposed site fundamental period (T_0) as the best performing single proxy and complimentary to V_{s30} .

3. SITE RESPONSE ANALYSIS METHOD

Amplitudes and frequency content of seismic waves change as they go through the near-surface soil layers and reach to ground surface. These alterations are known as site effects and should be quantified by conducting site response analyses. We will start by briefly discussing the cyclic soil behavior and reviewing the methods for site response analysis.

3.1. Cyclic Behavior of Soil

During earthquakes, soil layers are subjected to cyclic shear stress, τ , and the bonds between soil particles may be broken. The resulting relative displacements within soil elements would induce shear strains, γ . It was observed by Vucetic (1992) that all types of soils have a specific threshold cyclic shear strain level, γ_c , at which the soil structure would change permanently.

The ideal stress-strain behavior of a soil element under cyclic stresses is represented by hysteretic-type models (Kramer, 1996). Accordingly, stiffness (i.e., resistance to shear) and damping (i.e., energy dissipation) properties of soils are obtained from these hysteresis loops. The two key are the *dynamic shear modulus*, G_d , and the *damping ratio*, ζ . G_d is the secant of the hysteresis loop and ζ is the area of the hysteresis loop divided by the input energy. The modulus ratio (graphically stated as modulus reduction curve) is used for an easier way of representing the relation between cyclic shear strain, γ_c , and dynamic shear modulus which is also designated as G_{sec} (see, Figure 3.1). The figure shows the change of G_{sec} over G_{max} (i.e., the slope of the skeleton of hysteresis loop at the origin point where γ_c is zero) by increasing cyclic shear strains. Hysteretic soil models can be approximated by equivalent-linear models, in which soil behaves according to modulus reduction curve and develops a hysteresis loop for each cycle of loading. There are various parameters affecting the soil stiffness, hence the shape of modulus reduction curve; the number of loading cycles and the plasticity index for fine grained soils (PI, measure of plasticity of soil defined by the difference of water content limits where the soil behaves plastic and

liquid) are two of them (Zen et al., 1978, Kokusho et al., 1982, Dobry and Vucetic, 1987, Sun et al., 1988). The increasing number of cycles causes to reduction in shear strength (i.e., soil stiffness). Besides, soils with (i.e., clays) higher PI behave more flexible since the threshold shear strain is higher for them, hence the degradation of soil stiffness starts at higher γ_c , and they have lower damping ratio than those with lower PI at the same γ_c (Kokusho et al., 1982, Dobry and Vucetic, 1987, Sun et al., 1988). The PI is effective on soil amplification as well. Soils with higher PI have higher soil amplification since the damping ratio is low, and for soil with low PI (or PI=0), the stiffness degradation develops fast by cyclic loading and amplification hardly occurs since the damping is high even at smaller shear strains (Vucetic, 1992).

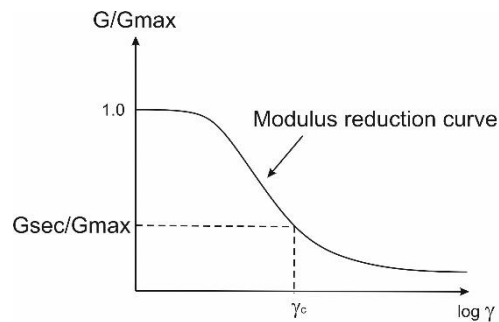


Figure 3.1. Graphical representation of cyclic shear strain, γ_c , and G/G_{max} relation by modulus reduction curve.

3.2. Equivalent-Linear Method

Site response is determined numerically by linear, equivalent-linear, and nonlinear analysis methods. In this study, we used both linear and equivalent-linear methods by running the software DEEPSOIL (Hashash et al., 2008). Equivalent-linear method presents an approximation of nonlinear behavior by using an iterative procedure. It was developed by Seed and Idriss (1968) to improve the application range (for higher shear strain levels) of linear method and implemented in a computer program SHAKE (Schnabel et al., 1972). The program was modified and updated as SHAKE91 (Idriss and Sun, 1992), and later as SHAKE2000 (Ordonez, 2011) by adding some pre- and post-processors. Various other one-dimensional softwares, like EERA (Bardet et al., 2000) and DEEPSOIL (Hashash et al., 2008), were introduced with more options.

DEEPSOIL has the option to use for both linear and equivalent-linear approach in frequency domain for one-dimensional analysis. The two key assumptions of DEEPSOIL are: all interfaces and boundaries are horizontal and extend to infinity, and site response is caused by vertically propagating SH-waves. The application procedure of DEEPSOIL for equivalent-linear analysis are as follows;

1. Initial G_{max} (DEEPSOIL automatically converts shear wave velocity to G_{max}) and damping ratio are entered in the software, then modulus reduction and damping ratio curves of each soil type are defined.
2. When the analysis starts, equation of motion is operated by using the initially defined $G^{(1)}$ and $\xi^{(1)}$ values, and strain-time histories are obtained for each soil layer. Effective shear strain values are obtained through the peak amplitude of shear strain-time histories by applying 65% of the peak shear strain amplitude.
3. New $G^{(2)}$ and $\xi^{(2)}$ values are selected through the G/G_{max} and ζ curves after determination of effective shear strains (Figure 3.2). The iterations continue until the effective shear strains obtained for each layer become compatible with the G/G_{max} and ζ curves. The analysis stops when the successive iterations result in relatively equal G and ζ values.

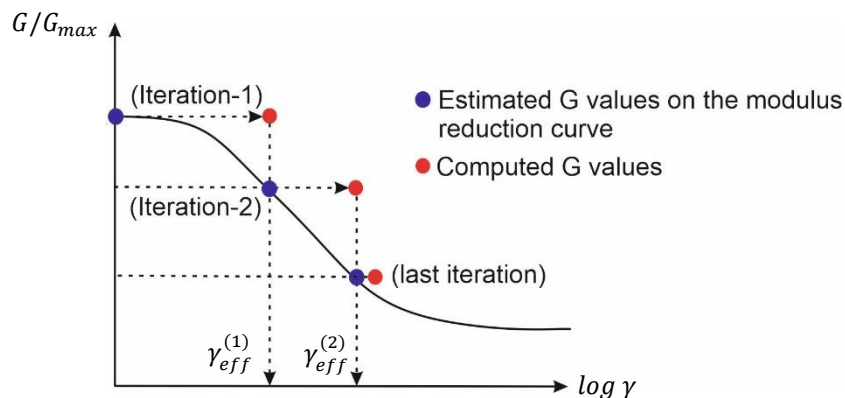


Figure 3.2. Iterative procedure for the selection of G corresponding to effective shear strain through the modulus reduction curve.

G and ζ stay constant through the analysis since the method is actually a linear approach. However, strain compatible G and ζ values are looked for until equivalent-linear

parameters are obtained on the modulus reduction curve. The method is found to be successful for determining the soil behavior in small and moderate strain levels.

4. SOIL MODELS

This Chapter investigates the performance of V_{s30} and the alternative parameters (V_{sz} , T_{tz} and f_0) suggested to characterize site amplification by considering a layered soil media lying on elastic bedrock and using the software DEEPSOIL (Hashash et al., 2008).

We consider a 100 m deep soil medium with 17 different shear wave velocity profiles, changing from convex to concave. The soil is divided into layers, first with equal thicknesses and then with equal wave travel times. Impulsive and white-noise type bedrock accelerations with gradually increasing amplitudes are used for the analysis. We investigate the correlations of the depth-averaged shear wave velocities, V_{sz} , and depth-averaged shear wave travel times, T_{tz} , for various depths (i.e., 5 m, 10 m, 20 m, 30 m, 40 m, 50 m and 100 m) with soil amplification factors and fundamental frequencies.

4.1. Validation of DEEPSOIL

We first tested DEEPSOIL for the accuracy of software by using a uniform soil profile. The uniform soil profile has a bedrock depth of 100 m and each layer has the same thickness (i.e., 1 m) and shear wave velocity (i.e., 100 m/sec), as shown in Figure 4.1. The elastic bedrock under the soil has a shear wave velocity, V_s , of 1524 m/sec. We used an impulse-type acceleration input at the bedrock because of its constant spectral amplitude. It has a PGA of 0.005g at 0.005 sec (Figure 4.2) and a Nyquist frequency of 100 Hz (Figure 4.3). An equivalent-linear analysis was carried out in the frequency domain by using the modulus reduction and damping ratio curve of Seed and Idriss (1970), (i.e., for sands in average bound) for all layers. We have validated accuracy of the software by comparing the theoretical fundamental frequency ($f=V_s / 4H$) with the analytical one (Figure 4.4-b). The analytical fundamental frequency was obtained from the surface-to-bedrock spectral ratio and found to be consistent with the theoretical one (0.2504 Hz).

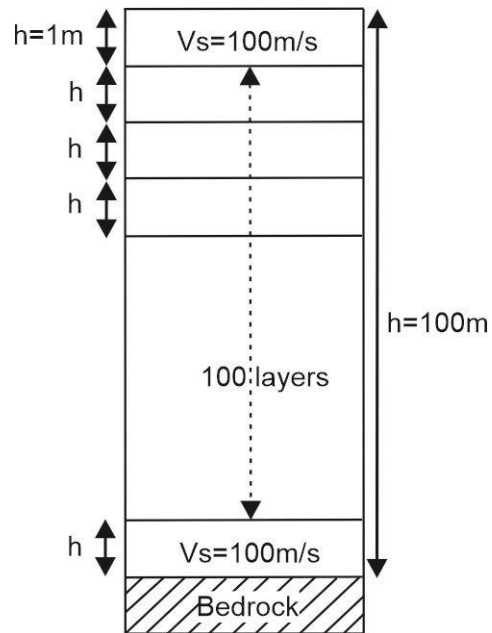


Figure 4.1. Uniform 100 m deep soil profile with $V_s=100$ m/sec for each layer with an elastic bedrock at the base, $V_{s\text{bedrock}}=1524$ m/sec.

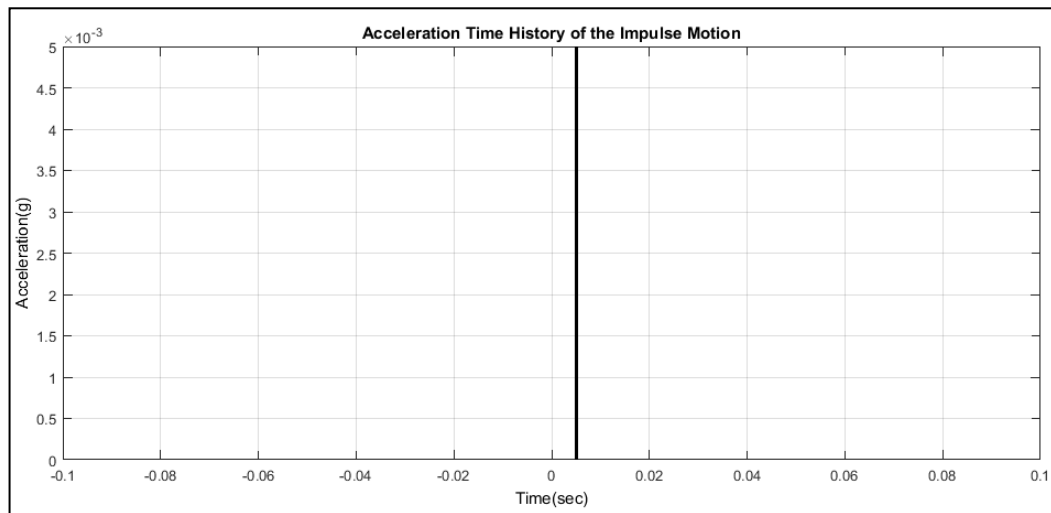


Figure 4.2. Acceleration-time history of the impulse displaying a peak at 0.005 sec.

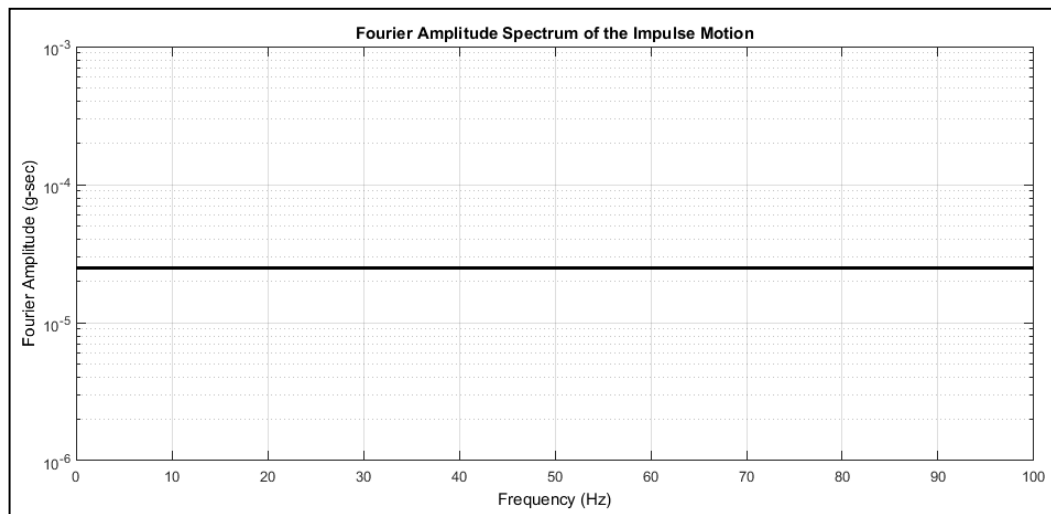


Figure 4.3. Fourier amplitude spectrum of the impulse.

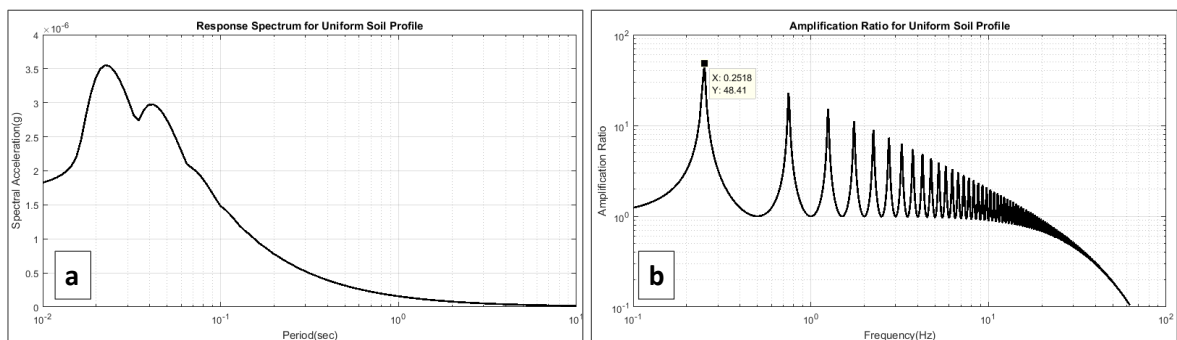


Figure 4.4. For the uniform soil profile: a) Response spectra of surface motions, b) Surface to bedrock spectral ratio that reveals the fundamental frequency at 0.25 Hz.

Next, to investigate the reliability of V_{s30} , we considered four different soil profiles with the same V_{s30} . The soil profiles consist of three layers as presented in Figure 4.5. The site response analysis has been carried out by using a single degradation and damping ratio curve for all soil layers. We chose the input ground motion randomly among the earthquake records. The properties of the soil profiles are given in Table 4.1. Although they all have the same V_{s30} , the results showed different soil amplification factors for the profiles. It is clear that the use of V_{s30} to characterize site amplification requires further investigation.

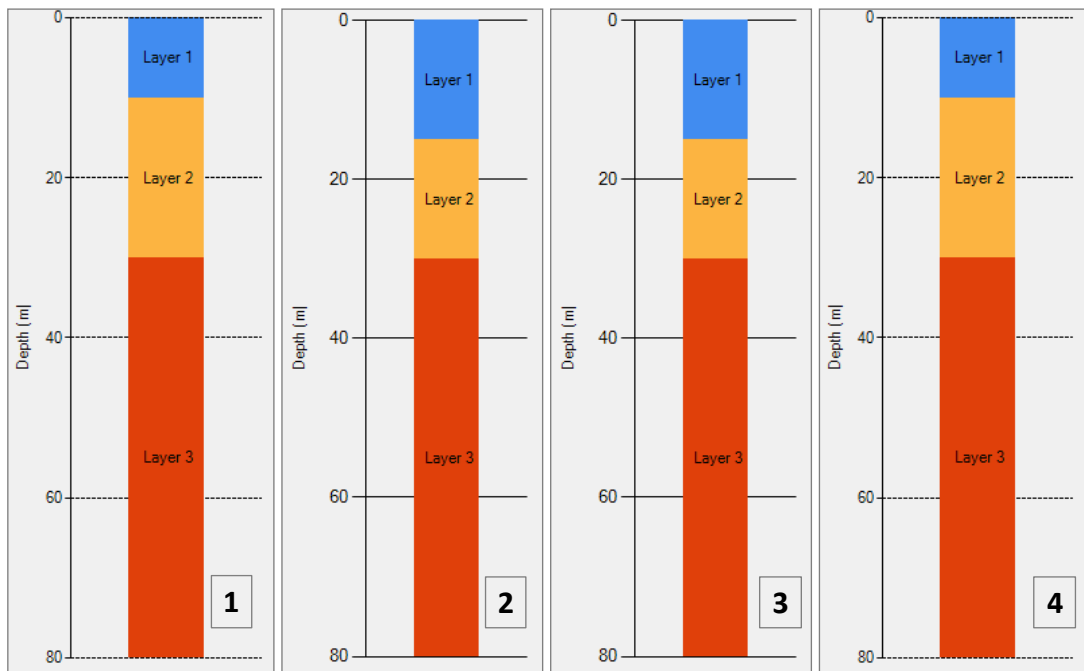


Figure 4.5. Soil profiles with the same V_{s30} (i.e., 133.3 m/sec) reveal different soil amplification factors.

Table 4.1. Properties and site response results of the soil profiles.

Layer No	Soil Profile-1		Soil Profile-2		Soil Profile-3		Soil Profile-4	
	Layer Thick.-H (m)	V_s (m/s)	Layer Thick.-H (m)	V_s (m/s)	Layer Thick.-H (m)	V_s (m/s)	Layer Thick.-H (m)	V_s (m/s)
1	10	80	15	120	15	120	10	80
2	20	200	15	150	15	150	20	200
3	50	300	50	700	50	300	50	700
Theo. Nat. Freq. (Hz)	0.64		0.84		0.64		0.84	
V_{s30} (m/s)	133.3		133.3		133.3		133.3	
Amp. Ratio	8.776		11.519		9.485		12.158	
Predom. Freq. (Hz)	0.87		1.11		0.81		1.31	

4.2. Soil Models of Equal Thickness and Equal Travel Time for Each Layer

We considered 17 shear wave velocity profiles for the bedrock depth of 100 m, changing from convex (i.e., the velocities changing faster near the surface and slower near the bedrock) to concave (i.e., the velocities changing slower near the surface and faster

near the bedrock). For analysis, we divided the soil media into layers, first with equal thickness, and then with equal wave travel times.

The soil model with equal layer thickness has 50 layers and the thickness of each layer is defined as 2 m. All shear wave velocity profiles are beginning with 50 m/sec at the first layer ending with 1000 m/sec at the last layer. The soil profiles are overlying an elastic bedrock with a shear wave velocity of 2000 m/sec. The generalized soil model for equal layer thickness is shown in Figure 4.6. We divided the shear wave velocity profiles into three groups according to the geometric shapes of them; as concave, linear and convex (Figure 4.7). For the concave profile, the velocities increase slower near the surface and faster near the bedrock, whereas for the convex profile, the velocities increase faster near the surface and slower near the bedrock. The linear profile represents the transition from concave to convex.

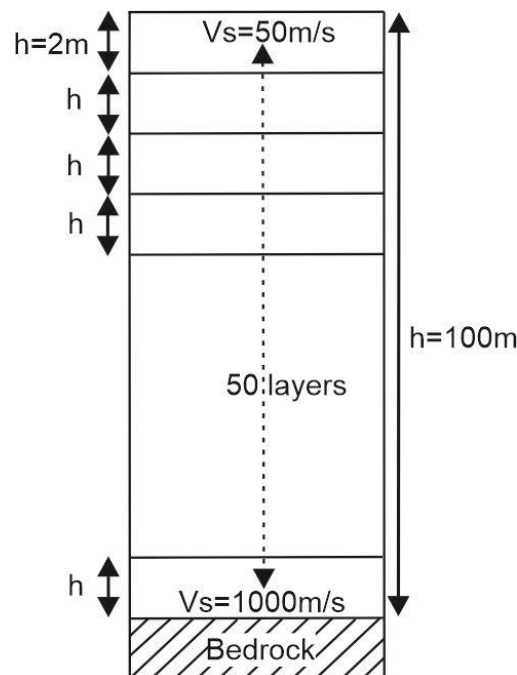


Figure 4.6. Generalized soil profile for concave, convex and linear types; $V_s=50$ m/sec for the top and $V_s=1000$ m/sec for the 50th layer.

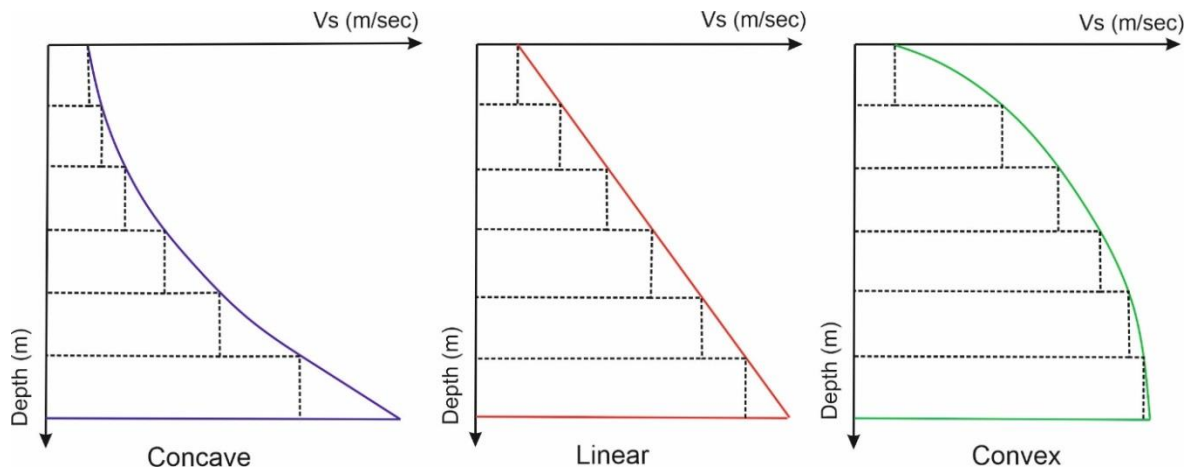


Figure 4.7. Geometric shapes of concave, linear and convex type shear wave velocity profiles.

Among the shear wave velocity profiles used, 10 are concave type, 1 is linear and 6 are convex type. In order to investigate the variation of soil amplification for softer profiles in more detail, we used higher number of concave profiles. The profiles are numbered from 1 to 10 representing decreasing stiffness for concave type and 1 to 6 representing increasing stiffness for convex type (Figure 4.8). The velocities increase rapidly near the surface as the soil profile turns from concave to convex. Therefore, Convex-6 type profile shows a higher stiffness than Concave-10. We generated these velocity profiles by using a single equation just by changing the coefficients of a and c and constant of n ;

$$y = ax^c + n \quad (4.1)$$

in which x represents shear wave velocity of each soil layer, and y represents the layer number from the surface. The values of coefficients a and c , and the constant n are given in Table 4.2.

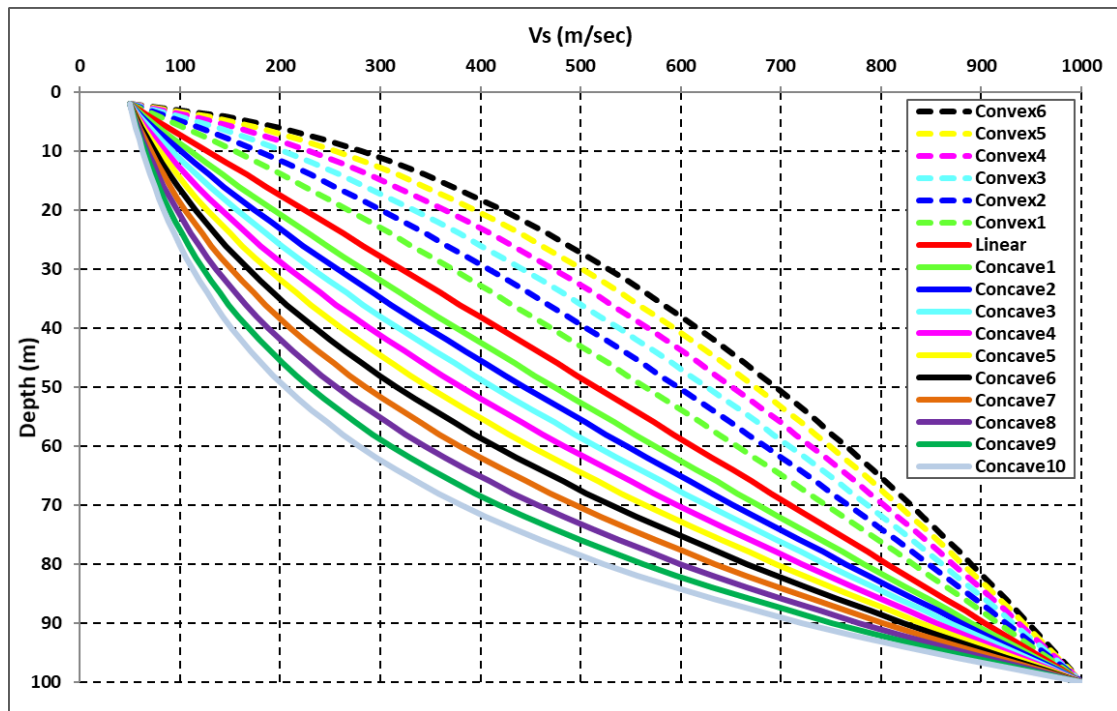


Figure 4.8. Shear wave velocity profiles changing from concave to convex (i.e., from left to right).

Table 4.2. Coefficients and constants of general equation for concave, linear and convex type soil profiles.

Soil Profile Type	a	n	c
Convex-1	0.01270	-0.38	1.20
Convex-2	0.00445	0.12	1.35
Convex-3	0.00157	0.44	1.50
Convex-4	0.00055	0.64	1.65
Convex-5	0.00019	0.77	1.80
Convex-6	0.00006	0.85	1.95
Linear	0.05158	-1.57	1
Concave-1	0.14984	-3.16	0.85
Concave-2	0.30812	-4.79	0.75
Concave-3	0.64128	-7.15	0.65
Concave-4	1.35848	-10.6	0.55
Concave-5	2.95672	-16.2	0.45
Concave-6	6.72342	-25.4	0.35
Concave-7	16.5302	-42.9	0.25
Concave-8	48.0320	-85.3	0.15
Concave-9	249.369	-302.2	0.05
Concave-10	-428.342	353.2	-0.05

For the soil model with equal wave travel time, the number of layers and the bedrock depths vary according to the velocity profiles (Figure 4.9). The equal travel time of each

layer is defined as 0.04 sec, since it corresponds to the lowest V_s and layer thickness, 50 m/sec (i.e., for the first layer) and 2 m, respectively.

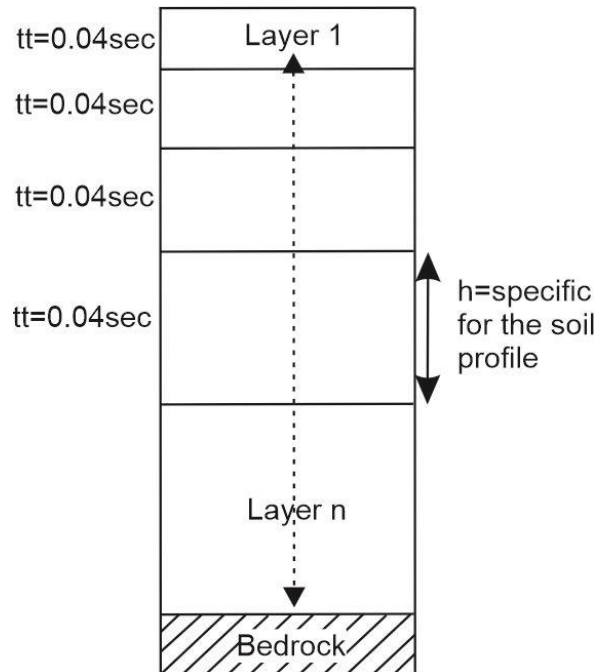


Figure 4.9. Generalized soil profile with equal wave travel time for each layer.

We have obtained the layer thicknesses of equal wave travel time model by using the velocity profiles of equal layer thickness model as explained below:

1. Incremental wave travel times were calculated for each velocity profile, as the velocity in the profiles increased and the wave travel times decreased (Figure 4.10, from right to left).
2. We extracted the depth of each layer, corresponding to a wave travel time of 0.04 sec, by using the wave travel time profiles.
3. Shear wave velocities corresponding to the identified depths (by item 2) were obtained by using the velocity profiles of equal layer thickness model (Figure 4.8).
4. We obtained the soil profiles with equal wave travel times (i.e., 0.04 sec for each layer) changing from concave to convex. The top layer of all profiles has V_s of 50

m/sec, and the layer thickness increases near the bedrock as the wave velocity increases with depth (Figure 4.11). The thicknesses of the soil layers are different for all profiles, because of the requirement of equal wave travel times in each layer.

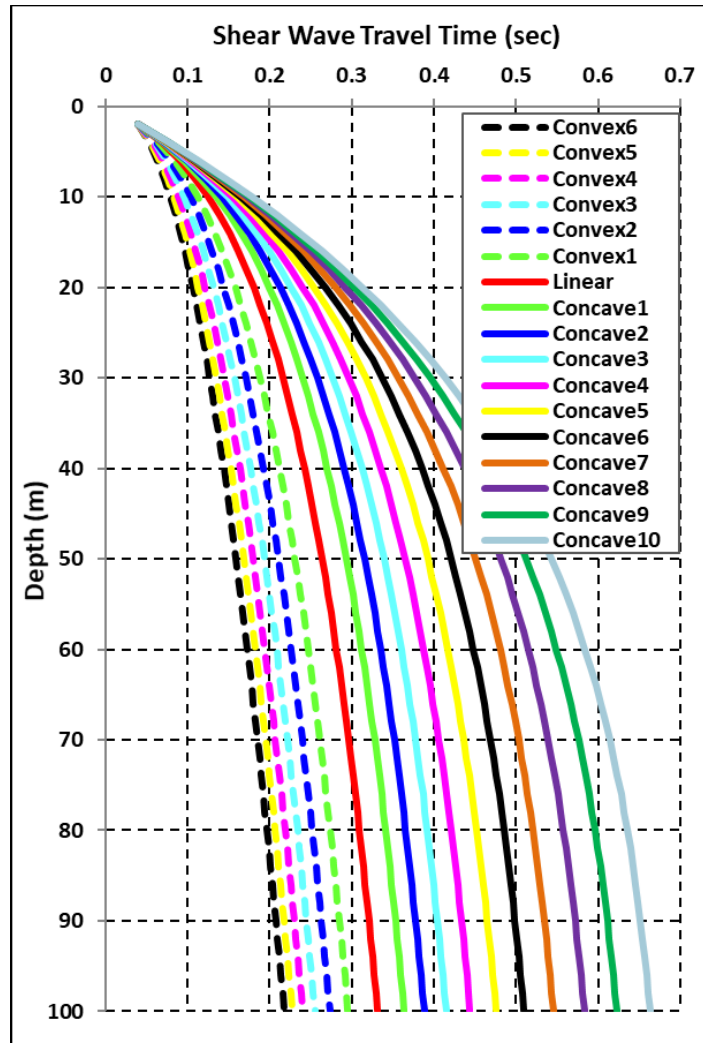


Figure 4.10. Incremental shear wave travel times for the velocity profiles of equal layer thickness model.

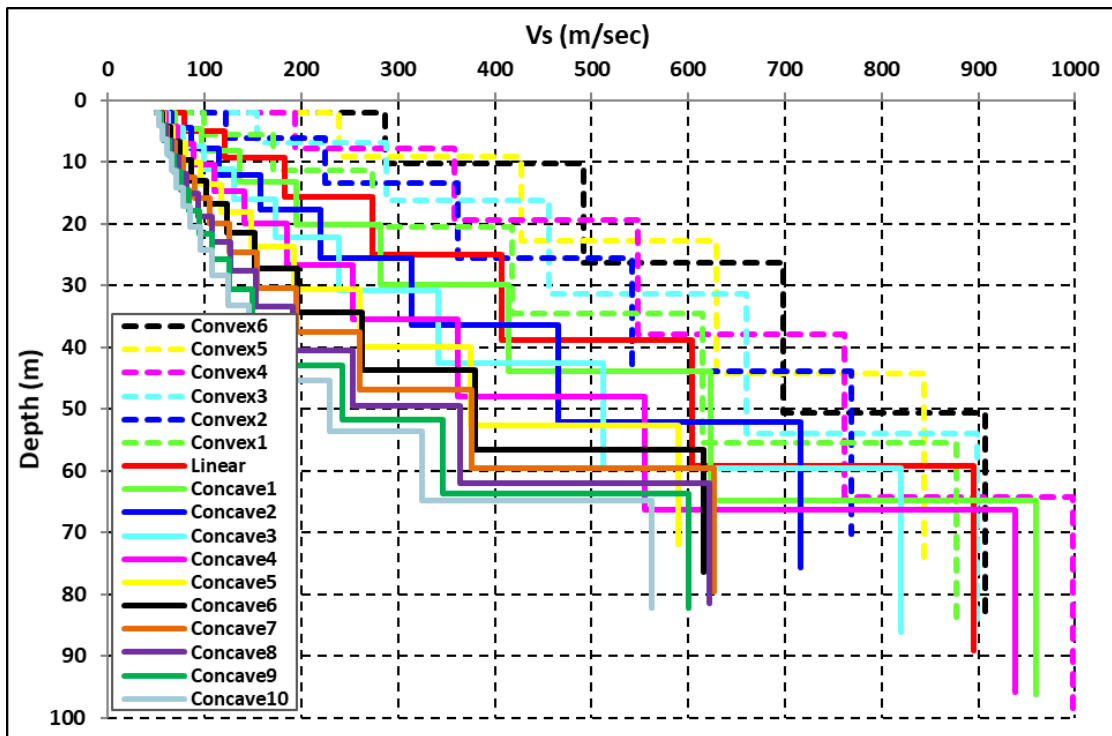


Figure 4.11. Soil profiles with equal shear wave travel time (0.04 sec) for each soil layer.

4.3. Impulsive and White-Noise Bedrock Motions

We used impulsive and white-noise bedrock motions, with gradually increasing peak acceleration levels for the analyses. They are considered as the boundaries of variations in the frequency content and amplitude of bedrock motions. The PGA levels of the bedrock accelerations varied between 0.005g and 1.0g. We preferred to use artificial ground motions since the earthquake records have complex properties with wide ranges of amplitudes, frequency content and duration.

The impulsive bedrock accelerations used for the analyses, and their Fourier amplitude and response spectra are shown in Figure 4.12.

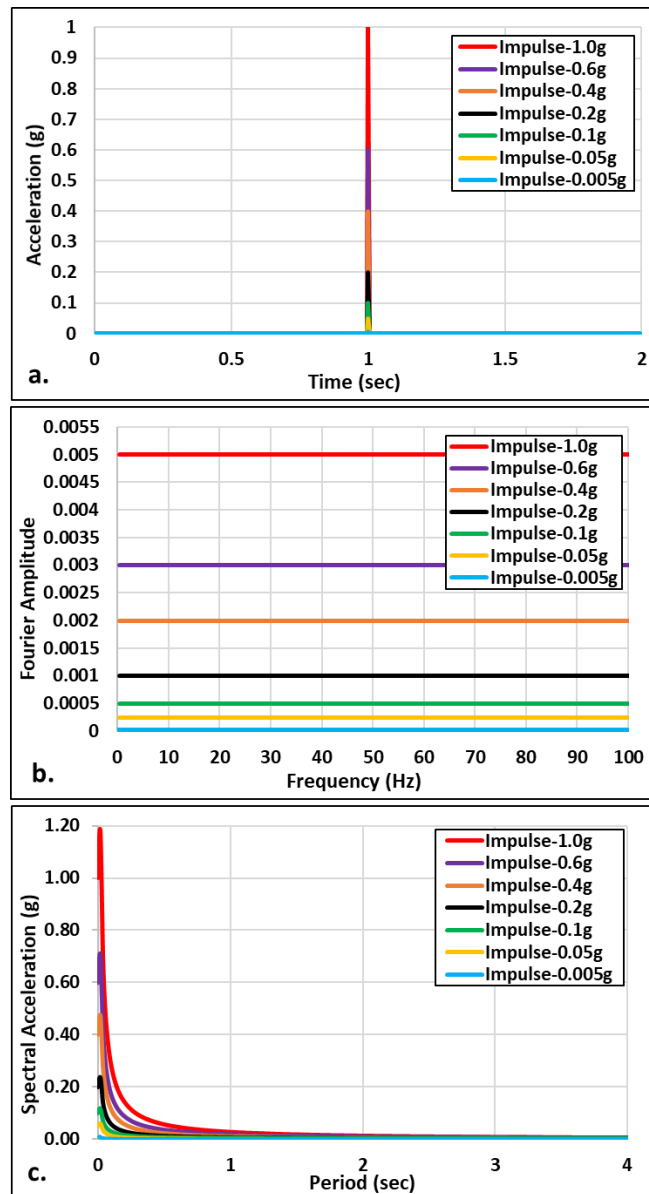


Figure 4.12. Bedrock impulsive accelerations with different amplitudes (gradually increasing PGAs: 0.005g, 0.05g, 0.1g, 0.2g, 0.4g, 0.6g, and 1.0g): a) Acceleration-time history, b) Fourier amplitude spectra, c) Response spectra.

The second type of bedrock motion used for the analysis is zero-mean Gaussian white-noise. Figure 4.13, shows the white-noise bedrock accelerations with PGA values varying from 0.005g to 1.0 g, along with their Fourier amplitude and response spectra. The sampling rate of the simulated impulsive and white-noise bedrock accelerations are 200 sps, corresponding to a Nyquist frequency of 100 Hz.

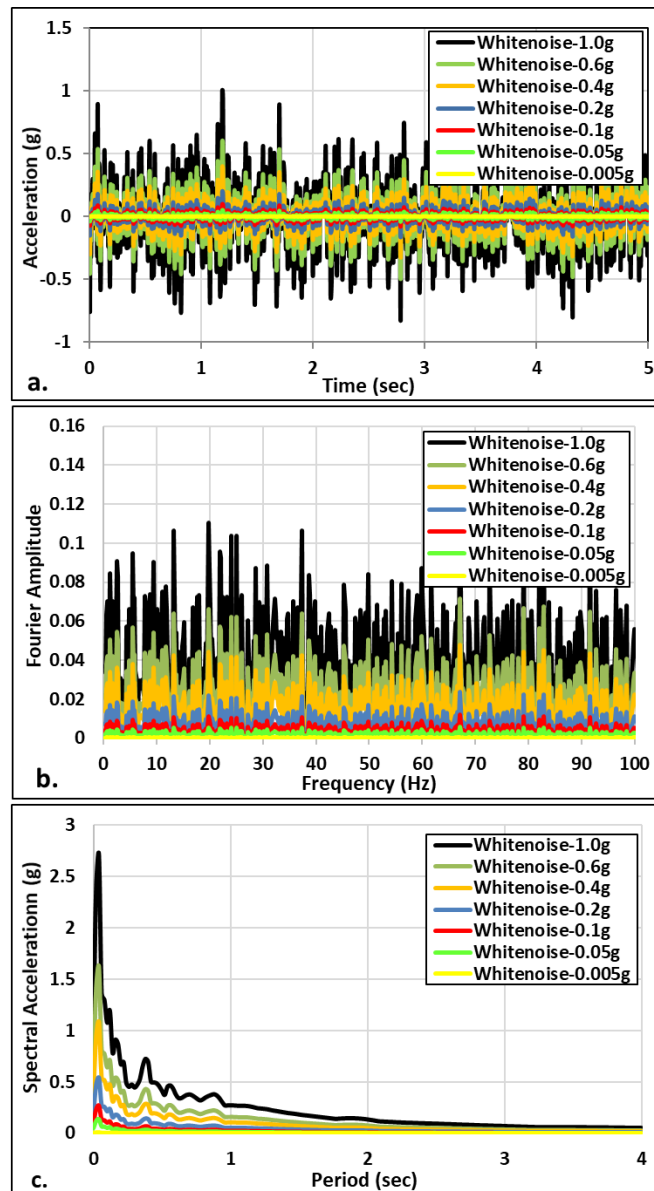


Figure 4.13. White-noise motions with gradually increasing PGAs: a) Acceleration-time history, b) Fourier amplitude spectrum, c) Response spectra.

4.4. Soil Properties for Site Response Analysis

We have carried out both linear and equivalent-linear analyses of soil profiles for the given bedrock motions by using DEEPSOIL. We identified the site amplification factors and fundamental frequencies for each soil profile and layering method (i.e., equal thickness and equal travel time).

Linear model uses the same shear modulus, G_{max} , and damping ratio, ζ , for all the profiles and layers. The damping ratio is assumed to be 0.48%, while the initial shear

modulus (i.e., G_{max}) was computed from the shear wave velocity and the density, ρ , by the equation of $V_s = \sqrt{G_{max}/\rho}$ embedded in DEEPSOIL. We assigned the unit weight, γ , of each layer above the bedrock as 18 kN/m^3 and the following properties for the bedrock; $V_s=2000 \text{ m/sec}$, $\gamma=22 \text{ kN/m}^3$ and $\xi=2\%$.

For equivalent-linear analysis, the unit weight and initial damping ratio were defined as $\gamma=18 \text{ kN/m}^3$ and $\xi=0.48\%$, respectively, same as the linear analysis. Equivalent-linear model requires the determination of modulus reduction and damping ratio curves at discrete points. In order to observe the effect of changing velocity profiles under the same conditions, we used the same degradation and damping ratio curve of Seed and Idriss (1970) for all soil layers (Figure 4.14). Seed and Idriss (1970) suggest three types of curves for sands, based on their stiffness. We have chosen “mean sand”, which presents a moderate stiffness and damping ratio.

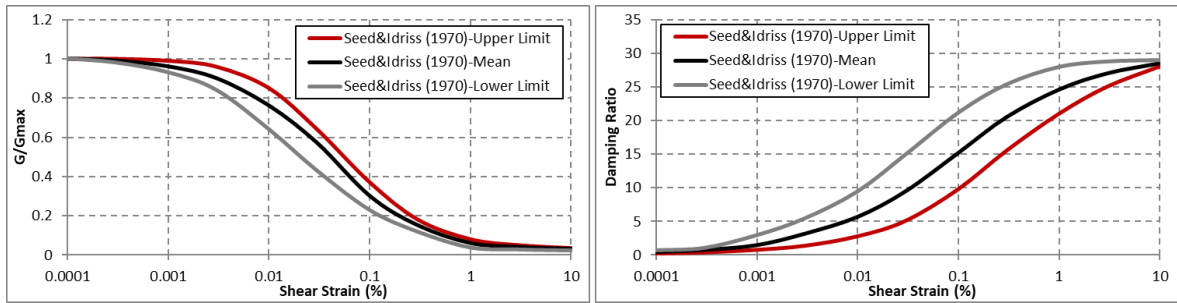


Figure 4.14. Modulus reduction, G/G_{max} , and damping ratio, ξ , curves defined by Seed and Idriss (1970) with respect to shear strains, γ_c .

4.5. Site Amplification Characterization Parameters

We calculated the averaged shear wave velocities, V_{sz} , and the shear wave travel times, T_{tz} , for different depths, z , in order to investigate the correlation with site amplification factors and fundamental frequencies. We have also investigated the correlation of f_0 with these parameters, V_{sz} and T_{tz} . We defined V_{sz} for $z=5 \text{ m}$, 10 m , 20 m , 30 m , 40 m , 50 m and 100 m by the following equation;

$$V_{sz} = \frac{\sum h_i}{\sum \left(\frac{h_i}{V_{si}}\right)} \quad (4.2)$$

where h equals to layer thickness. It is clear that V_{sz} is indirectly related to the shear wave travel time, as it is seen by the term in the denominator of the equation. We next investigated the performance of T_{tz} for site amplification characterization. Shear wave travel times were generated for 5 m, 10 m, 20 m, 30 m, 40 m, 50 m and 100 m by the following equation;

$$T_{tz} = \sum \frac{h_i}{V_{si}} \quad (4.3)$$

Shear wave travel time at a specific depth, z , is obtained by the sum of wave travel times (i.e., sum of the *layer thickness / shear wave velocity* ratios). V_{sz} and T_{tz} are presented in Tables 4.3 to 4.6 for each layering model and the 17 soil profiles. As the velocity profiles change from concave to convex, the stiffness of soil increases and the wave travel times decrease due to increasing wave velocity. V_{s100}/V_{sz} reflects the averaged shear wave velocity and T_{t100}/T_{tz} reflects the total wave travel time down to bedrock.

Table 4.3. V_{sz} of the soil profiles with equal layer thickness.

Soil Profile No	Soil Type	V_{s05} (m/sec)	V_{s10} (m/sec)	V_{s20} (m/sec)	V_{s30} (m/sec)	V_{s40} (m/sec)	V_{s50} (m/sec)	V_{s100} (m/sec)
1	Convex-6	85	127	188	236	277	314	459
2	Convex-5	82	120	177	222	261	297	439
3	Convex-4	78	112	165	207	244	278	416
4	Convex-3	74	104	152	191	226	258	392
5	Convex-2	70	96	139	175	207	237	366
6	Convex-1	67	89	126	159	189	217	338
7	Linear	62	80	111	139	165	190	302
8	Concave-1	60	74	100	125	148	170	275
9	Concave-2	58	70	94	116	138	159	258
10	Concave-3	57	67	88	108	128	147	241
11	Concave-4	56	65	83	101	119	137	225
12	Concave-5	55	63	79	95	111	127	210
13	Concave-6	54	61	75	89	104	119	196
14	Concave-7	54	59	71	84	97	111	183
15	Concave-8	53	58	68	80	91	104	171
16	Concave-9	53	57	66	76	86	98	161
17	Concave-10	52	56	64	73	82	92	151

Table 4.4. T_{tz} of the soil profiles with equal layer thickness.

Soil Profile No	Soil Type	T_{t05} (sec)	T_{t10} (sec)	T_{t20} (sec)	T_{t30} (sec)	T_{t40} (sec)	T_{t50} (sec)	T_{t100} (sec)
1	Convex-6	0.059	0.079	0.106	0.127	0.144	0.159	0.218
2	Convex-5	0.061	0.084	0.113	0.135	0.153	0.169	0.228
3	Convex-4	0.064	0.089	0.122	0.145	0.164	0.180	0.240
4	Convex-3	0.067	0.096	0.132	0.157	0.177	0.194	0.255
5	Convex-2	0.071	0.104	0.144	0.171	0.193	0.211	0.274
6	Convex-1	0.075	0.113	0.158	0.189	0.212	0.231	0.295
7	Linear	0.080	0.126	0.181	0.216	0.243	0.264	0.331
8	Concave-1	0.084	0.136	0.200	0.241	0.270	0.293	0.364
9	Concave-2	0.086	0.142	0.213	0.258	0.291	0.315	0.388
10	Concave-3	0.088	0.148	0.227	0.277	0.313	0.339	0.415
11	Concave-4	0.089	0.154	0.241	0.297	0.336	0.365	0.444
12	Concave-5	0.091	0.160	0.254	0.317	0.360	0.393	0.476
13	Concave-6	0.092	0.165	0.268	0.337	0.386	0.421	0.510
14	Concave-7	0.093	0.169	0.281	0.357	0.412	0.451	0.545
15	Concave-8	0.094	0.173	0.292	0.377	0.438	0.482	0.583
16	Concave-9	0.095	0.176	0.303	0.396	0.463	0.513	0.623
17	Concave-10	0.096	0.179	0.313	0.414	0.488	0.544	0.663

Table 4.5. V_{sz} of the soil profiles with equal wave travel time for each layer.

Soil Profile No	Soil Type	V_{s05} (m/sec)	V_{s10} (m/sec)	V_{s20} (m/sec)	V_{s30} (m/sec)	V_{s40} (m/sec)	V_{s50} (m/sec)	V_{sz} (m/sec)
1	Convex-6	99	147	225	281	330	369	657
2	Convex-5	95	139	210	265	310	350	433
3	Convex-4	90	131	193	246	288	329	483
4	Convex-3	84	121	178	223	266	302	413
5	Convex-2	77	110	161	203	240	275	338
6	Convex-1	71	98	142	181	215	248	349
7	Linear	64	85	122	154	183	213	314
8	Concave-1	61	78	107	135	162	188	299
9	Concave-2	59	74	100	125	149	173	232
10	Concave-3	58	70	93	115	137	160	236
11	Concave-4	57	66	86	107	127	146	238
12	Concave-5	55	64	81	99	117	135	176
13	Concave-6	55	62	77	92	108	125	170
14	Concave-7	54	60	73	86	101	116	163
15	Concave-8	53	58	69	81	94	108	154
16	Concave-9	53	57	67	77	89	101	144
17	Concave-10	52	56	64	74	84	95	135

Table 4.6. T_{tz} of the soil profiles with equal wave travel time for each layer.

Soil Profile No	Soil Type	T_{t05} (sec)	T_{t10} (sec)	T_{t20} (sec)	T_{t30} (sec)	T_{t40} (sec)	T_{t50} (sec)	T_{tz} (sec)
1	Convex-6	0.050	0.068	0.089	0.107	0.121	0.135	0.172
2	Convex-5	0.053	0.072	0.095	0.113	0.129	0.143	0.171
3	Convex-4	0.055	0.076	0.104	0.122	0.139	0.152	0.206
4	Convex-3	0.059	0.083	0.112	0.134	0.151	0.166	0.207
5	Convex-2	0.065	0.091	0.125	0.148	0.167	0.182	0.208
6	Convex-1	0.070	0.102	0.141	0.166	0.186	0.202	0.245
7	Linear	0.078	0.117	0.164	0.195	0.219	0.235	0.284
8	Concave-1	0.082	0.128	0.187	0.222	0.247	0.266	0.322
9	Concave-2	0.084	0.136	0.200	0.240	0.268	0.289	0.327
10	Concave-3	0.087	0.136	0.216	0.261	0.291	0.313	0.365
11	Concave-4	0.088	0.151	0.232	0.281	0.316	0.341	0.402
12	Concave-5	0.090	0.157	0.246	0.304	0.343	0.370	0.410
13	Concave-6	0.092	0.162	0.261	0.325	0.369	0.399	0.449
14	Concave-7	0.093	0.167	0.276	0.348	0.397	0.431	0.489
15	Concave-8	0.094	0.171	0.288	0.368	0.425	0.465	0.529
16	Concave-9	0.095	0.175	0.300	0.389	0.451	0.497	0.569
17	Concave-10	0.095	0.178	0.310	0.407	0.478	0.529	0.610

5. INVESTIGATION OF SITE AMPLIFICATION CHARACTERIZATION PARAMETERS

We carried out both linear and equivalent-linear analyses by using the velocity profiles defined. We used two different layering scheme for analysis, first by dividing them into layers with equal thickness (i.e., 2 m), and next into layers with equal wave travel time (i.e., 0.04 sec). For each layering scheme and soil profile, we calculated soil amplification factors and fundamental frequencies by assuming impulsive and white-noise bedrock accelerations with gradually increasing amplitudes. We then studied their correlations with averaged V_{sz} and T_{tz} for different depths. We have also investigated the correlations of soil amplification factors with surface PGAs, maximum shear strains, and fundamental frequencies for each case. The optimal (i.e., those with the highest correlations) averaging depths for V_{sz} and T_{tz} have been identified. Moreover, we studied the correlation of nonlinear site amplification parameters with the linear ones by gradually increasing the bedrock acceleration amplitudes. Guidelines are presented to estimate nonlinear site amplification factors and fundamental frequencies from the linear ones.

5.1. Linear Analyses

We carried out linear analyses for equal layer thickness model by using an impulse at the bedrock level with peak PGA amplitudes 0.1g, 0.4g and 1.0g. We calculated soil amplification factors, fundamental frequencies, maximum shear strains, and surface PGAs for each bedrock acceleration level. Soil amplification factors and fundamental frequencies were obtained from the surface to bedrock transfer functions. Maximum value in the surface to bedrock spectral ratio of Fourier Amplitude spectra is defined as the soil amplification factor, AF , and the corresponding frequency as the fundamental frequency, f_0 . These are presented in Table 5.1 for each velocity profile. Since the soil model was linear, the soil amplification factors and fundamental frequencies are the same for all bedrock acceleration levels.

Table 5.1. Soil amplification factors (AF) and fundamental frequencies (f_0) for each velocity profile calculated by linear analysis.

Soil Profile No	Soil Type	f_0 -0.1g	f_0 -0.4g	f_0 -1.0g	AF-0.1g	AF-0.4g	AF-1.0g
1	Convex-6	5.823	5.823	5.823	16.354	16.354	16.354
2	Convex-5	5.609	5.609	5.609	15.329	15.329	15.329
3	Convex-4	5.359	5.359	5.359	14.243	14.243	14.243
4	Convex-3	5.066	5.066	5.066	13.213	13.213	13.213
5	Convex-2	4.742	4.742	4.742	12.335	12.335	12.335
6	Convex-1	2.869	2.869	2.869	11.708	11.708	11.708
7	Linear	1.337	1.337	1.337	11.884	11.884	11.884
8	Concave-1	1.190	1.190	1.190	13.747	13.747	13.747
9	Concave-2	1.099	1.099	1.099	15.033	15.033	15.033
10	Concave-3	1.007	1.007	1.007	16.293	16.293	16.293
11	Concave-4	0.922	0.922	0.922	17.506	17.506	17.506
12	Concave-5	0.848	0.848	0.848	18.668	18.668	18.668
13	Concave-6	0.775	0.775	0.775	19.783	19.783	19.783
14	Concave-7	0.708	0.708	0.708	20.831	20.831	20.831
15	Concave-8	0.647	0.647	0.647	21.724	21.724	21.724
16	Concave-9	0.598	0.598	0.598	22.440	22.440	22.440
17	Concave-10	0.549	0.549	0.549	23.363	23.363	23.363

The transfer functions are presented in Figure 5.1 to observe the variation of soil amplification with frequency for all velocity profiles. The same transfer functions were obtained for all bedrock acceleration levels, because no stiffness degradation occurs in linear range. We have seen a drastic difference in f_0 as the velocity profiles changed from concave to convex. f_0 was the first peak of transfer functions for the linear and concave profiles (Figure 5.2), whereas it was the second or third peak for the convex profiles (Figure 5.3). This indicates that convex velocity profiles amplify the high frequencies of the bedrock motion more than the low frequencies.

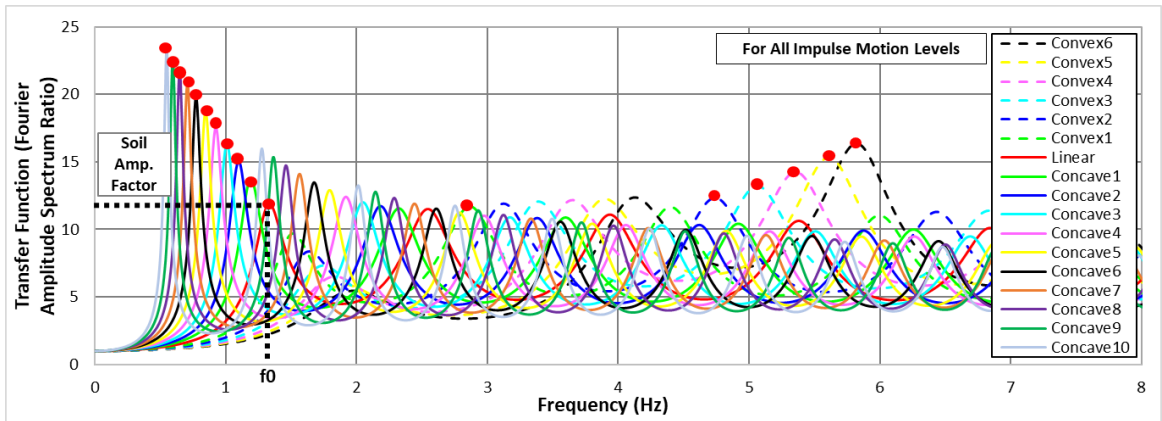


Figure 5.1. Transfer functions of all velocity profiles; red dots are representing the soil amplification factors and the corresponding fundamental frequencies.

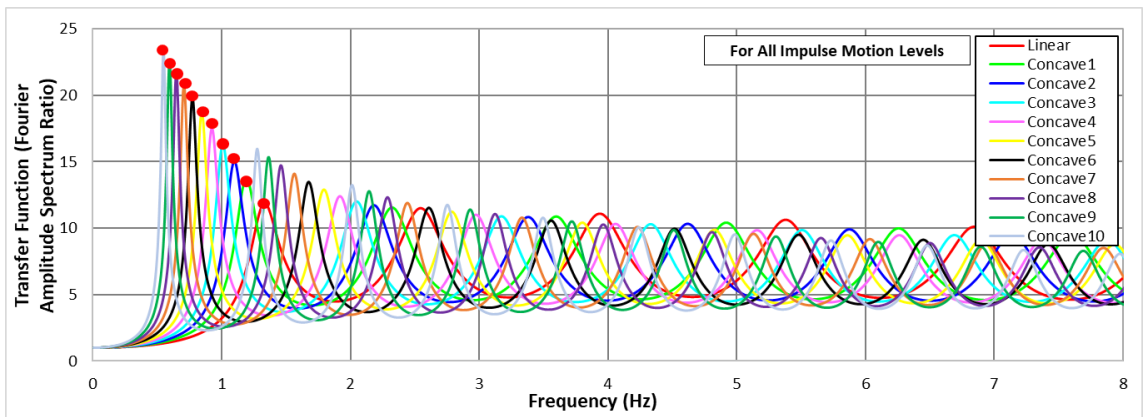


Figure 5.2. Transfer functions of concave and linear type velocity profiles.

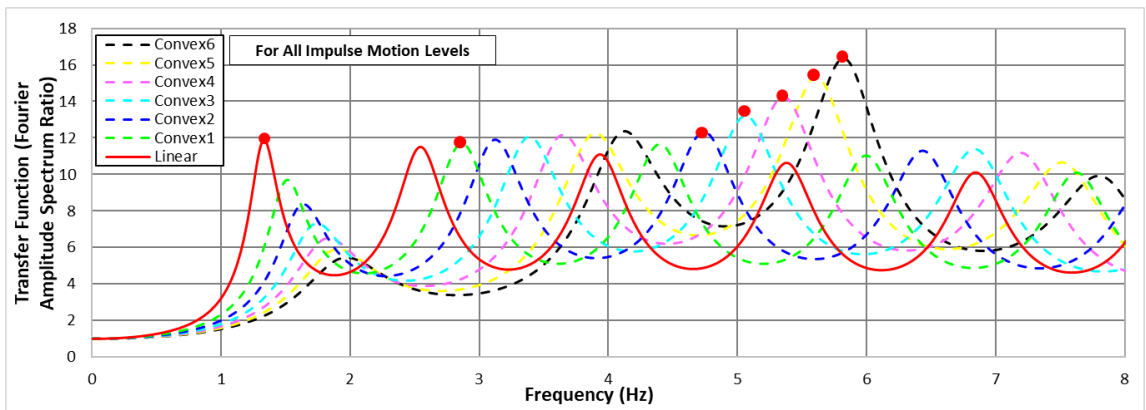


Figure 5.3. Transfer functions of linear and convex type velocity profiles.

The soil amplification factor of Concave-10 was higher than Concave-1, and the soil amplification factor of Convex-6 was higher than Convex-1. The soil amplification factor of Linear profile was observed lower than the amplification factor of Concave-1 and higher than the amplification factor of Convex-1. The reason of this fluctuation was explained in detail below:

1. The damping ratios stayed constant for all velocity profiles during the linear analysis, although the bedrock accelerations increased gradually.
2. Shear wave velocities, hence shear modulus, were lower for Concave-10 compared to Concave-1, which resulted in lower shear resistance against cyclic stresses. Besides, the impedance ratio between consecutive layers was higher near the surface and lower near the bedrock. Low damping ratio, low shear modulus and low impedance ratio near the bedrock contributed to a high soil amplification factor for Concave-10.
3. Stiffness of soil increased gradually as the velocity profiles changed from Concave-10 to Concave-1 and the shear resistance also increased. The impedance ratio was lower near the surface layers and higher near the bedrock. Higher soil stiffness and higher impedance ratio near the bedrock caused soil amplification factors to be lower for Concave-1.
4. The rate of change of the V_s values of top layers caused to a lower impedance ratio for Convex-6 than Convex-1. The impedance ratio between consecutive layers increased faster near the bedrock for Convex-6 with respect to Convex-1. Even if the stiffness of soil was higher, the high impedance contrast between the top two layers resulted in higher soil amplification factor for Convex-6 profile.

The surface PGAs and the maximum shear strains are presented for increasing bedrock acceleration levels in Tables 5.2 and 5.3, respectively. The transfer functions for linear soil behavior are identical for all velocity profiles and bedrock acceleration levels. The surface accelerations change based on the amplitude of bedrock accelerations. Surface

PGAs were amplified linearly proportional to the increase in bedrock accelerations (e.g., surface PGA of Convex-6 at 0.4g is four times the surface PGA at 0.1g; Table 5.2).

Table 5.2. Surface PGAs for each bedrock acceleration level.

Soil Profile No	Soil Type	Surface PGAs	Bedrock PGA-0.1g	Bedrock PGA-0.4g	Bedrock PGA-1.0g
1	Convex-6		0.300	1.200	3.000
2	Convex-5		0.315	1.260	3.151
3	Convex-4		0.400	1.601	4.003
4	Convex-3		0.400	1.601	4.002
5	Convex-2		0.354	1.417	3.542
6	Convex-1		0.391	1.564	3.911
7	Linear		0.352	1.409	3.523
8	Concave-1		0.341	1.363	3.408
9	Concave-2		0.308	1.233	3.083
10	Concave-3		0.349	1.395	3.489
11	Concave-4		0.328	1.311	3.279
12	Concave-5		0.319	1.275	3.188
13	Concave-6		0.310	1.239	3.097
14	Concave-7		0.298	1.194	2.984
15	Concave-8		0.249	0.994	2.486
16	Concave-9		0.216	0.866	2.164
17	Concave-10	0.233	0.932	2.331	

Table 5.3. Maximum shear strains for each bedrock acceleration level.

Soil Profile No	Soil Type	$\gamma(\%)$ - Bedrock PGA 0.1g	$\gamma(\%)$ - Bedrock PGA 0.4g	$\gamma(\%)$ - Bedrock PGA 1.0g
1	Convex-6	0.0252	0.1010	0.2524
2	Convex-5	0.0259	0.1038	0.2595
3	Convex-4	0.0266	0.1063	0.2658
4	Convex-3	0.0271	0.1083	0.2708
5	Convex-2	0.0274	0.1096	0.2741
6	Convex-1	0.0276	0.1105	0.2763
7	Linear	0.0276	0.1103	0.2757
8	Concave-1	0.0274	0.1097	0.2743
9	Concave-2	0.0272	0.1087	0.2718
10	Concave-3	0.0274	0.1096	0.2739
11	Concave-4	0.0271	0.1085	0.2711
12	Concave-5	0.0269	0.1078	0.2694
13	Concave-6	0.0267	0.1066	0.2665
14	Concave-7	0.0264	0.1055	0.2638
15	Concave-8	0.0257	0.1030	0.2574
16	Concave-9	0.0254	0.1018	0.2544
17	Concave-10	0.0250	0.0999	0.2498

Surface PGAs are presented for each velocity profile with respect to bedrock acceleration levels (Figure 5.4); a linear increase of PGA was observed. In order to verify the linearity of analysis, the surface PGAs were divided by the lowest surface PGAs belonging to each profile as well and the same rate of increase was observed for each profile (Figure 5.5).

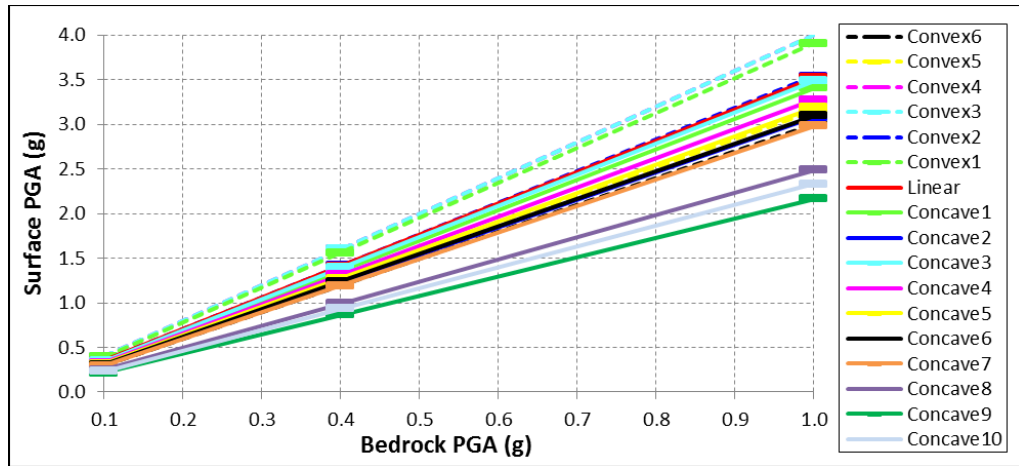


Figure 5.4. Surface PGAs for each velocity profile with respect to bedrock acceleration levels.

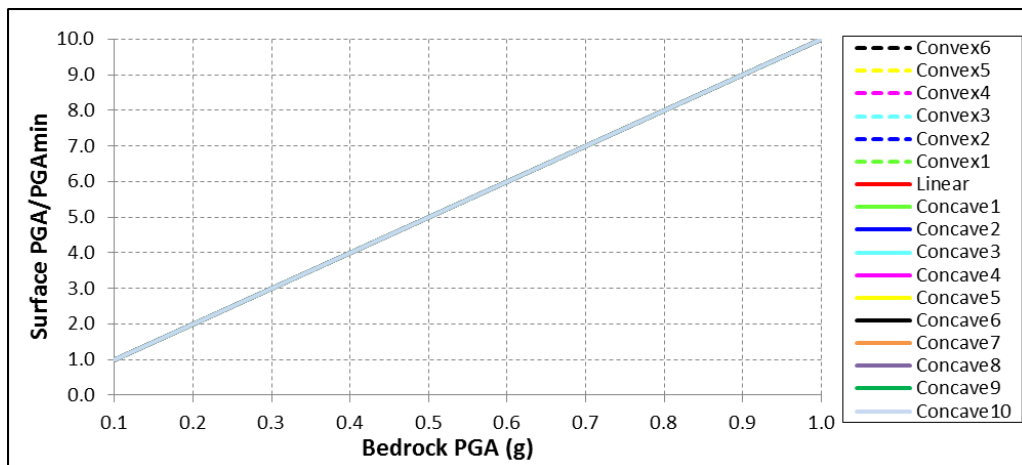


Figure 5.5. The linearity of the analysis by the same rate of increase for all profiles.

Maximum shear strains (γ -%) are presented with respect to bedrock accelerations (Figure 5.6); it is seen that the shear strains increased as the bedrock acceleration levels increased. The strains were observed in similar ranges for all velocity profiles when the bedrock PGA was smaller. For higher bedrock PGAs, the surface PGAs and maximum shear strains were observed quite high, indicating that the linearity assumption causes an

overestimation. However linear approach is still applicable for lower ground accelerations that result in linear elastic soil behavior.

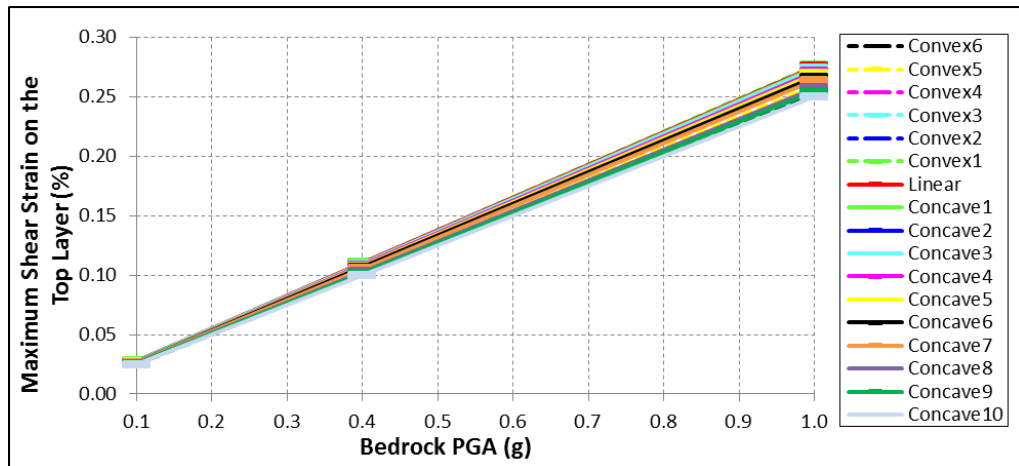


Figure 5.6. Maximum shear strains (γ -%) for each velocity profile with respect to bedrock accelerations.

5.1.1. Evaluation of Site Amplification and Fundamental Frequency Characterization Parameters

We have investigated the correlation of soil amplification factors and fundamental frequencies with averaged shear wave velocities, V_{sz} , and shear wave travel times, T_{tz} , at various depths. Besides, we have studied the correlation of soil amplification factors with fundamental soil frequencies, surface PGAs, and maximum shear strains. The optimal V_{sz} and T_{tz} parameters for site amplification has been decided by plotting AF/V_{sz} (or, AF/T_{tz}) values for each velocity profile and finding the one that is closest to a horizontal straight line (i.e., the mean of data set AF/V_{sz}), (Figure 5.7). The relation between the soil amplification factor (the spectral ratio of surface motion Fourier amplitude to bedrock motion Fourier amplitude) and surface PGA with respect to bedrock PGA is presented in Figure 5.8. The same information is also presented in Figure 5.9 with respect to the velocity profile number, after normalizing the data set (i.e., $AF/\text{surface PGA}$) with the largest value. Both figures do not show a good correlation. We have also studied the correlation of soil amplification factors with maximum shear strain with respect to bedrock PGA (Figure 5.10), and with respect to profile numbers after normalization (Figure 5.11). Again, the correlations were not good.

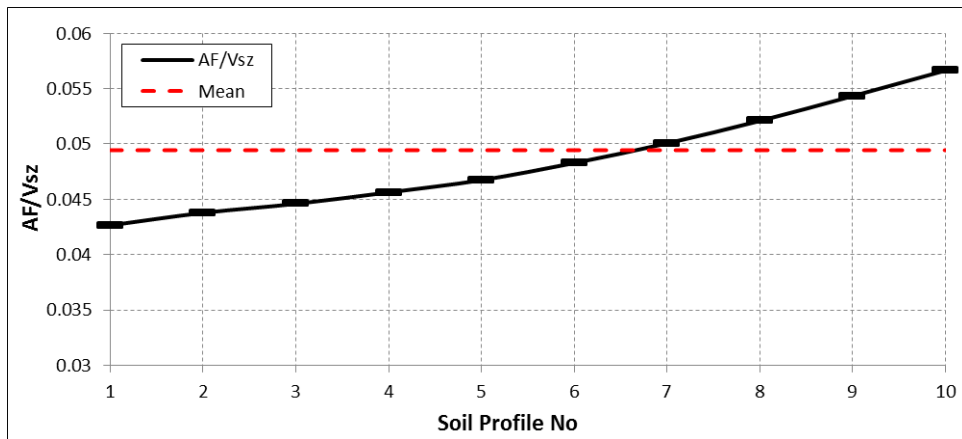


Figure 5.7. AF/V_{sz} data set and the mean of the data set as the best fitting straight line.

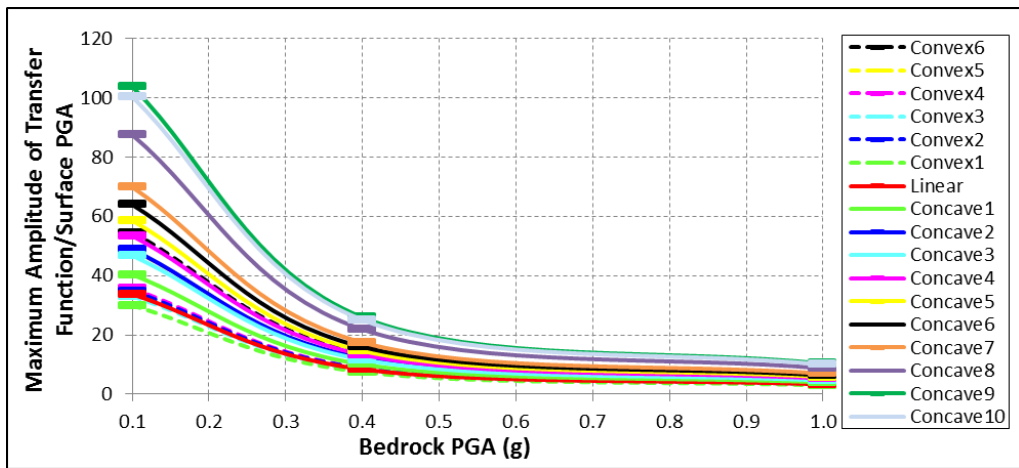


Figure 5.8. Correlation between soil amplification factors and surface PGAs with gradually increasing bedrock PGAs.

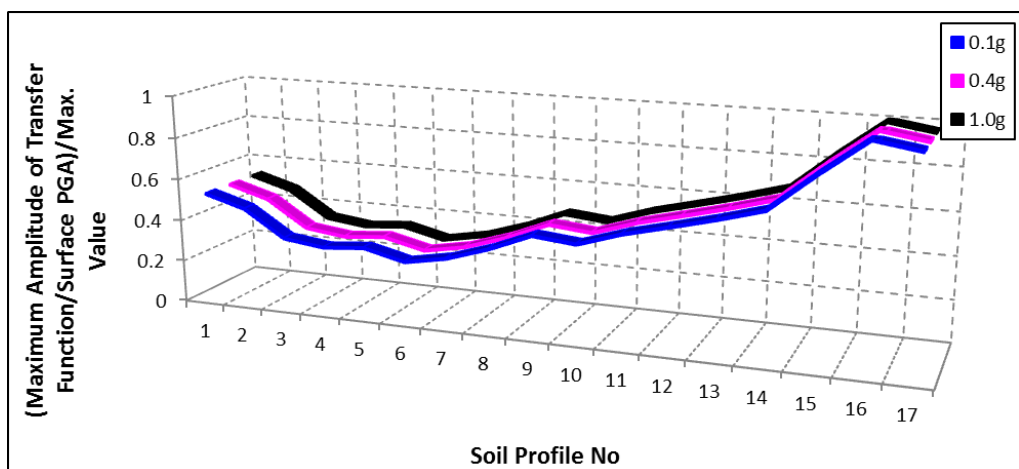


Figure 5.9. Normalized relation between soil amplification factors and surface PGAs for the profiles.

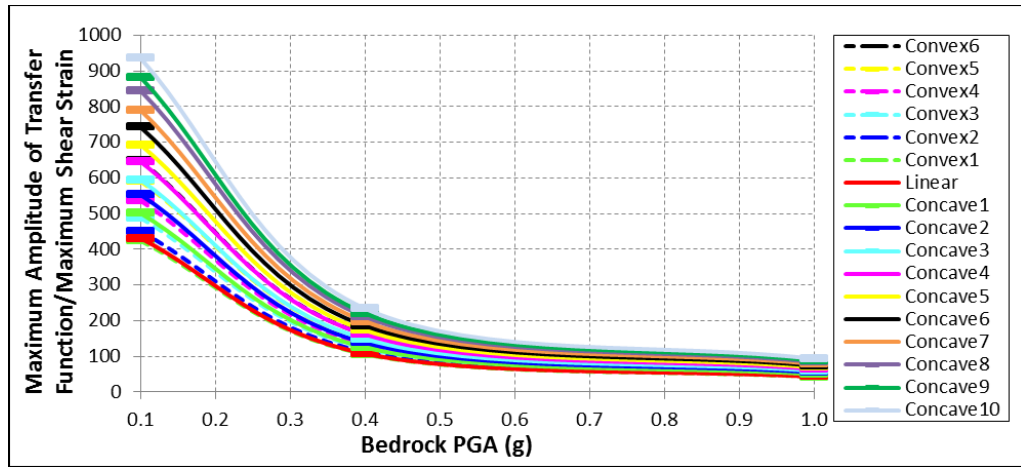


Figure 5.10. Relation between the soil amplification factors and maximum shear strains with respect to gradually increasing bedrock PGAs.

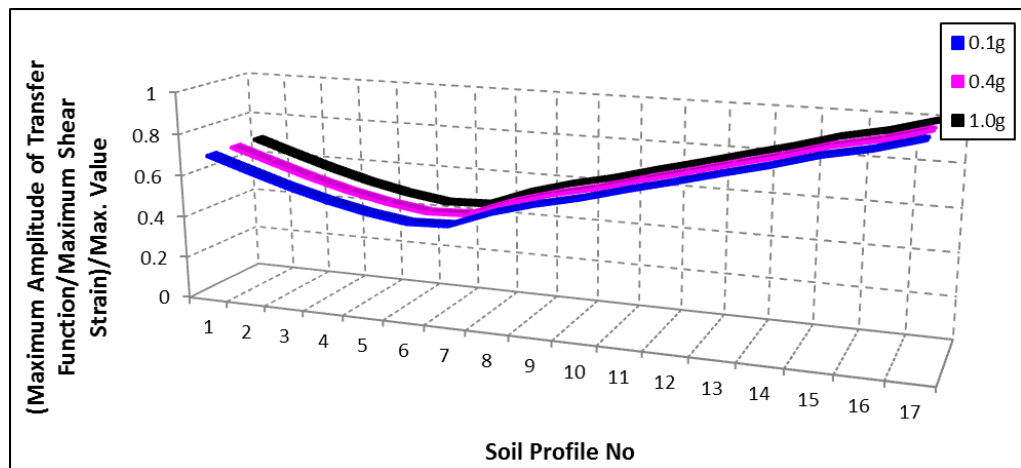


Figure 5.11. Normalized relation between the soil amplification factor and maximum shear strain for the profiles.

To investigate the correlation with frequency, we plotted the ratios of soil amplification factors to the fundamental frequencies, as shown in Figure 5.12. We have observed a fairly constant ratio for convex type velocity profiles for all bedrock acceleration levels. This indicates that soil amplification can be characterized by the fundamental frequency in linear elastic range.

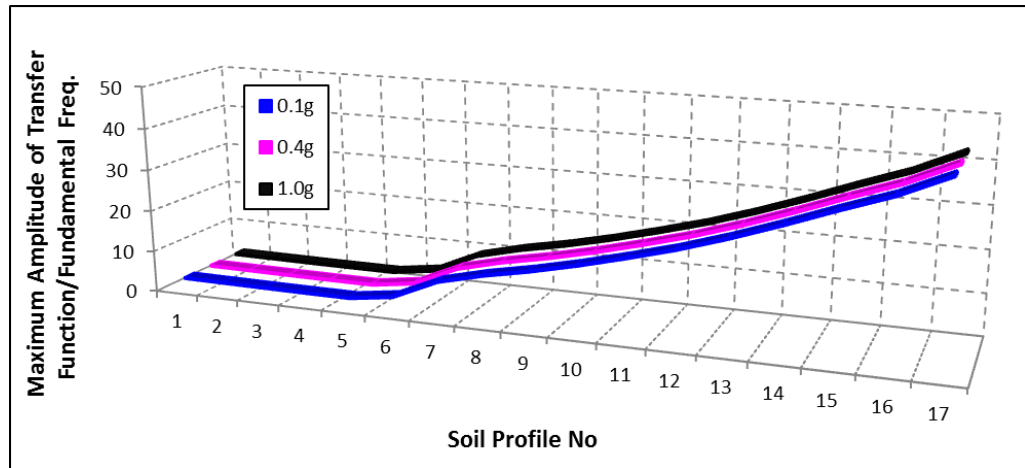


Figure 5.12. Correlation between soil amplification factor and fundamental frequency with respect to profiles.

In order to quantify the performance of the parameters used, we calculated the absolute error (AE) of each parameter for each profile with respect to the mean value of the parameter. The error is quantified as the spread of the parameter around the mean by the following equation:

$$AE = |y - \hat{y}| \quad (5.1)$$

where y equals to data point among the data set and the \hat{y} equals to mean of the data set. We presented the absolute errors for the convex and linear/concave velocity profiles separately for each bedrock acceleration level.

The correlation of soil amplification factors with time averaged shear wave velocities at various depths, AF/V_{sz} , are shown in Figure 5.13 for all bedrock accelerations (for linear analysis, bedrock input level does not change the values). The V_{sz} showed a good correlation just for convex velocity profiles since AF/V_{sz} presented a constant relation. We observed a linear relation rather than a constant relation for linear and concave velocity profiles (Figure 5.14). The mean of each AF/V_{sz} data set (Figure 5.15) and AE (Figure 5.16) were calculated for convex profiles. The best characterizing parameters for soil amplification factor were calculated as V_{s50} , V_{s10} , V_{s100} , V_{s100} , V_{s50} and V_{s100} for Convex-6, 5, 4, 3, 2 and 1, respectively.

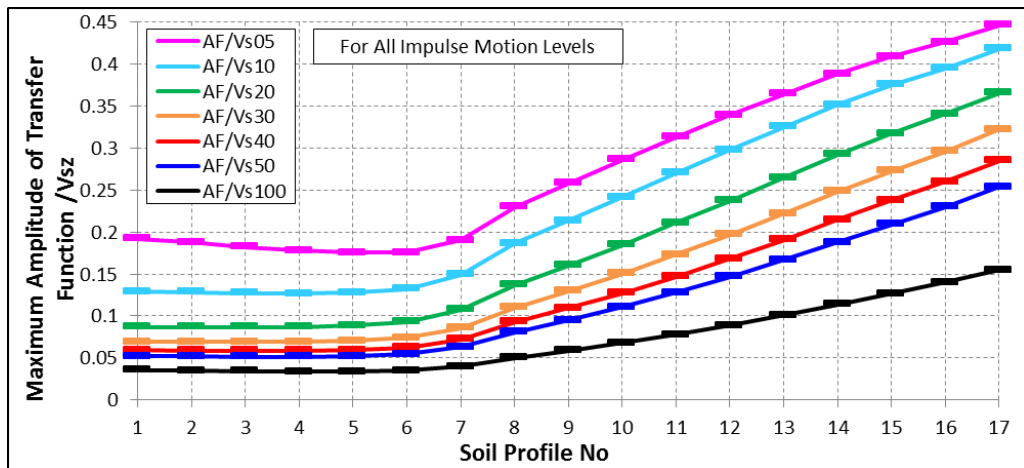


Figure 5.13. Correlation between soil amplification factors and V_{sz} at various depths for all bedrock acceleration levels.

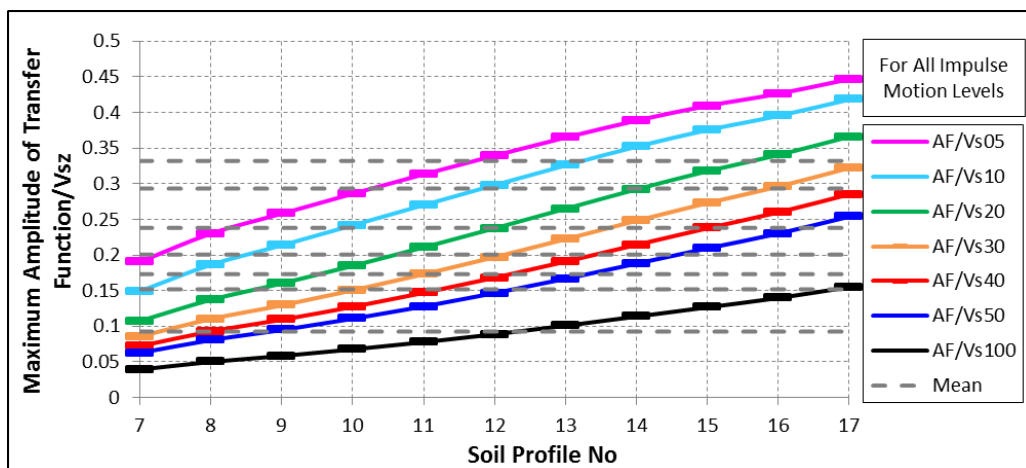


Figure 5.14. AF/V_{sz} values and the means (gray dashed lines) for linear/concave profiles.

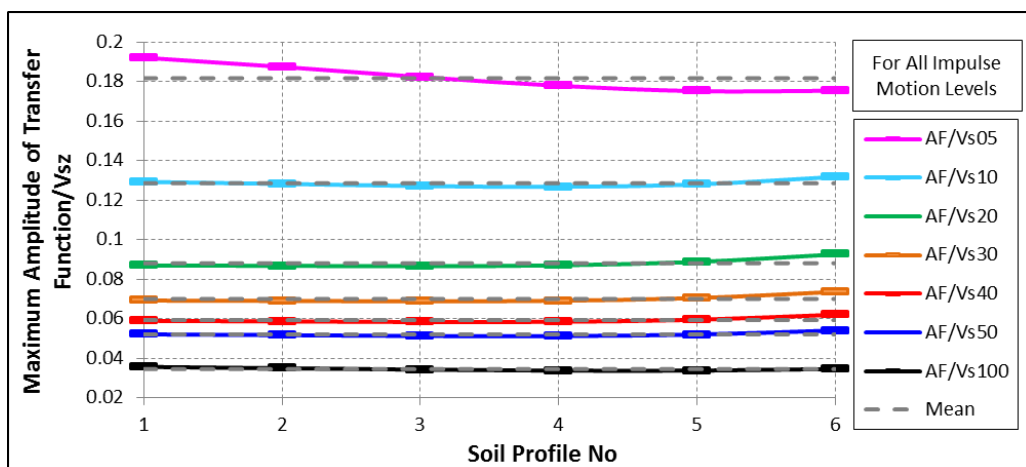


Figure 5.15. AF/V_{sz} values and the means (gray dashed lines) for convex profiles.

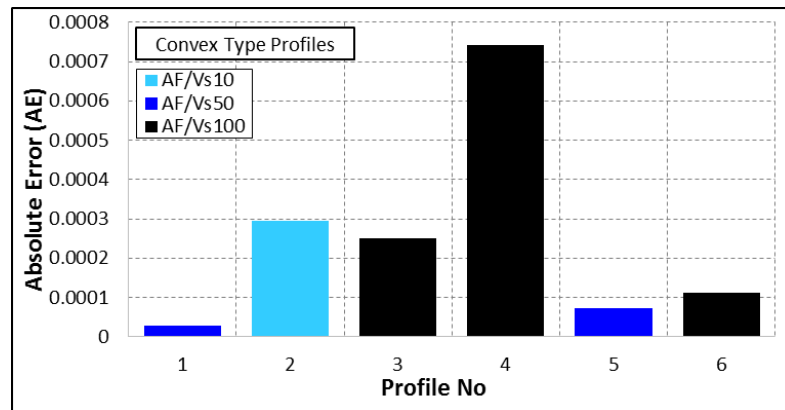


Figure 5.16. AE values for AF/V_{sz} at various depths for each convex type profile.

We have alternatively investigated the correlation of soil amplification factor with shear wave travel times at various depths (Figure 5.17). T_{tz} presented a constant relation only for linear and concave type profiles, as V_{sz} presented a constant relation only for convex profiles. So we showed the AE values just for linear/concave profiles; the best characterizing proxy parameters for soil amplification factor were defined as T_{t50} , T_{t100} , T_{t30} , T_{t20} , T_{t20} , T_{t50} , T_{t50} , T_{t30} , T_{t30} and T_{t30} for Linear to Concave-10 profiles from left to right (No 7 to 17), respectively (Figure 5.18).

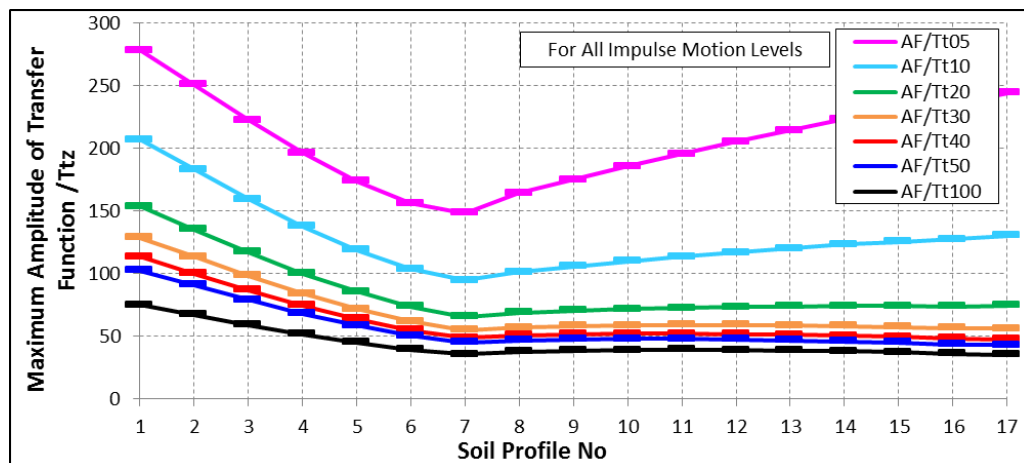


Figure 5.17. Correlation of soil amplification factors with T_{tz} for various depths.

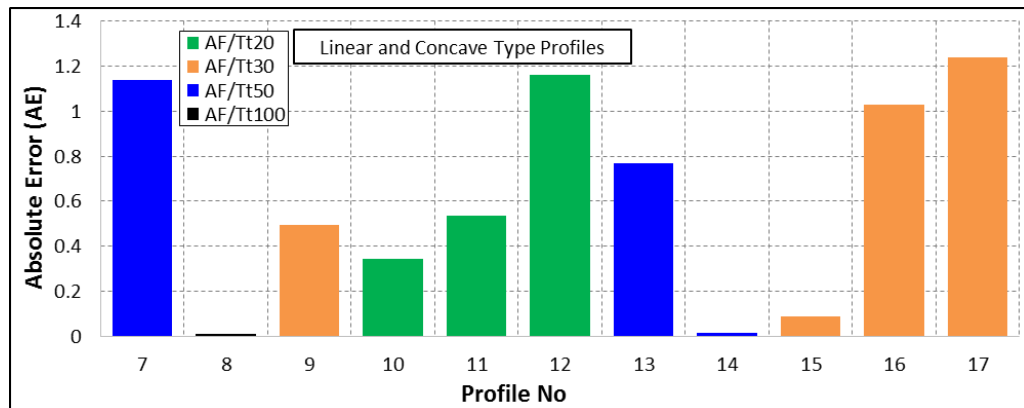


Figure 5.18. AE values for AF/T_{tz} at various depths for linear and concave type profiles.

The correlation between f_0 and T_{tz} has been investigated by multiplying these two parameters in order to see if it results in a constant value (recall that for a single layer over bedrock: $V_s=H/T_1$ and $f_0=V_s/4H$). We observed that T_{tz} was well correlated with f_0 for both concave and convex profiles (Figure 5.19). The best correlation with f_0 was obtained by T_{t20} for Convex-6 and 5, and by T_{t05} for Convex-4 to 1 (Figure 5.20). For linear and concave profiles, T_{t40} , T_{t50} , T_{t05} , T_{t40} , T_{t50} , T_{t05} were observed as the best characterizing parameters for Linear, Concave-1, Concave-2 to 5, Concave-6, Concave-7, and Concave-8 to 10, respectively (Figure 5.21).

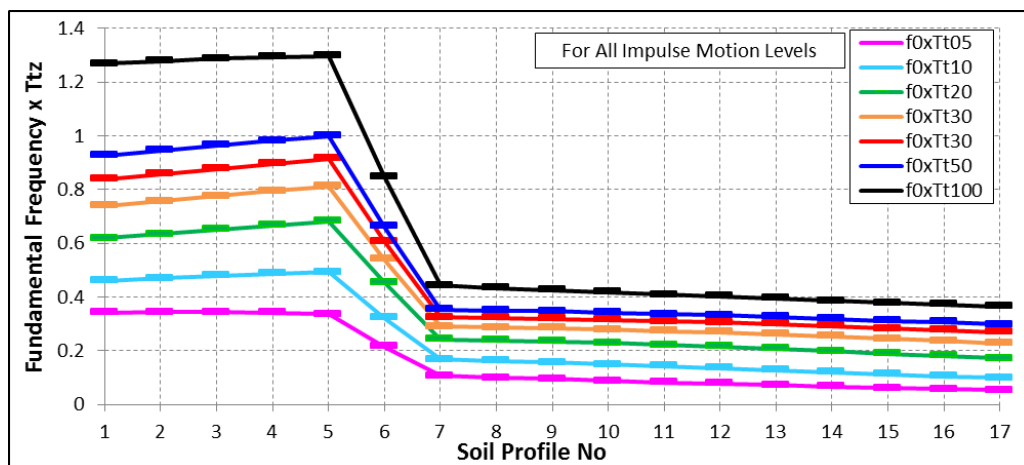


Figure 5.19. Correlation of fundamental frequency with T_{tz} at various depths.

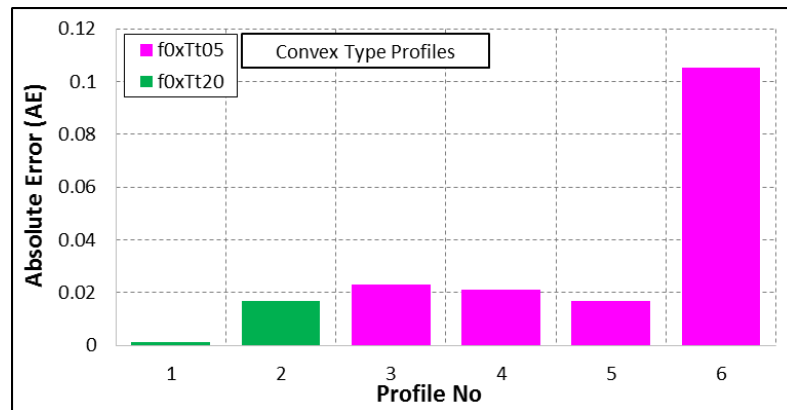


Figure 5.20. AE values of f_0xT_{tz} for convex type profiles.

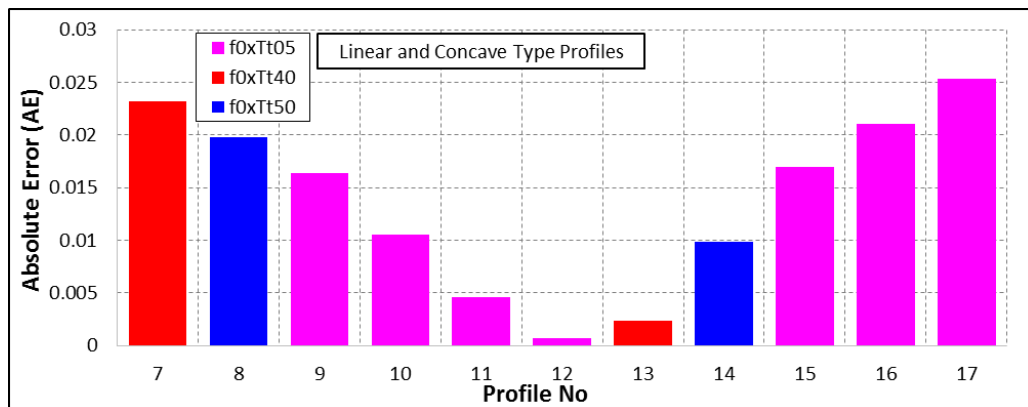


Figure 5.21. AE values of f_0xT_{tz} for linear and concave type profiles.

Fundamental frequency can be characterized by V_{sz} at various depths as well (Figure 5.22). For convex profiles, AE points out V_{s20} , V_{s50} and V_{s100} for Convex-6, Convex-5, and Convex-4 to 1 as the best performing parameters, respectively (Figure 5.23). For linear and concave profiles, V_{s50} for Concave-6 and V_{s100} for the other profiles were defined as the best performing parameters to characterize f_0 (Figure 5.24).

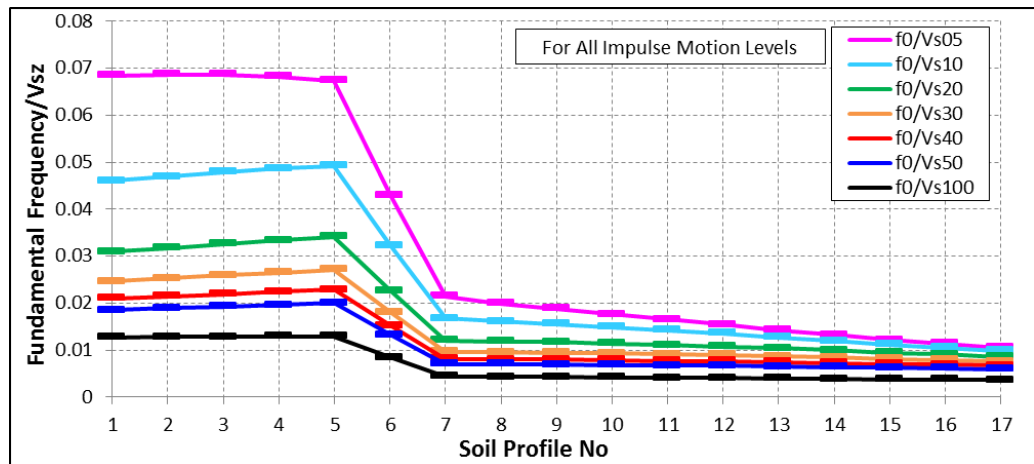


Figure 5.22. Correlation of fundamental frequency with V_{sz} at various depths.

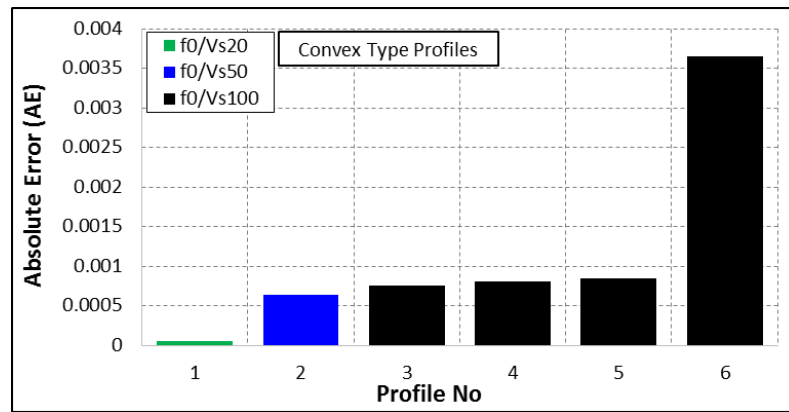


Figure 5.23. AE values of f_0/V_{sz} for convex type profiles.

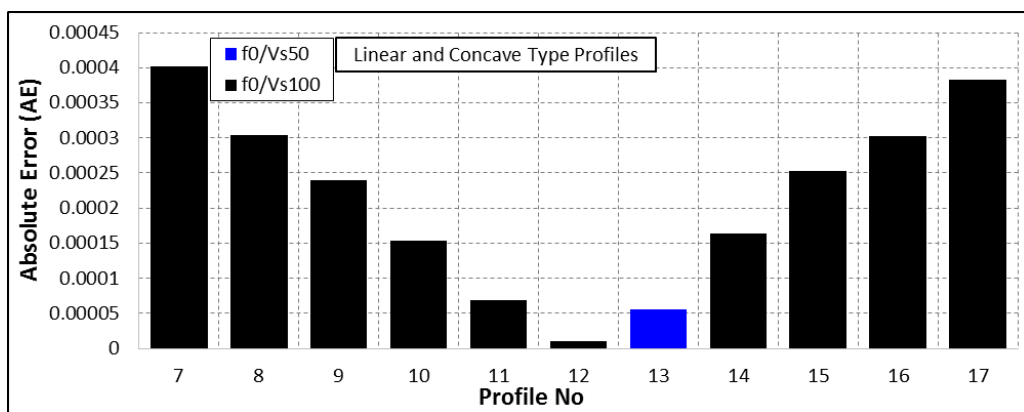


Figure 5.24. AE values of f_0/V_{sz} for linear and concave type profiles.

The investigation on proxy parameters for site amplification and fundamental frequency can be summarized as follows:

1. The results presented in this section are for linear elastic strain range.
2. There is a sharp difference between the soil amplification behavior of convex and linear/concave type velocity profiles. Therefore, the averaging depths of characterizing parameters for soil amplification and fundamental frequency differ for each profile type.
3. Surface PGAs and maximum shear strains do not correlate well with soil amplification.
4. Fundamental frequency can be used to characterize soil amplification only for convex profiles.
5. Soil amplification factors can be characterized by V_{sz} for convex profiles and by T_{tz} for linear/concave profiles; the best performing parameters were defined as V_{s50} and V_{s100} for convex profiles, and T_{t20} , T_{t30} and T_{t50} for linear/concave profiles.
6. Fundamental frequency can be characterized by both T_{tz} and V_{sz} parameters for all type of profiles; T_{t05} , T_{t20} and V_{s100} for convex profiles, T_{t05} and V_{s100} for linear/concave profiles.

5.2. Equivalent-Linear Analyses

Equivalent-linear approach is suitable for calculating site response for a broad range of strain rates. We used equivalent-linear approach for each layering type and velocity profile by using impulsive and white-noise bedrock accelerations to observe linear and nonlinear soil behavior.

5.2.1. Analyses of Equal Thickness Model Under Impulsive Bedrock Motion

We calculated soil amplification factors, fundamental frequencies, surface PGAs, and shear strains for gradually increasing impulsive bedrock motions with PGAs from 0.005g to 1.0g. The soil amplification factors (AF) and fundamental frequencies (f_0) are

presented in Table 5.4 and Table 5.5 for all bedrock acceleration levels. The values of AF and f_0 computed by the lowest bedrock acceleration level of 0.005g were nearly the same as those obtained by linear analysis.

Table 5.4. Fundamental frequencies (f_0) for gradually increasing bedrock accelerations.

Soil Profile No	Soil Type	f_0 -0.005g	f_0 -0.05g	f_0 -0.1g	f_0 -0.2g	f_0 -0.4g	f_0 -0.6g	f_0 -1.0g
1	Convex-6	5.780	4.004	3.906	3.717	3.265	2.924	1.862
2	Convex-5	5.573	3.784	3.693	3.528	3.125	2.832	1.770
3	Convex-4	5.322	3.546	3.461	3.308	2.960	2.716	1.666
4	Convex-3	5.035	3.290	3.204	3.070	2.783	1.611	1.544
5	Convex-2	4.718	3.027	2.948	2.820	2.588	1.483	1.404
6	Convex-1	2.856	2.771	2.698	1.440	1.385	1.337	1.251
7	Linear	1.331	1.306	1.282	1.245	1.184	1.135	1.044
8	Concave-1	1.282	1.160	1.135	1.099	1.038	0.983	0.891
9	Concave-2	1.099	1.068	1.044	1.007	0.946	0.891	0.800
10	Concave-3	1.007	0.977	0.952	0.916	0.854	0.806	0.720
11	Concave-4	0.922	0.891	0.867	0.830	0.775	0.726	0.647
12	Concave-5	0.842	0.812	0.793	0.757	0.702	0.653	0.580
13	Concave-6	0.769	0.745	0.720	0.684	0.635	0.592	0.519
14	Concave-7	0.702	0.677	0.653	0.623	0.574	0.537	0.470
15	Concave-8	0.647	0.616	0.598	0.568	0.525	0.488	0.427
16	Concave-9	0.592	0.568	0.549	0.519	0.482	0.446	0.391
17	Concave-10	0.543	0.525	0.507	0.476	0.439	0.409	0.354

Table 5.5. Soil amplification factors (AF) for gradually increasing bedrock accelerations.

Soil Profile No	Soil Type	AF-0.005g	AF-0.05g	AF-0.1g	AF-0.2g	AF-0.4g	AF-0.6g	AF-1.0g
1	Convex-6	15.25	11.95	11.35	10.20	8.25	7.36	7.97
2	Convex-5	14.49	11.69	11.12	10.17	8.55	7.69	8.35
3	Convex-4	13.62	11.42	10.84	10.03	8.79	8.00	8.66
4	Convex-3	12.72	11.09	10.49	9.76	8.88	8.30	8.93
5	Convex-2	11.92	10.71	10.10	9.40	8.72	8.77	9.06
6	Convex-1	11.57	10.30	9.68	9.30	9.20	9.08	8.80
7	Linear	11.88	11.27	10.81	10.22	9.53	9.06	8.08
8	Concave-1	12.46	12.39	11.58	10.59	9.45	8.72	7.46
9	Concave-2	14.85	12.99	11.93	10.68	9.28	8.40	7.07
10	Concave-3	16.01	13.46	12.14	10.66	9.06	8.08	6.72
11	Concave-4	17.10	13.81	12.24	10.56	8.82	7.78	6.40
12	Concave-5	18.08	14.03	12.24	10.41	8.58	7.52	6.15
13	Concave-6	18.98	14.14	12.21	10.25	8.35	7.28	5.94
14	Concave-7	19.71	14.24	12.11	10.08	8.14	7.07	5.77
15	Concave-8	20.41	14.22	12.04	9.92	7.97	6.90	5.64
16	Concave-9	21.05	14.24	11.94	9.77	7.80	6.75	5.52
17	Concave-10	21.44	14.15	11.81	9.64	7.69	6.63	5.43

As the bedrock PGA level increased, fundamental frequencies were shifted to smaller values due to stiffness degradation. Increasing shear stress reduced the stiffness (G_{sec}) of soil, and caused to a decrease in V_s due the fact that $V_s \propto \sqrt{G_{sec}/\rho}$, hence caused to a decrease in fundamental frequency. The fundamental frequencies of convex velocity profiles were observed higher than the other velocity profiles due to high stiffness properties. As the bedrock acceleration level increased, soil amplification factors decreased for each velocity profile due to stiffness degradation and increase in damping ratio.

In order to investigate the cyclic behavior of profiles in detail, shear strains, corresponding modulus reductions, and damping ratios are presented in Figures 5.25-5.30 for only 0.005g and 1.0g bedrock acceleration levels, since they represent the inputs for linear and nonlinear soil behavior. The G/G_{max} and ξ (%) were obtained depending on the effective shear strains ($\gamma\%$) at the last iteration of equivalent-linear analysis. It is observed that stiffness degradations and damping ratios are so low (and even no stiffness degradation for the soil layers close to bedrock, $G/G_{max}=1.0$) at 0.005g bedrock motion for all profiles (Figure 5.25 and 5.26), that the strains are in linear elastic range (i.e., linear behavior; Figure 5.27). For the bedrock acceleration level of 1.0g, stiffness degradations and damping ratios are high for all velocity profiles (Figure 5.28 and 5.29), so the shear strains are in elasto-plastic range (i.e., nonlinear behavior; Figure 5.30). According to shear strain rates calculated for each velocity profile, the strain ranges were defined as perfectly linear elastic at 0.005g bedrock acceleration level, and perfectly elasto-plastic at 1.0g bedrock acceleration level.

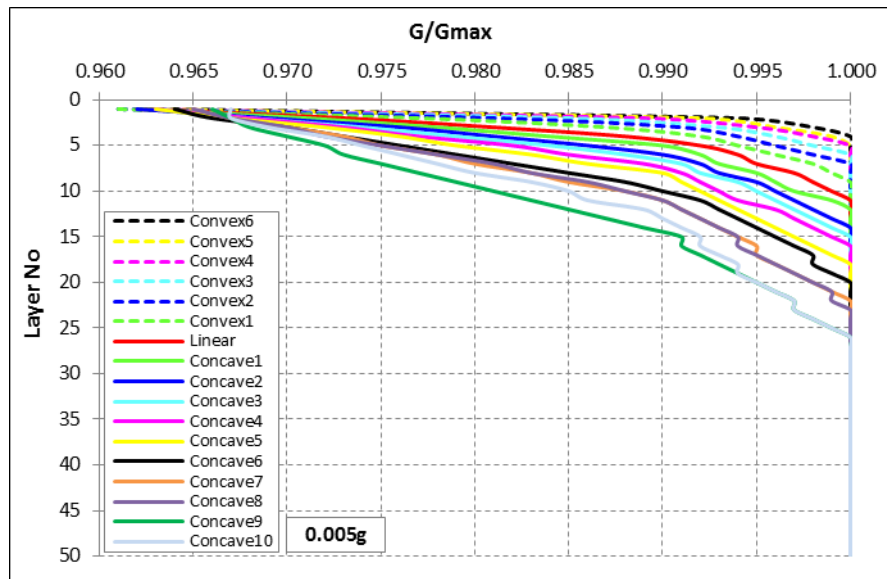


Figure 5.25. Modulus reductions for each layer at 0.005g bedrock acceleration level.

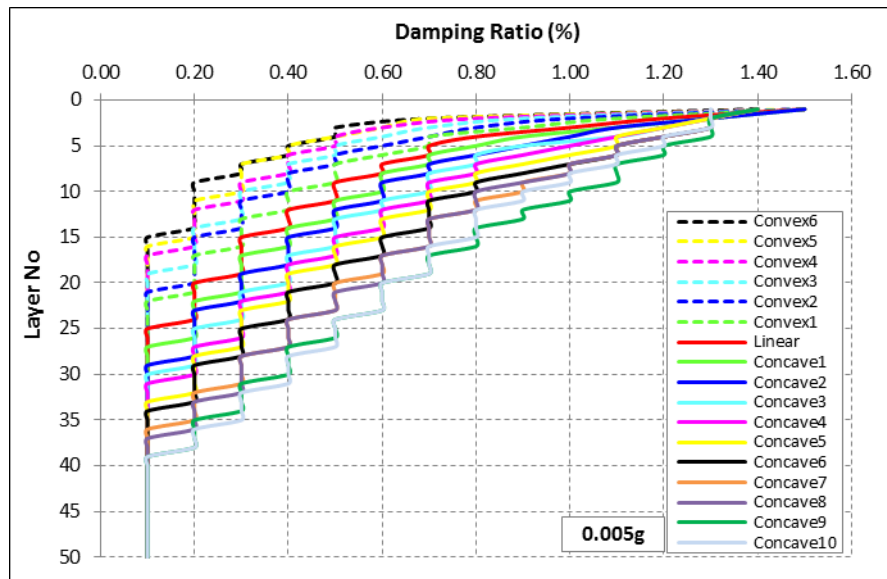


Figure 5.26. Damping ratios for each layer at 0.005g bedrock acceleration level.

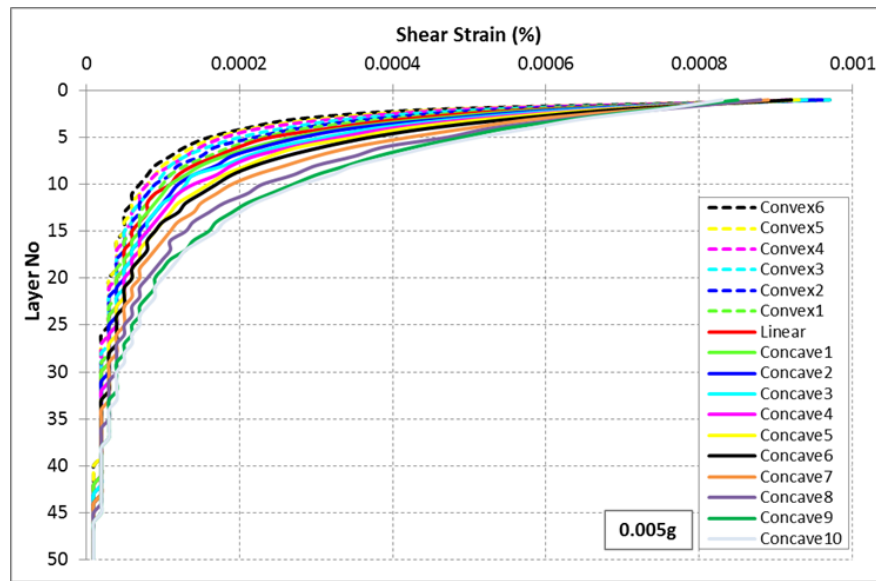


Figure 5.27. Shear strains for each layer at 0.005g bedrock acceleration level.

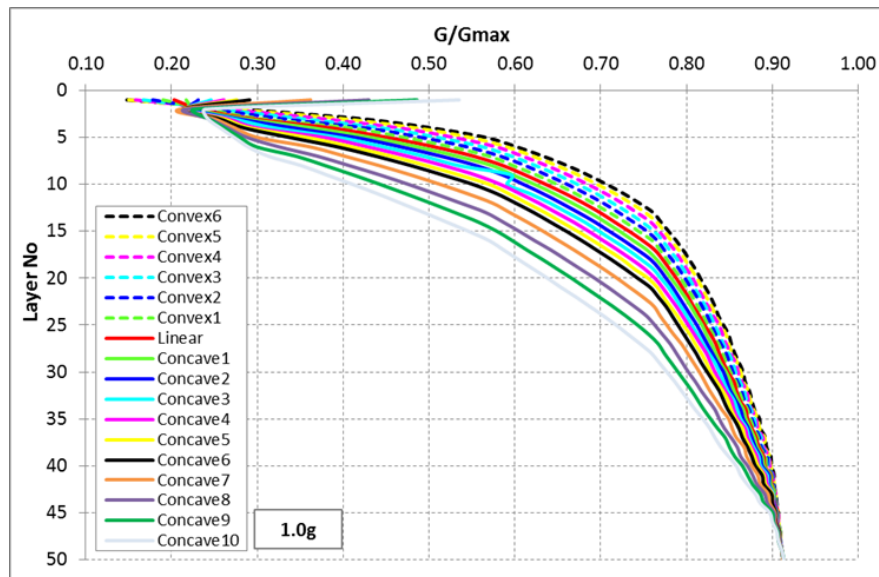


Figure 5.28. Modulus reductions for each layer at 1.0g bedrock acceleration level.

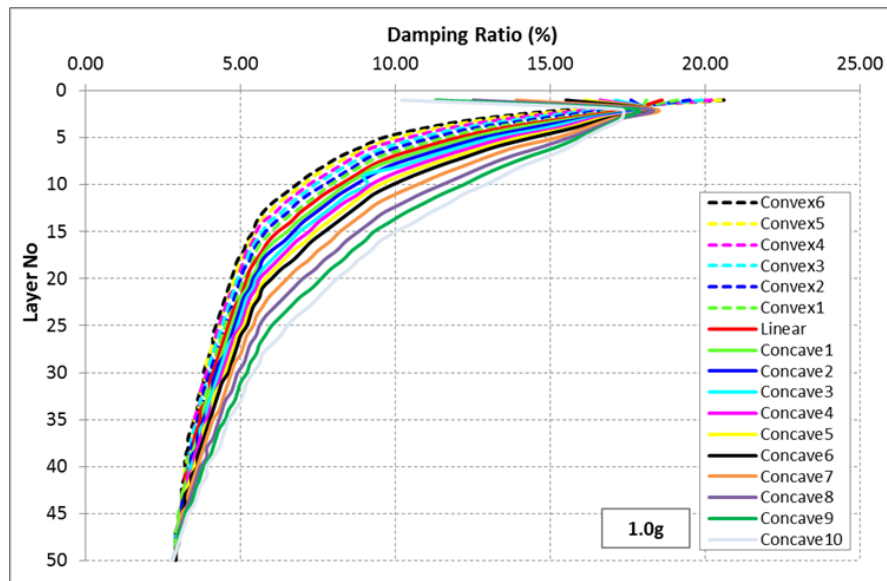


Figure 5.29. Damping ratios for each layer at 1.0g bedrock acceleration level.

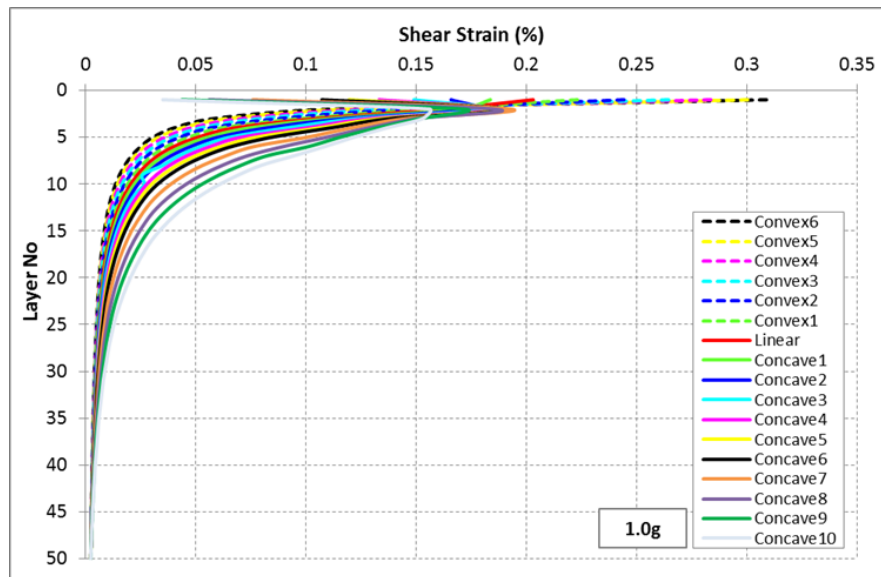


Figure 5.30. Shear strains for each layer at 1.0g bedrock acceleration level.

Due to low stiffness properties in linear and concave profiles, the G/G_{\max} rates are lower (i.e., stiffness degradation is high), damping ratios and shear strains are higher than those for the convex profiles. However, G/G_{\max} rate, damping ratio and shear strain on the top layer of velocity profiles present different characteristics from the other layers. G/G_{\max} rates are higher, damping ratios and shear strains are lower at the top layer of concave profiles compared to the ones at the top layer of convex profiles by the effect of impedance

ratio between layers (Figure 5.25 to 5.30). The impedance ratio (i.e., the ratio of the upper to lower layer since the wave propagation is from bedrock to surface) is increasing from bedrock to top layer for Concave-10, and decreasing from bedrock to top layer for the other profiles (Table 5.6). Besides, the sharp transition between the V_s of top layers for convex profiles causes to low impedance ratio (i.e., high contrast) while the smooth transition between the V_s of top layers for concave profiles presents high impedance ratio.

We have tested the effect of stiffness and impedance ratio on the soil amplification factor and the shear strain by using equal shear wave velocities (i.e., 50 m/sec) for the top two layers of velocity profiles, hence damping ratio and G/G_{\max} on the top layer decreased and increased, respectively. Also, the shear strains on the top layer and soil amplification factors were less than before for all profiles. We observed that the effect of impedance ratio between the top layers was more prevalent for convex profiles because the transition between the top layers was sharper for them. We can say that the sudden decrease of V_s , hence shear modulus, at the top layer causes stiffness degradation and increase in shear strains, especially for convex profiles. High impedance ratio near the surface for concave profiles may be the reason for higher G/G_{\max} and lower shear strain for the top layer.

Table 5.6. V_s and α_z for Concave-10, Linear and Convex-6 profiles.

Layer No	Concave-10		Linear		Convex-6	
	V_s (m/sec)	Impedance Ratio, α_z	V_s (m/sec)	Impedance Ratio, α_z	V_s (m/sec)	Impedance Ratio, α_z
1	50.0	0.9447	50.0	0.721	50.0	0.3441
2	52.9	0.9446	69.4	0.782	145.3	0.7244
3	56.0	0.9444	88.8	0.821	200.6	0.8217
4	59.3	0.9443	108.2	0.848	244.1	0.8679
5	62.8	0.9441	127.6	0.868	281.3	0.8950
6	66.5	0.9440	146.9	0.883	314.3	0.9129
7	70.5	0.9438	166.3	0.896	344.2	0.9256
8	74.7	0.9436	185.7	0.905	371.9	0.9350
9	79.2	0.9435	205.1	0.914	397.8	0.9423
10	83.9	0.9433	224.5	0.921	422.1	0.9482
.....						
48	876.8	0.9365	961.2	0.980	978.9	0.9893
49	936.3	0.9363	980.6	0.981	989.5	0.9895
50	1000.0	0.5000	1000.0	0.500	1000.0	0.5000
Bedrock	2000.0	-	2000.0	-	2000.0	-

Figure 5.31 presents the variation of surface PGAs with gradually increasing bedrock PGAs. As the nonlinearity increases due to higher bedrock accelerations, the surface PGAs become lower than the bedrock PGAs due to stiffness degradation. We see higher surface PGAs for the stiffer velocity profiles, when compared to the softer profiles, due to low impedance ratios near the surface and due to low damping ratios.

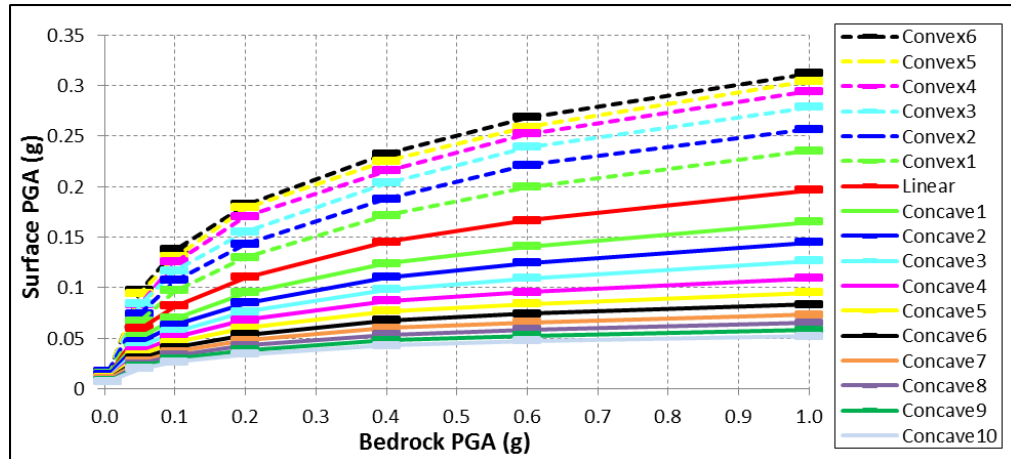


Figure 5.31. Surface PGAs with respect to gradually increasing bedrock PGAs.

The variation of PGAs with depth is presented in Figure 5.32-5.35 for gradually increasing bedrock impulse levels. At 0.005g bedrock accelerations, the surface PGAs were amplified for all profiles. As the bedrock PGA increased to 0.05g, the surface PGAs were amplified for Concave-1 up to Convex-6 and de-amplified for Concave-2 up to Concave-10. The surface PGAs were de-amplified for the rest of the bedrock acceleration levels, since the damping ratio increased for all profiles.

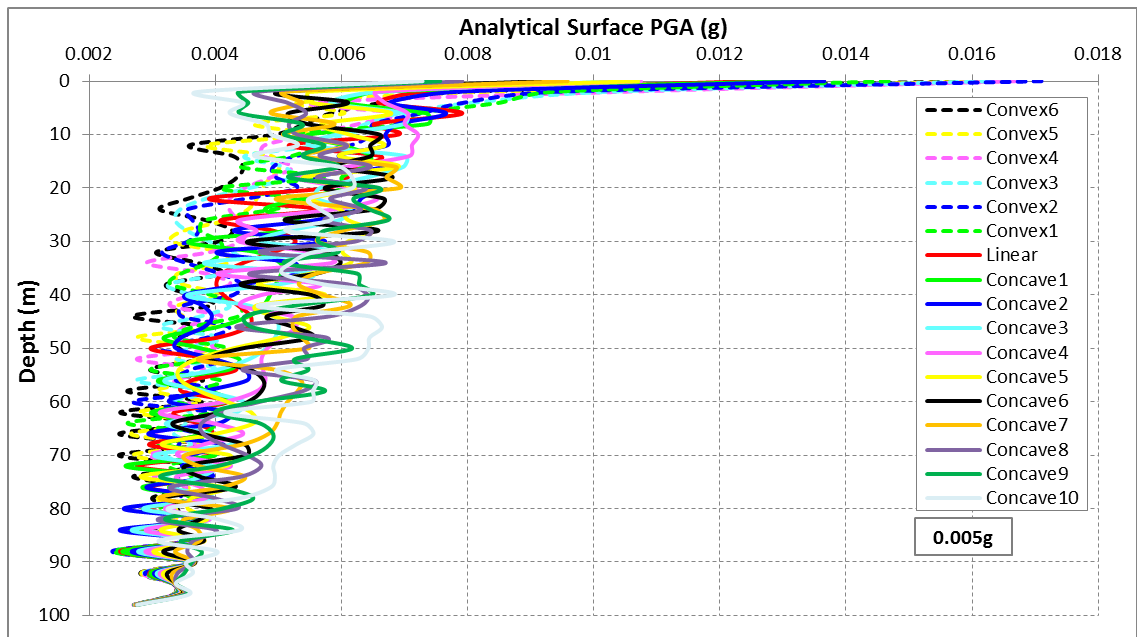


Figure 5.32. PGAs along the velocity profiles for 0.005g bedrock acceleration level.

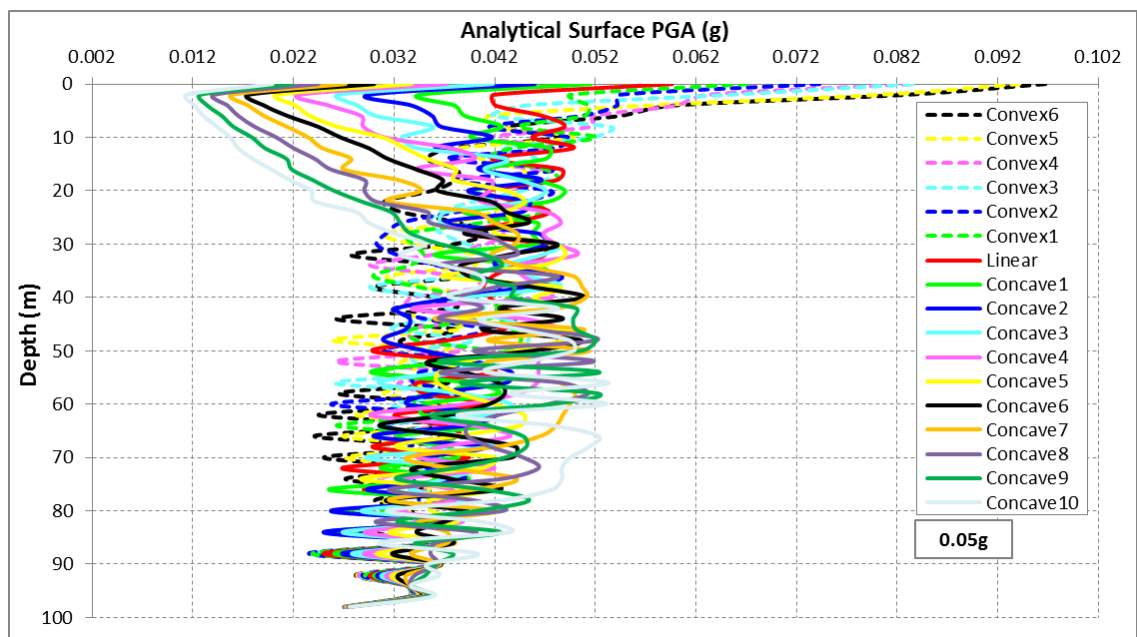


Figure 5.33. PGAs along the velocity profiles for 0.05g bedrock acceleration level.

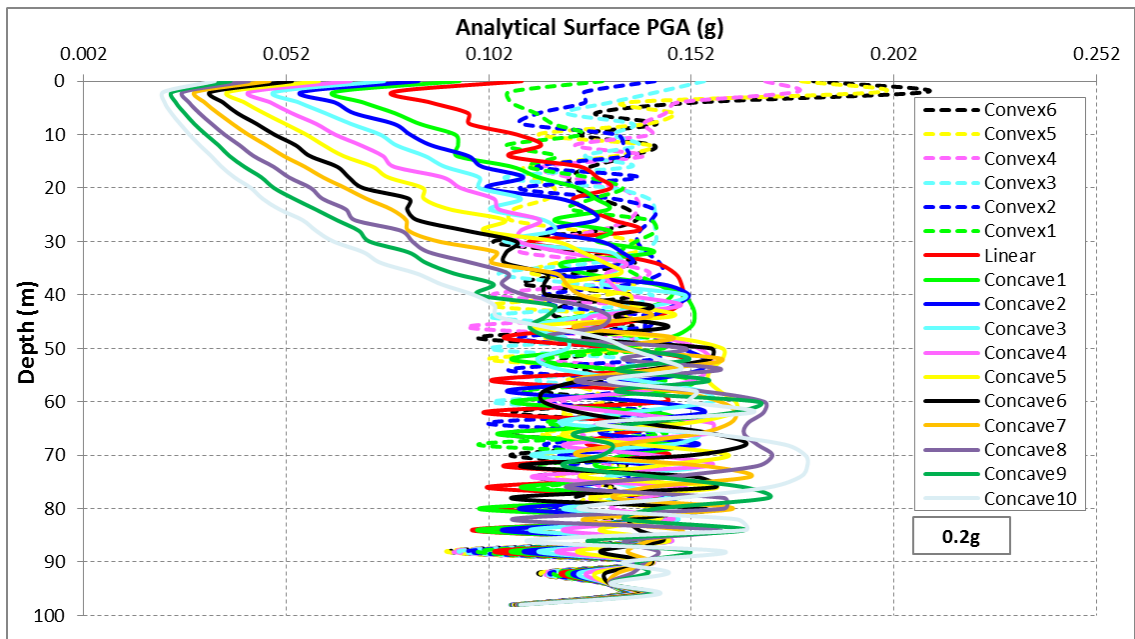


Figure 5.34. PGAs along the velocity profiles for 0.2g bedrock acceleration level.

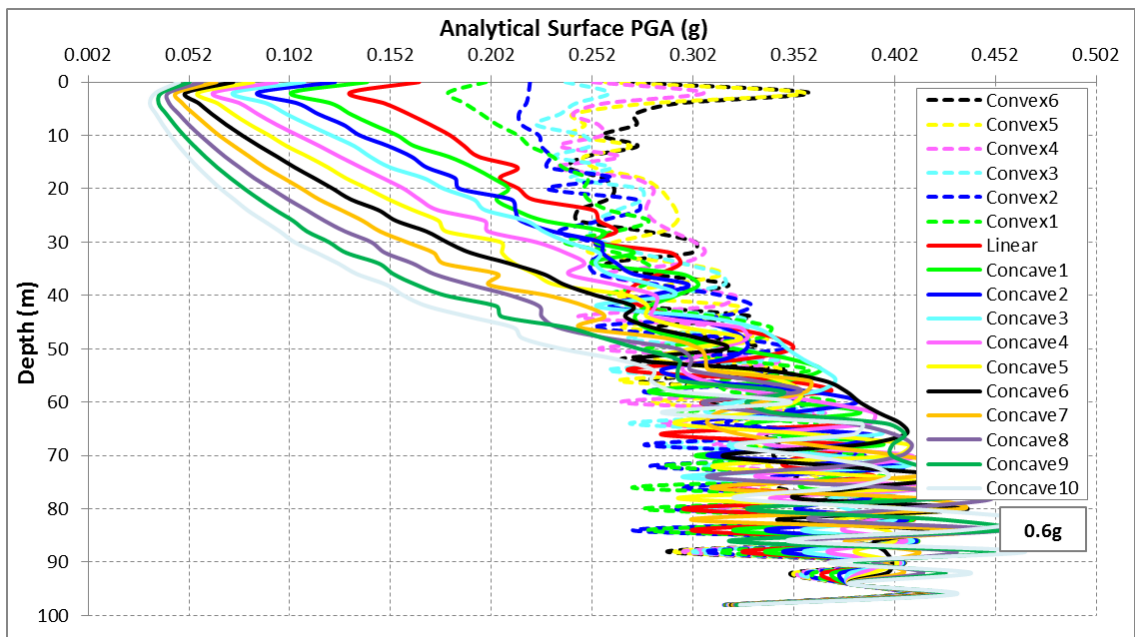


Figure 5.35. PGAs along the velocity profiles for 0.6g bedrock acceleration level.

We have studied the bedrock-to-surface transfer functions for gradually increasing bedrock acceleration levels in order to obtain soil amplification factors and fundamental frequencies. We computed the transfer functions as the surface-to-bedrock ratio of the Fourier Amplitude Spectra (FAS) of accelerations. In Figures 5.36 to 5.42, the variation of

transfer functions are shown for increasing bedrock acceleration levels from 0.005g to 1.0g. The maximum values of the FAS ratios (i.e., the soil amplification factor; y axis) are marked by red dots on the figures.

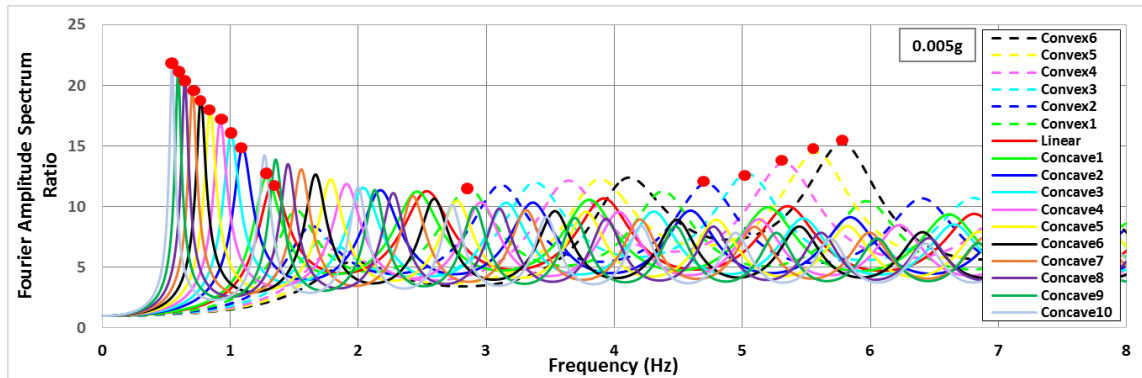


Figure 5.36. Transfer functions at 0.005g impulsive acceleration level.

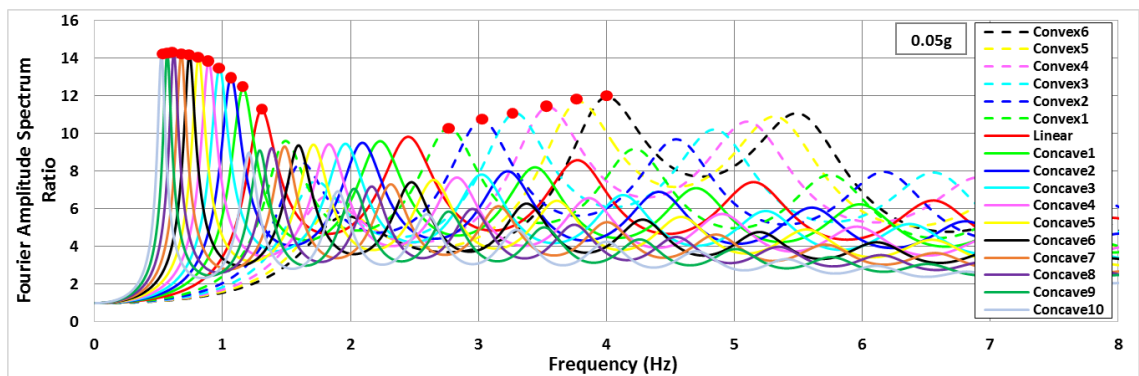


Figure 5.37. Transfer functions at 0.05g impulsive acceleration level.

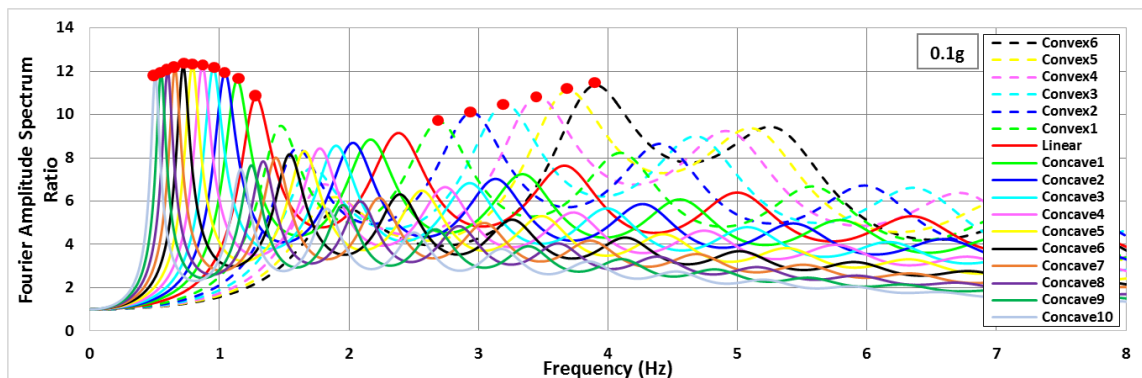


Figure 5.38. Transfer functions at 0.1g impulsive acceleration level.

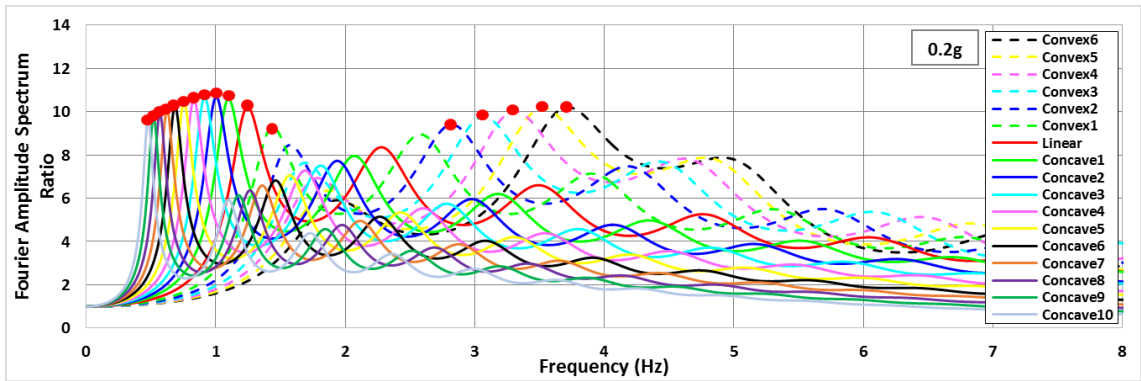


Figure 5.39. Transfer functions at 0.2g impulsive acceleration level.

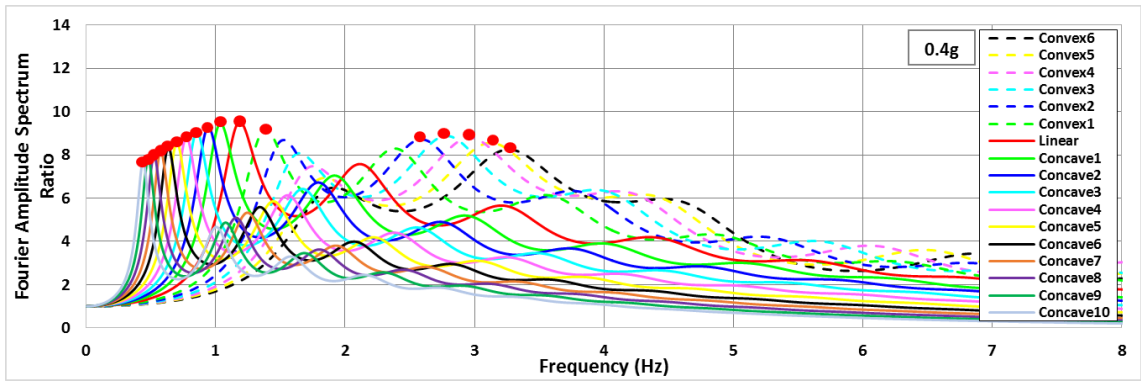


Figure 5.40. Transfer functions at 0.4g impulsive acceleration level.

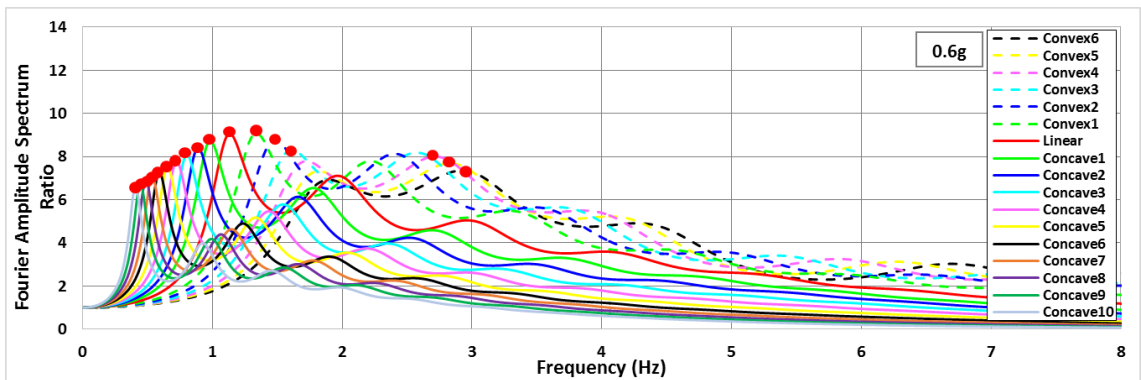


Figure 5.41. Transfer functions at 0.6g impulsive acceleration level.

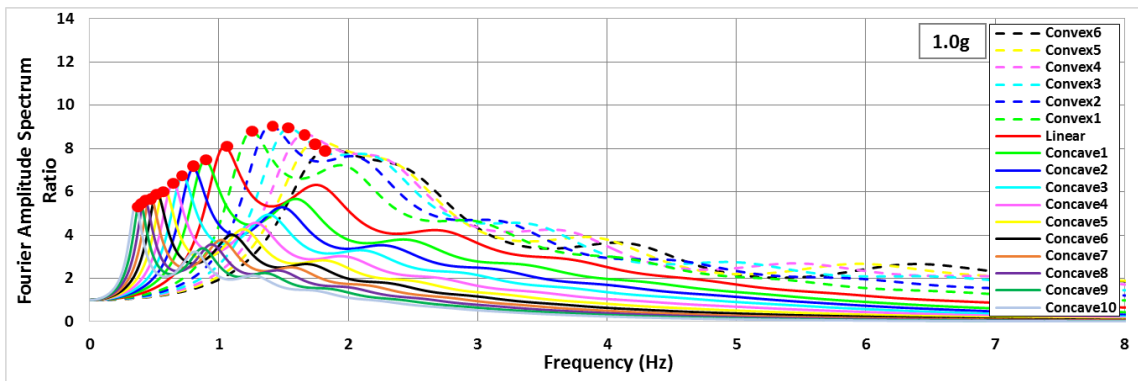


Figure 5.42. Transfer functions at 1.0g impulsive acceleration level.

The soil amplification factors and corresponding fundamental frequencies of each profile are shown in Figure 5.43 for gradually increasing bedrock acceleration levels.

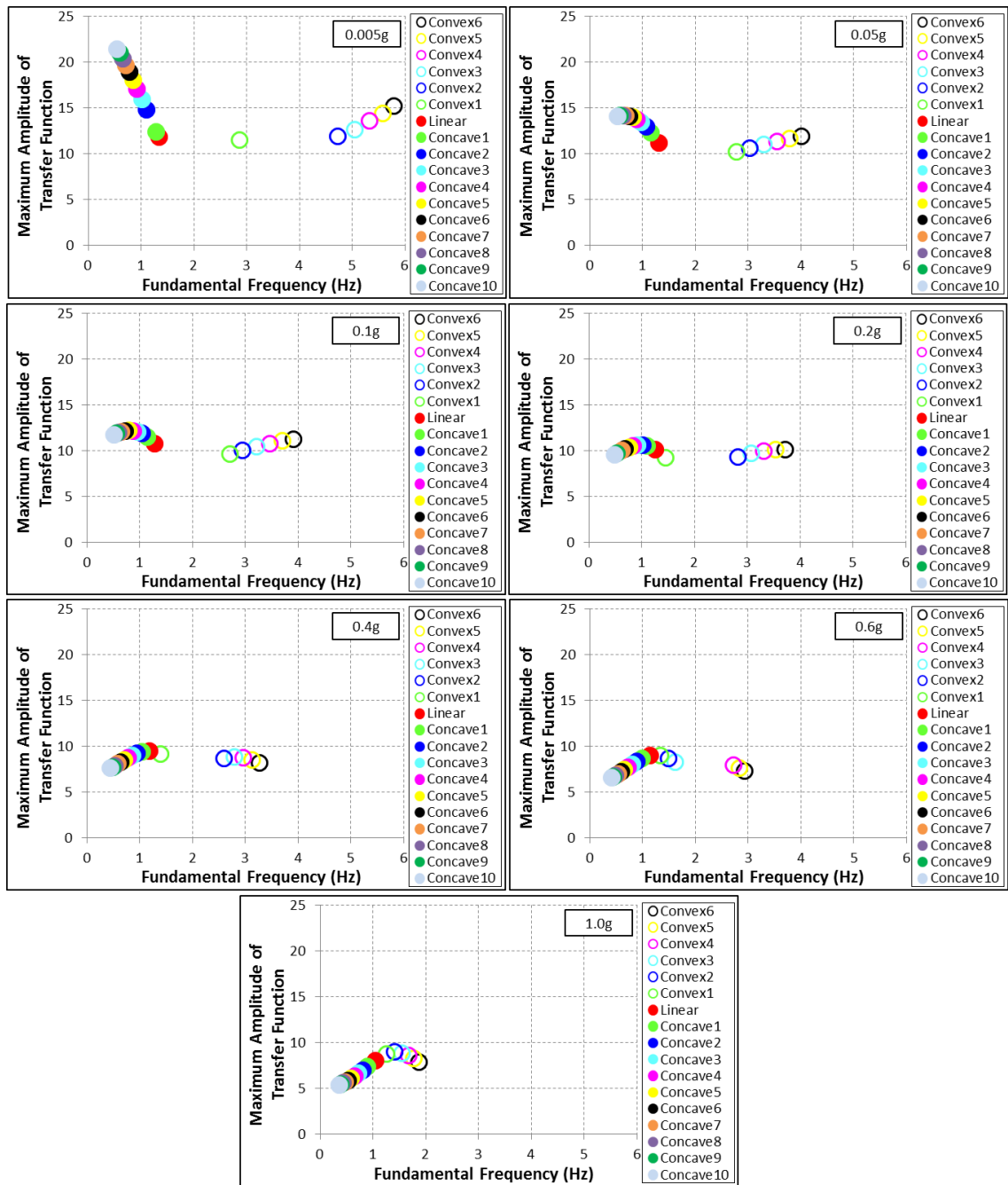


Figure 5.43. Maximum amplitude of transfer functions and corresponding fundamental frequencies for impulsive bedrock accelerations.

The following observations can be made from the figures of transfer functions:

1. The transfer functions at 0.005g impulse level were the same as those for linear analysis (Figure 5.36). The shear strains were in linear elastic range ($0.001\% <$), hence the stiffness of profiles did not change ($G/G_{\max} > 0.96$). The stiffness

degradations and the damping ratios were higher for softer profiles, except for the top layer, when compared to the stiffer profiles due to low shear resistance. Due to lower stiffness and decreasing impedance ratio towards the bedrock, the soil amplification factor was the highest for Concave-10. The impedance contrast between shallower layers was higher for convex profiles. The damping ratio was lower for Convex-6 than Convex-1; hence soil amplification factor was higher for Convex-6 than Convex-1.

2. At 0.05g impulse level, the soil amplification decreased due to increasing modulus reduction and damping ratio for all profiles (Figure 5.37). Especially, the decreasing linear trend from Concave-10 to Concave-1 was softened by the effect of increased damping ratio. The Concave-10 profile reached to high strain levels more rapidly than Concave-1 due to its lower shear resistance. The soil amplification factors for convex profiles showed a linear increasing trend from Convex-1 to Convex-6.
3. At 0.1g impulse level, the decreasing trend of soil amplification factors from Concave-10 to Concave-1 changed its direction due to increasing damping ratio, particularly for the softer profiles (Figure 5.38). The fundamental frequencies were shifted to first order peaks for convex profiles because of the decreasing stiffness.
4. At 0.2g impulse level, the soil amplification factors were lower for Concave-10 and higher for Concave-1, since the damping ratio was higher for the softer profiles (Figure 5.39).
5. We have observed the stiffness degradation for convex profiles for the 0.4g bedrock acceleration level (Figure 5.40). The fundamental frequency was shifted to the first order peak for Convex-1, and the soil amplification factors started to decrease from Convex-1 to Convex-6. The stiffness degradation, hence the damping ratio for the top layer of Convex-6, was higher than Convex-1 since the shear stresses and strains transferred to the top layer were higher for Convex-6.

6. At 0.6g bedrock acceleration level, the fundamental frequencies were shifted to the first order peaks for the remaining soil profiles as well (Figure 5.41). As the shear stresses increased for 1.0g bedrock acceleration, the shear strains reached to elasto-plastic range and the softer profiles presented lower soil amplification factors than the stiffer profiles (Figure 5.42).
7. Due to lower soil stiffness, the fundamental frequencies of concave type profiles were observed less than the fundamental frequencies of convex profiles and as the nonlinearity increased, the f_0 decreased for all profiles due to the fact that $V_s \propto \sqrt{G_{sec}/\rho}$ (Figure 5.43). Especially, high order f_0 peaks (2nd and 3rd) of convex profiles decreased more than the first order f_0 peaks of concave ones and they were shifted to the first order by gradually increasing bedrock accelerations. Because high frequency spectral amplitudes of convex profiles were damped by increased stiffness degradation at the top layers due to high amplitude shear stress transfer from bedrock.
8. We have detected that the fast transition from high impedance ratio to low impedance ratio (i.e., high impedance contrast) at thin layers (i.e., 2 m here) near surface caused to high order f_0 peaks in convex profiles.
9. The soil amplifications decreased for all profiles by the effect of stiffness degradation as the bedrock acceleration level increased. At perfectly linear elastic strain range, the softer velocity profiles presented higher soil amplifications than stiffer velocity profiles, and vice versa at perfectly elasto-plastic strain range. We observed a sharp difference between soil amplification behavior for the convex and linear/concave profiles.

5.2.1.1. Site Amplification Characterization by Surface PGA. We have investigated the soil amplification in terms of the surface PGAs and the bedrock PGAs. In order to study the effects of increasing nonlinearity, the surface PGAs were divided by the bedrock PGAs, as shown in Figure 5.44. The boundary between soil amplification and de-amplification was shown in the figure by the grey dashed line. At bedrock acceleration

levels higher than 0.2g, all profiles showed nonlinear behavior. The surface PGAs were found to be higher for convex types due to low impedance ratio between top layers, although the stiffness of layers was high.

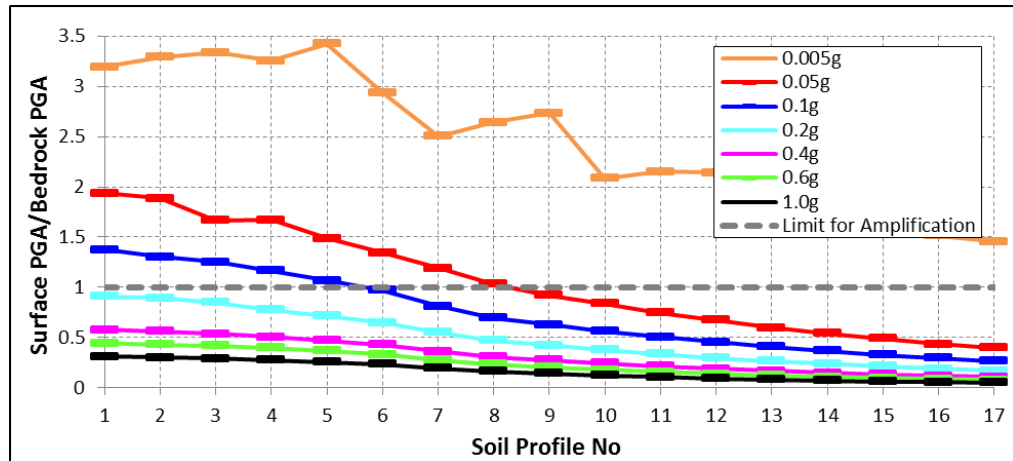


Figure 5.44. Amplification and de-amplification of surface PGAs for each profile.

Figure 5.45 shows the correlations between soil amplification factors and surface PGAs for increasing bedrock accelerations. Figure 5.46, the close up of Figure 5.45 for convex profiles (Profiles 1-6), presents that surface PGA can be taken as a characterizing parameter for soil amplification at bedrock acceleration levels $\geq 0.05g$ (i.e., nonlinear elastic and elasto-plastic strain range). For concave and linear profiles, there is not a constant ratio between the amplification factor and the surface PGA.

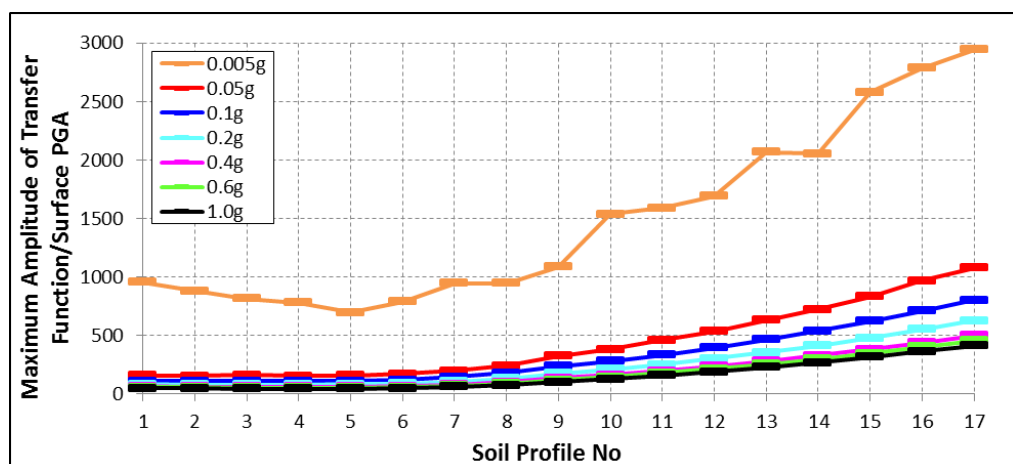


Figure 5.45. The correlation of soil amplification factors with surface PGAs with respect to velocity profiles.

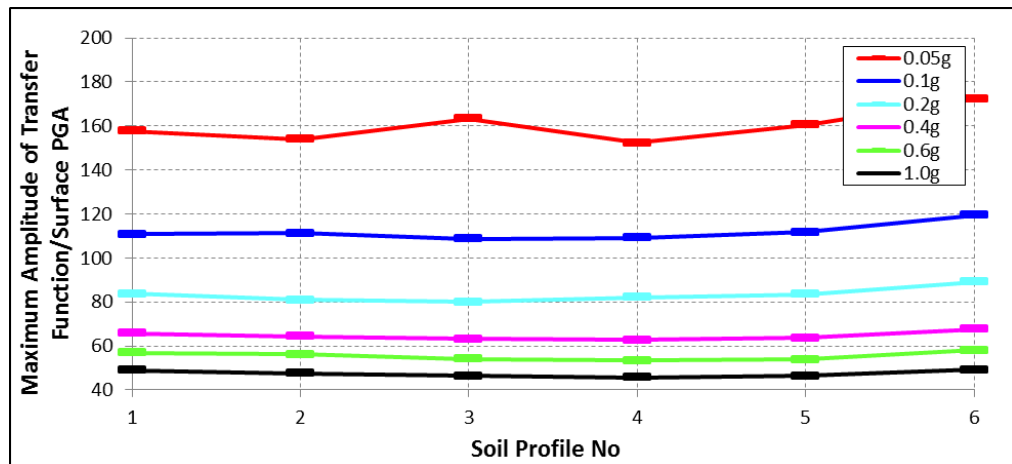


Figure 5.46. The correlation of soil amplification factors with surface PGAs with respect to convex profiles.

5.2.1.2. Site Amplification Characterization by Fundamental Soil Frequency, f_0 The variation of fundamental soil frequencies with increasing bedrock acceleration levels, and with profile numbers, are presented respectively in Figure 5.47 and Figure 5.48. We have observed a linear relation for fundamental frequency of linear/concave profiles at all bedrock acceleration levels. The fundamental frequencies of concave profiles were observed at the first peak of transfer functions and the fundamental frequencies for convex profiles were observed at the second and third peaks, and all decreased due to stiffness degradation as the bedrock accelerations increased.

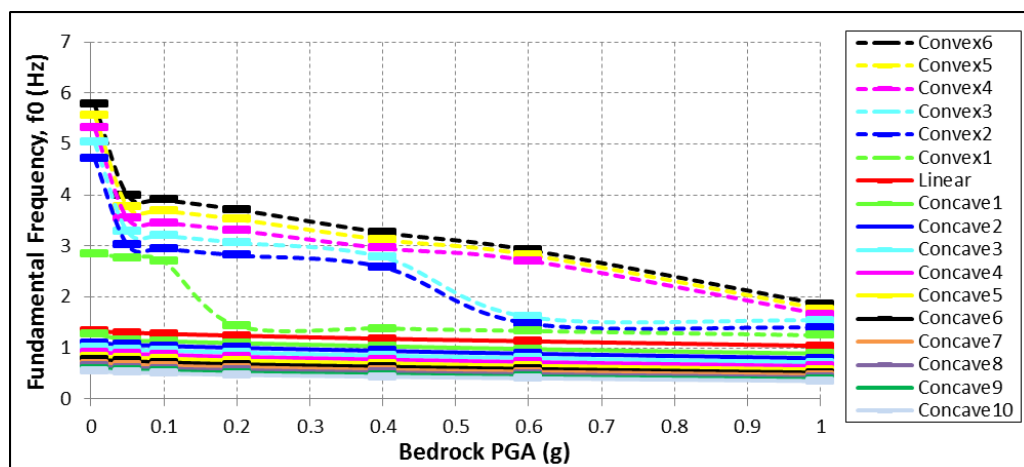


Figure 5.47. Fundamental frequencies with respect to bedrock PGAs for each profile.

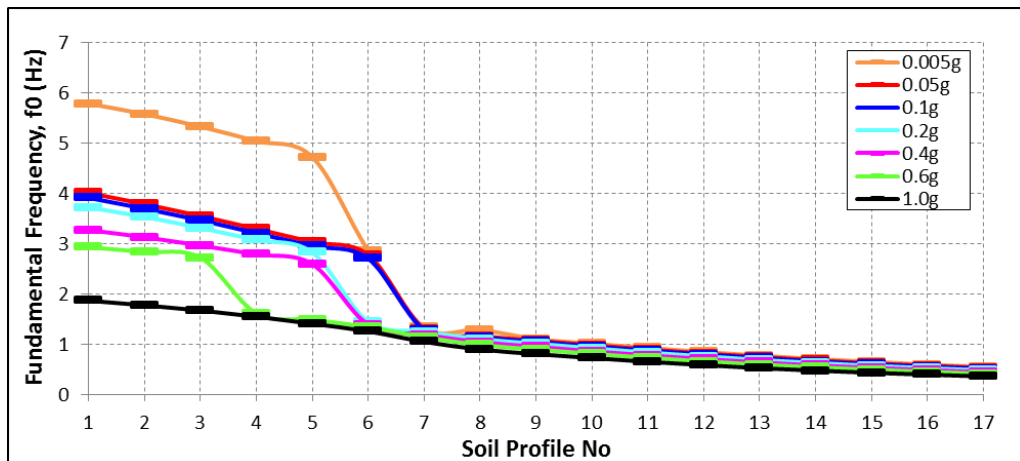


Figure 5.48. Fundamental frequencies with respect to profile numbers.

We have detected the reason of the high order f_0 peaks for convex profiles as the sharp transition of high impedance ratio to low impedance ratio at consecutive layers.

We have investigated the correlation between the ratio (soil amplification / fundamental frequency) with profile numbers (Figure 5.49). A constant ratio was observed between these parameters at linear elastic and nonlinear elastic strain range triggered by the acceleration levels below 0.4g for convex profiles. So, fundamental frequency can be used as a site amplification characterizing parameter for convex profiles at $\text{Acc.} \leq 0.4g$.

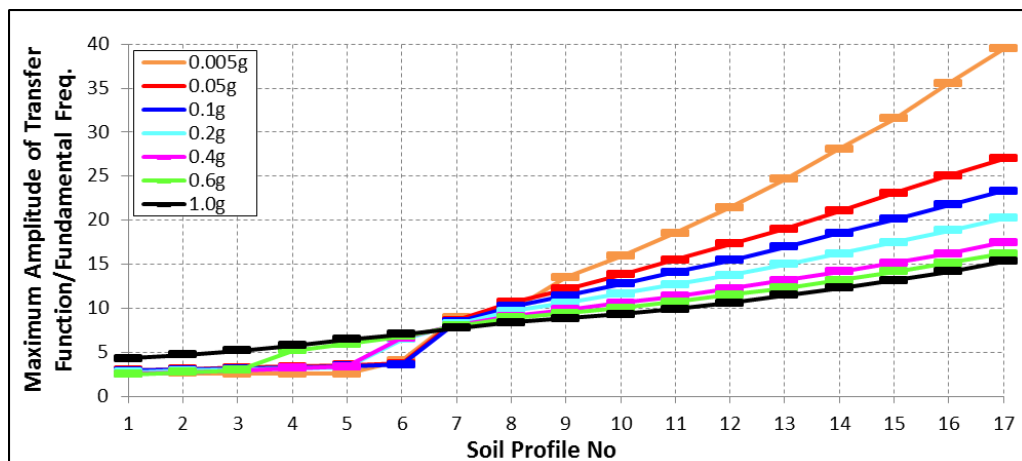


Figure 5.49. The correlation of soil amplification factor with f_0 with respect to profile number.

5.2.1.3. Site Amplification Characterization by V_{sz} . We have investigated the correlation of soil amplification factors (i.e., AF, maximum amplitudes of transfer functions) with time averaged shear wave velocities at various depths, V_{sz} , by checking if AF/V_{sz} ratios are close to a constant. The best performing averaging depths for site amplification characterization were defined by the AE (Absolute Error) method (i.e., the measure of scattering from a horizontal straight line) for gradually increasing bedrock acceleration levels. AF/V_{sz} ratios were presented for gradually increasing impulsive bedrock accelerations in Figure 5.50-5.56. At 0.005g, 0.05g and 0.1g bedrock acceleration levels, all AF/V_{sz} ratios showed nearly constant lines for convex profiles, while there was not any correlation for linear and concave profiles (Figure 5.50-5.53).

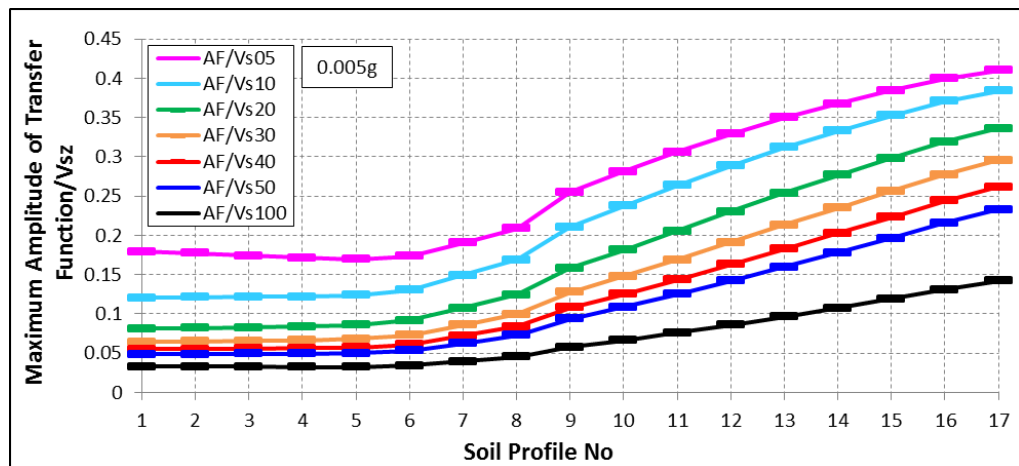


Figure 5.50. The correlation of AF with V_{sz} for 0.005g impulsive bedrock acceleration.

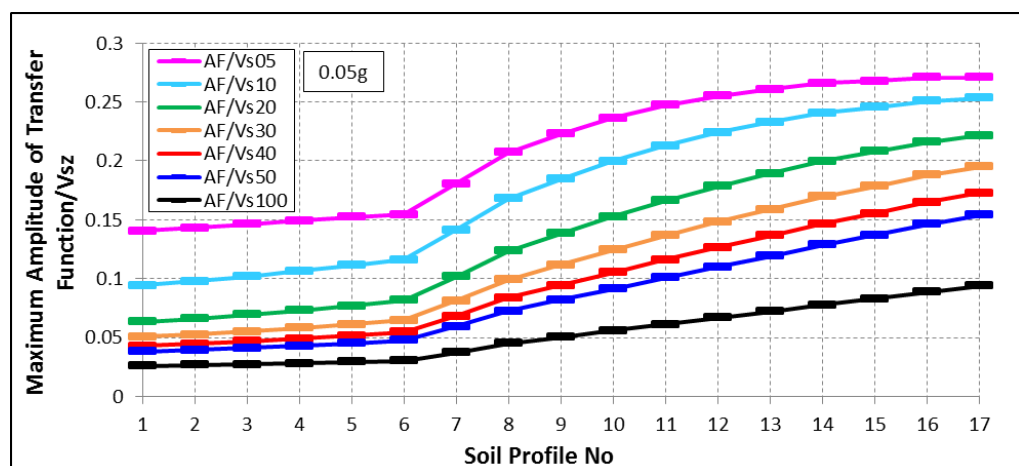


Figure 5.51. The correlation of AF with V_{sz} for 0.05g impulsive bedrock acceleration.

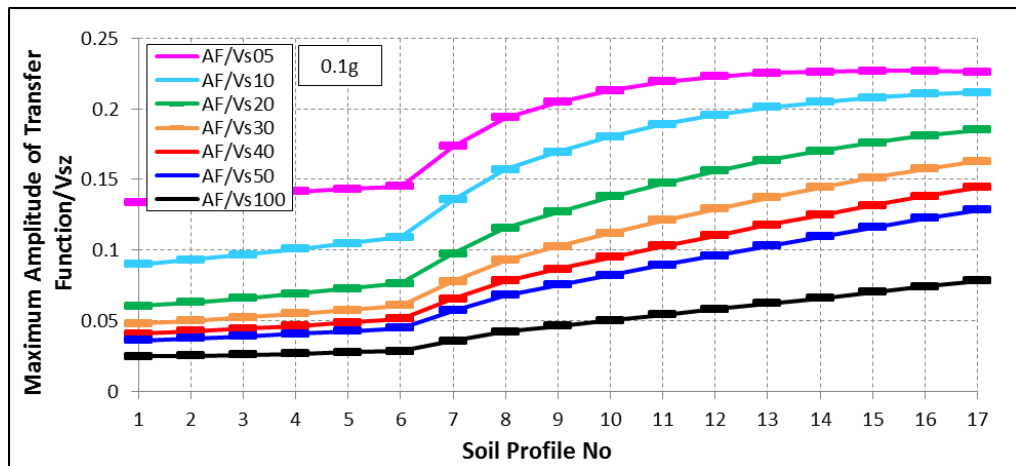


Figure 5.52. The correlation of AF with V_{sz} for 0.1g impulsive bedrock acceleration.

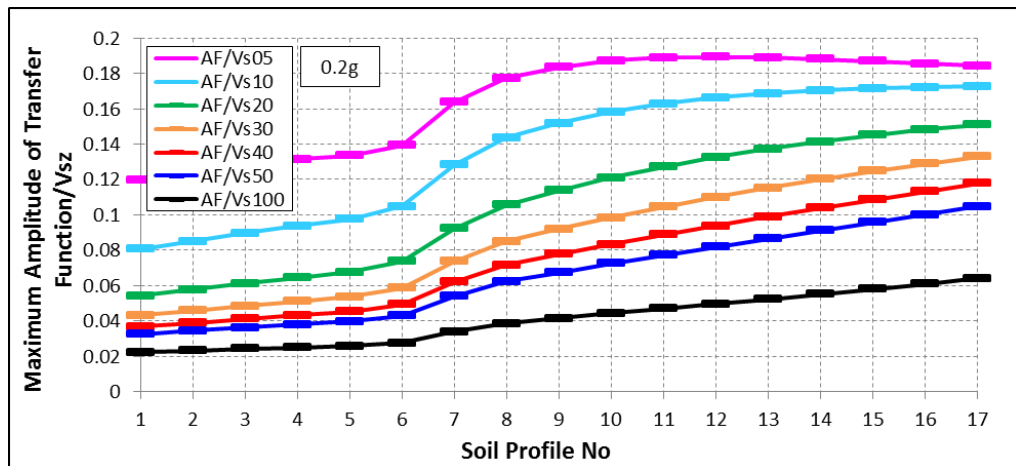


Figure 5.53. The correlation of AF with V_{sz} for 0.2g impulsive bedrock acceleration.

As the nonlinearity increased by 0.2g, 0.4g, 0.6g and then 1.0g bedrock accelerations, the constant ratio between AF and V_{sz} for convex profiles deteriorated especially for the shallow averaging depths, while V_{sz} presented a better performance of site amplification characterization for linear and concave profiles (Figure 5.54 to 5.56).

The AE performance levels (i.e., scattering level from a horizontal straight line) with respect to increasing bedrock PGAs are shown for convex and linear/concave profiles in Figure 5.57 and Figure 5.58, respectively. For convex profiles, the AE levels were lower at 0.005g, 0.05g, 0.1g and 0.2g acceleration levels than those for acceleration level $>0.2g$, which show a good performance of soil amplification characterization at linear elastic and nonlinear elastic strain range.

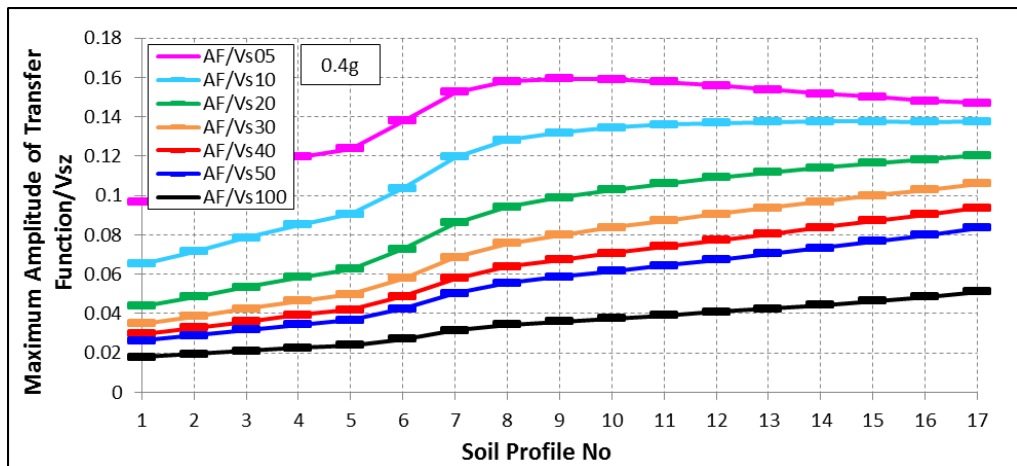


Figure 5.54. The correlation of AF with V_{sz} for 0.4g impulsive bedrock acceleration.

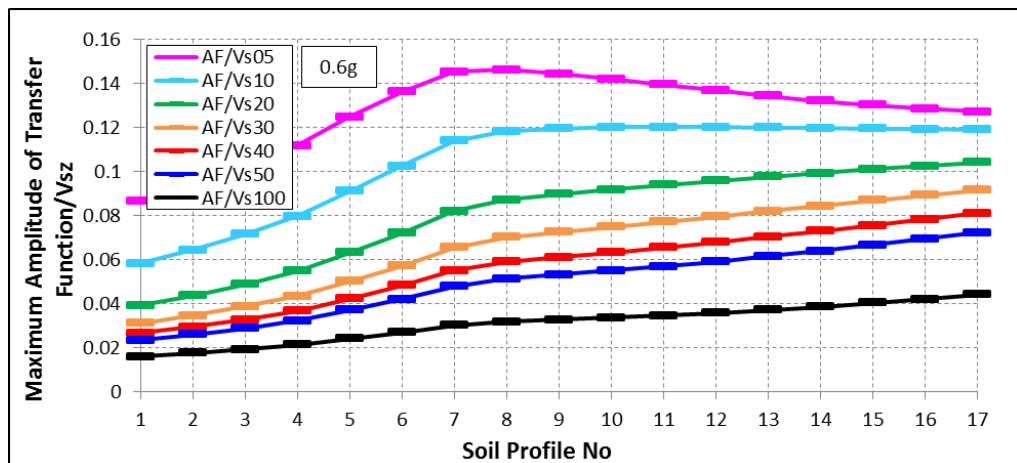


Figure 5.55. The correlation of AF with V_{sz} for 0.6g impulsive bedrock acceleration.

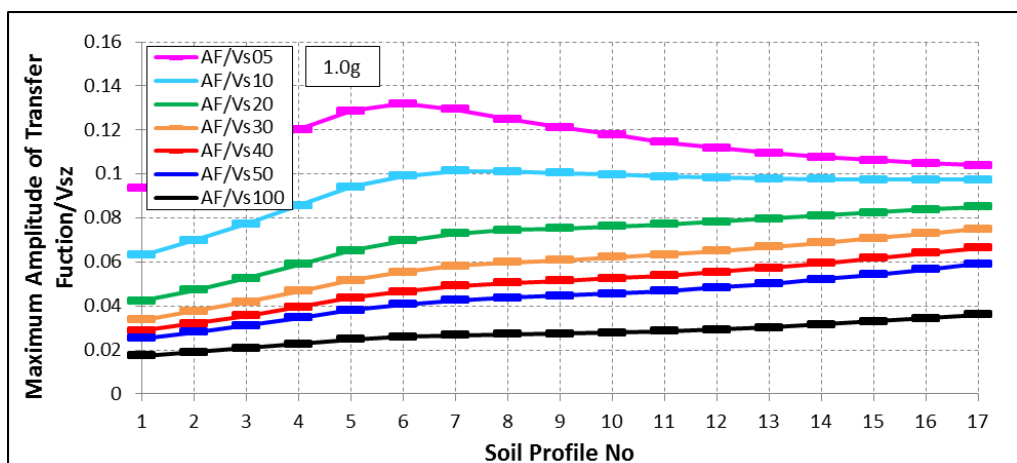


Figure 5.56. The correlation of AF with V_{sz} for 1.0g impulsive bedrock acceleration.

The best performing averaging depths were presented for each convex profile in Figure 5.57. V_{s100} had the best performance for all convex profiles at bedrock accelerations $>0.005g$. At $0.005g$ acceleration level, V_{s100} , V_{s100} , V_{s05} , V_{s100} , V_{s50} and V_{s100} had the best performance for profiles no 1, 2, 3, 4, 5 and 6, respectively. Though we haven't observed any constant relation for AF/V_{sz} at $Acc. >0.2g$, the AE levels are smaller at profiles no 3 and 4 compared to other profiles since their AF/V_{sz} values are close to the mean of data set (i.e., horizontal straight line). So the best performing parameter should be defined by considering both AF/V_{sz} and AE graphs.

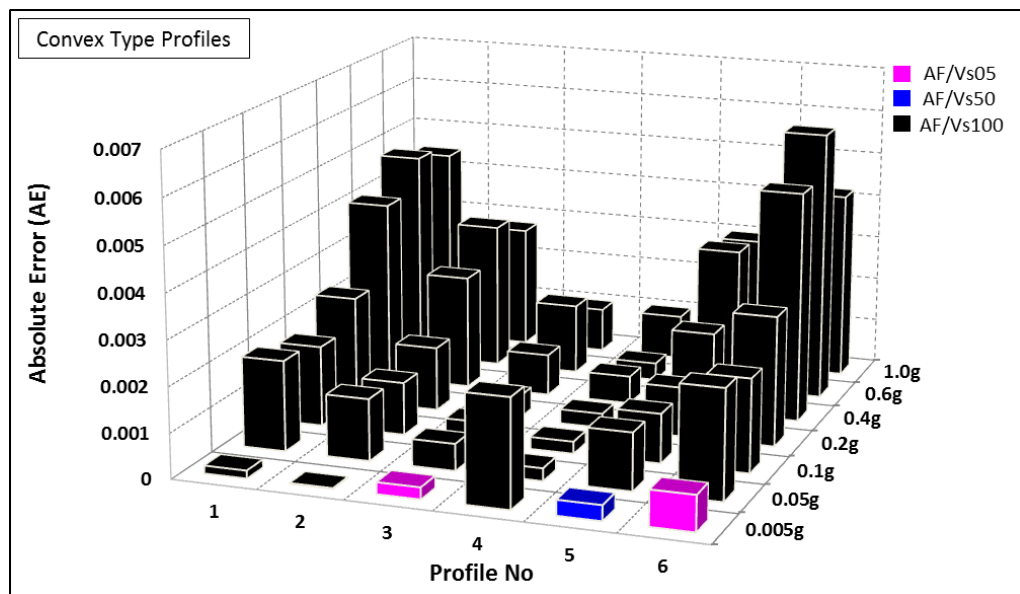


Figure 5.57. The variation of AE for AF/V_{sz} with increasing impulsive bedrock accelerations for convex profiles.

Linear and concave profiles presented lower AE at $0.2g$, $0.4g$, $0.6g$ and $1.0g$ bedrock accelerations leading to a good V_{sz} performance for soil amplification characterization at nonlinear elastic and elasto-plastic strain ranges (Figure 5.58). At $0.2g$ bedrock acceleration, the best performing parameters were defined as V_{s05} for profiles no 7, 8, 9, 10, 15, 16; V_{s100} for no 11, 12, 17; V_{s20} for no 13 and V_{s10} for no 14. At $0.4g$, the best performing parameters were defined as V_{s10} for profiles no 7, 8, 9, 14, 15; V_{s05} for 10, 11, 16, 17; V_{s50} for no 12 and V_{s20} for no 13. At $0.6g$, the best performing parameters were defined as V_{s10} for no 7, 8, 9, 10, 14, 15, 16, 17; V_{s100} for no 11; V_{s05} for no 12 and V_{s20} for no 13. At $1.0g$, the best performing parameters were defined as V_{s10} for profiles no 7, 8, 9, 10, 13, 14, 15, 16, 17; V_{s100} for no 11 and V_{s20} for no 12.

The optimal parameter was V_{s100} for convex profiles for $\text{Acc.} \leq 0.2g$, and V_{s10} and V_{s05} for linear/concave profiles for $\text{Acc.} \geq 0.2g$.

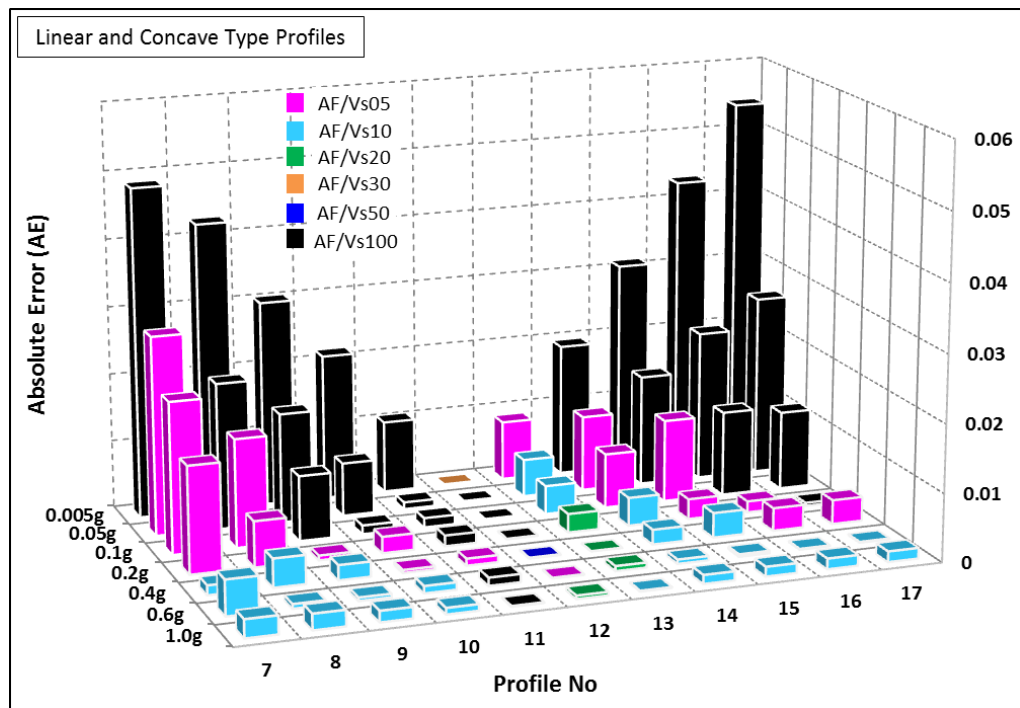


Figure 5.58. The variation of AE for AF/V_{sz} with increasing impulsive bedrock accelerations for linear/concave profiles.

5.2.1.4. Site Amplification Characterization by T_{tz} . As alternative to V_{sz} , we have also investigated the wave travel times for various depths, T_{tz} , as a parameter to characterize soil amplification. The correlation of soil amplification parameter T_{tz} is studied for gradually increasing bedrock acceleration levels and quantified in terms of AE. At bedrock acceleration level 0.005g, linear and concave profiles give a very good correlation for depths $z \geq 20$ m, while convex profiles presents a linear relation (i.e., a poor correlation according to AE method, scattering from a horizontal straight line), (Figure 5.59). As the bedrock acceleration level increased to 0.05g, 0.1g, 0.2g and 0.4g, the correlations for all profiles became closer to a linear straight line (i.e., not a constant line), (Figure 5.60 to 5.63). Also there is a very distinct transion point between convex and concave profiles. This is true for all bedrock input levels. As the bedrock acceleration level increases, the transion from convex to concave becomes softer. At 0.6g and 1.0g, constant relations were observed just for convex profiles (Figure 5.64 and 5.65). The variation of AE showing the

best performing T_{tz} parameters for AF characterization is presented in Figure 5.66 and 5.67 for convex and linear/concave profiles, respectively.

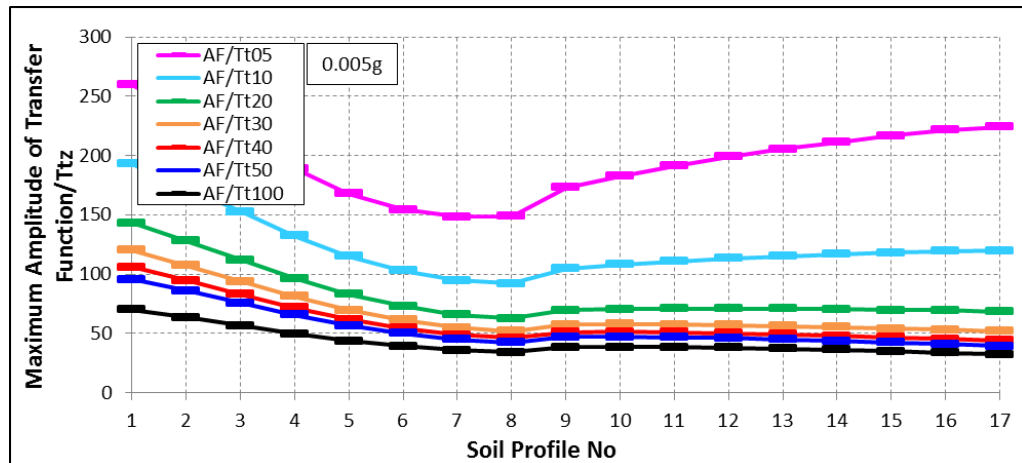


Figure 5.59. The correlation of AF with T_{tz} for 0.005g impulsive bedrock acceleration.

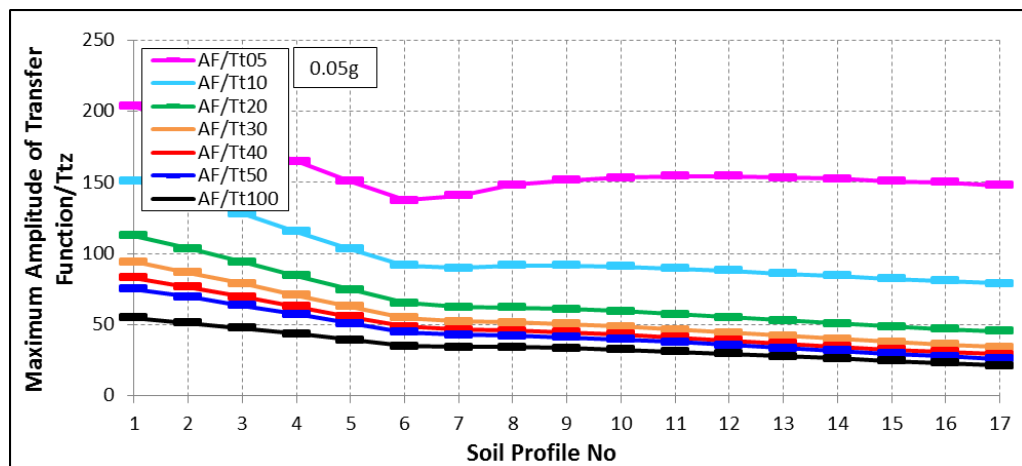


Figure 5.60. The correlation of AF with T_{tz} for 0.05g impulsive bedrock acceleration.

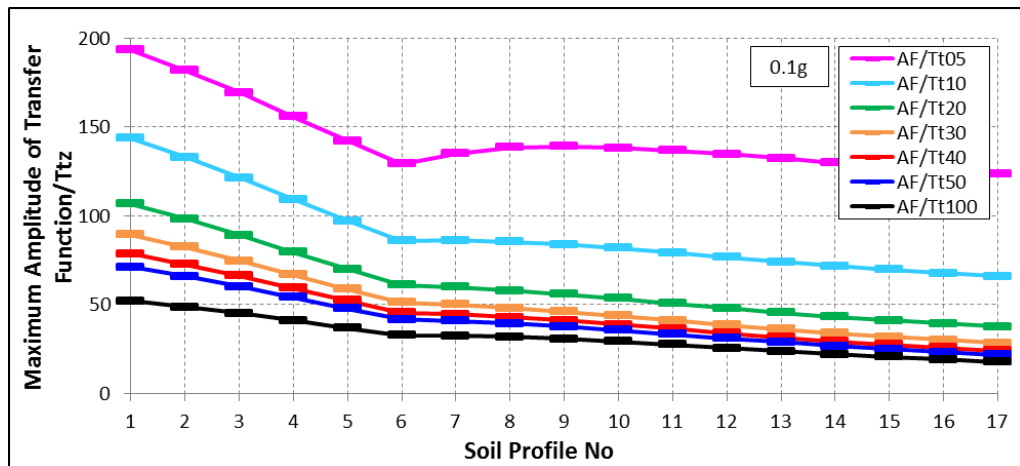


Figure 5.61. The correlation of AF with T_{tz} for 0.1g impulsive bedrock acceleration.

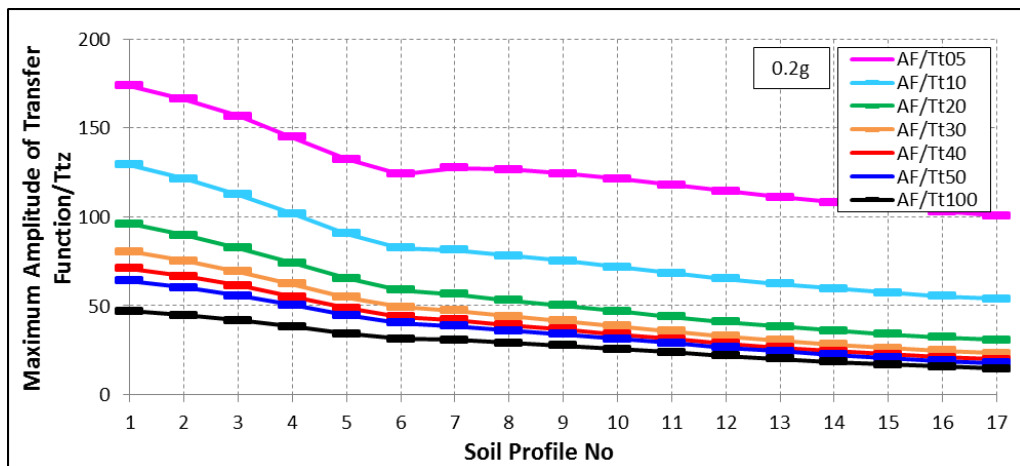


Figure 5.62. The correlation of AF with T_{tz} for 0.2g impulsive bedrock acceleration.

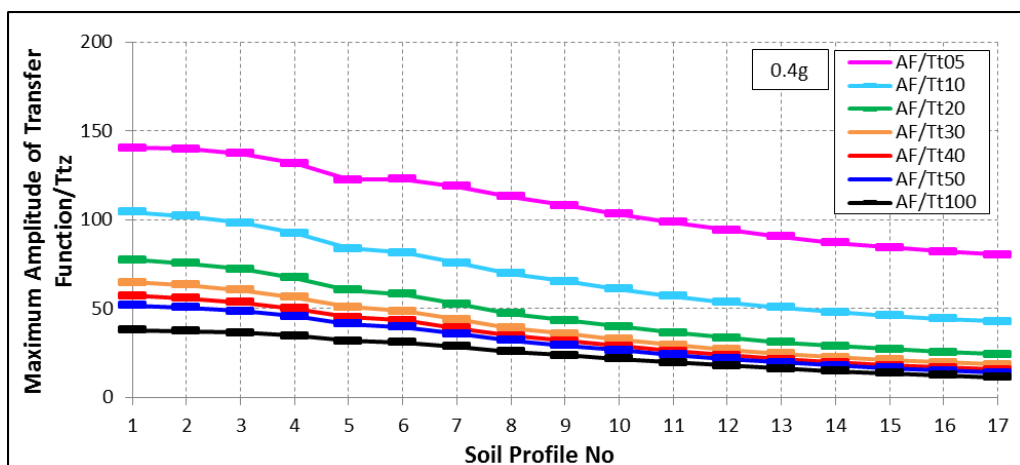


Figure 5.63. The correlation of AF with T_{tz} for 0.4g impulsive bedrock acceleration.

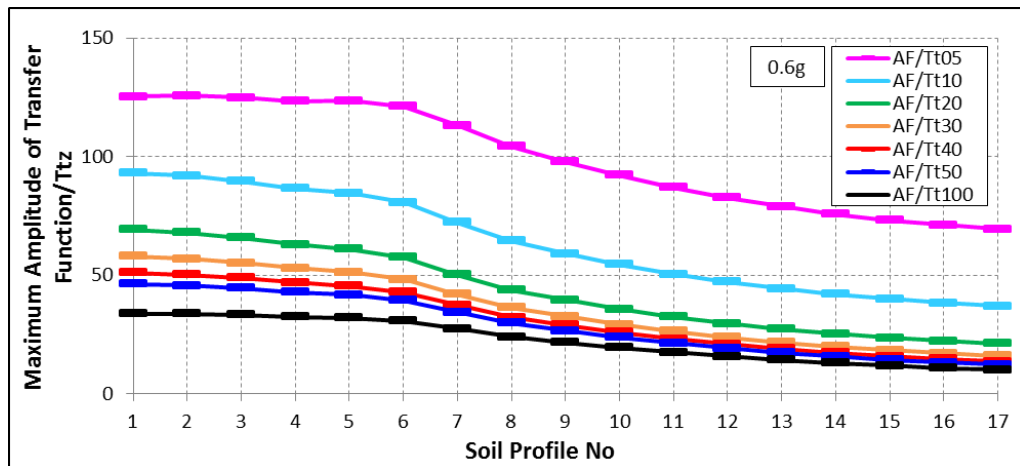


Figure 5.64. The correlation of AF with T_{tz} for 0.6g impulsive bedrock acceleration.

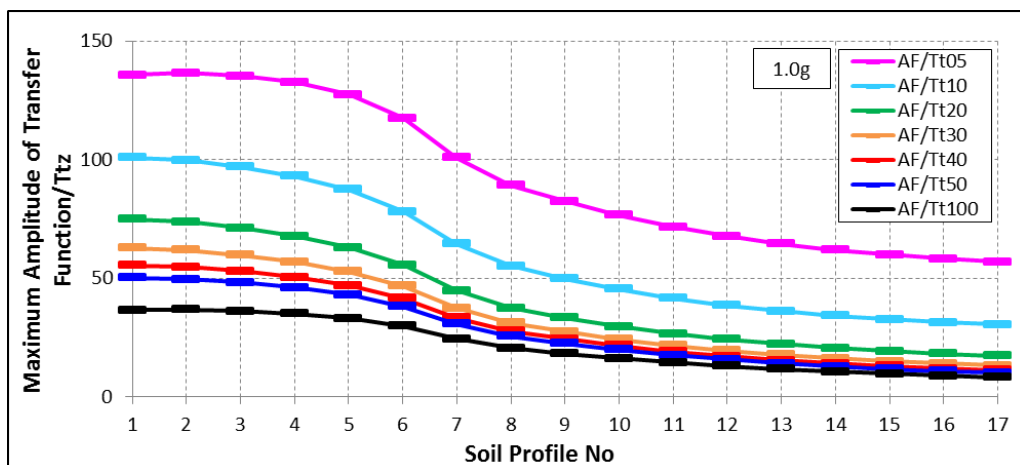


Figure 5.65. The correlation of AF with T_{tz} for 1.0g impulsive bedrock acceleration.

The AE levels were lower at 0.4g, 0.6g and 1.0g bedrock acceleration levels for convex profiles since AF/T_{tz} presented a more constant relation compared to smaller accelerations, pointing out a better performance at nonlinear elastic and elasto-plastic strain rates. T_{t100} had the best performance for all convex profiles at 0.4g; for no 1, 2, 3, 4, 6 at 0.6g; and for 1, 2, 3, 5, 6 at 1.0g. T_{t05} performed well for profile no 5 at 0.6g, and T_{t20} performed well for profile no 4 at 1.0g.

Linear and concave profiles presented a good correlation of AF and T_{tz} just at 0.005g and 0.05g bedrock acceleration levels pointing out linear elastic and nonlinear elastic strain ranges. At 0.005g acceleration level, the best performing parameters were defined as T_{t30}

for no 7; T_{t50} for no 8 and 13; T_{t20} for no 9, 10, 15, 16, 17; T_{t10} for no 11, and T_{t100} for no 12 and 14. At 0.05g acceleration level, the best performing parameters were defined as T_{t10} for no 7 and 13; T_{t05} for no 8, 9, 10, 14, 15, 16, 17; T_{t100} for no 11, and T_{t30} for no 12.

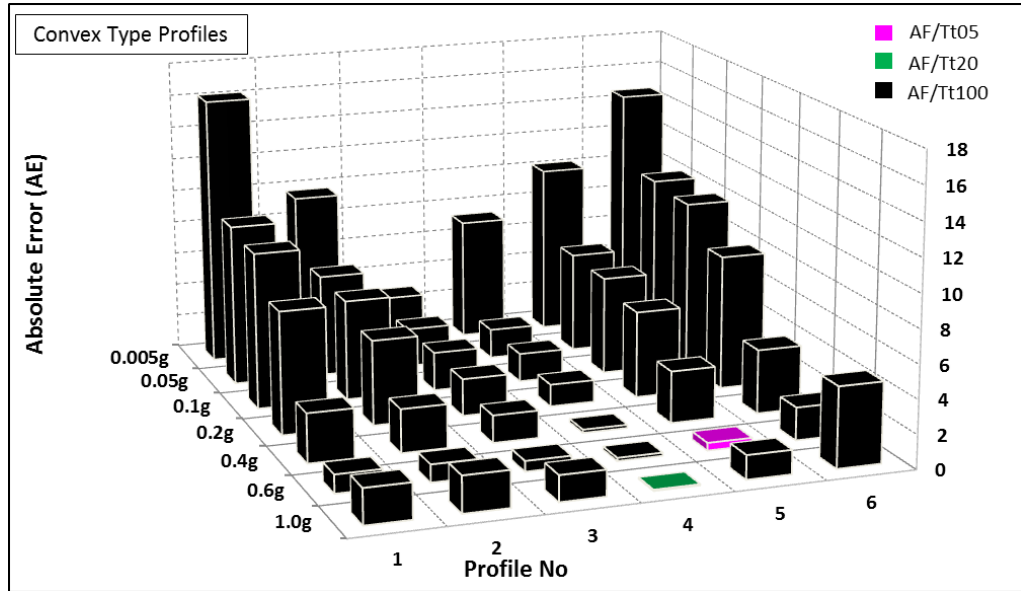


Figure 5.66. The variation of AE for AF/ T_{tz} with increasing impulsive bedrock accelerations for convex profiles.

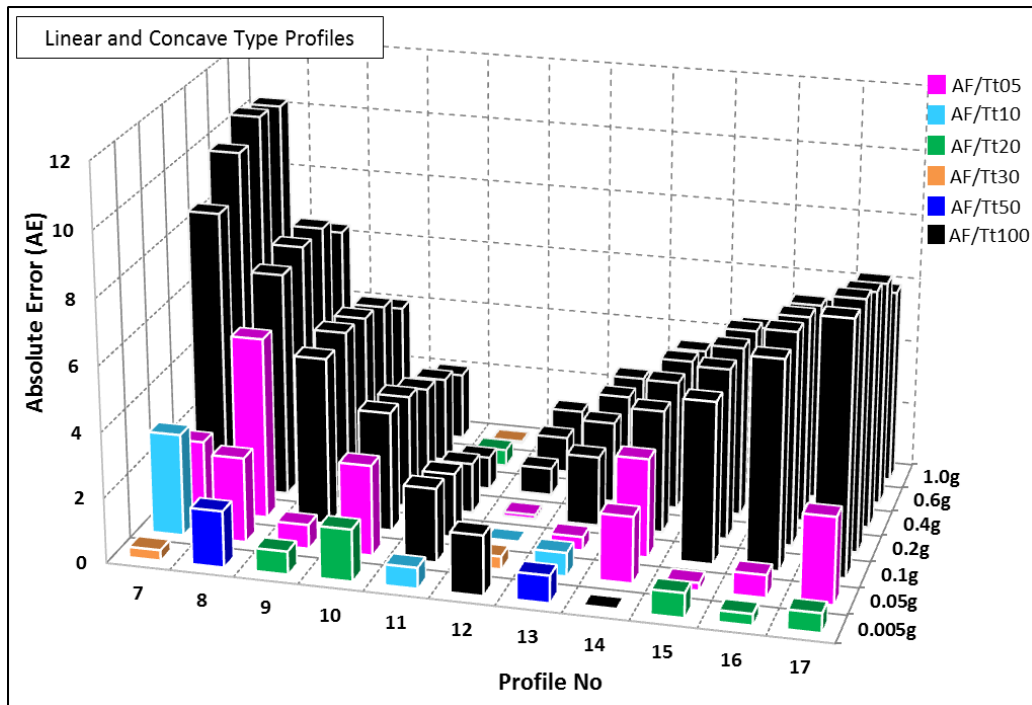


Figure 5.67. The variation of AE for AF/ T_{tz} with increasing impulsive bedrock accelerations for linear/concave profiles.

The optimal parameter for convex profiles was T_{t100} for $\text{Acc.} \geq 0.4g$, and T_{t20} for $0.005g$ and T_{t05} for $0.05g$ for linear/concave profiles.

5.2.1.5. Fundamental Frequency Characterization by V_{sz} . We have investigated the correlation of fundamental soil frequency with time averaged shear wave velocities at various depths (i.e., V_{s30} , V_{s40} , V_{s50} and V_{s100}) for gradually increasing bedrock accelerations. The fundamental soil frequencies were observed at the 1st peaks of transfer functions for linear/concave profiles at all bedrock accelerations, while they were observed at the 3rd, 2nd and 1st peaks as the bedrock accelerations increased for convex profiles (Table 5.7). By gradually increasing the bedrock acceleration level, the higher order peaks (e.g., 2nd and 3rd peaks) are damped and they are shifted towards the 1st peak. The order of peaks affected the correlations between f_0 and V_{sz} .

At $0.005g$ bedrock acceleration level, constant ratios were observed for profiles no 1 to 5 and no 7 to 17 since the f_0 was at 2nd peak for Convex-1, at 3rd peak for other convex profiles and at 1st peak for linear/concave profiles (Figure 5.68). At $0.05g$ and $0.1g$, f_0 was observed at 2nd peaks for all convex profiles, hence constant ratios were obtained for both convex and linear/concave profiles (Figure 5.69 and 5.70). At $0.2g$ and $0.4g$, the f_0 was at 1st peak for no 6 and at 2nd peak for the other convex profiles, hence a sharp change occurred at profile no 6 (Figure 5.71 and 5.72). At $0.6g$, the f_0 was at 1st peak for profiles no 4 to 17 and at 2nd peak for no 1 to 3 (Figure 5.73). As the peak bedrock acceleration reached to $1.0g$, all f_0 values were observed at the 1st peak, presenting constant ratios for convex profiles (Figure 5.74). The best performing parameters defined by AE method are given in Figure 5.75 and 5.76 for each profile type.

Table 5.7. The order of maximum peaks at transfer functions for f_0 .

Soil Profile No	Soil Type	0.005g	0.05g	0.1g	0.2g	0.4g	0.6g	1.0g
1	Convex-6	3 rd	2 nd	2 nd	2 nd	2 nd	2 nd	1 st
2	Convex-5	3 rd	2 nd	2 nd	2 nd	2 nd	2 nd	1 st
3	Convex-4	3 rd	2 nd	2 nd	2 nd	2 nd	2 nd	1 st
4	Convex-3	3 rd	2 nd	2 nd	2 nd	2 nd	1 st	1 st
5	Convex-2	3 rd	2 nd	2 nd	2 nd	2 nd	1 st	1 st
6	Convex-1	2 nd	2 nd	2 nd	1 st	1 st	1 st	1 st

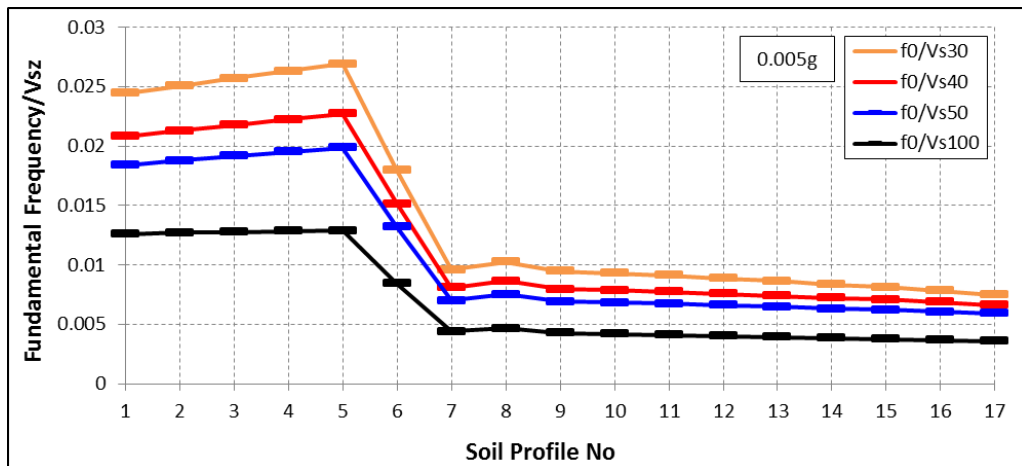


Figure 5.68. The correlation of f_0 with V_{sz} for 0.005g impulsive bedrock acceleration.

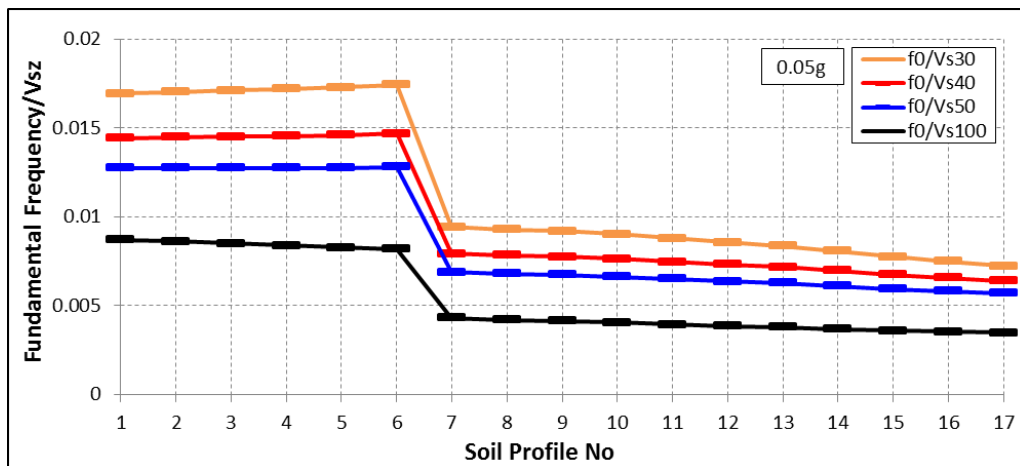


Figure 5.69. The correlation of f_0 with V_{sz} for 0.05g impulsive bedrock acceleration.

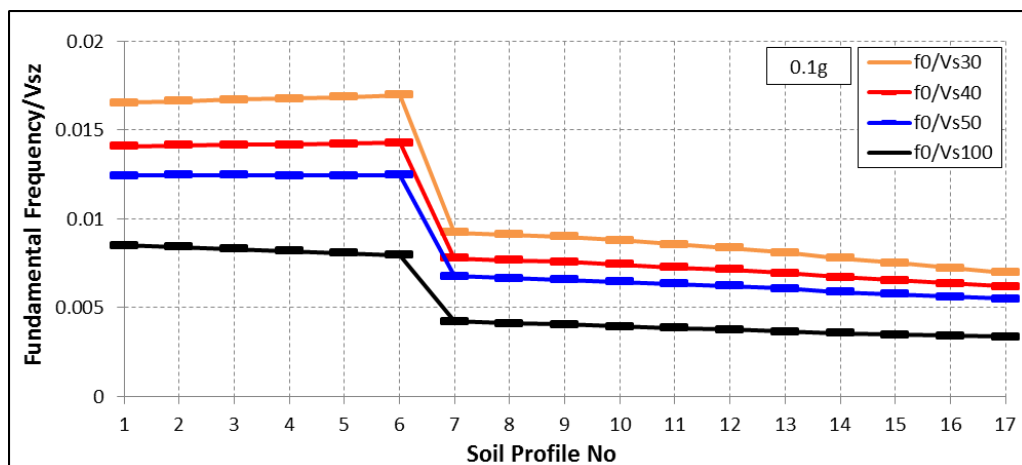


Figure 5.70. The correlation of f_0 with V_{sz} for 0.1g impulsive bedrock acceleration.

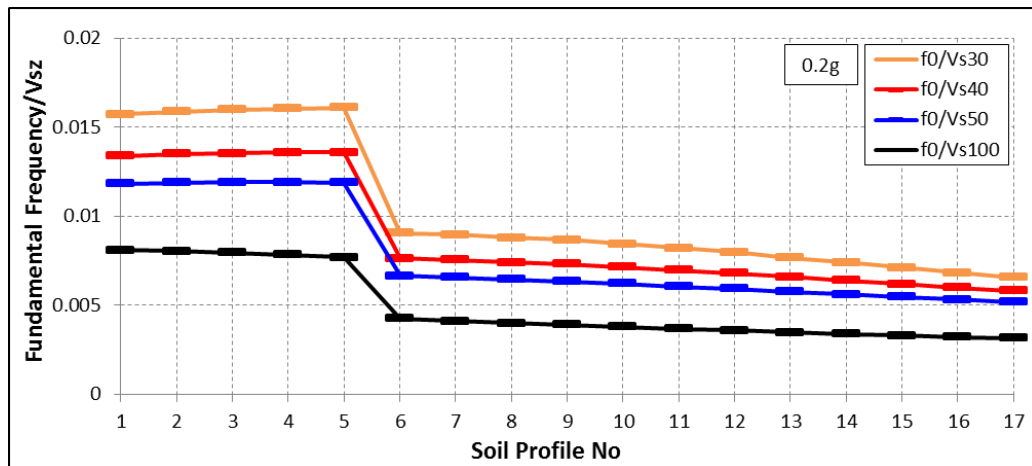


Figure 5.71. The correlation of f_0 with V_{sz} for 0.2g impulsive bedrock acceleration.

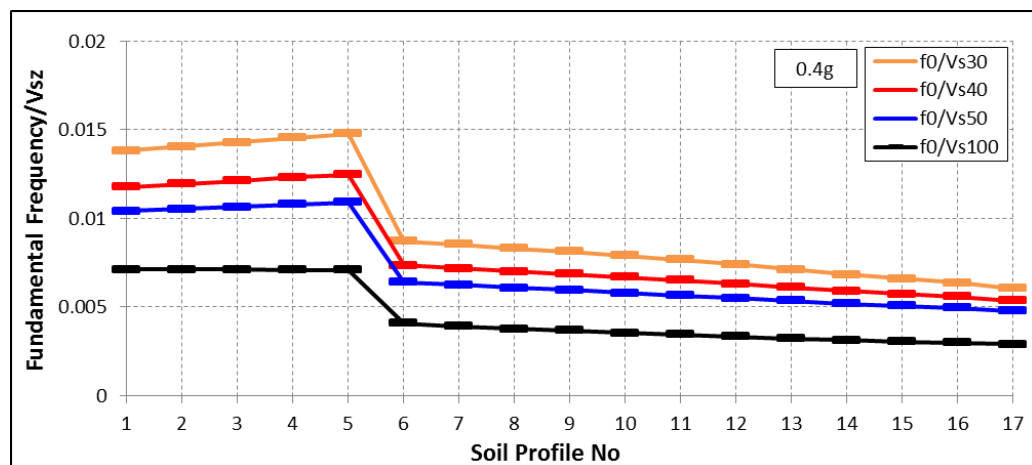


Figure 5.72. The correlation of f_0 with V_{sz} for 0.4g impulsive bedrock acceleration.

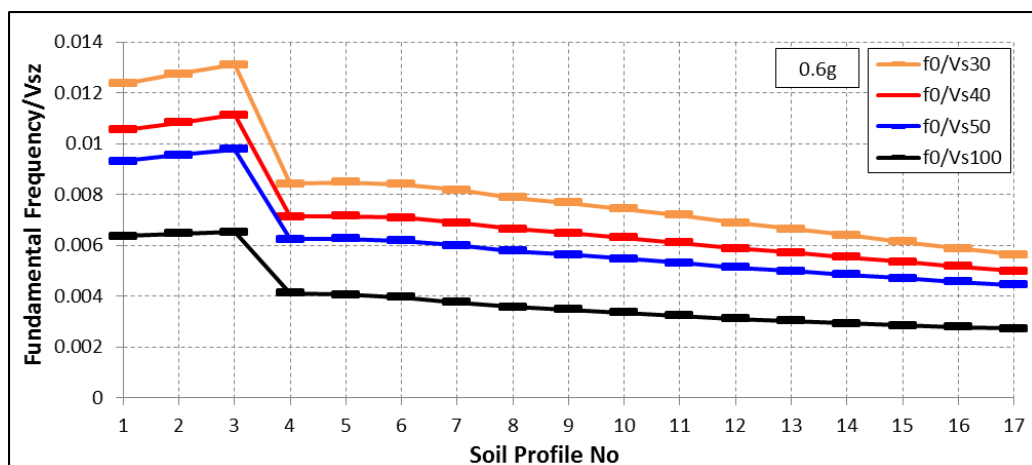


Figure 5.73. The correlation of f_0 with V_{sz} for 0.6g impulsive bedrock acceleration.

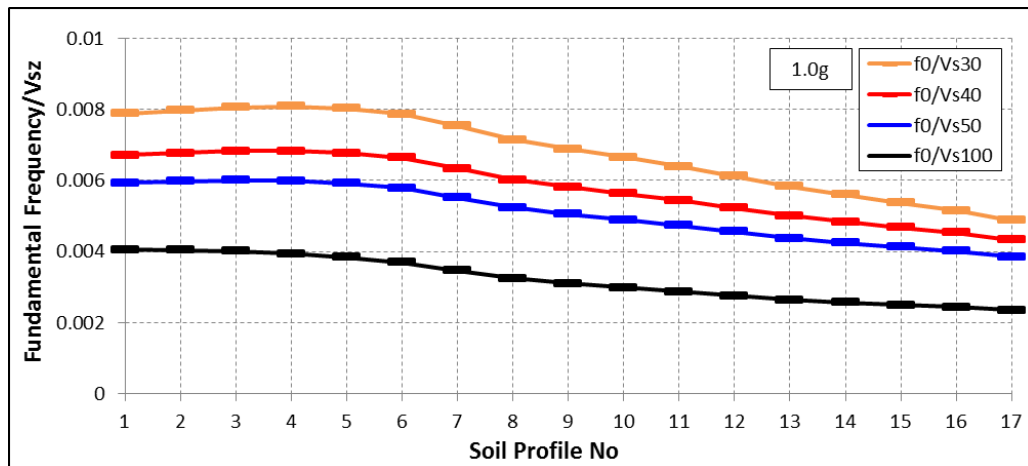


Figure 5.74. The correlation of f_0 with V_{sz} for 1.0g impulsive bedrock acceleration.

The smallest absolute errors were observed at 0.05g, 0.1g and 1.0g bedrock accelerations for convex profiles, where f_0 was at the same order peaks for all profiles (Figure 5.75). V_{s50} had the best performance for all profiles at 0.05g acceleration level, for profiles no 1, 2, 5, 6 at 0.1g and for profile no 1 at 1.0g. V_{s40} had the best performance for profiles no 3 and 4 at 0.1g, and for profiles no 3 and 5 at 1.0g. V_{s30} had the best performance for no 2 and 6 at 1.0g acceleration level.

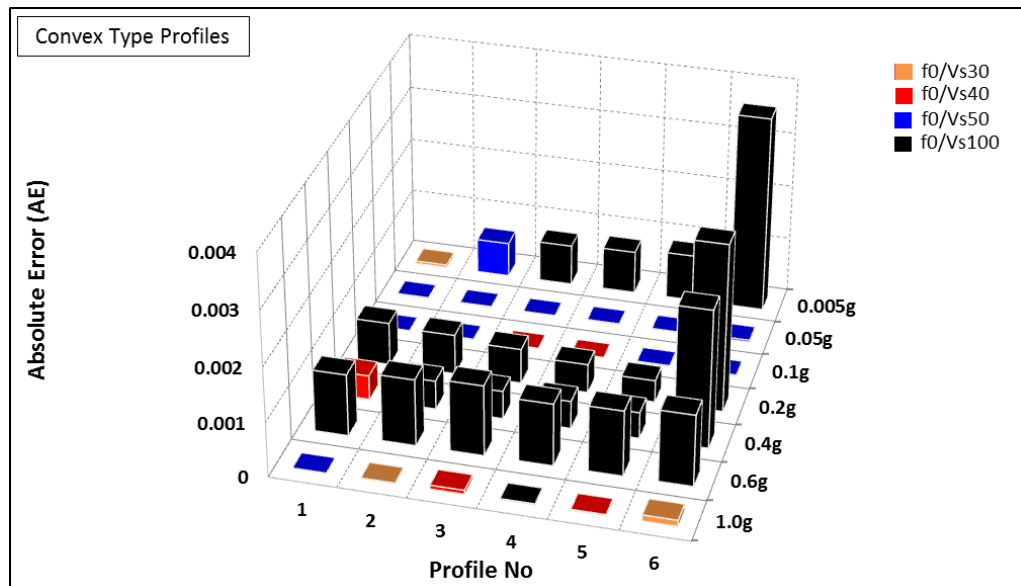


Figure 5.75. The variation of AE for f_0/V_{sz} with increasing impulsive bedrock accelerations for convex profiles.

The correlations for linear/concave profiles were nearly the same; they presented relations closer to a linear line instead of a constant one. Even so, the best performing parameter was defined as V_{s100} which can be used at all bedrock accelerations pointing out a wide range of strains (Figure 5.76). Besides, V_{s30} and V_{s50} are the best performing parameters observed for profiles no 12 and 13.

As a general statement, the most common parameters for convex profiles were V_{s50} at 0.05g and 0.1g; and V_{s30} and V_{s40} at 1.0g. They can be used at nonlinear elastic and elasto-plastic strain ranges. For linear/concave profiles, V_{s100} was the most common parameter for all bedrock acceleration levels.

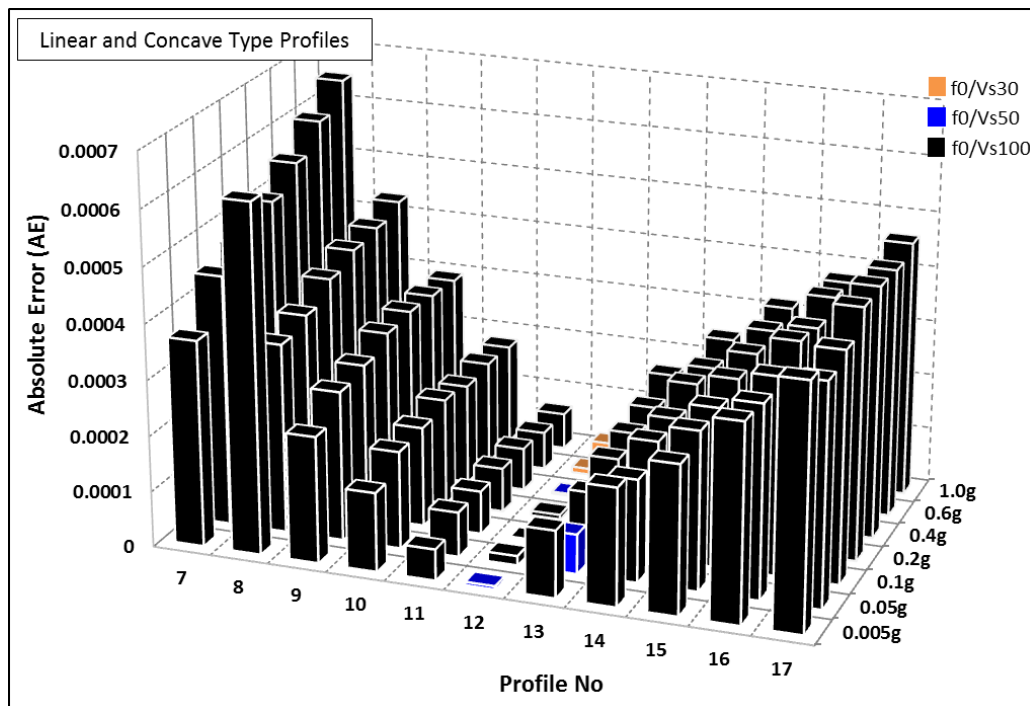


Figure 5.76. The variation of AE for f_0/V_{sz} with increasing impulsive bedrock accelerations for linear/concave profiles.

5.2.1.6. Fundamental Frequency Characterization by T_{tz} . We have investigated the correlation of fundamental soil frequency, f_0 , with shear wave travel times at various depths, T_{tz} , by multiplying f_0 with T_{tz} to check if we get a constant line (Figure 5.77 to 5.83). As in the correlation between f_0 and V_{sz} , the order of f_0 peaks in the transfer functions affected the correlation between f_0 and T_{tz} as well. We have observed a distinct transition point for $f_0 \times T_{tz}$ correlations between convex and linear/concave profiles

because all fundamental frequencies for linear/concave profiles were at the first peak, and for convex profiles at the 2nd/3rd peaks. As the bedrock acceleration increased, the transition point was softened between convex and linear/concave profile types since the f_0 values of convex profiles were shifted to lower peaks (i.e., from the 3rd to 2nd, and from the 2nd to 1st peaks). We have observed more constant relations for convex profiles at specific bedrock accelerations where f_0 values were observed at the same order peaks. For linear/concave profiles, the correlations were close to a linear line, rather than a constant line for all acceleration levels, even so T_{tz} can be used as a characterizing parameter for f_0 .

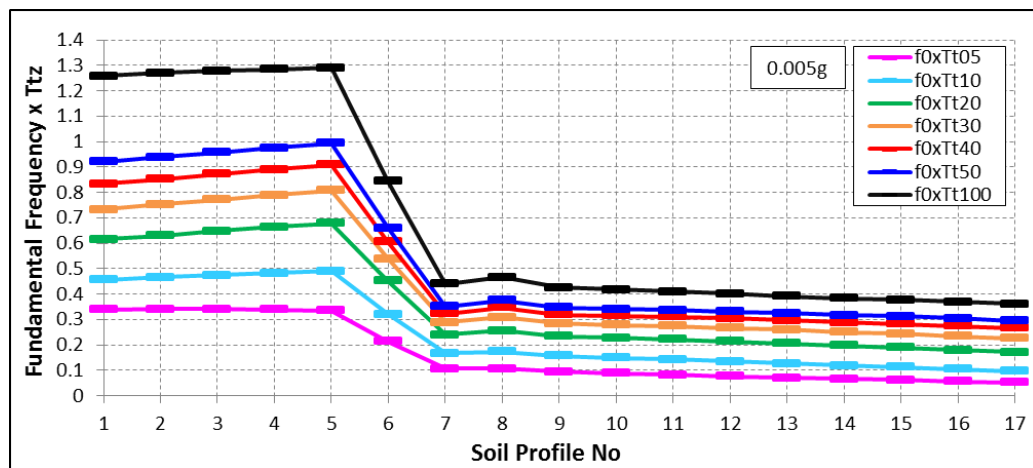


Figure 5.77. The correlation of f_0 with T_{tz} for 0.005g impulsive bedrock acceleration.

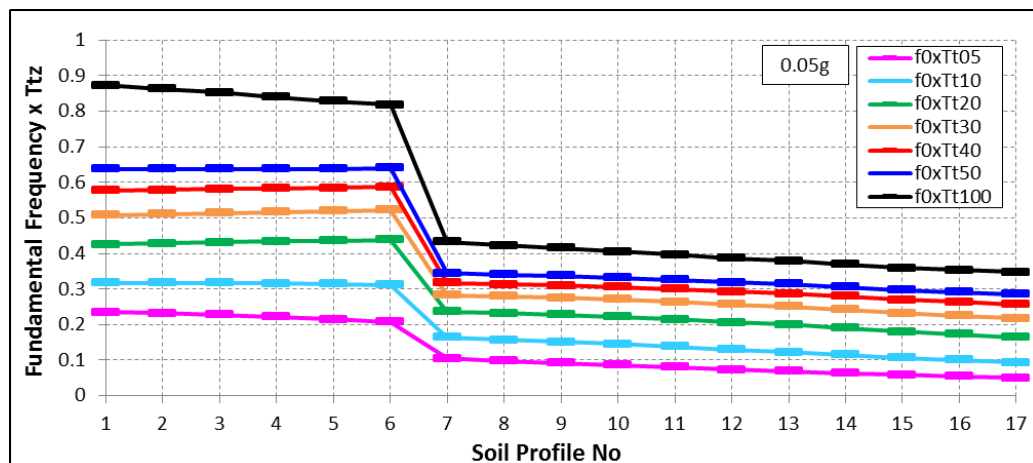


Figure 5.78. The correlation of f_0 with T_{tz} for 0.05g impulsive bedrock acceleration.

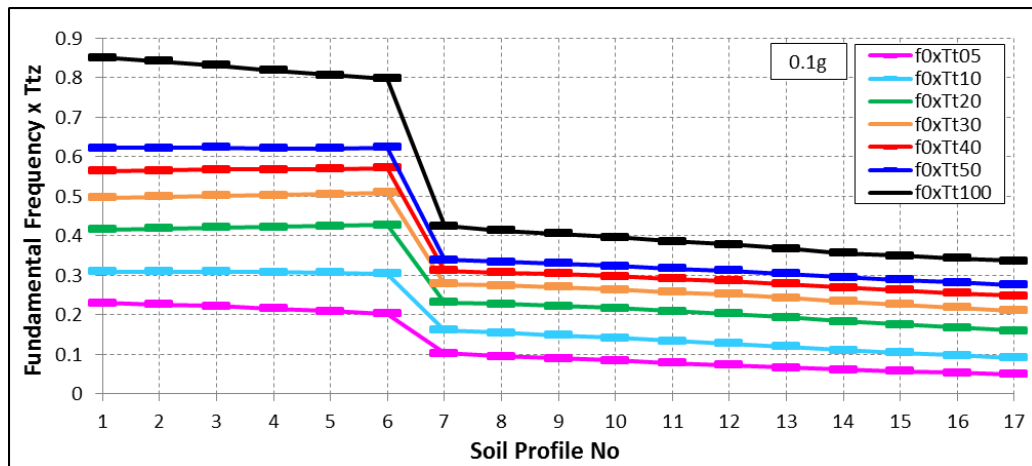


Figure 5.79. The correlation of f_0 with T_{tz} for 0.1g impulsive bedrock acceleration.

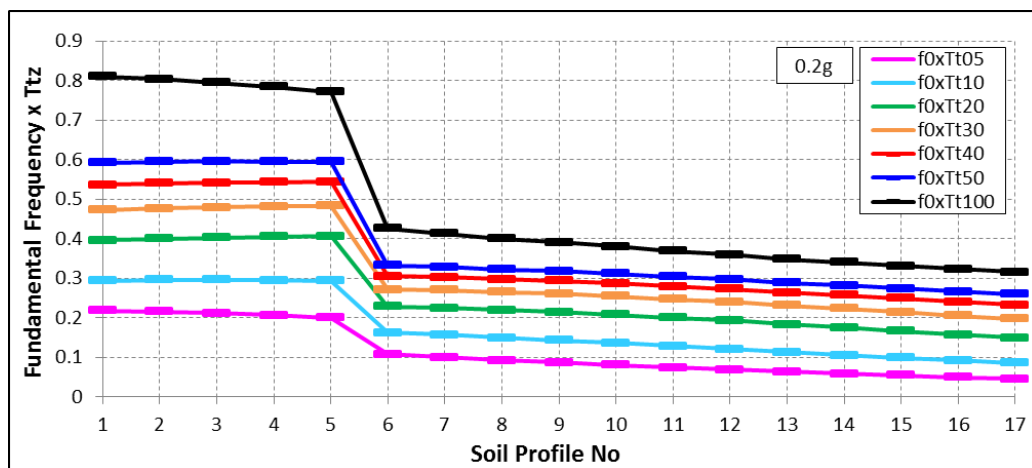


Figure 5.80. The correlation of f_0 with T_{tz} for 0.2g impulsive bedrock acceleration.

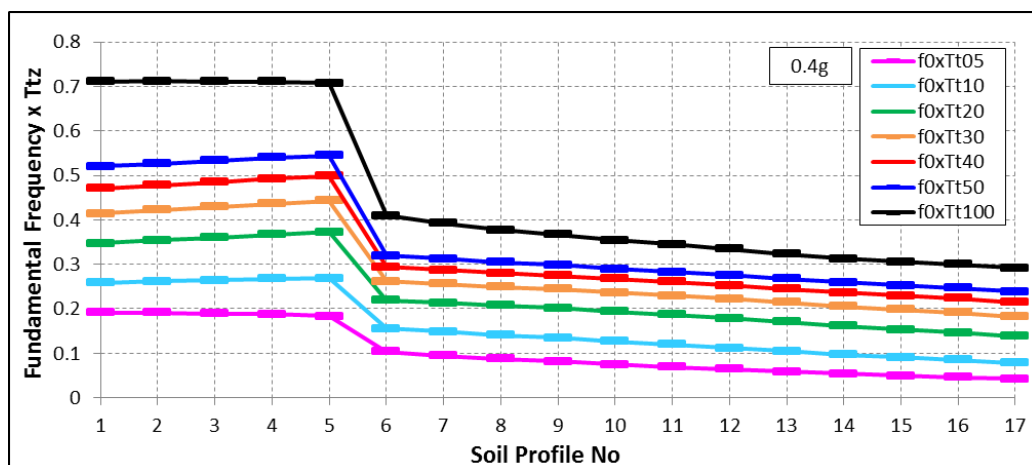


Figure 5.81. The correlation of f_0 with T_{tz} for 0.4g impulsive bedrock acceleration.

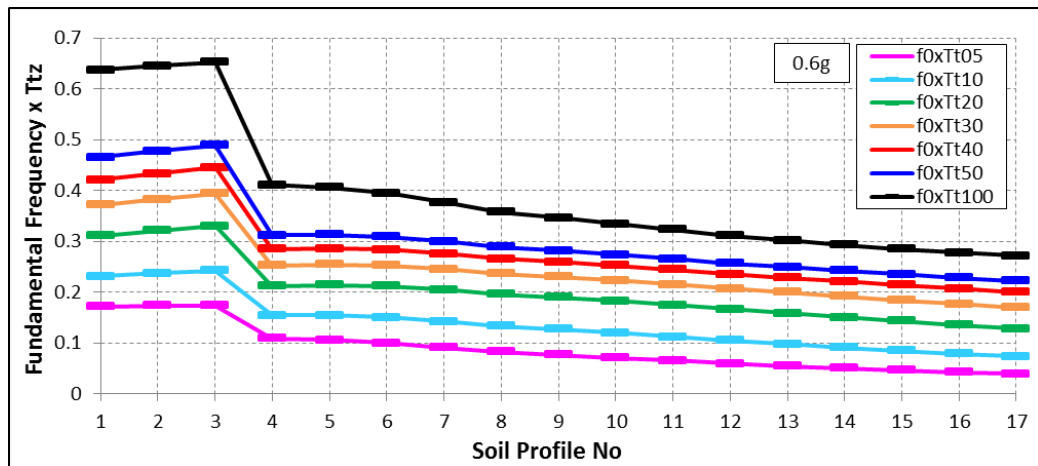


Figure 5.82. The correlation of f_0 with T_{tz} for 0.6g impulsive bedrock acceleration.

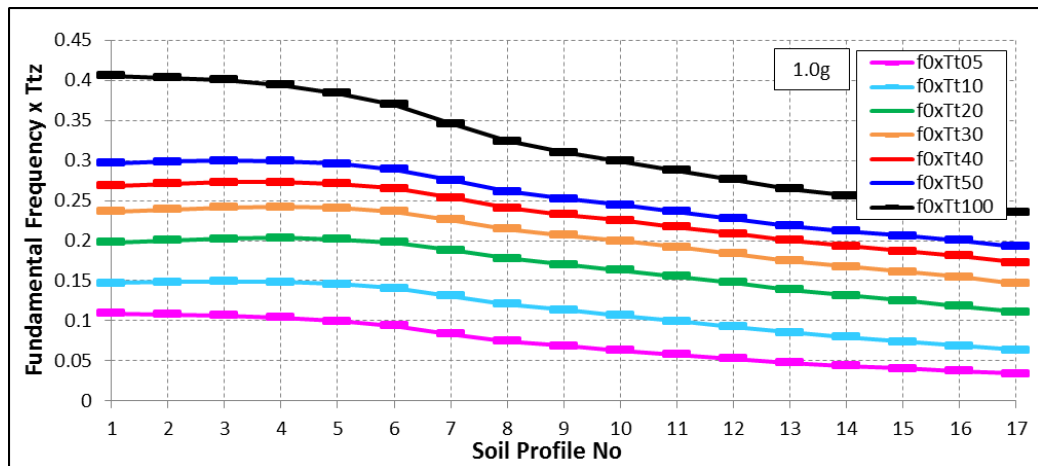


Figure 5.83. The correlation of f_0 with T_{tz} for 1.0g impulsive bedrock acceleration.

The AE variation of convex profiles showed the best performance for T_{tz} at 0.05g, 0.1g and 1.0g bedrock acceleration levels, where the errors were the lowest (Figure 5.84). At 0.05g, the best performing parameter was T_{t40} for profile no 4, and T_{t50} for the other profiles. At 0.1g, T_{t40} had the best performance for profile no 4 and 5, and T_{t50} for the rest of profiles. At 1.0g, the best performing parameters were defined as T_{t50} , T_{t30} , T_{t20} , T_{t05} , T_{t40} and T_{t20} for profile no 1 to 6, respectively. T_{t05} had the best performance for linear/concave profiles at all bedrock acceleration levels (Figure 5.85). Besides, T_{t10} , T_{t20} , T_{t30} , T_{t40} , T_{t50} and T_{t100} were the observed parameters for profiles no 7, 12, 13 and 14.

As a general comment, T_{tz} performed well for convex profiles at nonlinear elastic (0.05g and 0.1g) and elasto-plastic (1.0g) strain levels; the most common parameter was

T_{150} among all profiles. T_{105} was the dominant parameter for linear and concave profiles, which can be used at all strain ranges, hence at all bedrock acceleration levels.

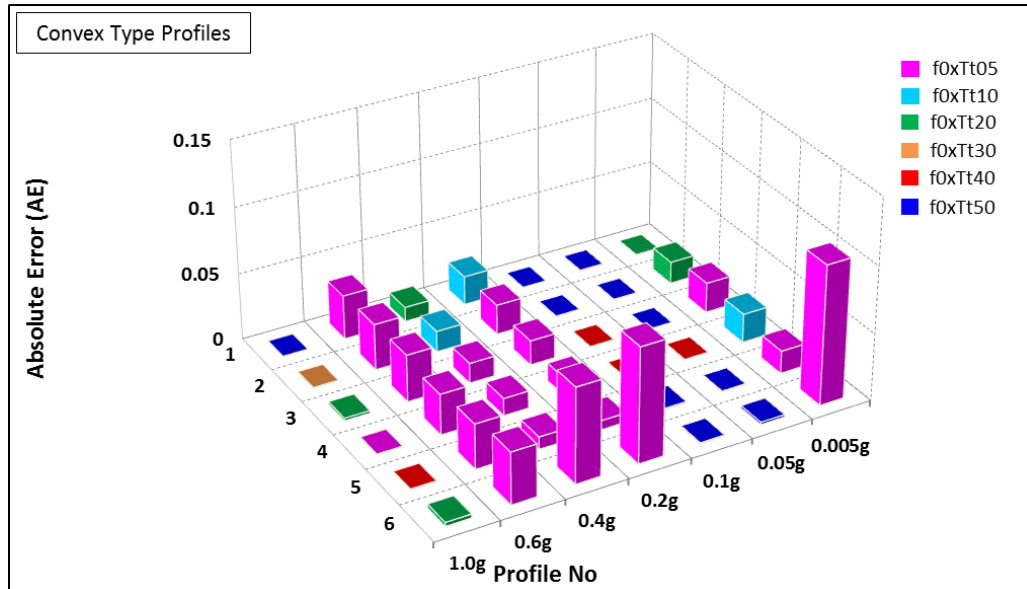


Figure 5.84. The variation of AE for f_0xT_z with increasing impulsive bedrock accelerations for convex profiles.

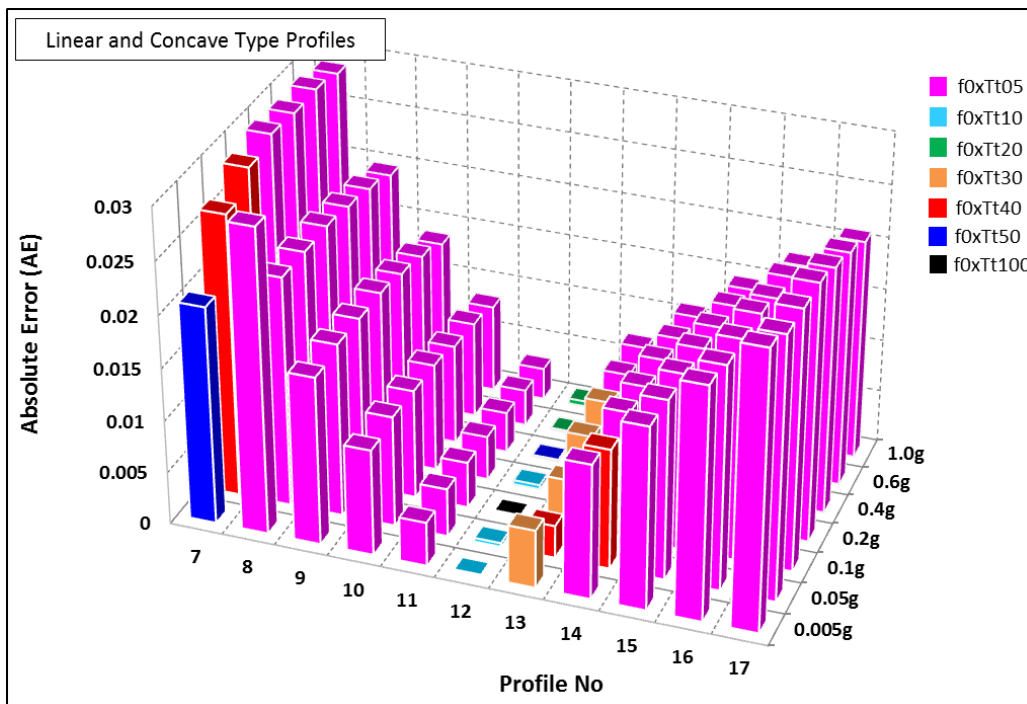


Figure 5.85. The variation of AE for f_0xT_z with increasing impulsive bedrock accelerations for linear/concave profiles.

5.2.2. Analyses of Equal Thickness Model Under White-Noise Bedrock Motion

We calculated the soil amplification factors, fundamental frequencies, surface PGAs and shear strains for gradually increasing white-noise bedrock motions by using the equal layer-thickness model. Due to the frequency content of white-noise motions (i.e., the energy is randomly distributed in all frequencies), the shear strains were increased by the increased nonlinearity, and the soil amplification factors and fundamental frequencies were decreased due to the effects of stiffness degradation, when compared to those for impulsive motions (see, Table 5.8 and Table 5.9).

Table 5.8. Fundamental frequencies (f_0) for gradually increasing bedrock accelerations.

Soil Profile No	Soil Type	f_0 -0.005g	f_0 -0.05g	f_0 -0.1g	f_0 -0.2g	f_0 -0.4g	f_0 -0.6g	f_0 -1.0g
1	Convex-6	5.688	3.796	3.577	2.795	1.733	1.508	1.367
2	Convex-5	5.493	3.601	3.387	1.782	1.642	1.465	1.318
3	Convex-4	5.261	3.387	3.131	1.685	1.489	1.392	1.239
4	Convex-3	4.987	3.119	2.875	1.575	1.392	1.300	1.111
5	Convex-2	3.082	2.838	2.625	1.428	1.263	1.135	0.916
6	Convex-1	2.820	1.434	1.373	1.270	1.099	0.946	0.757
7	Linear	1.318	1.233	1.160	1.044	0.854	0.726	0.610
8	Concave-1	1.172	1.074	1.007	0.867	0.714	0.598	0.513
9	Concave-2	1.080	0.977	0.891	0.775	0.641	0.543	0.446
10	Concave-3	0.989	0.879	0.806	0.702	0.574	0.488	0.397
11	Concave-4	0.903	0.800	0.732	0.629	0.513	0.433	0.354
12	Concave-5	0.824	0.726	0.659	0.568	0.458	0.385	0.317
13	Concave-6	0.751	0.659	0.598	0.507	0.409	0.342	0.275
14	Concave-7	0.690	0.598	0.543	0.458	0.366	0.305	0.238
15	Concave-8	0.629	0.543	0.488	0.415	0.330	0.275	0.208
16	Concave-9	0.580	0.494	0.446	0.378	0.299	0.250	0.189
17	Concave-10	0.531	0.458	0.409	0.348	0.269	0.226	0.171

Surface PGAs were computed for each profile and presented in Figure 5.86 with respect to gradually increasing bedrock accelerations. As the bedrock accelerations increased, the surface PGAs were observed less than the bedrock PGAs for all velocity profiles. The surface PGAs of convex profiles were higher than the linear and concave ones. The rapid increase in stiffness degradation and damping ratio may have resulted in lower PGA values for the softer velocity profiles, when compared to the stiffer profiles. The surface PGAs for white-noise bedrock motion were observed less than the ones computed by impulsive motions.

Table 5.9. Soil amplification factors (AF) for gradually increasing bedrock accelerations.

Soil Profile No	Soil Type	AF-0.005g	AF-0.05g	AF-0.1g	AF-0.2g	AF-0.4g	AF-0.6g	AF-1.0g
1	Convex-6	13.259	10.524	9.267	7.006	8.590	7.426	6.679
2	Convex-5	12.825	10.342	9.247	7.337	8.877	7.741	6.941
3	Convex-4	12.358	9.985	9.055	7.935	8.686	8.008	7.134
4	Convex-3	11.738	9.564	8.780	8.575	8.876	8.157	6.906
5	Convex-2	11.227	9.124	8.332	8.963	8.841	7.674	5.843
6	Convex-1	10.887	9.063	8.857	8.786	7.866	6.501	5.017
7	Linear	11.554	9.870	9.084	7.959	6.091	5.131	4.543
8	Concave-1	12.832	10.004	8.747	7.031	5.373	4.590	4.203
9	Concave-2	13.577	9.880	8.349	6.608	5.097	4.507	3.959
10	Concave-3	14.267	9.596	8.093	6.278	4.928	4.397	3.856
11	Concave-4	14.641	9.460	7.777	6.019	4.812	4.260	3.761
12	Concave-5	14.944	9.264	7.498	5.813	4.624	4.137	3.601
13	Concave-6	15.324	9.109	7.277	5.635	4.474	3.938	3.518
14	Concave-7	15.596	8.935	7.062	5.505	4.408	3.889	3.378
15	Concave-8	15.922	8.670	6.868	5.336	4.305	3.829	3.289
16	Concave-9	15.852	8.403	6.737	5.239	4.215	3.721	3.184
17	Concave-10	15.432	8.435	6.581	5.191	4.116	3.617	3.140

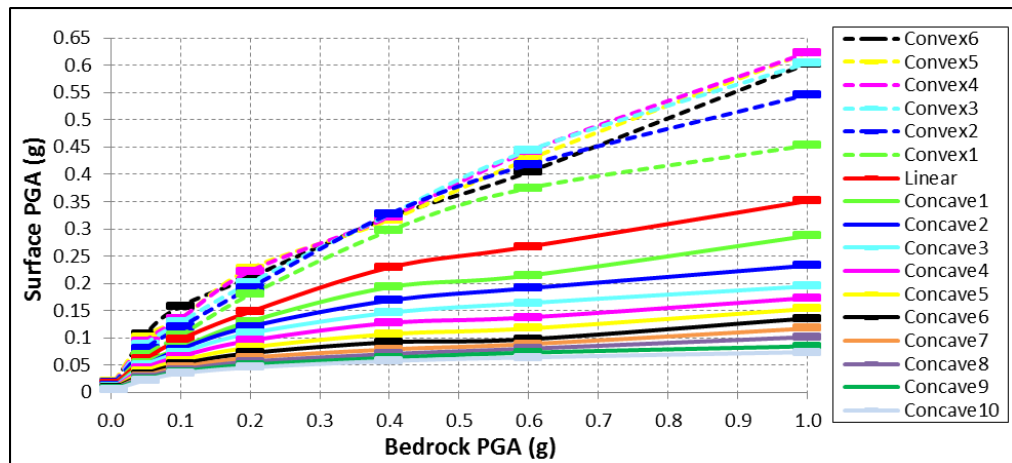


Figure 5.86. Surface PGAs with respect to gradually increasing white-noise accelerations.

We presented in Figure 5.87 to Figure 5.93, the transfer functions for gradually increasing bedrock acceleration levels to explain the variation of soil amplification factors (marked with red dots) and fundamental frequencies in more detail. The Fourier amplitudes of bedrock-to-surface transfer functions for white-noise input were higher than those for the impulsive input, although the bedrock PGAs were the same. Higher high-frequency content of white-noise motions caused the soil to reach nonlinear strain range

quicker, hence resulting in lower soil amplification factors and fundamental frequencies, when compared to those for the impulsive motions.

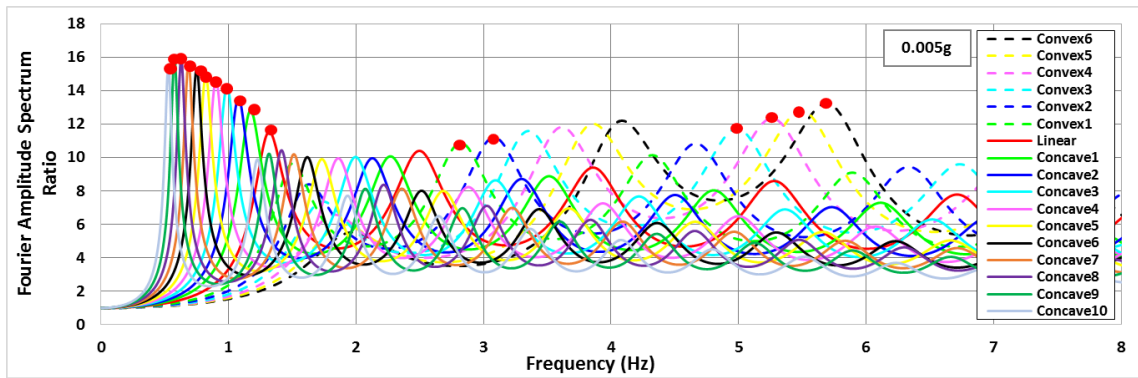


Figure 5.87. Transfer functions at 0.005g white-noise acceleration level.

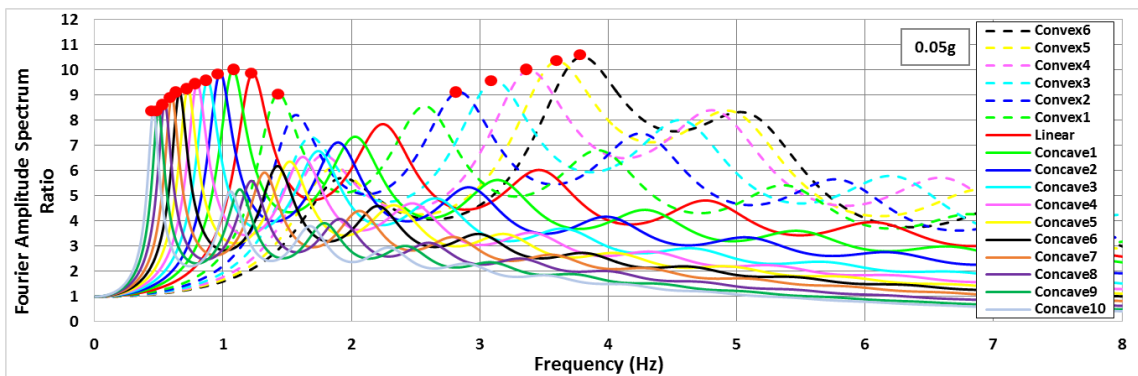


Figure 5.88. Transfer functions at 0.05g white-noise acceleration level.

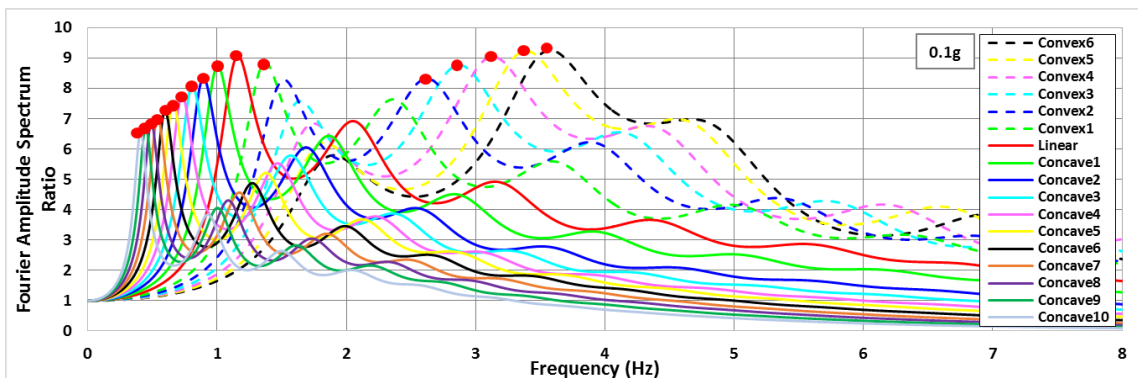


Figure 5.89. Transfer functions at 0.1g white-noise acceleration level.

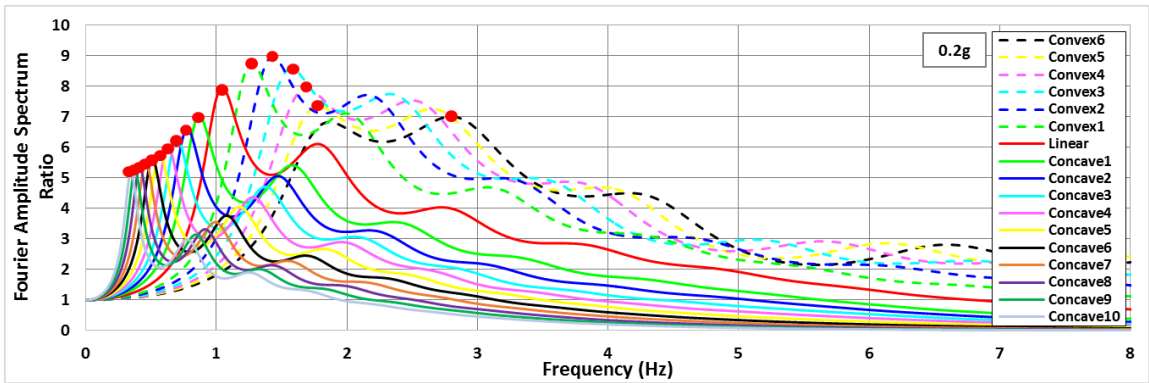


Figure 5.90. Transfer functions at 0.2g white-noise acceleration level.

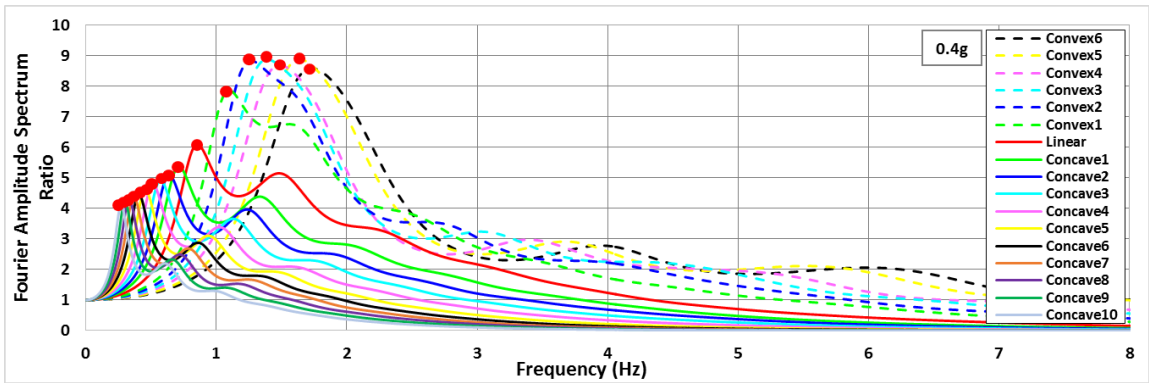


Figure 5.91. Transfer functions at 0.4g white-noise acceleration level.

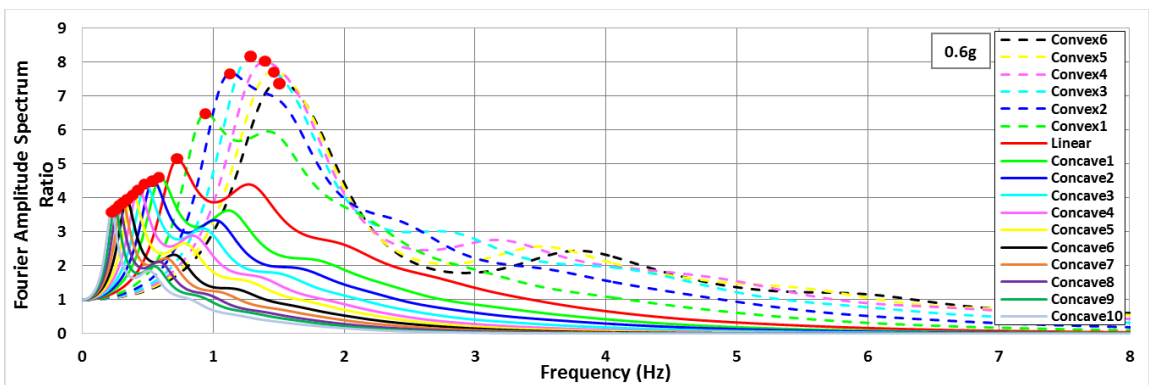


Figure 5.92. Transfer functions at 0.6g white-noise acceleration level.

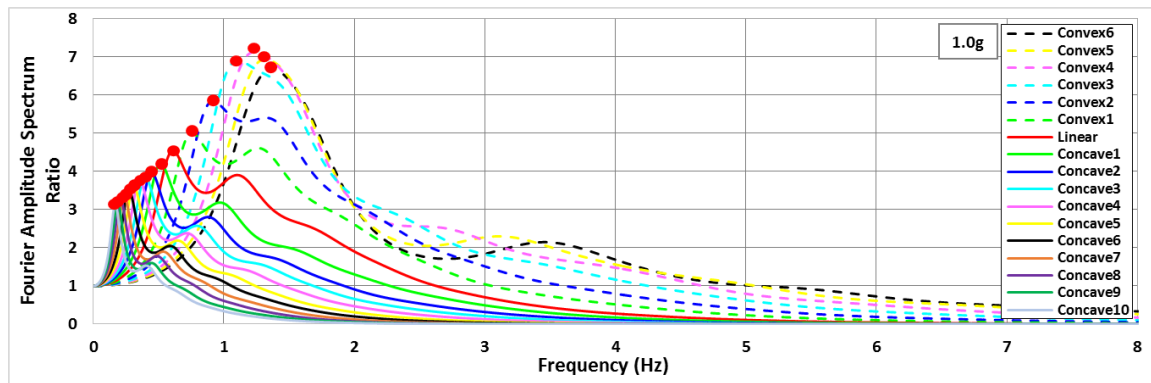


Figure 5.93. Transfer functions at 1.0g white-noise acceleration level.

Beginning with the 0.005g bedrock acceleration level, the high order fundamental frequencies of convex profiles were shifted to the first order peaks by the effect nonlinearity. The soil amplification factors for concave profiles decreased as the bedrock PGA level increased. For each bedrock acceleration level, we showed the maximum amplitude of transfer functions (amplification factor) with fundamental frequencies of each soil profile type (Figure 5.94). An increasing trend of soil amplification factors from Concave-10 to Convex-6 was observed for the bedrock acceleration levels $\geq 0.4g$.

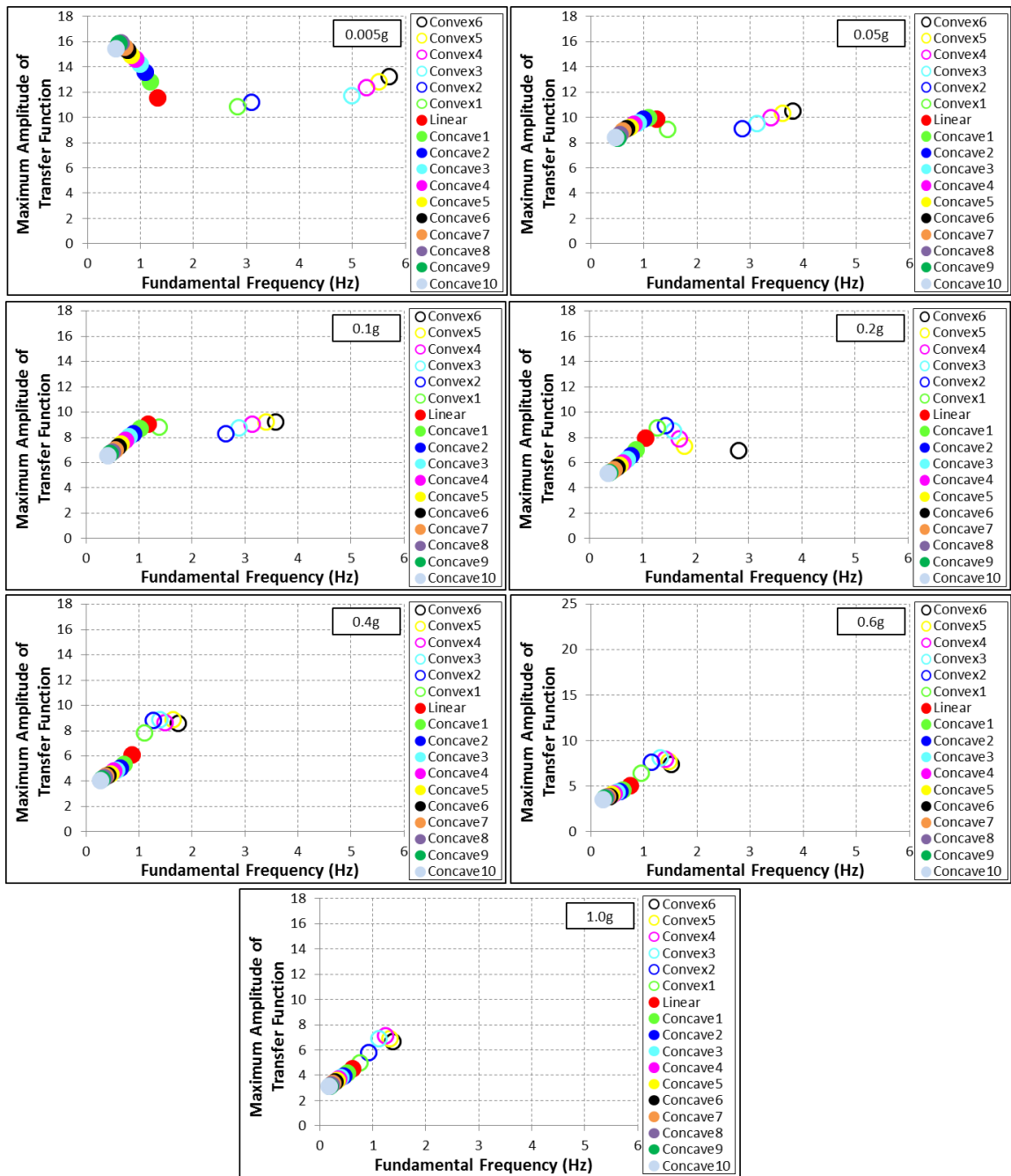


Figure 5.94. Maximum amplitude of transfer functions and corresponding fundamental frequencies for white-noise bedrock accelerations.

5.2.2.1. Site Amplification Characterization by Surface PGA. We have investigated the amplification and de-amplification of surface PGAs with gradually increasing bedrock acceleration levels for each profile (Figure 5.95). We have observed amplification for all profiles at 0.005g bedrock acceleration level, especially more for convex profiles.

As the bedrock acceleration level increased to 0.4g, de-amplification was seen for all profiles. Linear and concave profiles reached to nonlinear elastic and elasto-plastic strain ranges more rapidly than convex profiles, hence the surface PGAs were lower by the effect of nonlinearity and higher damping ratio. We have studied the correlation of soil amplification factors with surface PGAs for gradually increasing bedrock accelerations (Figure 5.96). A better correlation was observed for convex profiles, when compared with linear and concave profiles.

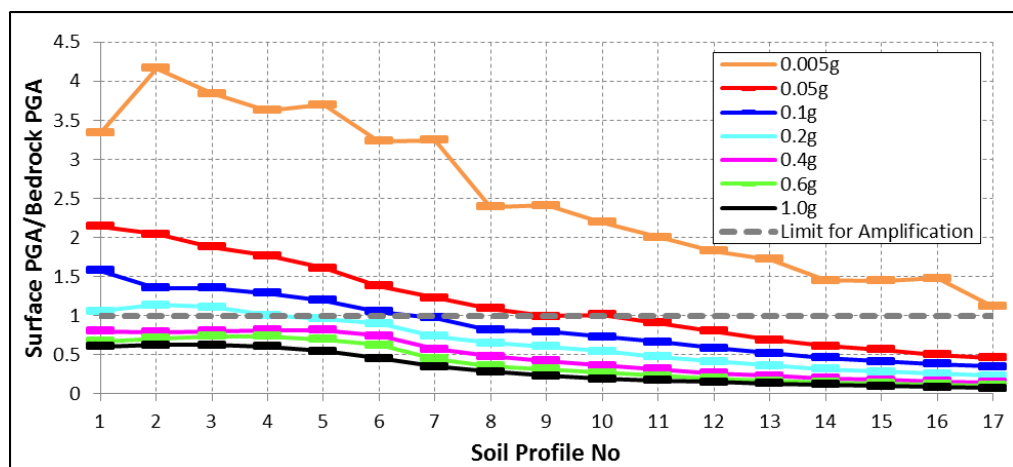


Figure 5.95. Amplification and de-amplification of surface PGAs for each profile.

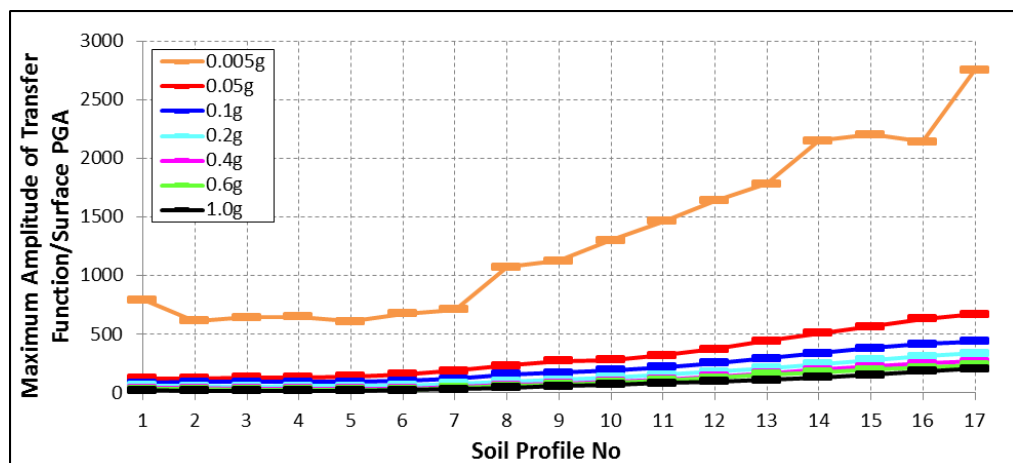


Figure 5.96. The correlation of soil amplification factors with surface PGAs with respect to profiles.

In Figure 5.97, a constant ratio is seen for convex profiles for gradually increasing bedrock accelerations. Surface PGAs can be used to characterize soil amplification for convex profiles at $\text{Acc.} \geq 0.05\text{g}$, corresponding to nonlinear elastic and elasto-plastic strain ranges.

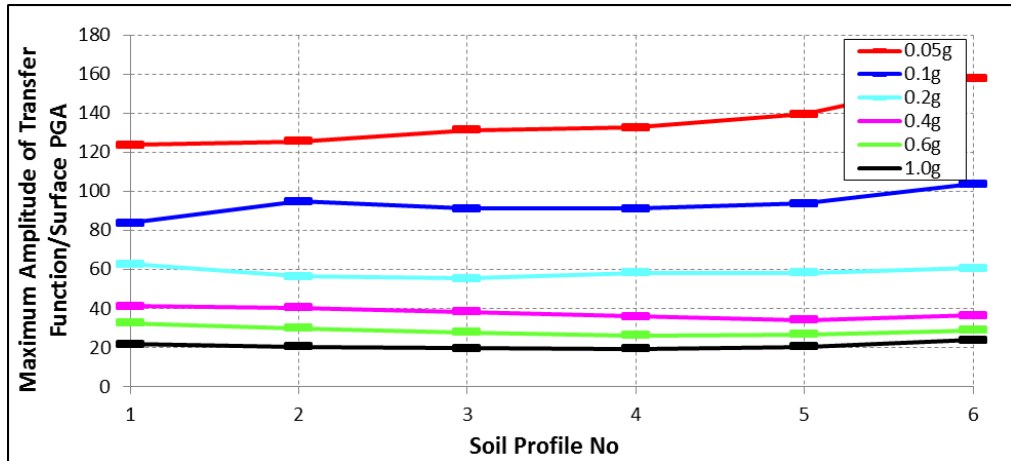


Figure 5.97. The correlation of soil amplification factors with surface PGAs for convex profiles.

5.2.2.2. Site Amplification Characterization by Fundamental Soil Frequency, f_0 .

Fundamental soil frequencies were presented with respect to bedrock PGAs and soil profile numbers in Figure 5.98 and Figure 5.99, respectively. The higher order fundamental frequencies of convex profiles were shifted to lower values rapidly by gradually increasing bedrock accelerations.

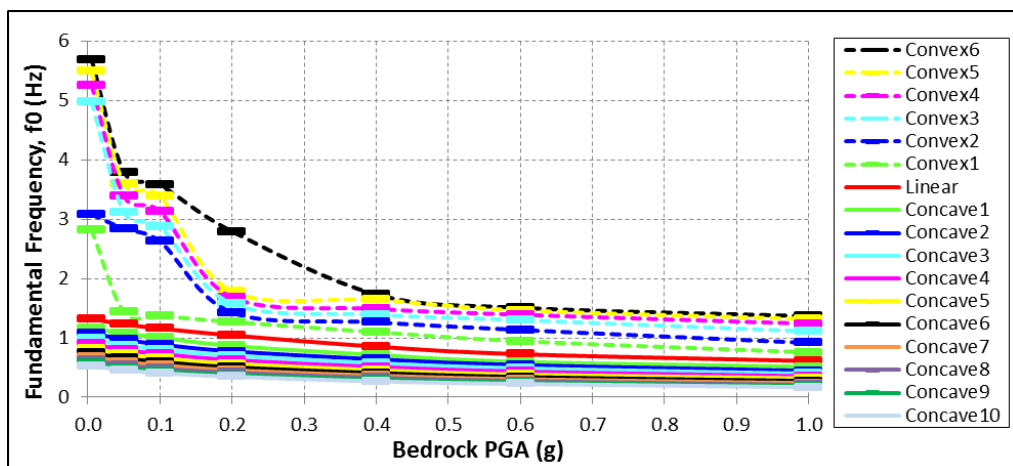


Figure 5.98. Fundamental soil frequencies with respect to bedrock PGAs for each profile.

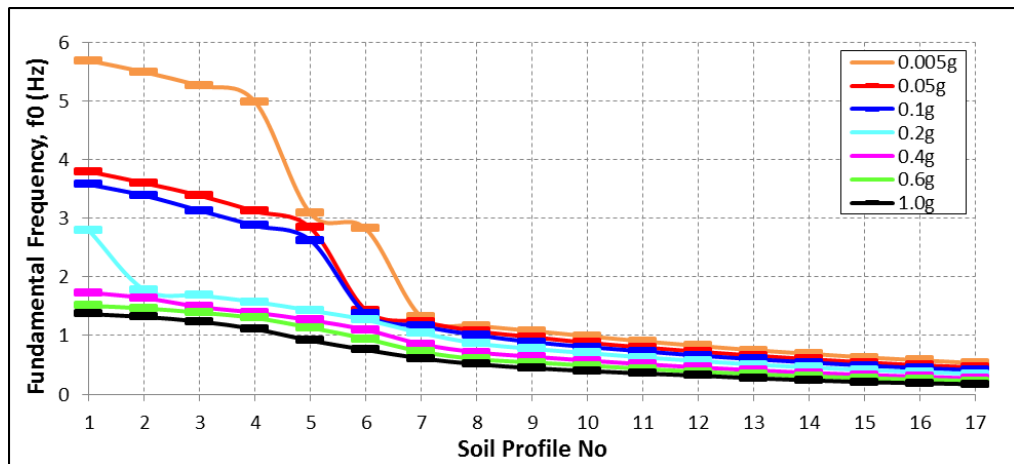


Figure 5.99. Fundamental soil frequencies with respect to profile numbers.

We have studied the correlation of soil amplification factors with fundamental frequencies (Figure 5.100). The correlation that is presented with respect to profile numbers showed a constant ratio just for convex profiles at 0.005g, 0.05g and 0.1g bedrock acceleration levels. The fundamental frequency can be used as a characterizing parameter for convex profiles at linear elastic and nonlinear elastic strain ranges triggered by $\text{Acc.} \leq 0.1g$.

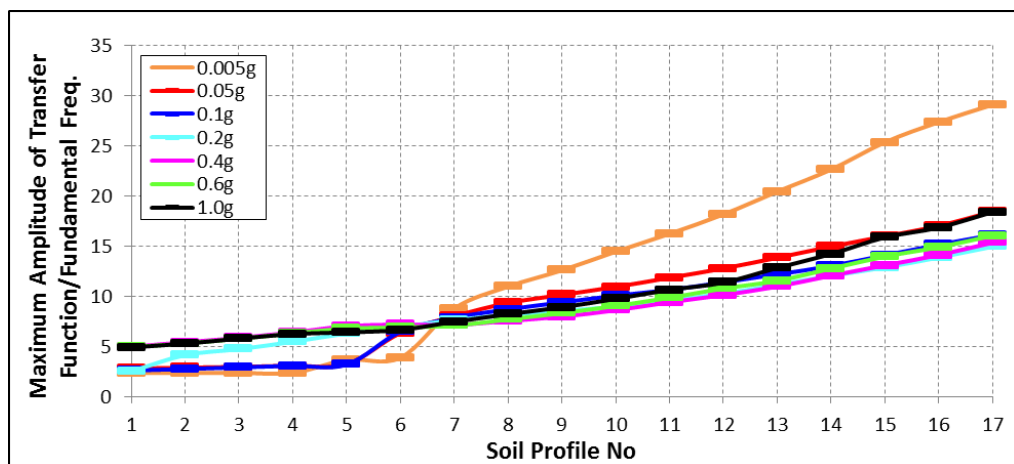


Figure 5.100. The correlation of soil amplification factor with f_0 with respect to profile no.

5.2.2.3. Site Amplification Characterization by V_{sz} . We have investigated the correlation of soil amplification factors with time averaged shear wave velocities, V_{sz} , for gradually increasing white-noise motions. The ratios of AF/V_{sz} were presented for each bedrock acceleration level in Figure 5.101-5.108.

For convex profiles, constant relations were observed at all averaging depths for $\text{Acc.} \geq 0.2\text{g}$, however the correlations with shallow averaging depths were closer to a linear straight line rather than a constant one for $\text{Acc.} \geq 0.2\text{g}$. For the bedrock $\text{Acc.} \geq 0.05\text{g}$, linear and concave profiles presented constant relations.

The variation of absolute errors for the correlation between AF and V_{sz} , were shown in Figures 5.109 and 5.110 with gradually increasing bedrock acceleration levels. The best performing parameter for convex profiles was V_{s100} at all acceleration levels though AE values were a bit higher for $\text{Acc.} \geq 0.2\text{g}$ compared to other acceleration levels. For linear and concave profiles, the AE values were lower for bedrock $\text{Acc.} \geq 0.05\text{g}$. At 0.05g bedrock acceleration level, the best performing parameters were defined as V_{s05} for profiles no 7, 8, 14, 15, 17; V_{s10} for profiles no 9, 10, 16; V_{s20} for no 11; V_{s50} for no 12, and V_{s100} for no 13.

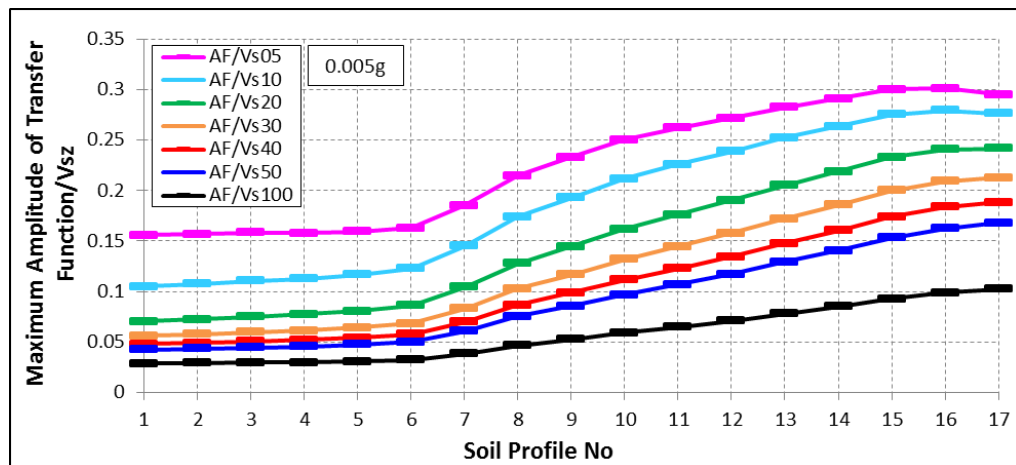


Figure 5.101. The correlation of AF with V_{sz} for 0.005g white-noise bedrock acceleration.

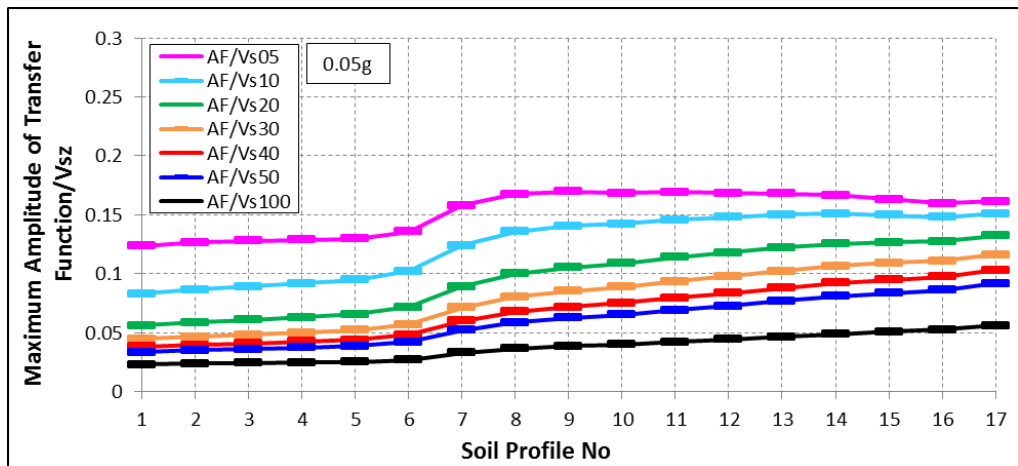


Figure 5.102. The correlation of AF with V_{sz} for 0.05g white-noise bedrock acceleration.

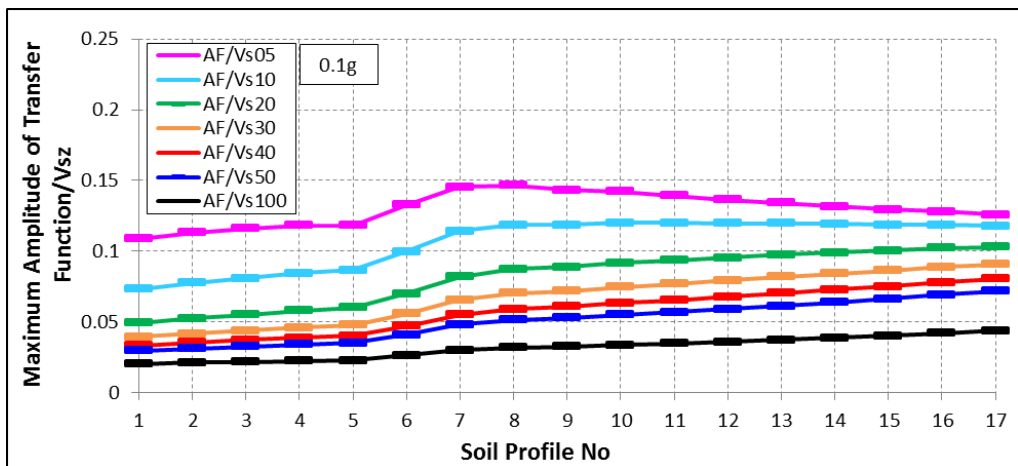


Figure 5.103. The correlation of AF with V_{sz} for 0.1g white-noise bedrock acceleration.

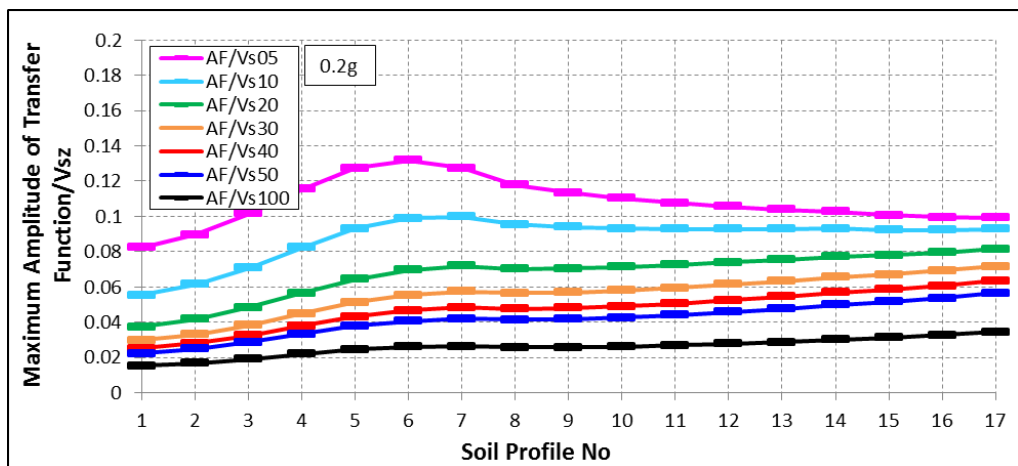


Figure 5.104. The correlation of AF with V_{sz} for 0.2g white-noise bedrock acceleration.

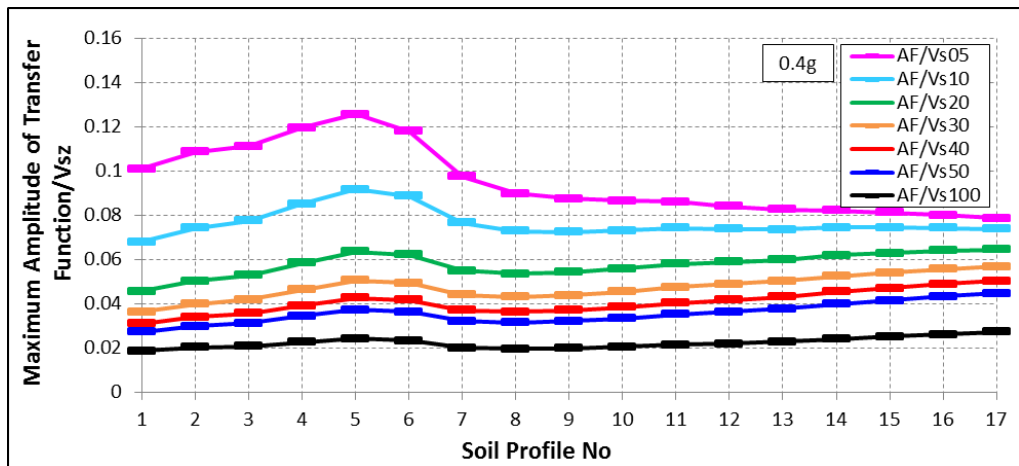


Figure 5.105. The correlation of AF with V_{sz} for 0.4g white-noise bedrock acceleration.

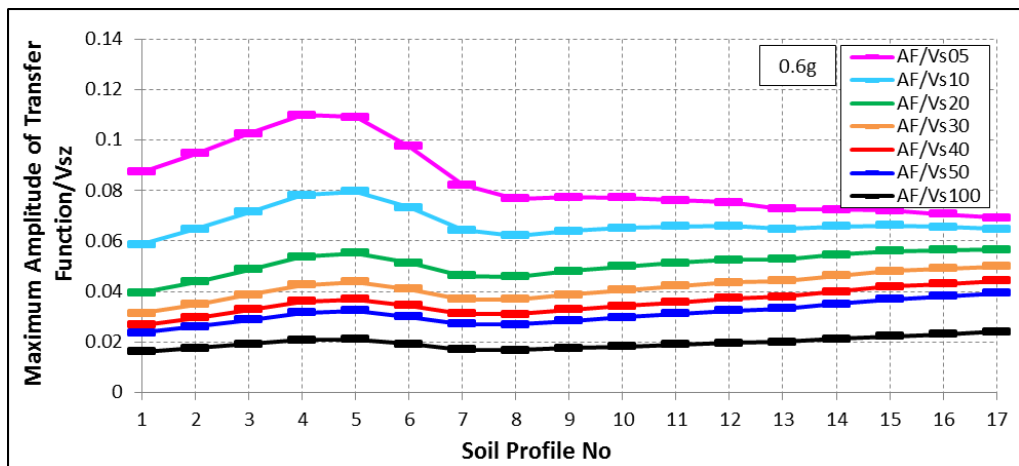


Figure 5.106. The correlation of AF with V_{sz} for 0.6g white-noise bedrock acceleration.

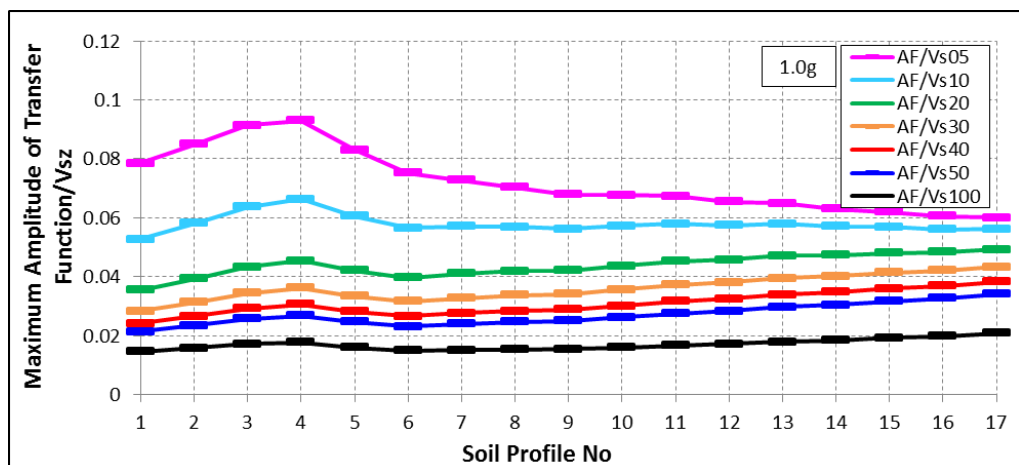


Figure 5.107. The correlation of AF with V_{sz} for 1.0g white-noise bedrock acceleration.

At 0.1g acceleration level, the best performing parameters were V_{s10} for profiles no 7, 8, 9, 10, 14, 15, 16, 17; V_{s20} for no 11; V_{s30} for no 12, and V_{s100} for no 13. At 0.2g, V_{s100} for profile no 7, 13; V_{s10} for no 8, 9, 10, 14, 15, 16, 17; V_{s05} for no 11; and V_{s20} for no 12, were the best performing parameters. At 0.4g, the best performing parameters were V_{s100} for profiles no 7, 13; and V_{s10} for no 8, 9, 10, 11, 14, 15, 16, 17. At 0.6g, V_{s10} for profiles no 7, 9, 10, 13, 14, 15, 16, 17; V_{s05} for no 8; V_{s20} for no 11; and V_{s40} for no 12 were the best performing parameters. At 1.0g bedrock acceleration level, V_{s10} for profiles no 7, 8, 9, 10, 14, 15, 16, 17; V_{s20} for no 11; V_{s30} for no 12; and V_{s100} for no 13 were the best ones.

As a general statement, the optimal parameter was V_{s100} for convex profiles at all acceleration levels, and V_{s10} for linear/concave profiles for $\text{Acc.} \geq 0.05\text{g}$.

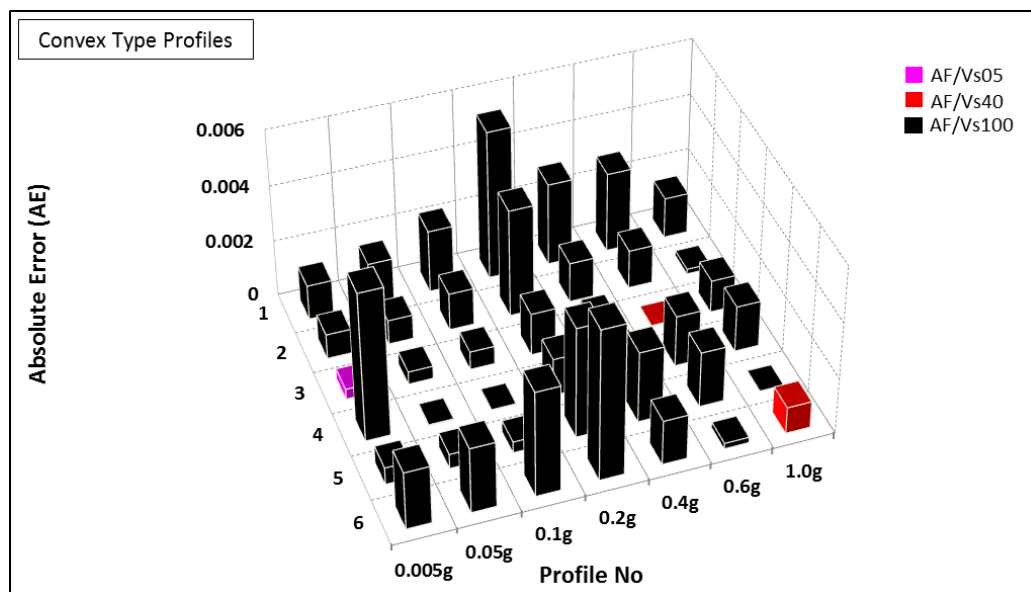


Figure 5.108. The variation of AE for AF/V_{sz} with increasing white-noise bedrock accelerations for convex profiles.

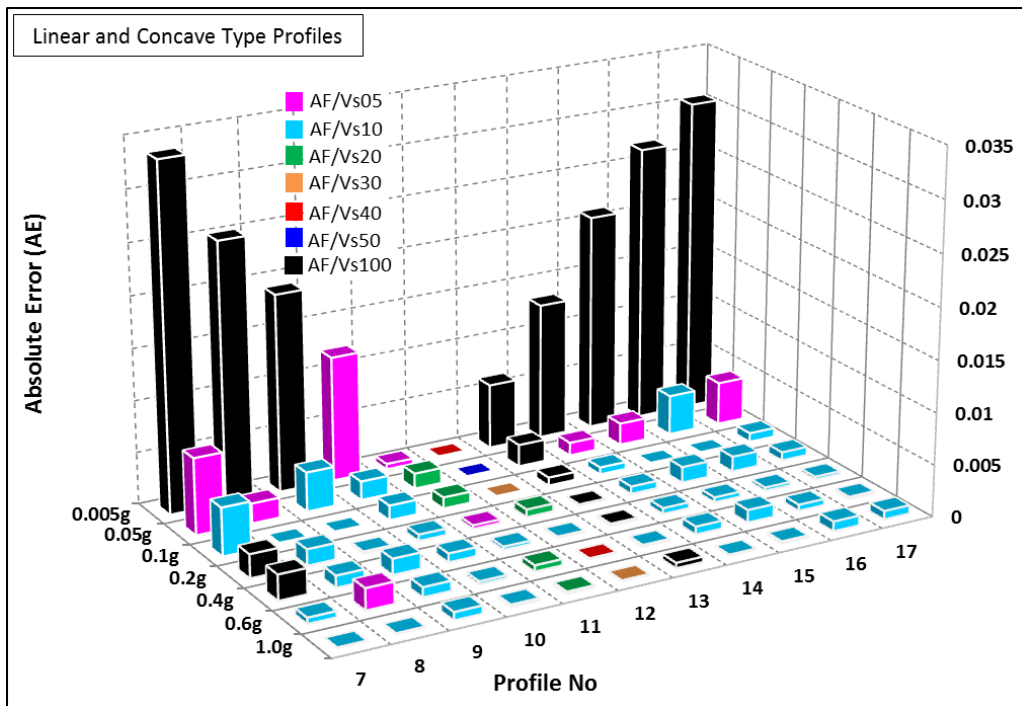


Figure 5.109. The variation of AE for AF/V_{sz} with increasing white-noise bedrock accelerations for linear/concave profiles.

5.2.2.4. Site Amplification Characterization by T_{tz} . We have investigated the correlation of soil amplification factors with T_{tz} parameters for gradually increasing white-noise accelerations (Figure 5.110-5.116). Convex profiles presented linear relations for Acc. <0.2g, and nearly constant relations for 0.2g and higher acceleration levels. Linear and concave profiles showed a constant relation at 0.005g acceleration level, and they presented linear relations for the higher bedrock accelerations.

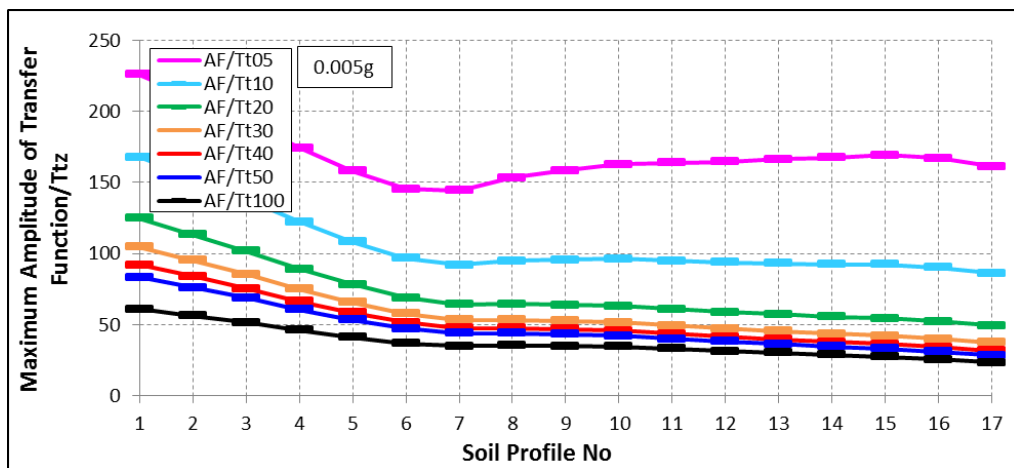


Figure 5.110. The correlation of AF with T_{tz} for 0.005g white-noise bedrock acceleration.

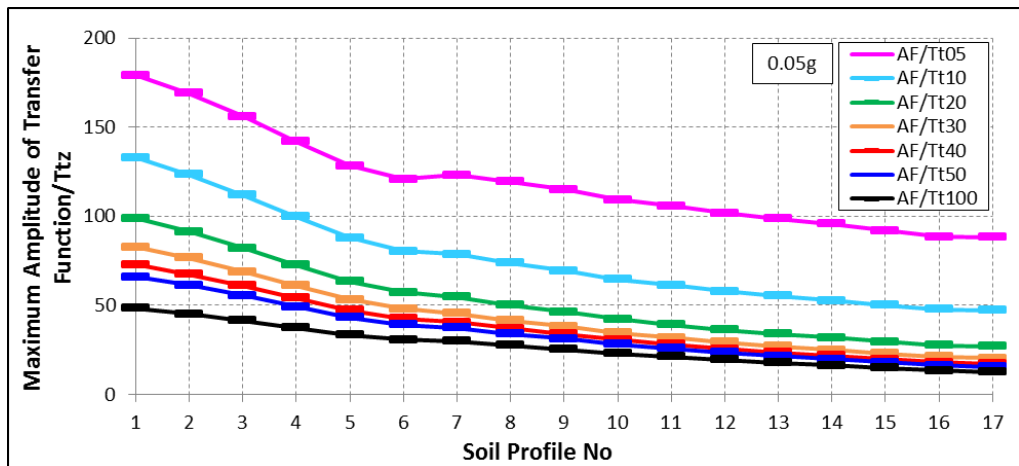


Figure 5.111. The correlation of AF with T_{tz} for 0.05g white-noise bedrock acceleration.

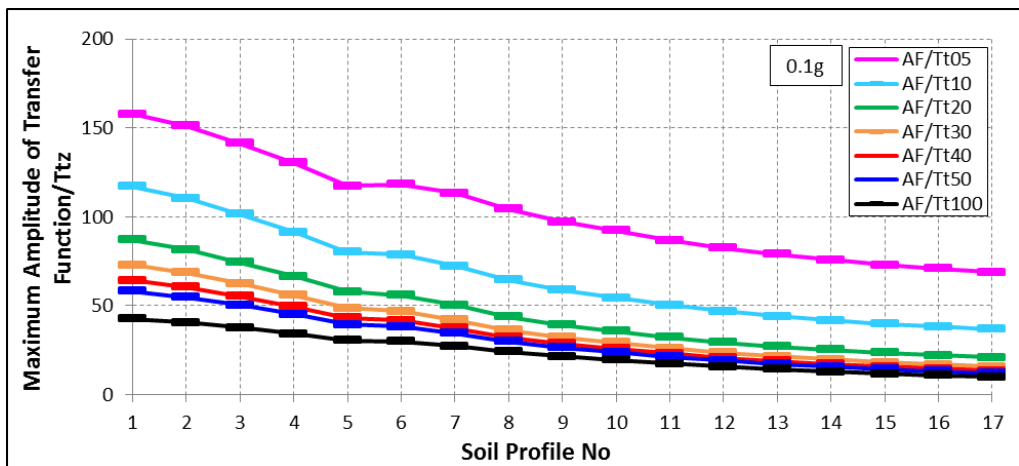


Figure 5.112. The correlation of AF with T_{tz} for 0.1g white-noise bedrock acceleration.

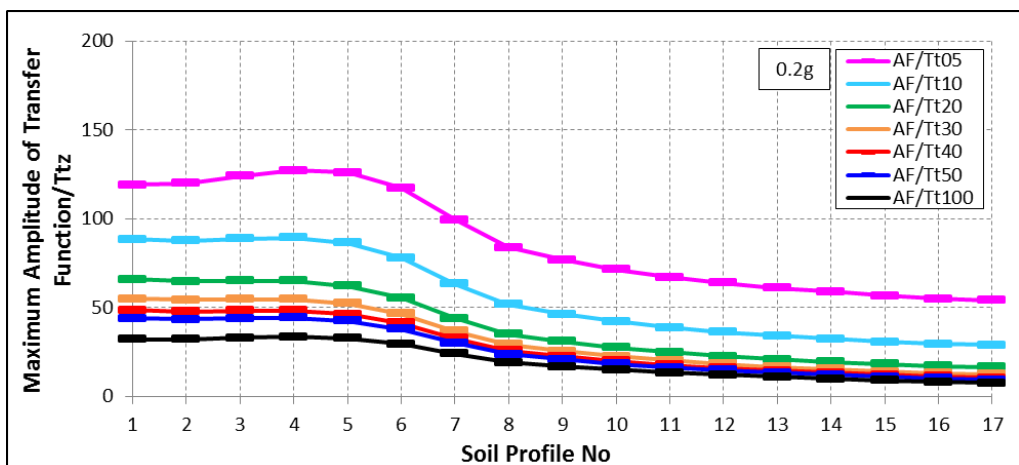


Figure 5.113. The correlation of AF with T_{tz} for 0.2g white-noise bedrock acceleration.

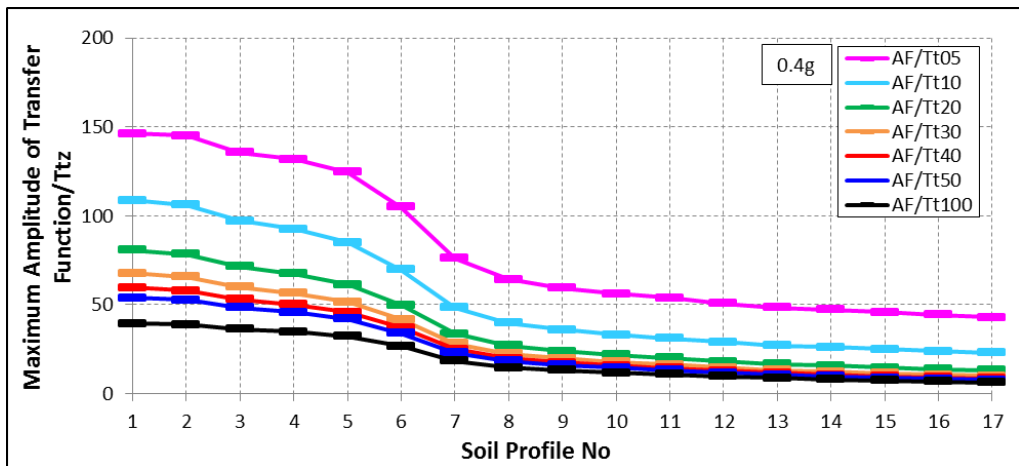


Figure 5.114. The correlation of AF with T_{tz} for 0.4g white-noise bedrock acceleration.

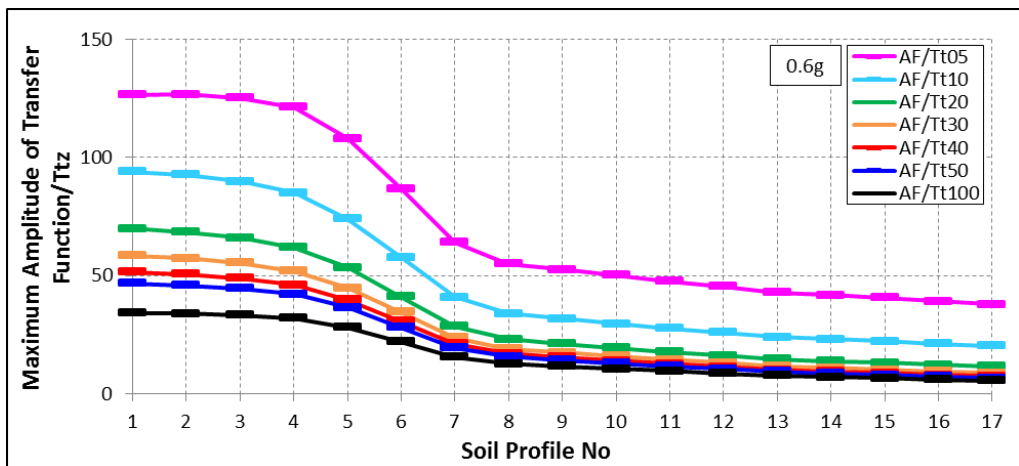


Figure 5.115. The correlation of AF with T_{tz} for 0.6g white-noise bedrock acceleration.

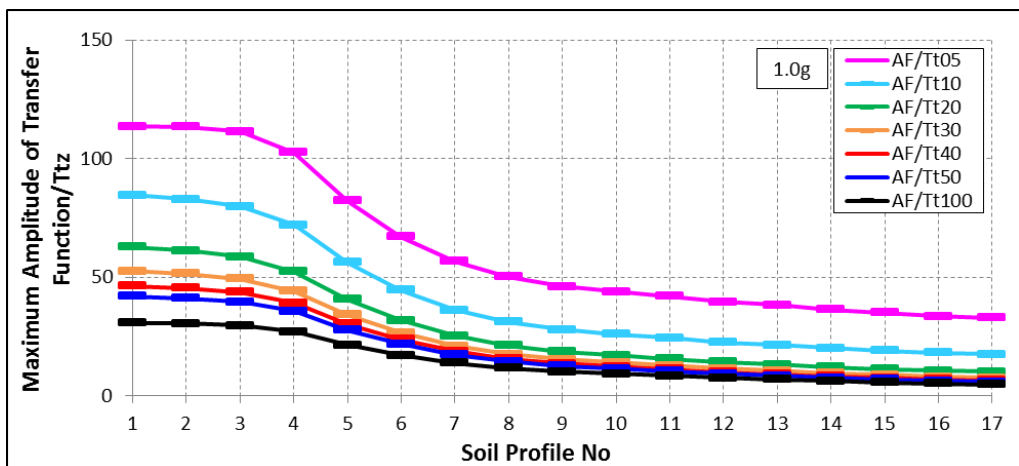


Figure 5.116. The correlation of AF with T_{tz} for 1.0g white-noise bedrock acceleration.

The AE values for the correlations between AF and T_{tz} showed the best performing parameters in Figure 5.117 and 5.118. For convex profiles, AE values were lower for $\text{Acc.} \geq 0.2g$ which revealed T_{t100} as the best performing parameter for all profiles. Linear and concave profiles showed lower AE values for $0.005g$ and $\text{Acc.} \geq 0.2g$. At $0.005g$ bedrock acceleration level, the best performing parameters were defined as T_{t10} for profiles no 7, 8, 9, 13, 14, 15, 16; T_{t05} for no 10, 11, 17; and T_{t20} for no 12. For $\text{Acc.} \geq 0.2g$, the best performing parameter was T_{t100} for all profiles.

As a general comment, the optimal parameter was T_{t100} for $\text{Acc.} \geq 0.2g$ for convex profiles; T_{t10} for $0.005g$ acceleration level and T_{t100} for $\text{Acc.} \geq 0.2g$ for linear/concave profiles.

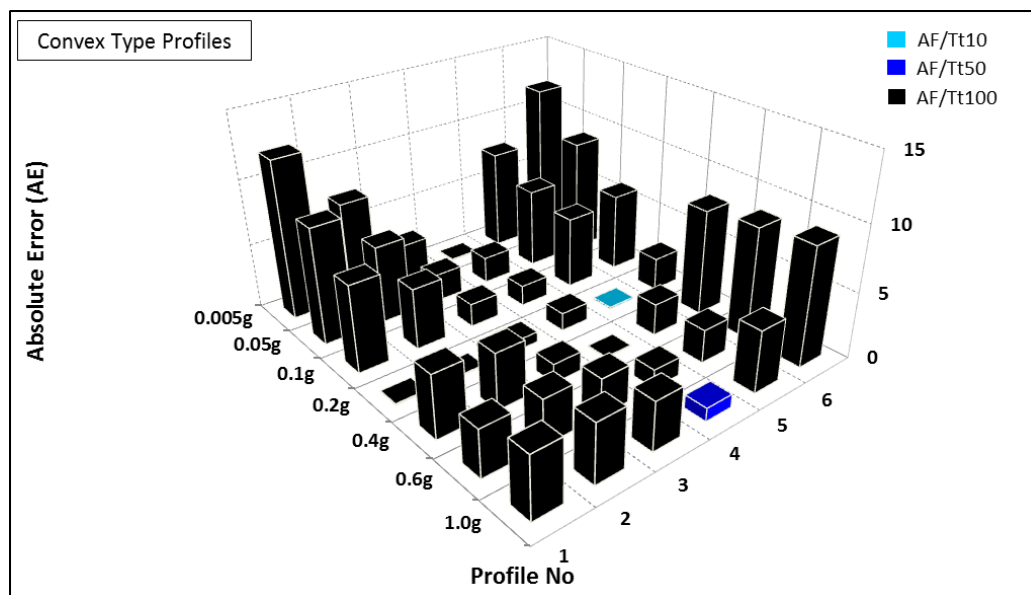


Figure 5.117. The variation of AE for AF/ T_{tz} with increasing white-noise bedrock accelerations for convex profiles.

The correlations for gradually increasing bedrock accelerations were presented in Figure 5.119-5.125. For convex profiles, we haven't observed constant relations for $\text{Acc.} \leq 0.2g$, since there is a sharp transition between the peaks of fundamental frequencies, however for $\text{Acc.} \geq 0.4g$ we have observed linear relations. Linear and concave profiles presented linear relations for all acceleration levels. The AE variations for the correlation between f_0 and V_{sz} were given in Figure 5.126 and 5.127.

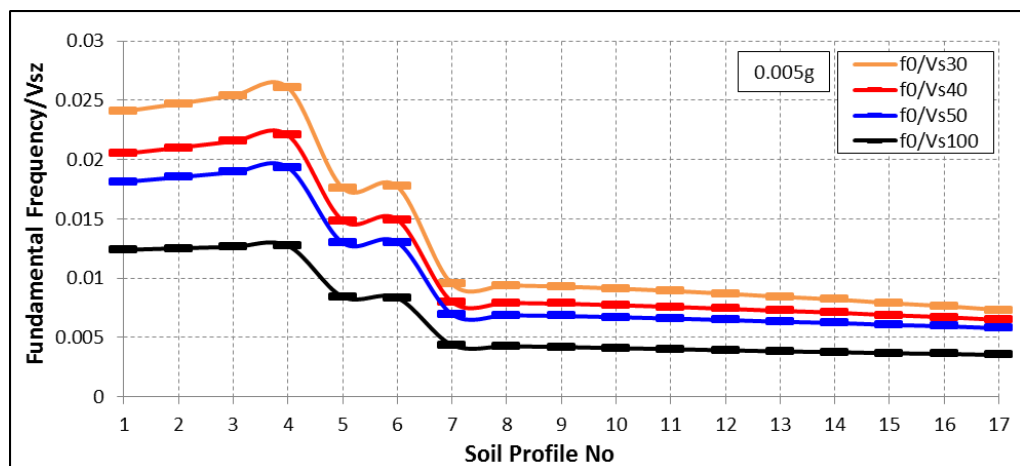


Figure 5.119. The correlation of f_0 with V_{sz} for 0.005g white-noise bedrock acceleration.

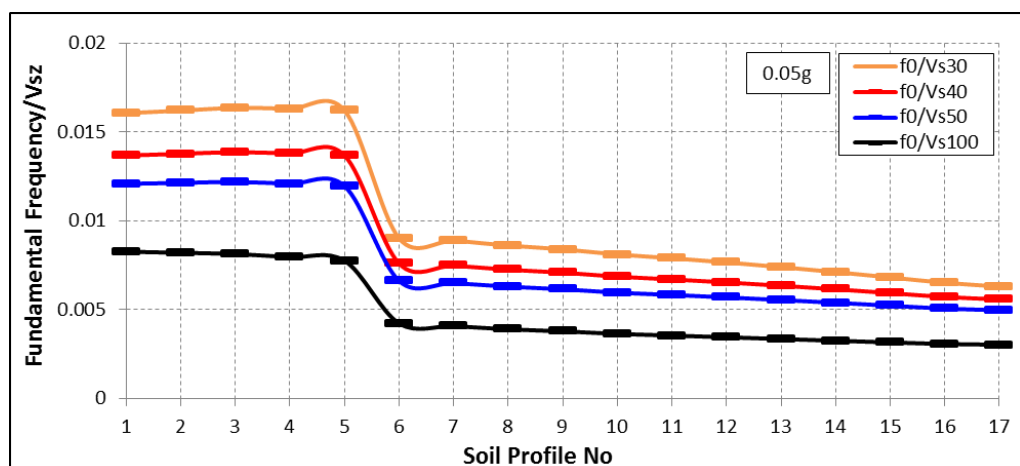


Figure 5.120. The correlation of f_0 with V_{sz} for 0.05g white-noise bedrock acceleration.

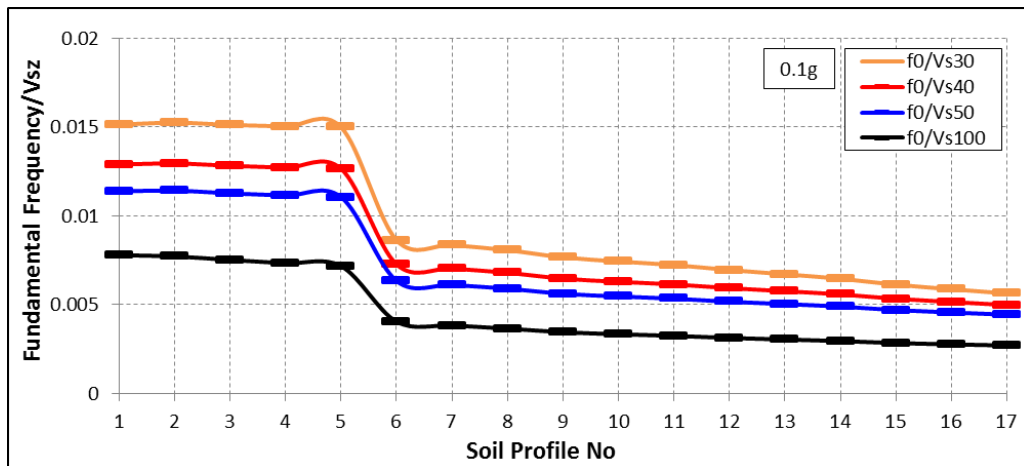


Figure 5.121. The correlation of f_0 with V_{sz} for 0.1g white-noise bedrock acceleration.

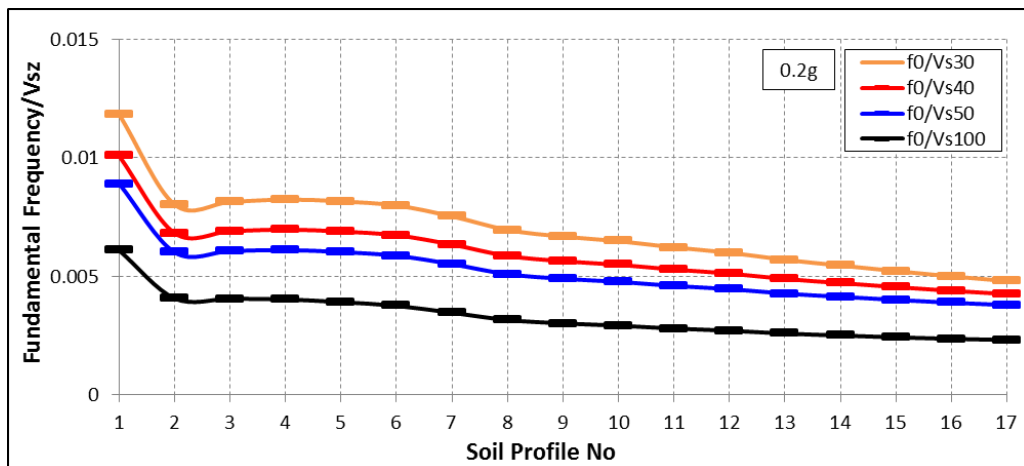


Figure 5.122. The correlation of f_0 with V_{sz} for 0.2g white-noise bedrock acceleration.

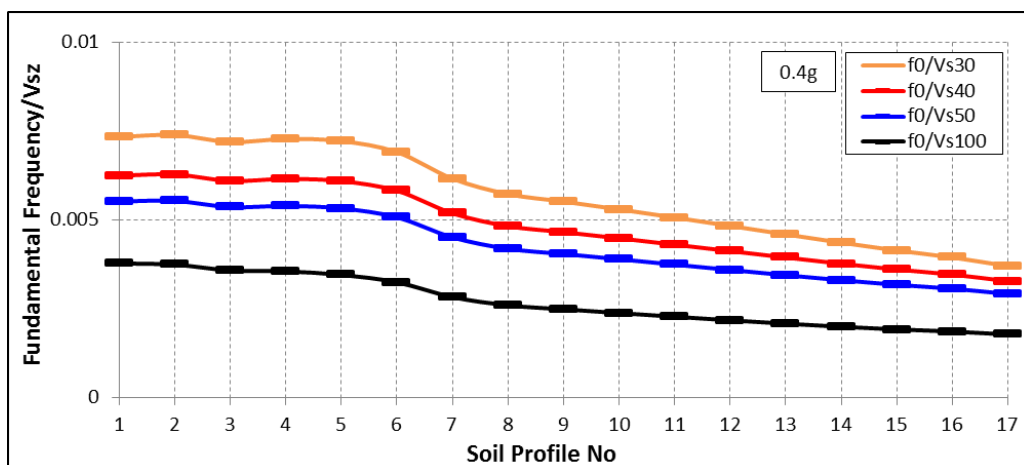


Figure 5.123. The correlation of f_0 with V_{sz} for 0.4g white-noise bedrock acceleration.

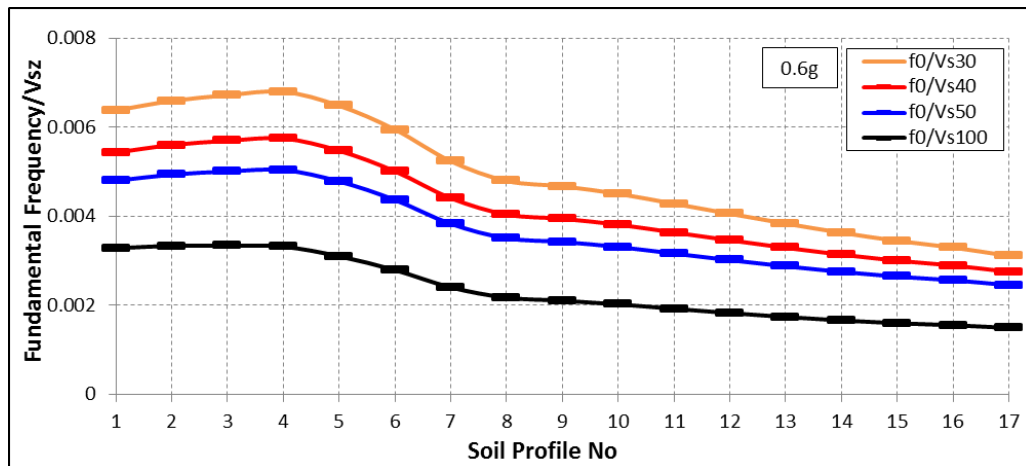


Figure 5.124. The correlation of f_0 with V_{sz} for 0.6g white-noise bedrock acceleration.

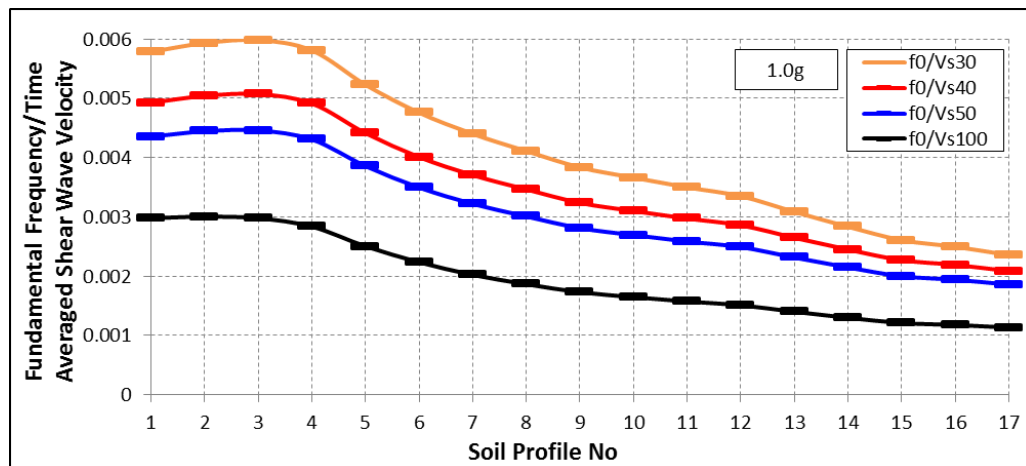


Figure 5.125. The correlation of f_0 with V_{sz} for 1.0g white-noise bedrock acceleration.

Convex profiles presented lower AE values for $\text{Acc.} \geq 0.4g$, pointing out a better characterization at nonlinear elastic and elasto-plastic strains. At 0.4g acceleration level, the best performing parameters were V_{s30} for no 1, 5; V_{s40} for no 2; V_{s50} for no 3, 6; and V_{s100} for no 4. At 0.6g, the best performing parameters were V_{s50} for no 1; V_{s30} for no 2, 5; V_{s100} for no 3 and 4. At 1.0g, the best performing parameters were V_{s40} for no 1 and V_{s100} for the rest. Linear and concave profiles presented similar AE values for all acceleration levels pointing out V_{s100} as the best performing parameter for all profiles.

As a general statement, the optimal parameter was V_{s100} for all profile types that can be used for $\text{Acc.} \geq 0.4g$ for convex and for all acceleration levels for linear/concave type profiles.

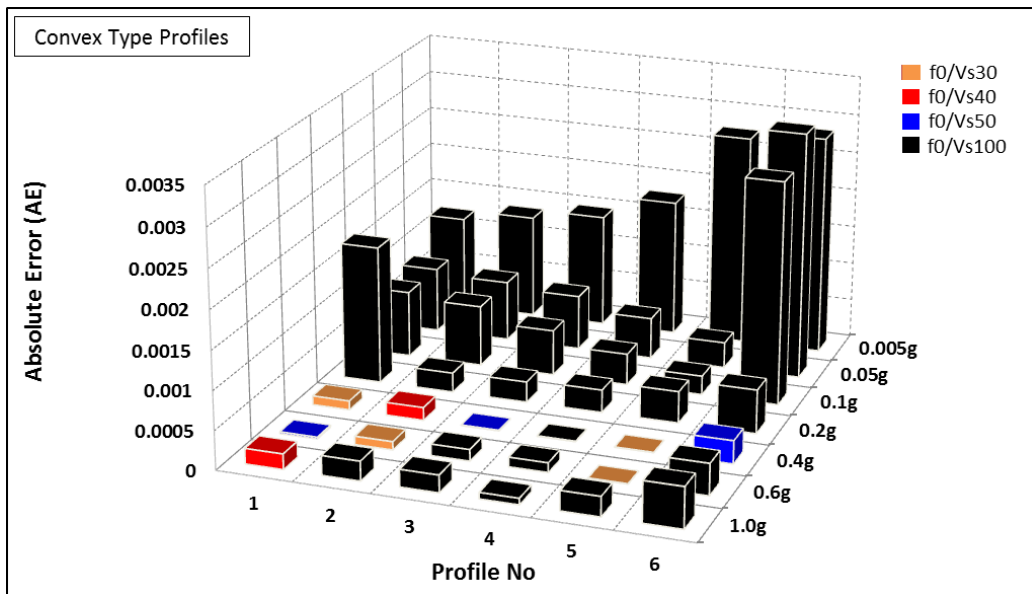


Figure 5.126. The variation of AE for f_0/V_{sz} with increasing white-noise bedrock accelerations for convex profiles.

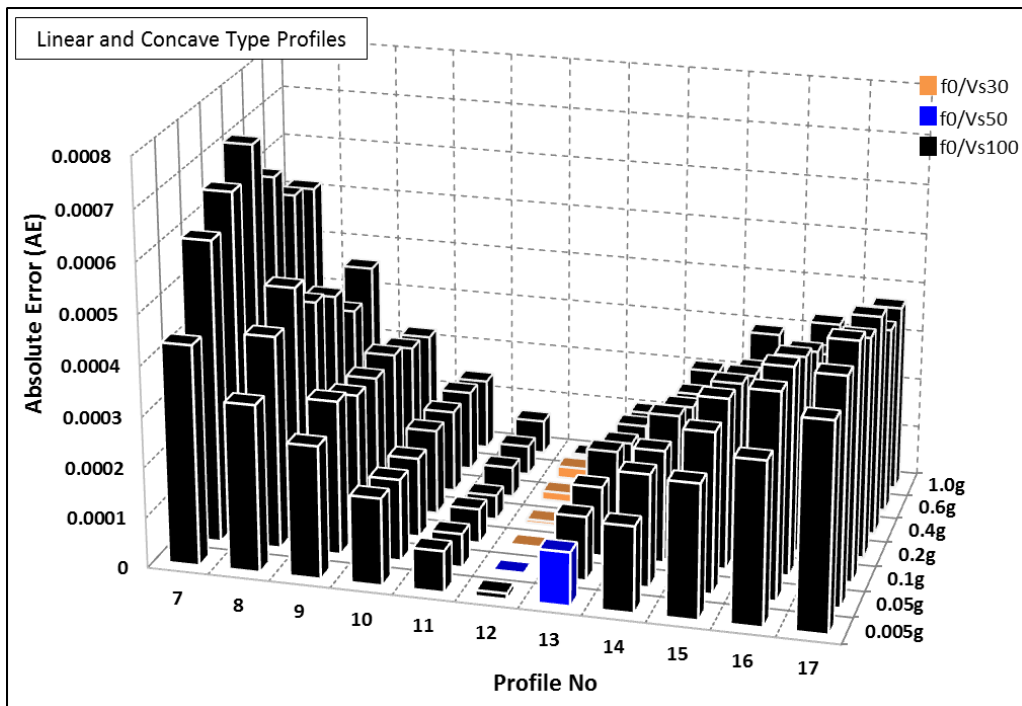


Figure 5.127. The variation of AE for f_0/V_{sz} with increasing white-noise bedrock accelerations for linear/concave profiles.

5.2.2.6. Fundamental Frequency Characterization by T_{tz} . We have investigated the correlation of fundamental frequency with T_{tz} for gradually increasing white-noise type bedrock motions by checking if $(f_0 \times T_{tz})$ is close to a constant. As mentioned in the section of characterization of f_0 by V_{sz} , the correlations of $f_0 \times T_{tz}$ are affected by the f_0 values of convex profiles which are observed at the 1st, 2nd and 3rd peaks of transfer functions. The correlations were shown in Figure 5.128-5.134 for gradually increasing white-noise bedrock acceleration levels. For convex profiles, we have observed linear relations rather than constant ones for accelerations $\geq 0.4g$. Linear and concave profiles presented linear relations as well for all acceleration levels. We calculated the AE values for each profile type and bedrock acceleration level (Figure 5.135 and 5.136).

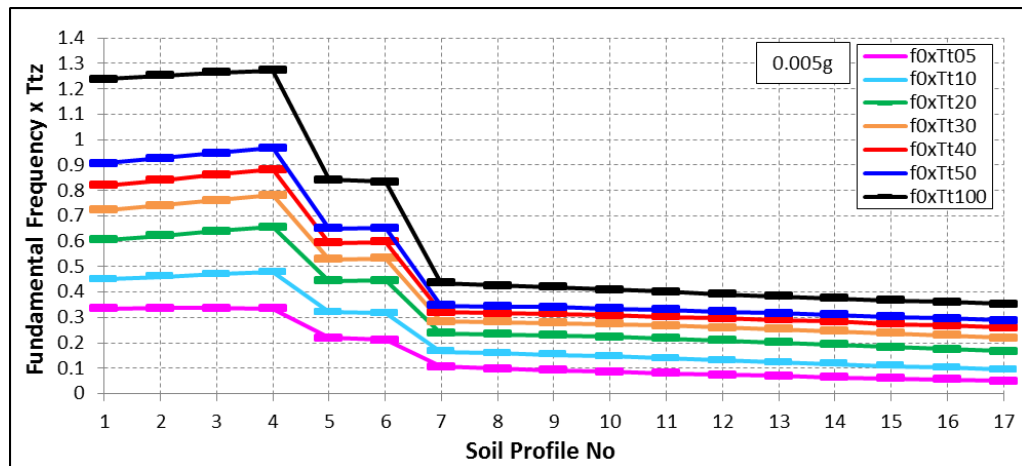


Figure 5.128. The correlation of f_0 with T_{tz} for 0.005g white-noise bedrock acceleration.

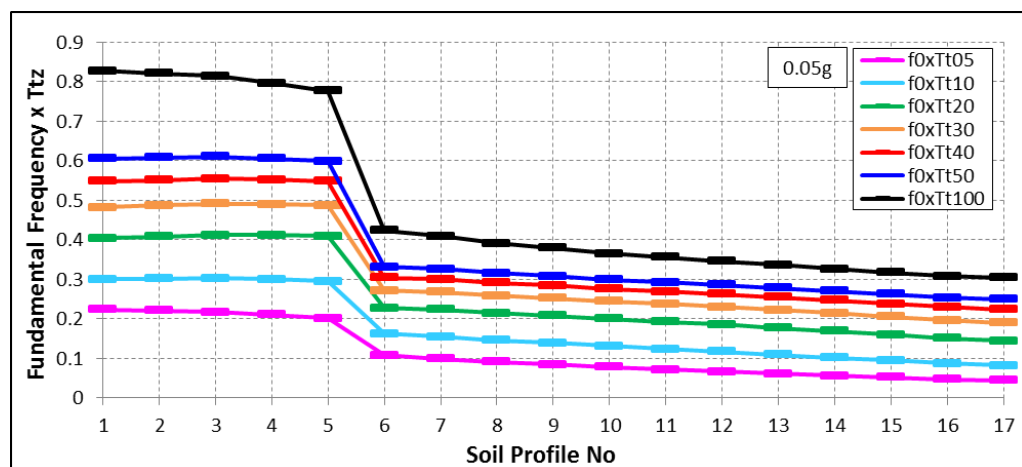


Figure 5.129. The correlation of f_0 with T_{tz} for 0.05g white-noise bedrock acceleration.

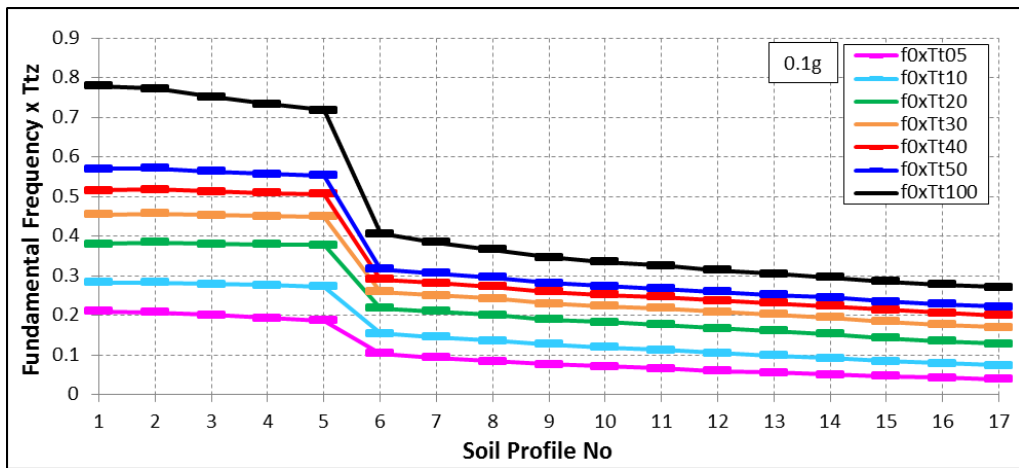


Figure 5.130. The correlation of f_0 with T_{tz} for 0.1g white-noise bedrock acceleration.

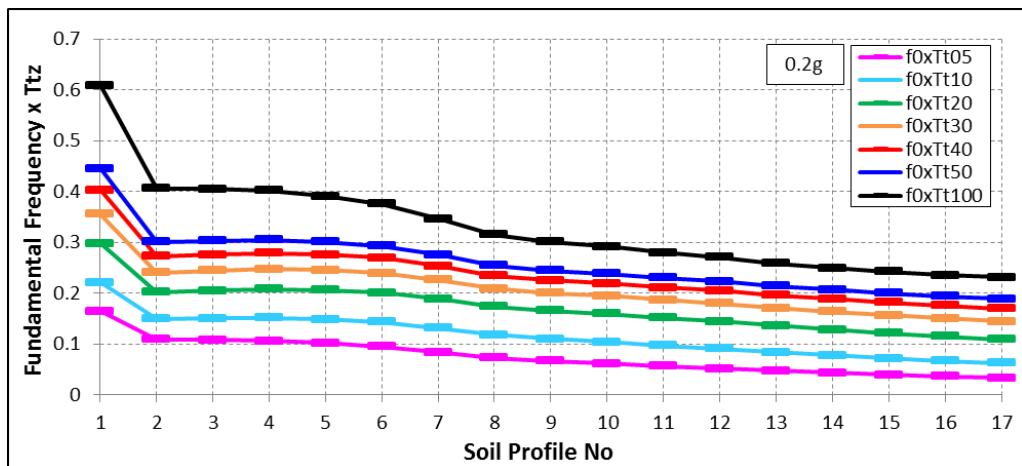


Figure 5.131. The correlation of f_0 with T_{tz} for 0.2g white-noise bedrock acceleration.

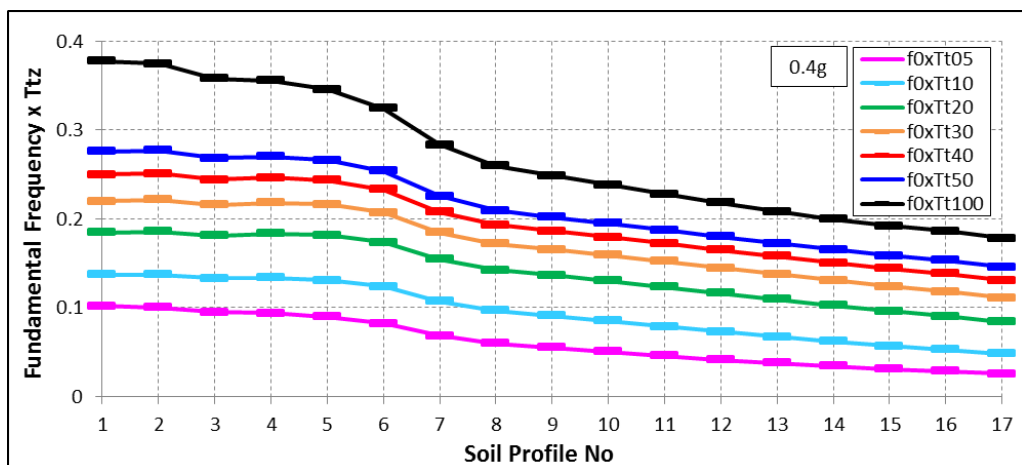


Figure 5.132. The correlation of f_0 with T_{tz} for 0.4g white-noise bedrock acceleration.

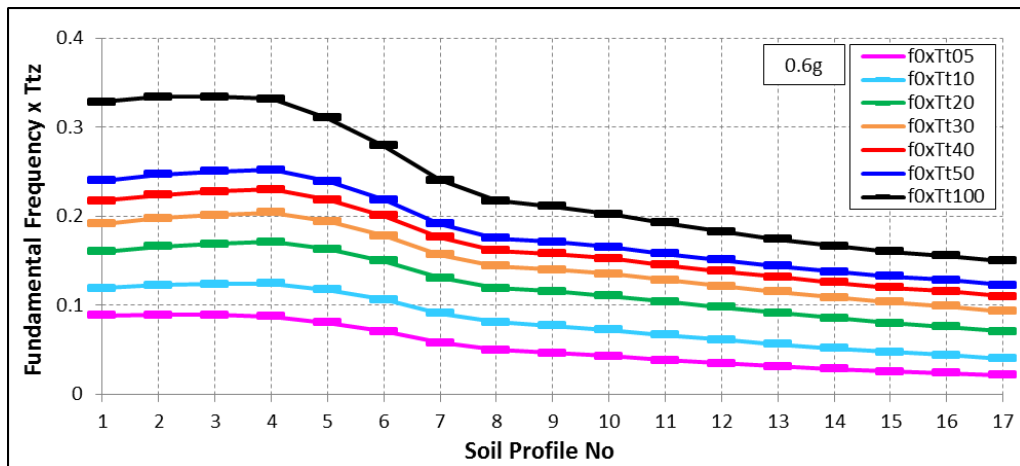


Figure 5.133. The correlation of f_0 with T_{tz} for 0.6g white-noise bedrock acceleration.

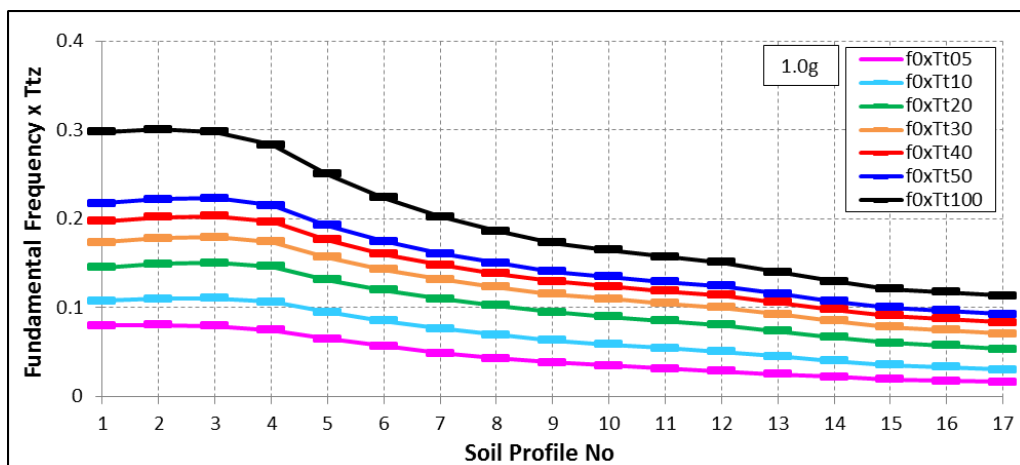


Figure 5.134. The correlation of f_0 with T_{tz} for 1.0g white-noise bedrock acceleration.

For convex profiles, the AE values were lower at $\text{Acc.} \geq 0.4g$. At 0.4g bedrock acceleration level, the best performing parameters were T_{t20} for no 1, 2, 5, 6; T_{t10} for no 3 and T_{t05} for no 4. At 0.6g, the best performing ones were T_{t10} for no 1, 6; T_{t20} for no 2, 5; and T_{t05} for no 3, 4. At 1.0g acceleration level, the best performing ones were T_{t20} for no 1; T_{t10} for no 2, 5; and T_{t05} for 3, 4, 6. For linear and concave profiles, the AE levels were obtained so similar for each bedrock acceleration. The best performing parameter was T_{t05} for all profiles and acceleration levels.

As a general statement, the optimal parameter was T_{t20} for 0.4g, T_{t05} for 0.6g and 1.0g for convex profiles; and T_{t05} for all acceleration levels for linear/concave profiles.

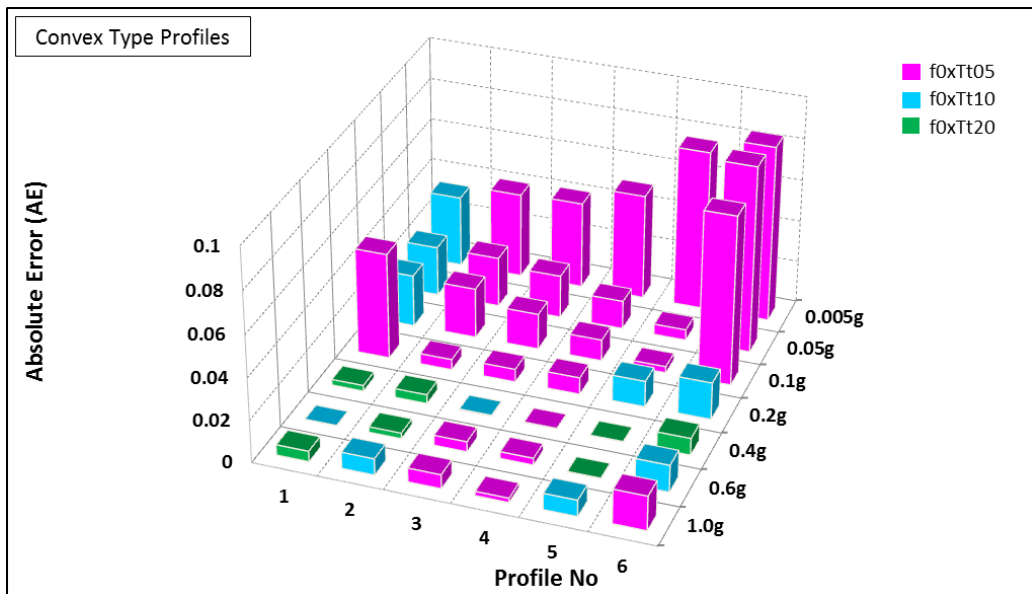


Figure 5.135. The variation of AE for f_{0xT_tz} with increasing white-noise bedrock accelerations for convex profiles.

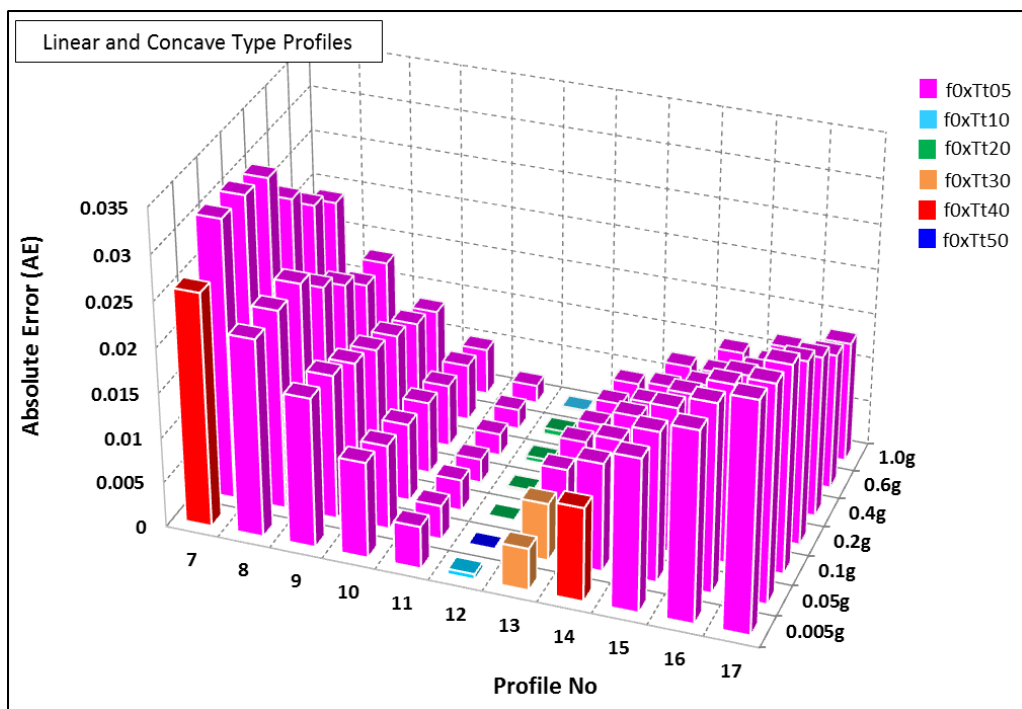


Figure 5.136. The variation of AE for f_{0xT_tz} with increasing white-noise bedrock accelerations for linear/concave profiles.

5.2.3. Analyses of Equal Wave Travel Time Model Under Impulsive Bedrock Motions

We have investigated the site amplification for the 17 velocity profiles under impulsive bedrock accelerations by dividing them into layers with equal wave travel time ($t=0.04$ sec) and gradually increasing the amplitude of the impulse. Unlike equal-thickness layer model, the layer thicknesses, layer numbers and bedrock depths of these profiles are different from each other (Table 5.11 and 5.12). The profile numbers 1 to 6 represent Convex-6 to Convex-1 and 7 to 17 represent Linear to Concave-10. For convex type profiles, the number of layers is less than those for linear/concave profiles and the thickness of layers increases from Concave-10 to Convex-6 in order to have equal wave travel time in each layer.

Table 5.11. Layer properties of convex profiles with equal wave travel time.

Layer No	Layer Thickness for each Profile Type (m)					
	1	2	3	4	5	6
1	2.0	2.0	2.0	2.0	2.0	2.0
2	8.3	7.1	5.9	4.9	4.1	3.5
3	16.1	13.8	11.5	9.3	7.4	5.8
4	24.2	21.5	18.4	15.2	12.0	9.2
5	32.4	29.7	26.4	22.6	18.3	14.1
6			35.4	31.4	26.4	20.8
7						30.0

Table 5.12. Layer properties of linear/concave profiles with equal wave travel time.

Layer No	Layer Thickness for each Profile Type (m)										
	7	8	9	10	11	12	13	14	15	16	17
1	2.0	2.0	2.0	2.0	2.0	2.0	2.0	2.0	2.0	2.0	2.0
2	3.0	2.7	2.6	2.5	2.4	2.3	2.2	2.2	2.2	2.1	2.1
3	4.3	3.6	3.2	3.0	2.8	2.7	2.5	2.4	2.4	2.3	2.3
4	6.3	4.9	4.3	3.8	3.4	3.1	2.9	2.7	2.6	2.5	2.4
5	9.4	6.9	5.7	4.8	4.2	3.7	3.3	3.1	2.8	2.7	2.6
6	13.8	9.8	7.8	6.3	5.2	4.4	3.9	3.5	3.2	3.0	2.8
7	20.4	14.1	10.9	8.5	6.7	5.5	4.6	4.0	3.6	3.3	3.1
8	30.0	20.8	15.7	11.8	9.0	7.0	5.7	4.8	4.1	3.7	3.3
9		31.5	23.6	17.2	12.4	9.2	7.1	5.7	4.8	4.2	3.7
10				26.5	18.4	12.9	9.3	7.1	5.7	4.8	4.2
11					29.4	19.2	13.0	9.3	7.0	5.6	4.8
12							19.8	12.8	9.0	6.9	5.5
13								19.8	12.4	8.7	6.6
14									19.4	11.9	8.3
15										18.6	11.2
16											17.4

We calculated soil amplification factors and fundamental frequencies for gradually increasing acceleration levels, and presented in Table 5.13 and Table 5.14. The soil amplification factors decreased with increasing nonlinearity, and they were close to the soil amplification factors of equal-thickness layer models.

Table 5.13. Fundamental frequencies (f_0) for gradually increasing bedrock accelerations.

Soil Profile No	Soil Type	f_0 -0.005g	f_0 -0.05g	f_0 -0.1g	f_0 -0.2g	f_0 -0.4g	f_0 -0.6g	f_0 -1.0g
1	Convex-6	5.121	4.913	4.730	4.419	3.741	2.393	2.313
2	Convex-5	5.035	4.822	4.645	4.340	3.668	2.368	2.258
3	Convex-4	6.030	4.175	4.071	3.870	3.394	2.997	1.996
4	Convex-3	6.036	4.034	3.925	3.723	3.278	1.990	1.892
5	Convex-2	4.010	3.882	3.766	3.577	1.941	1.880	1.758
6	Convex-1	3.418	3.314	3.223	1.740	1.672	1.611	1.495
7	Linear	1.569	1.538	1.508	1.465	1.392	1.324	1.208
8	Concave-1	1.367	1.337	1.306	1.257	1.184	1.117	1.007
9	Concave-2	1.270	1.233	1.202	1.154	1.080	1.013	0.903
10	Concave-3	1.135	1.105	1.074	1.025	0.958	0.891	0.793
11	Concave-4	1.025	0.989	0.964	0.916	0.848	0.793	0.702
12	Concave-5	0.940	0.903	0.879	0.836	0.775	0.720	0.635
13	Concave-6	0.848	0.812	0.787	0.751	0.690	0.647	0.568
14	Concave-7	0.763	0.732	0.714	0.677	0.623	0.580	0.507
15	Concave-8	0.696	0.665	0.641	0.610	0.562	0.519	0.458
16	Concave-9	0.635	0.604	0.586	0.555	0.507	0.470	0.415
17	Concave-10	0.580	0.555	0.537	0.507	0.464	0.433	0.378

Table 5.14. Soil amplification factors (AF) for gradually increasing bedrock accelerations.

Soil Profile No	Soil Type	AF-0.005g	AF-0.05g	AF-0.1g	AF-0.2g	AF-0.4g	AF-0.6g	AF-1.0g
1	Convex-6	15.24	13.29	11.74	9.68	7.52	7.25	8.22
2	Convex-5	15.54	13.20	11.61	9.68	7.77	8.06	8.78
3	Convex-4	14.66	11.55	11.09	10.13	8.45	7.64	8.34
4	Convex-3	13.58	11.64	10.93	9.93	8.56	8.31	9.03
5	Convex-2	13.12	11.52	10.58	9.60	9.05	9.15	9.13
6	Convex-1	11.65	10.45	9.82	9.14	9.21	9.13	8.88
7	Linear	11.65	11.12	10.71	10.18	9.54	9.04	8.03
8	Concave-1	13.46	12.28	11.50	10.54	9.41	8.62	7.27
9	Concave-2	15.66	13.40	12.13	10.70	9.13	8.16	6.77
10	Concave-3	16.46	13.65	12.20	10.58	8.88	7.84	6.47
11	Concave-4	17.40	13.86	12.20	10.41	8.59	7.52	6.16
12	Concave-5	19.08	14.36	12.35	10.33	8.39	7.31	5.97
13	Concave-6	19.75	14.38	12.24	10.14	8.17	7.09	5.79
14	Concave-7	20.42	14.37	12.10	9.94	7.98	6.91	5.64
15	Concave-8	21.07	14.37	11.98	9.79	7.82	6.75	5.53
16	Concave-9	21.58	14.32	11.90	9.65	7.67	6.63	5.43
17	Concave-10	22.15	14.31	11.79	9.55	7.58	6.54	5.37

The variation of V_s with depth and the impedance ratio (i.e., α_z : the ratio of the upper to lower layer impedances for upgoing waves) between consecutive layers are presented for Concave-10, Linear and Convex-6 profiles (Table 5.15).

Table 5.15. V_s and α_z for Concave-10, Linear and Convex-6 profiles.

Layer No	Concave-10			Linear			Convex-6		
	V_s (m/sec)	Depth (m)	α_z	V_s (m/sec)	Depth (m)	α_z	V_s (m/sec)	Depth (m)	α_z
1	50.0	2.0	0.941	50.0	2.0	0.633	50.0	2.0	0.175
2	53.1	4.1	0.937	79.0	5.0	0.654	286.3	10.3	0.582
3	56.7	6.4	0.933	120.7	9.3	0.662	492.2	26.4	0.705
4	60.7	8.8	0.928	182.2	15.6	0.667	698.6	50.5	0.770
5	65.4	11.4	0.923	273.2	25.0	0.671	906.6	82.9	0.453
6	70.9	14.2	0.915	407.1	38.8	0.673			
7	77.5	17.2	0.907	604.4	59.2	0.675			
8	85.4	20.6	0.897	895.2	89.2	0.448			
9	95.2	24.3	0.885						
10	107.6	28.5	0.869						
11	123.8	33.2	0.848						
12	146.0	38.7	0.819						
13	178.3	45.4	0.777						
14	229.6	53.7	0.707						
15	324.7	64.9	0.578						
16	562.3	82.3	0.281						

The impedance ratio between the soil layers decreased with increasing depth for Concave-10 profile, and increased with increasing depth for both Linear and Convex-6 profiles. There was a sharp transition of V_s between the top and bottom layer of Convex-6, hence impedance contrast was seen higher at the upper layers of convex profiles. The bedrock V_s was defined as 2000 m/sec for all profiles as before.

We presented in Figure 5.137 the surface PGAs with respect to bedrock acceleration levels. The increase in bedrock PGAs increased the nonlinearity and therefore decreased the surface PGAs. The surface PGAs were close to those for the equal-thickness layer models.

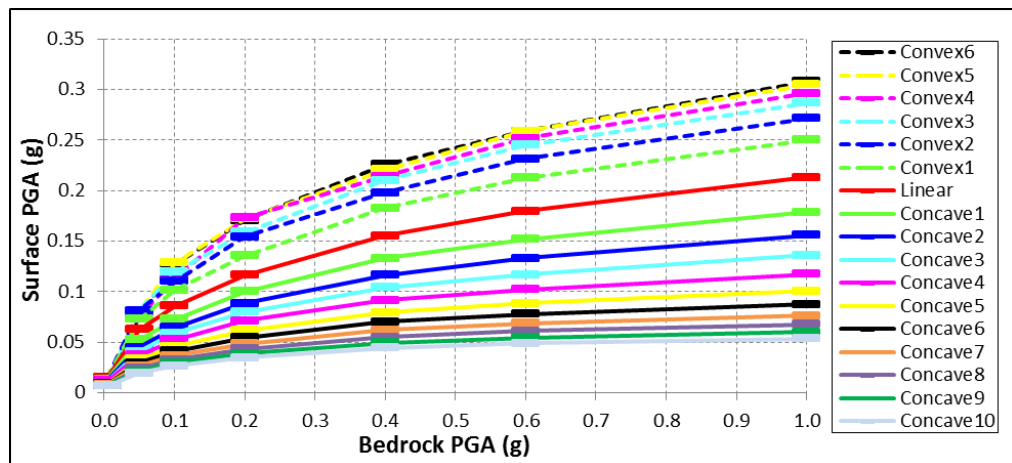


Figure 5.137. Surface PGAs with respect to gradually increasing bedrock PGAs.

The transfer functions are presented for 0.005g, 0.05g, 0.1g, 0.2g, 0.4g, 0.6g and 1.0g bedrock acceleration levels in Figure 5.138 to Figure 5.144, and the maximum amplitudes, corresponding to the amplification factor, were marked by red dots on the figures.

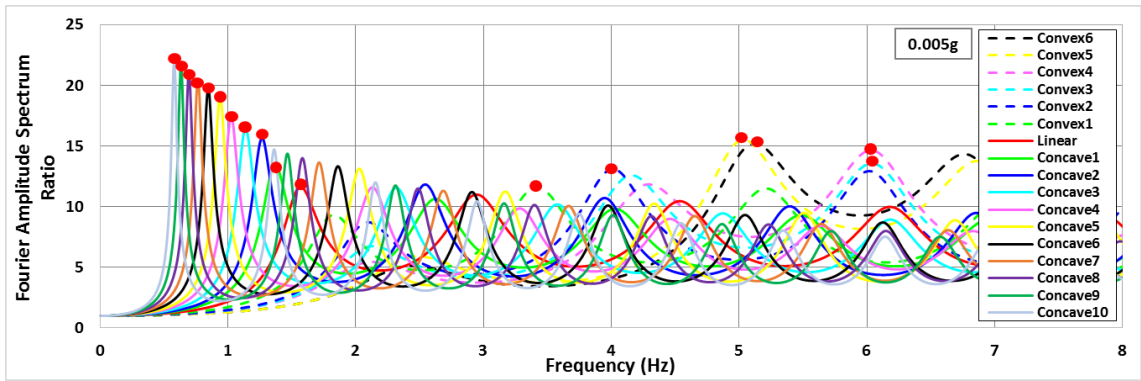


Figure 5.138. Transfer functions at 0.005g impulsive acceleration level.

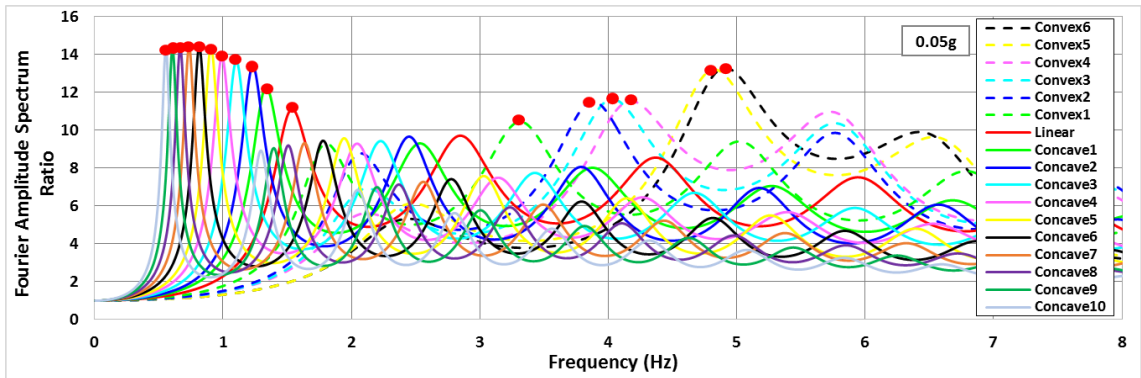


Figure 5.139. Transfer functions at 0.05g impulsive acceleration level.

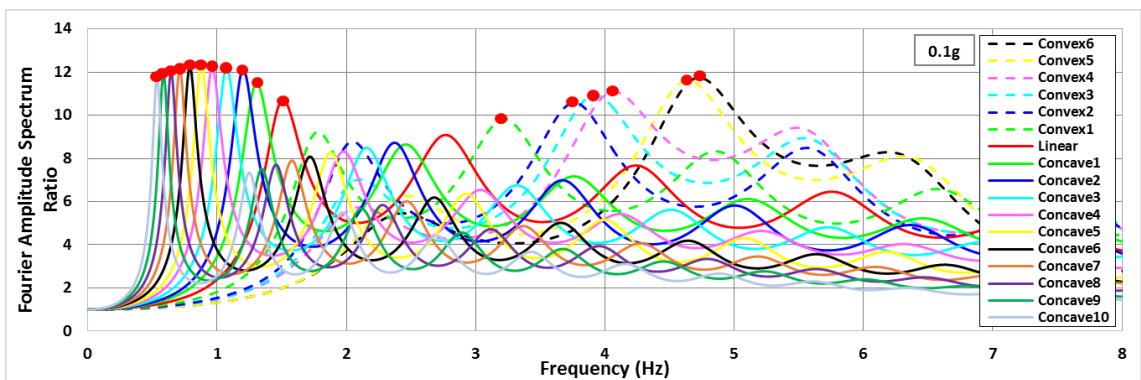


Figure 5.140. Transfer functions at 0.1g impulsive acceleration level.

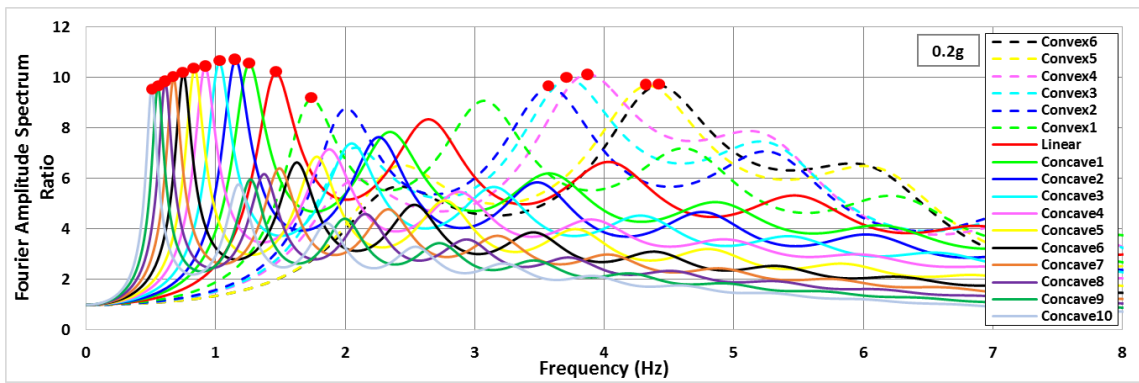


Figure 5.141. Transfer functions at 0.2g impulsive acceleration level.

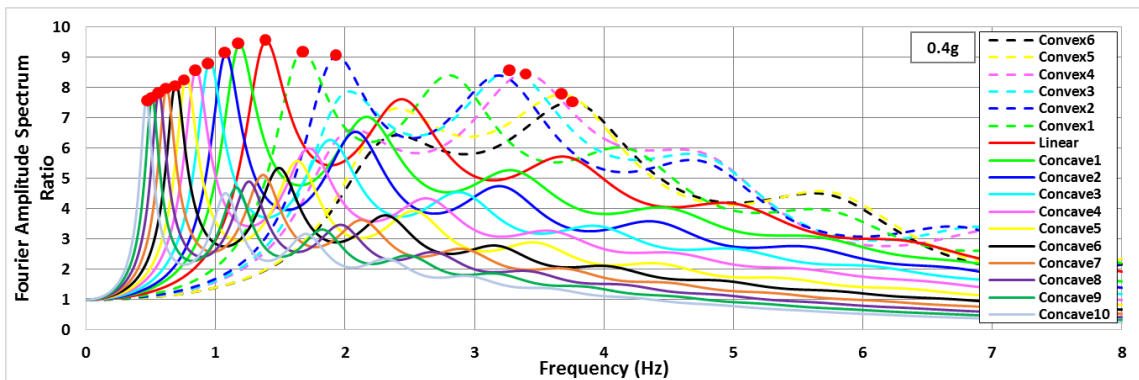


Figure 5.142. Transfer functions at 0.4g impulsive acceleration level.

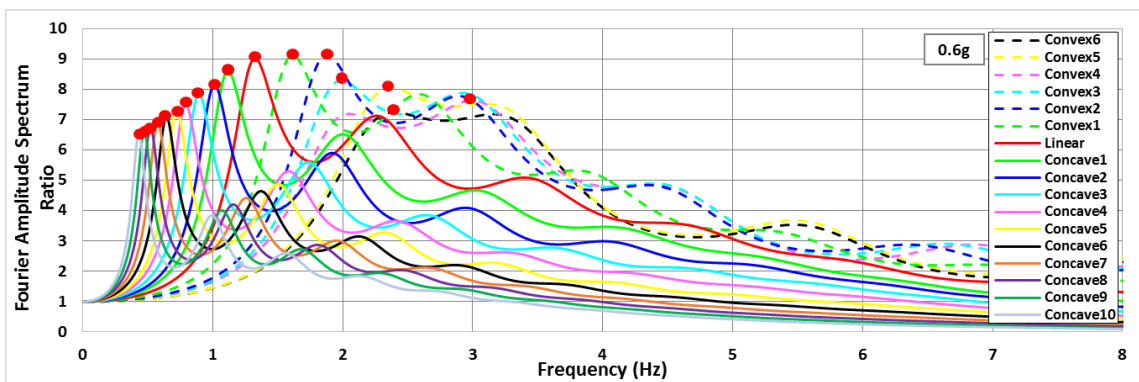


Figure 5.143. Transfer functions at 0.6g impulsive acceleration level.

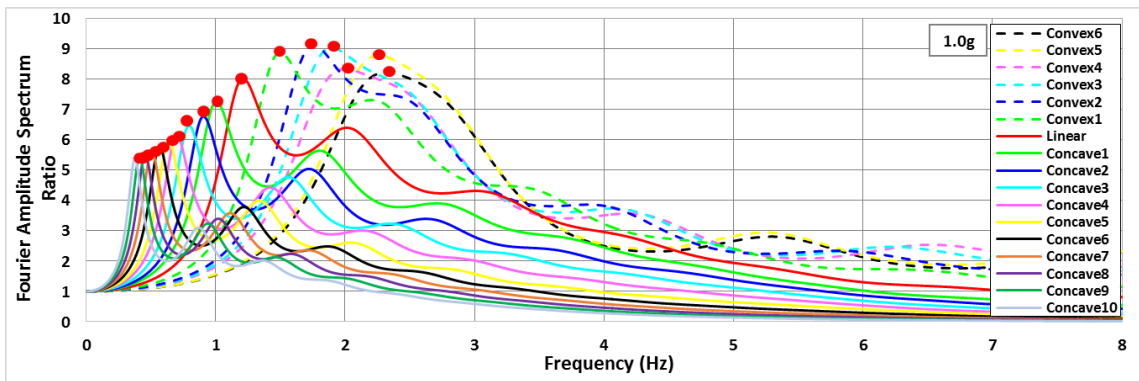


Figure 5.144. Transfer functions at 1.0g impulsive acceleration level.

The soil amplification factors and corresponding fundamental frequencies for each profiles were shown for increasing bedrock acceleration amplitudes in Figure 5.145.

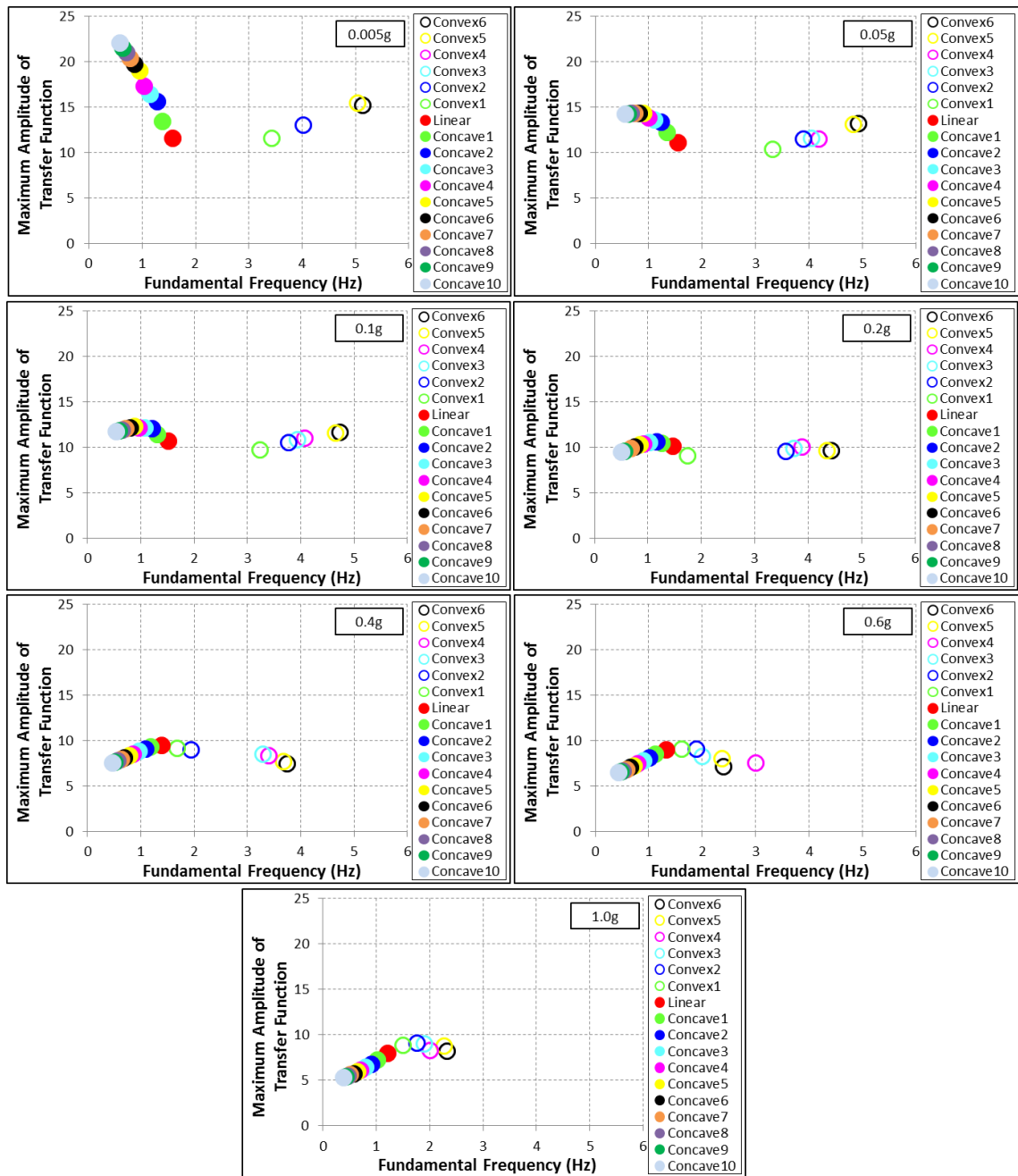


Figure 5.145. Maximum amplitudes of transfer functions and corresponding fundamental frequencies for impulsive bedrock accelerations.

The variations of soil amplification factors can be explained as follows:

1. The soil amplification factor of Concave-10 was higher compared to stiffer profiles at 0.005g bedrock acceleration level. As the bedrock PGAs increased gradually, the soil amplification factors decreased more rapidly for the softer profiles by the effect of rapid stiffness degradation.

- The soil amplification factor for Convex-6 was higher compared to Convex-1 for up to 0.2g bedrock accelerations. This can be explained by the higher impedance contrast between the top and consecutive layers and lower damping ratio. For 0.2g and higher bedrock accelerations, we see nonlinearity for convex profiles. The stiffness degradation and damping ratio increased at the top layer for Convex-6, hence the soil amplification factor was lower than that for Convex-1. Additionally, fundamental frequencies for convex profiles were at higher modes and low bedrock accelerations.

The transfer functions of velocity profiles for both layering models ($h=2$ m and $t=0.04$ sec) were close to each other. We can conclude that the same velocity profiles with different layering discretization result in closer cyclic behavior of soil, especially for linear and concave profiles.

5.2.3.1. Site Amplification Characterization by Surface PGA. The amplification and de-amplification of surface PGAs for each profile are presented in Figure 5.146 as the ratio of surface PGAs to bedrock PGAs. For 0.005g bedrock accelerations, all profiles show amplification.

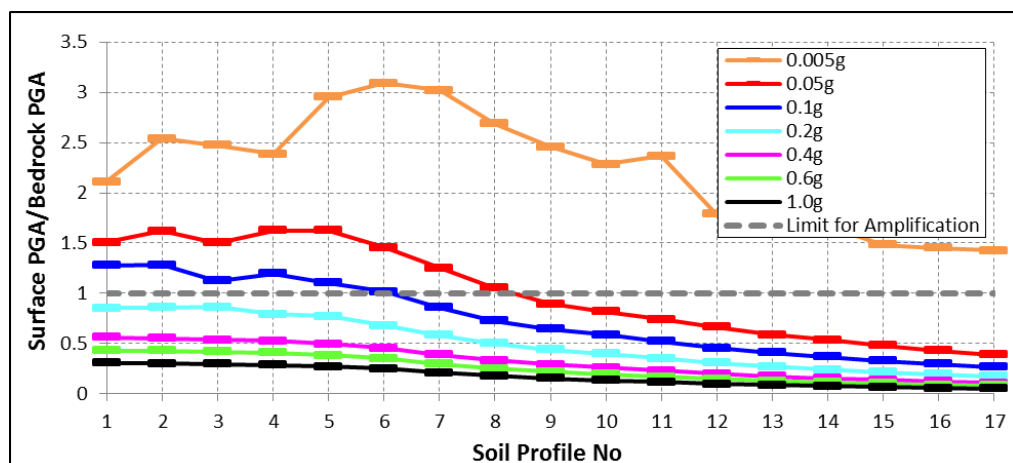


Figure 5.146. Amplification and de-amplification of surface PGAs for each profile.

At 0.05g, the amplification was seen just for convex and linear profiles, and at 0.1g just for convex profiles. For the rest of bedrock acceleration levels, we have observed de-amplification of surface PGAs due to increase in damping and nonlinearity. We have

investigated the correlation of soil amplification factors with surface PGAs for gradually increasing bedrock accelerations, as shown in Figure 5.147. The surface PGAs and soil amplification factors for 0.005g bedrock acceleration level are higher than those for higher bedrock accelerations by the effect of linearity. Hence, the 0.005g curves are much higher than the other curves in Figures 5.146 and 5.147.

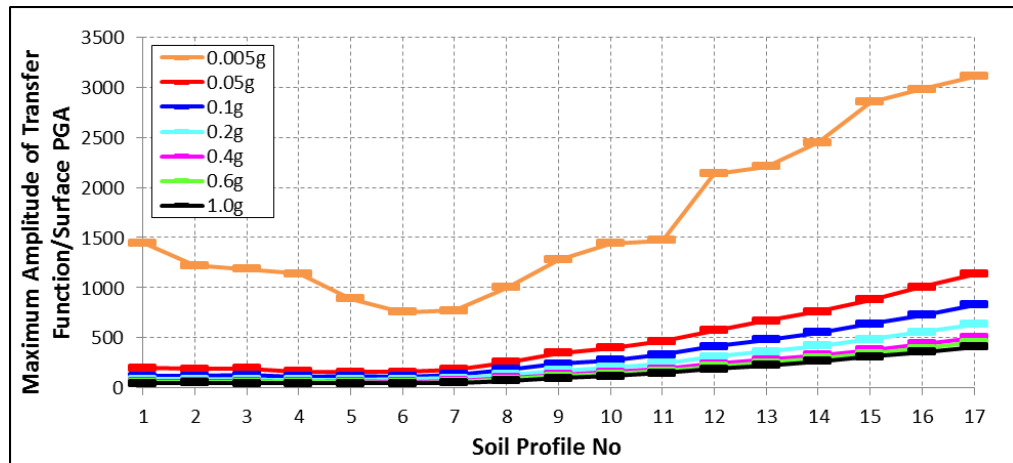


Figure 5.147. The correlation of soil amplification factors with surface PGAs with respect to velocity profiles.

Figure 5.148, which is the close up of Figure of 5.147 for convex profiles (Profiles 1-6), shows almost constant relation with increasing bedrock accelerations. For those profiles, surface PGA can be considered a good parameter for soil amplification factor at $\text{Acc.} \geq 0.1g$.

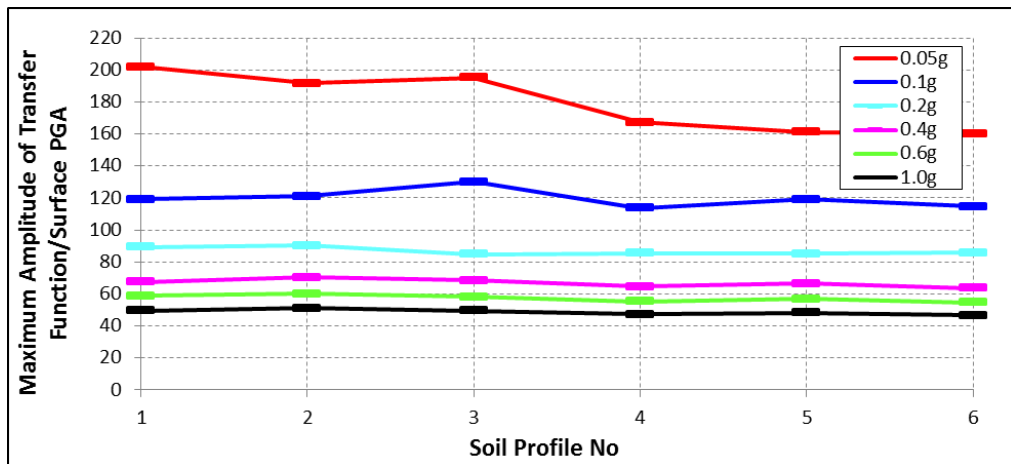


Figure 5.148. The correlation of soil amplification factors with surface PGAs with respect to convex profiles.

5.2.3.2. Site Amplification Characterization by Fundamental Soil Frequency, f_0 . We presented in Figure 5.149 and 5.150, respectively, the fundamental frequencies with respect to gradually increasing bedrock accelerations and the profile number. The fundamental frequencies of convex profiles were higher than those of linear and concave profiles, especially at low bedrock PGAs. For linear and concave profiles, the decrease with increasing bedrock accelerations were fairly linear.

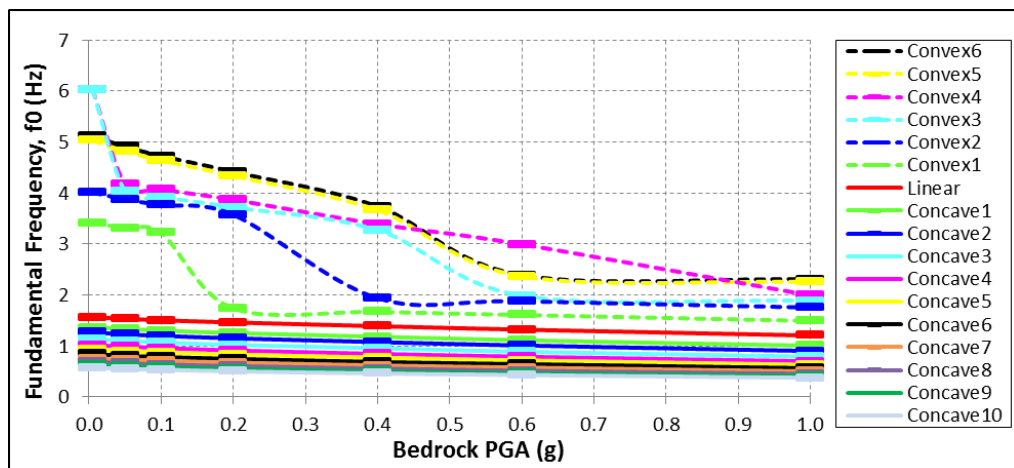


Figure 5.149. Fundamental frequencies with respect to bedrock PGAs for each profile.

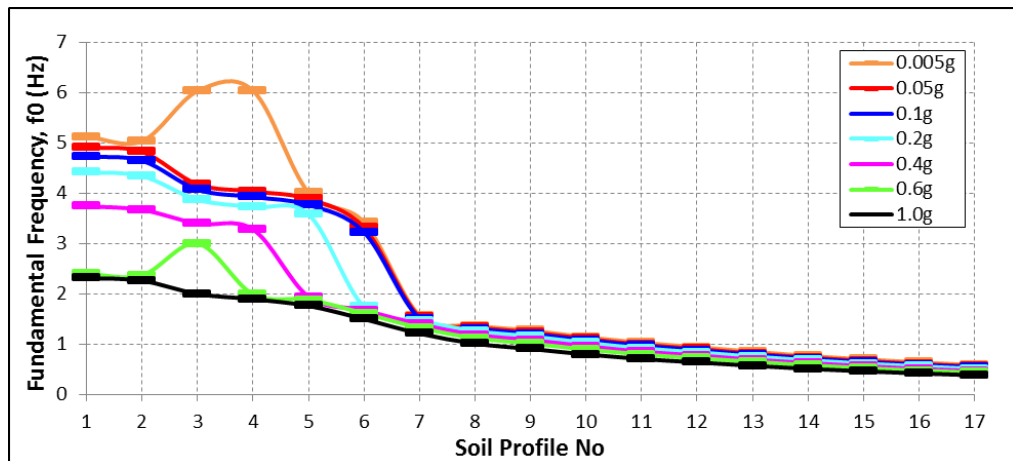


Figure 5.150. Fundamental frequencies with respect to profile numbers.

We have investigated the correlation of soil amplification factors with fundamental soil frequency for equal travel time model. The ratio of soil amplification factor to fundamental frequency was presented with respect to profile numbers in Figure 5.151. The ratios were constant just for convex profiles for $Acc. \leq 0.4g$, which indicates that the fundamental soil frequency can be used as a characterizing parameter for soil amplification in such profiles.

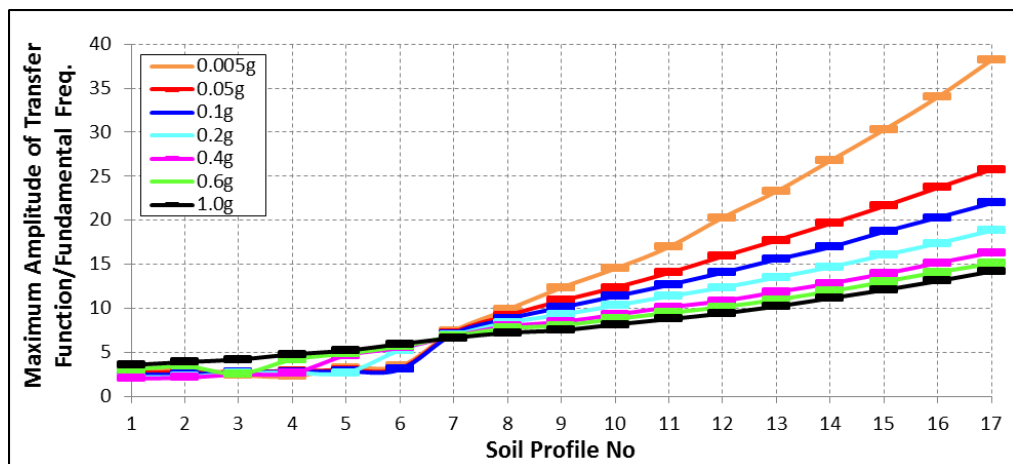


Figure 5.151. The correlation of soil amplification factor with f_0 with respect to profile number.

5.2.3.3. Site Amplification Characterization by V_{sz} . The correlation of soil amplification factors with V_{sz} for various depths was investigated for equal wave travel time. Since the velocity profiles were divided into layers with equal wave travel time, thickness of each layer and the bedrock depth are different for each profile. The depth value, z , in V_{sz} parameter is taken as 5 m, 10 m, 20 m, 30 m, 40 m, 50 m and the bedrock depth, which are different for each profile. For convex profiles, the correlations were observed to be constant for bedrock $Acc. \leq 0.2g$ and linear for $Acc. \geq 0.4g$, as seen in Figure 5.152-5.158. Linear/concave profiles presented linear relations with the profile number for $Acc. \leq 0.1g$ and constant relations for higher bedrock acceleration levels.

The best performing V_{sz} parameters to characterize site amplification were identified by the absolute error (AE) method, which defines the scatter from a constant, and shown in Figure 5.159 and 5.160 for gradually increasing bedrock accelerations. For convex profiles, the best performing parameters for 0.005g were V_{s50} for profiles no 1, 2, 4, 5; V_{s40} for no 3; and V_{sz} for no 6. For 0.05g, the optimal ones were V_{s50} for no 1, 3, 5; V_{s05} for no 2; V_{s20} for no 4; V_{sz} for no 6. For 0.1g, the best performing ones were V_{s50} for no 1, 3, 4, 5; and V_{sz} for no 2, 6. For 0.2g, the optimal ones were V_{s50} for no 1, 5; V_{sz} for no 2, 4, 6; and V_{s40} for no 3.

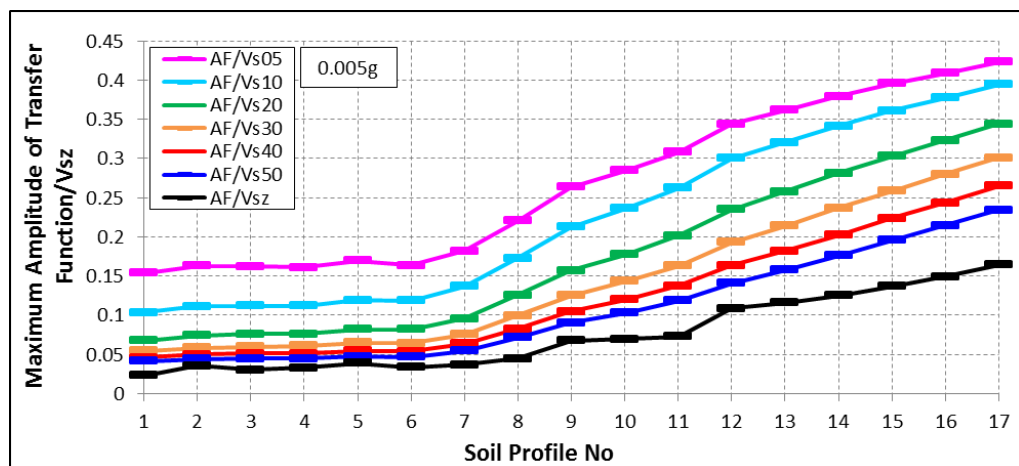


Figure 5.152. The correlation of AF with V_{sz} for 0.005g impulsive bedrock acceleration.

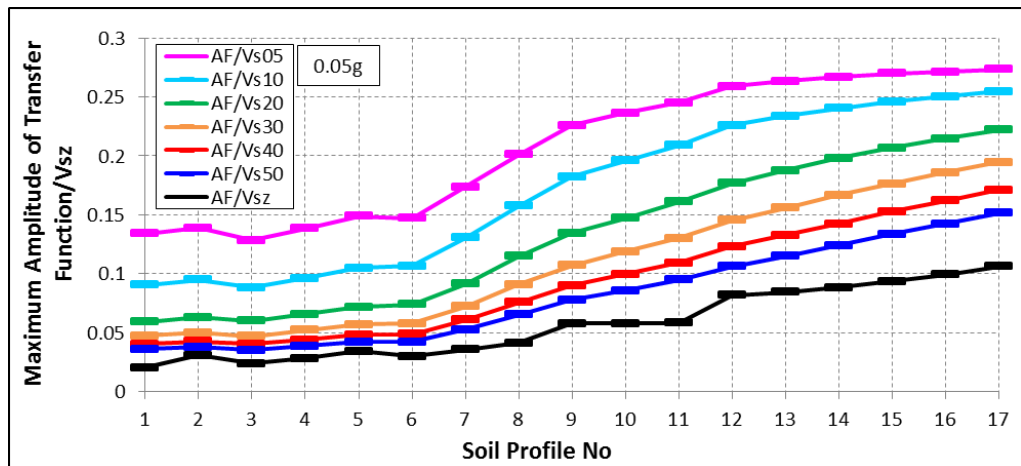


Figure 5.153. The correlation of AF with V_{sz} for 0.05g impulsive bedrock acceleration.

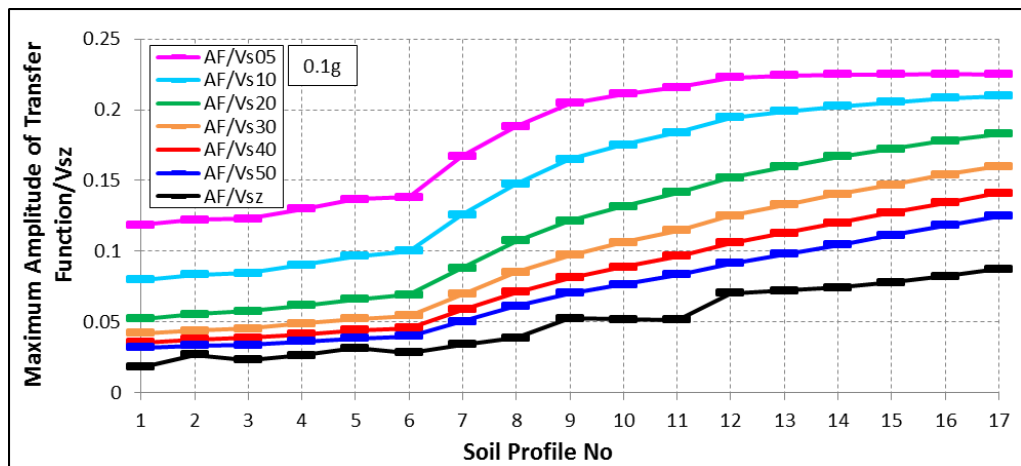


Figure 5.154. The correlation of AF with V_{sz} for 0.1g impulsive bedrock acceleration.

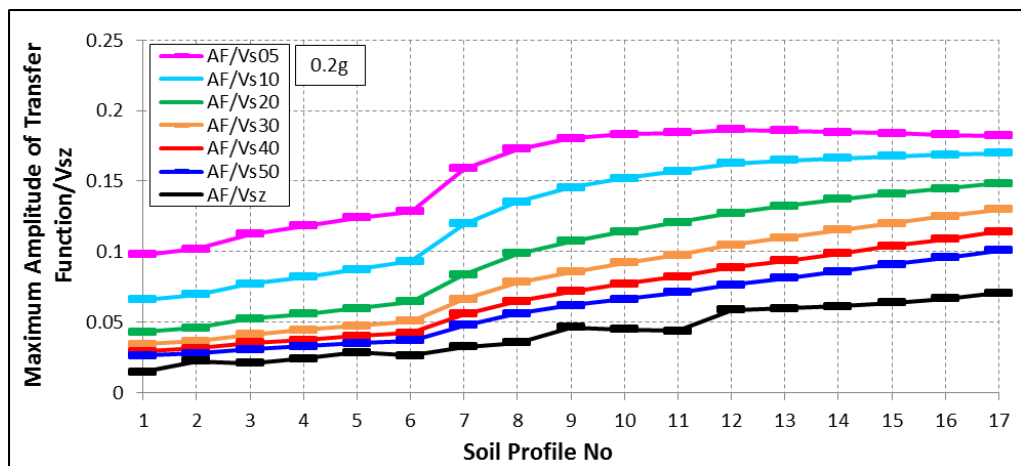


Figure 5.155. The correlation of AF with V_{sz} for 0.2g impulsive bedrock acceleration.

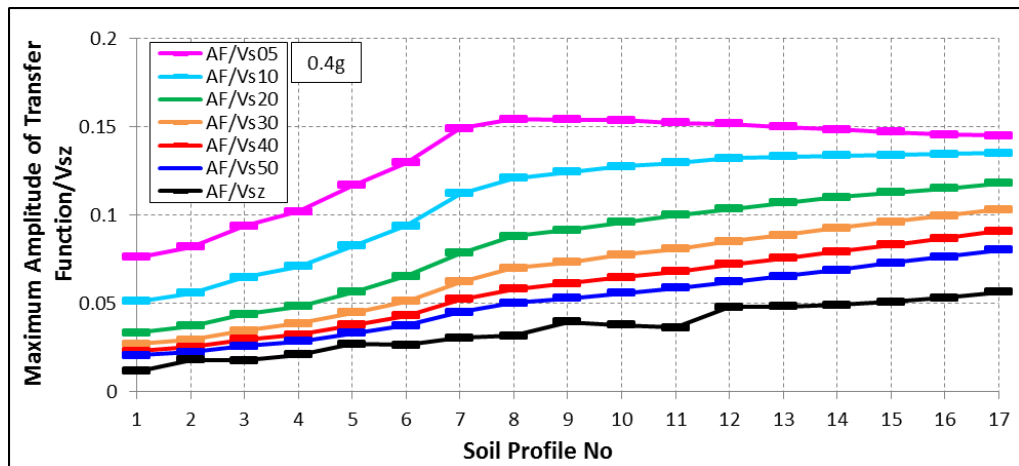


Figure 5.156. The correlation of AF with V_{sz} for 0.4g impulsive bedrock acceleration.

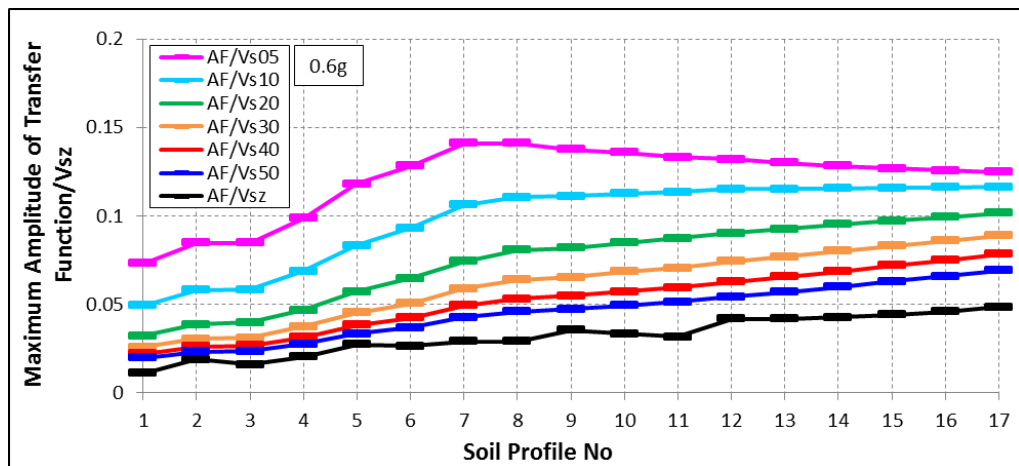


Figure 5.157. The correlation of AF with V_{sz} for 0.6g impulsive bedrock acceleration.

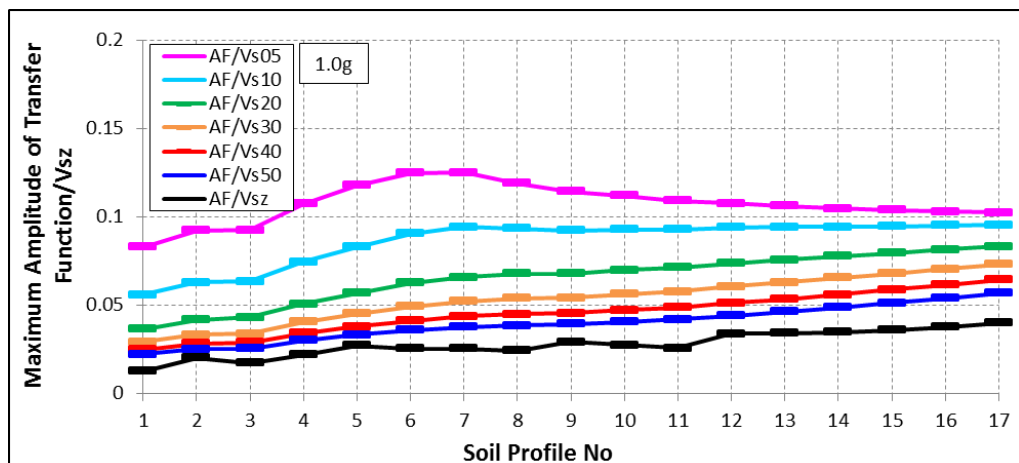


Figure 5.158. The correlation of AF with V_{sz} for 1.0g impulsive bedrock acceleration.

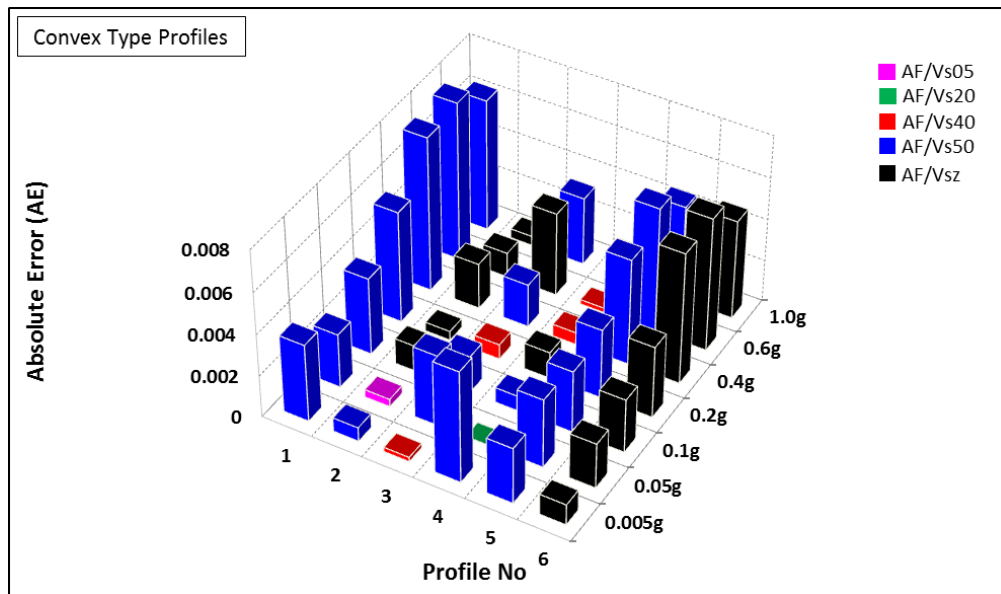


Figure 5.159. The variation of AE for AF/ V_{sz} with increasing impulsive bedrock accelerations for convex profiles.

For linear/concave profiles, the AE variation showed that the best performing parameters for 0.2g were V_{sz} for profile no 7; V_{s05} for no 8, 9, 10, 14, 15, 16, 17; V_{s10} for no 11; and V_{s50} for no 12, 13. For 0.4g acceleration level, the best performing ones were V_{s05} for no 7, 8, 9, 13, 14, 15, 16, 17; V_{s10} for no 10, 11; and V_{s40} for no 12. For 0.6g, the optimal parameters were V_{s10} for profiles no 7, 8, 9, 10, 11, 14, 15, 16, 17; V_{s30} for no 12; and V_{s50} for no 13. For 1.0g, the best performing parameters were V_{s10} for no 7, 8, 9, 10, 12, 13, 14, 15, 16, 17; and V_{s05} for no 11.

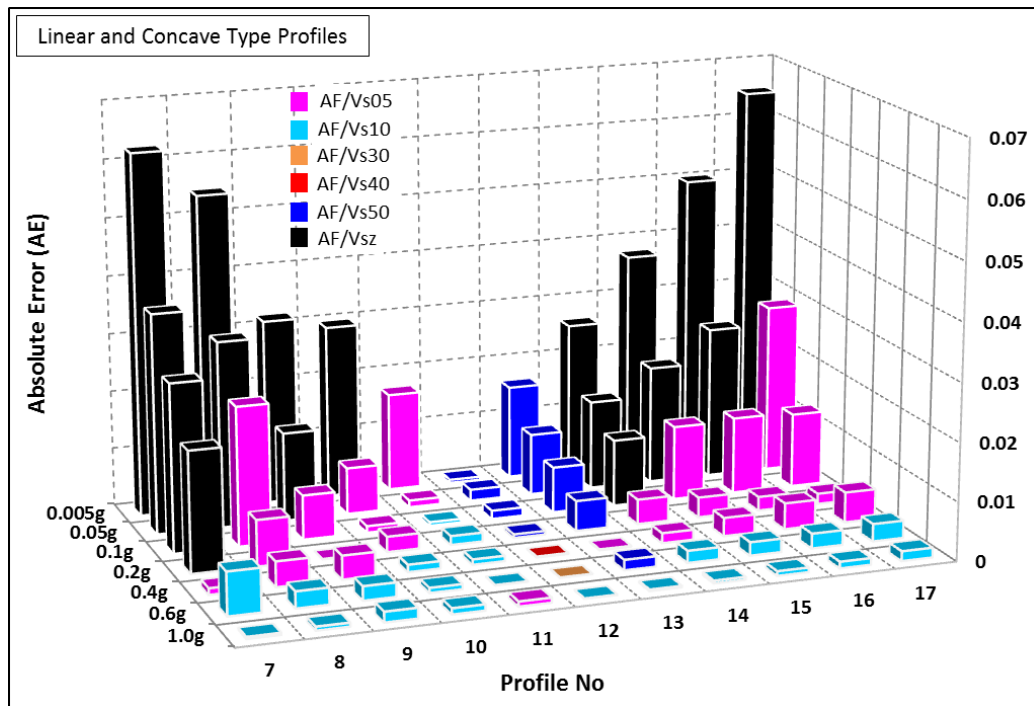


Figure 5.160. The variation of AE for AF/ V_{sz} with increasing impulsive bedrock accelerations for linear/concave profiles.

As a general statement, the optimal parameters were V_{s50} for $\text{Acc.} \leq 0.2g$ for convex profiles, where the AE values were the lowest, and V_{s05} and V_{s10} for $\text{Acc.} \geq 0.2g$ for linear and concave profiles.

5.2.3.4. Site Amplification Characterization by T_{tz} . We have investigated the correlation of soil amplification factor with T_{tz} at various depths for equal travel time soil model. The results are shown in Figures 5.161- 5.167. For convex profiles, the correlations were linear for $\text{Acc.} \leq 0.2g$, and constant for $\text{Acc.} \geq 0.4g$. For linear and concave profiles, the correlations were constant only for $\text{Acc.} \leq 0.05g$; linear relation were observed for higher bedrock accelerations.

The variation of AE for gradually increasing bedrock accelerations is presented in Figure 5.168 and 5.169. For convex profiles, the best performing parameters for 0.4g were T_{tz} for profiles no 1, 3, 5, 6; T_{t50} for no 2; and T_{t05} for no 4. For 0.6g, the best performing ones were T_{tz} for profiles no 1, 6; T_{t50} for no 2, 4, 5; and T_{t30} for no 3. For 1.0g, the optimal parameters for AF characterization were T_{tz} for no 1, 5, 6; T_{t50} for no 2; and T_{t20} for no 3, 4.

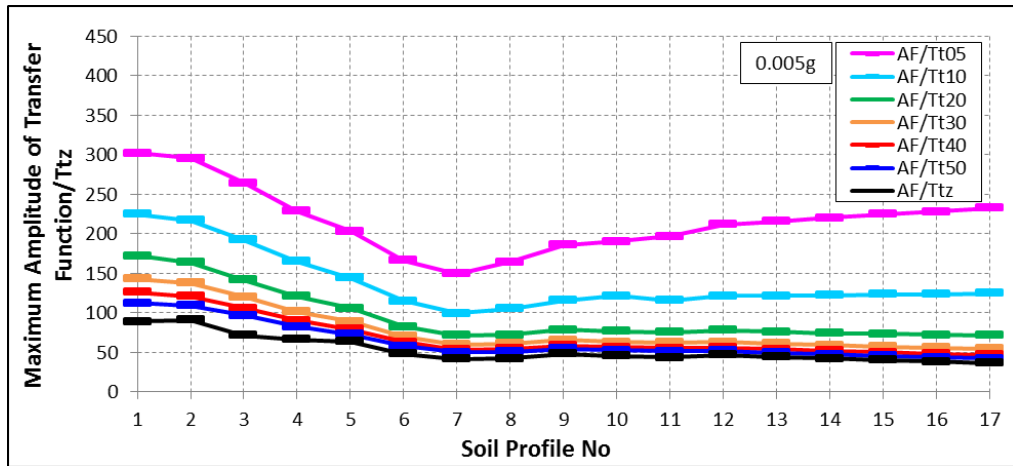


Figure 5.161. The correlation of AF with T_{tz} for 0.005g impulsive bedrock acceleration.

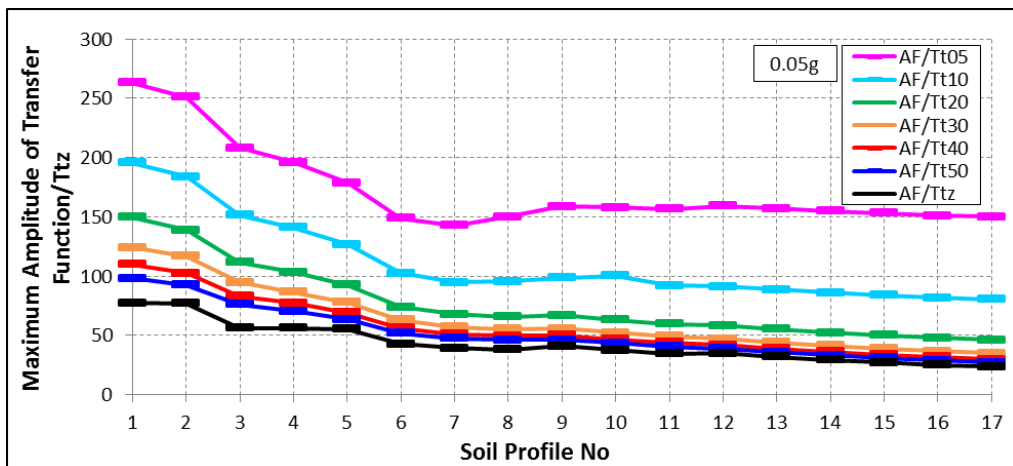


Figure 5.162. The correlation of AF with T_{tz} for 0.05g impulsive bedrock acceleration.

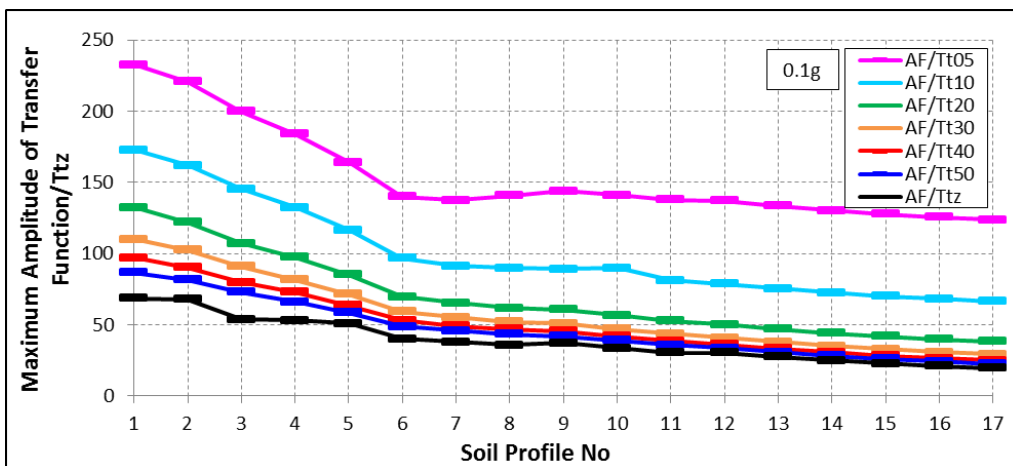


Figure 5.163. The correlation of AF with T_{tz} for 0.1g impulsive bedrock acceleration.

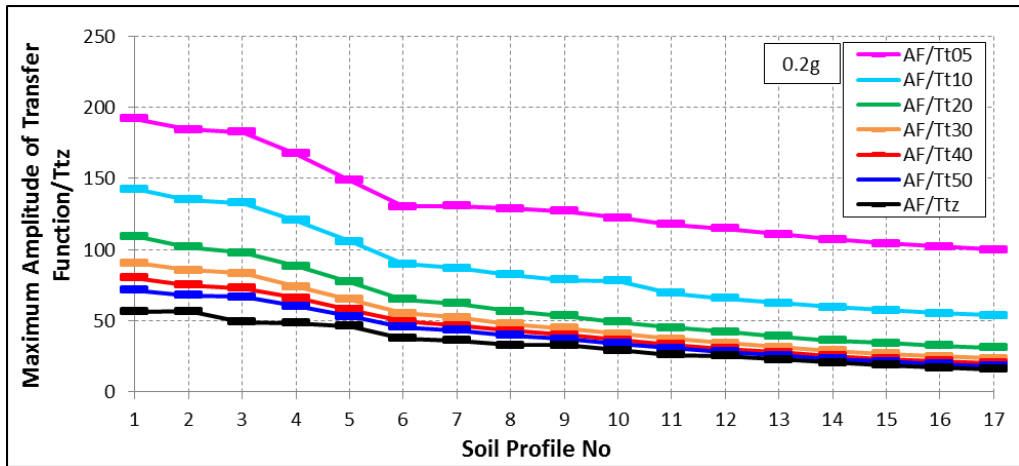


Figure 5.164. The correlation of AF with T_{tz} for 0.2g impulsive bedrock acceleration.

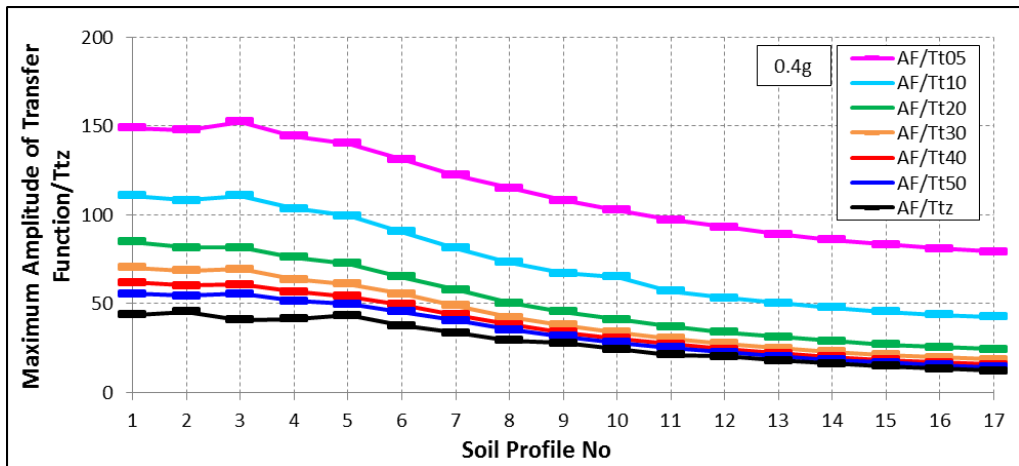


Figure 5.165. The correlation of AF with T_{tz} for 0.4g impulsive bedrock acceleration.

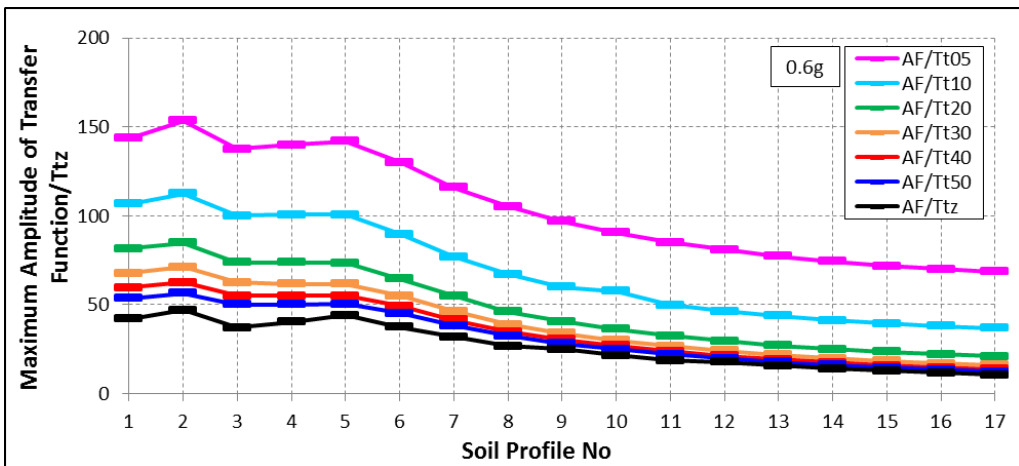


Figure 5.166. The correlation of AF with T_{tz} for 0.6g impulsive bedrock acceleration.

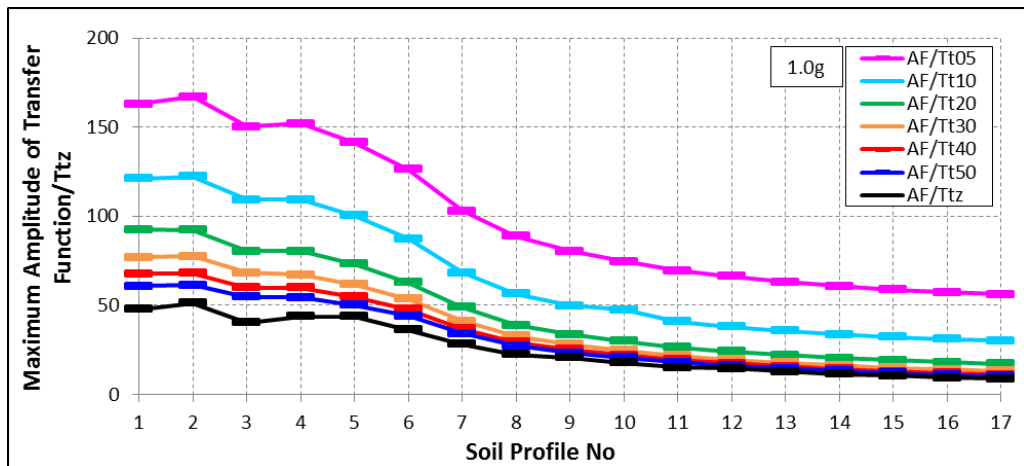


Figure 5.167. The correlation of AF with T_{tz} for 1.0g impulsive bedrock acceleration.

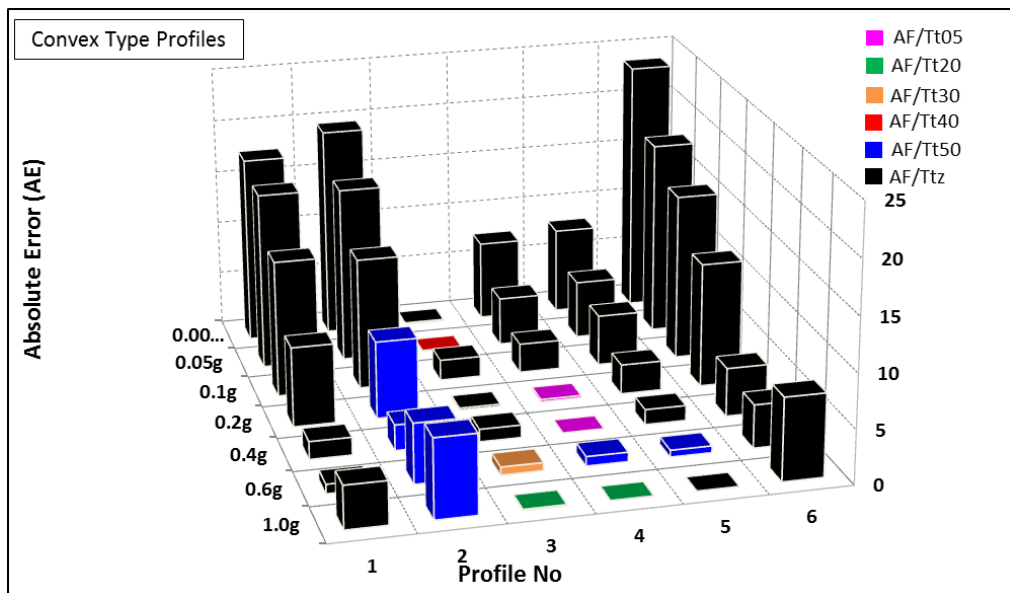


Figure 5.168. The variation of AE for AF/T_{tz} with increasing impulsive bedrock accelerations for convex profiles.

For linear and concave profiles, the best performing parameters for 0.005g were T_{t30} for profiles no 7; T_{tz} for no 8, T_{t10} for no 9; T_{t20} for no 10, 11, 14, 15, 16, 17; and T_{t40} for no 12, 13. For 0.05g, the optimal ones were T_{tz} for no 7, 8, 11, 13; T_{t05} for no 9, 10, 14, 15, 16, 17; and T_{t30} for no 12.

As a general comment, the optimal parameters were T_{tz} and T_{t50} for $Acc. \geq 0.4g$ for convex profiles, T_{t20} for 0.005g and T_{t05} for 0.05g for linear/concave profiles.

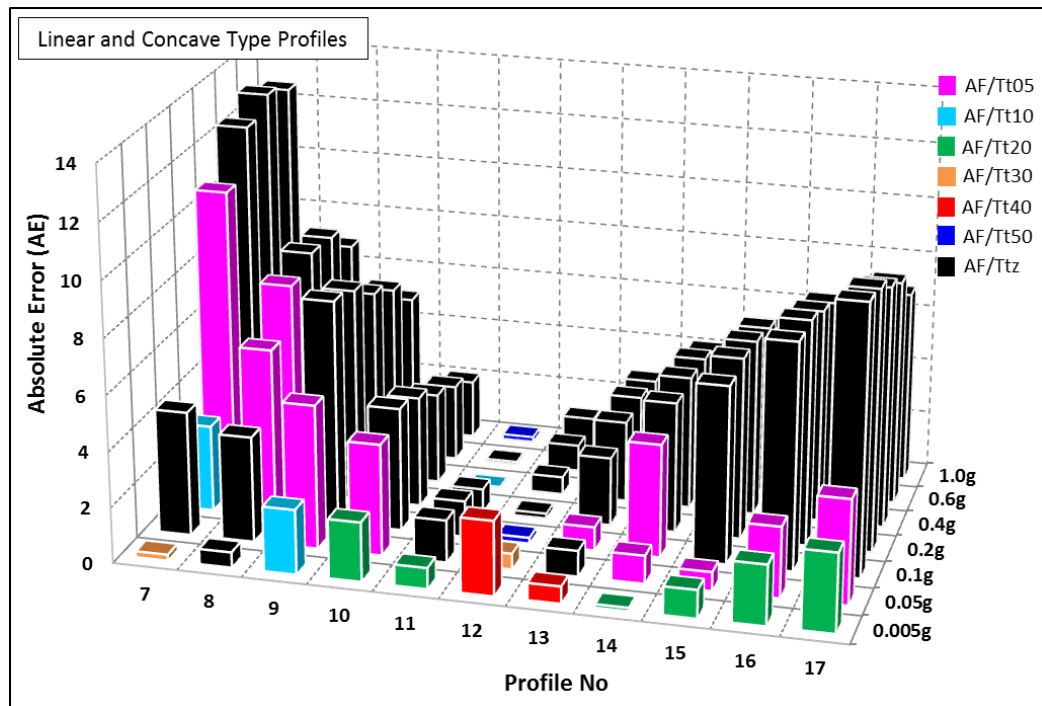


Figure 5.169. The variation of AE for AF/T_{tz} with increasing impulsive bedrock accelerations for linear/concave profiles.

5.2.3.5. Fundamental Frequency Characterization by V_{sz} . The correlation of fundamental soil frequency with V_{sz} at various depths was investigated for equal wave travel time model by impulsive type bedrock accelerations. The order of maximum peaks at transfer functions affected the correlations of f_0 with V_{sz} especially for convex profiles. The fundamental soil frequencies were at the 1st peaks of transfer functions for linear and concave profiles while they were at the 1st and 2nd peaks for convex profiles, as shown in Table 6.16. For $Acc. \leq 0.1g$, fundamental soil frequencies of convex profiles were at the 2nd peaks of transfer functions.

Table 5.16. The order of maximum peaks at transfer functions for f_0 .

Soil Profile No	Soil Type	0.005g	0.05g	0.1g	0.2g	0.4g	0.6g	1.0g
1	Convex-6	2 nd	2 nd	2 nd	2 nd	2 nd	1 st	1 st
2	Convex-5	2 nd	2 nd	2 nd	2 nd	2 nd	1 st	1 st
3	Convex-4	2 nd	2 nd	2 nd	2 nd	2 nd	2 nd	1 st
4	Convex-3	2 nd	2 nd	2 nd	2 nd	2 nd	1 st	1 st
5	Convex-2	2 nd	2 nd	2 nd	2 nd	1 st	1 st	1 st
6	Convex-1	2 nd	2 nd	2 nd	1 st	1 st	1 st	1 st

As the bedrock acceleration level increased, the high frequencies of transfer functions were damped and the f_0 were shifted to the 1st peaks.

The correlation of f_0 with V_{sz} was presented for gradually increasing impulsive bedrock accelerations in Figures 5.170-5.176. The fundamental frequency values of convex profiles were irregular (i.e., higher f_0 for profile no 4 compared to others at 0.005g) since they were affected more than linear/concave profiles by the equal wave travel time model in which the layer thickness and number, and the bedrock depth is different for each profile. For convex profiles, the correlations were close to constant just at 0.05g, 0.1g and 1.0g bedrock acceleration levels. For linear and concave profiles, the correlations were linear for all bedrock acceleration levels.

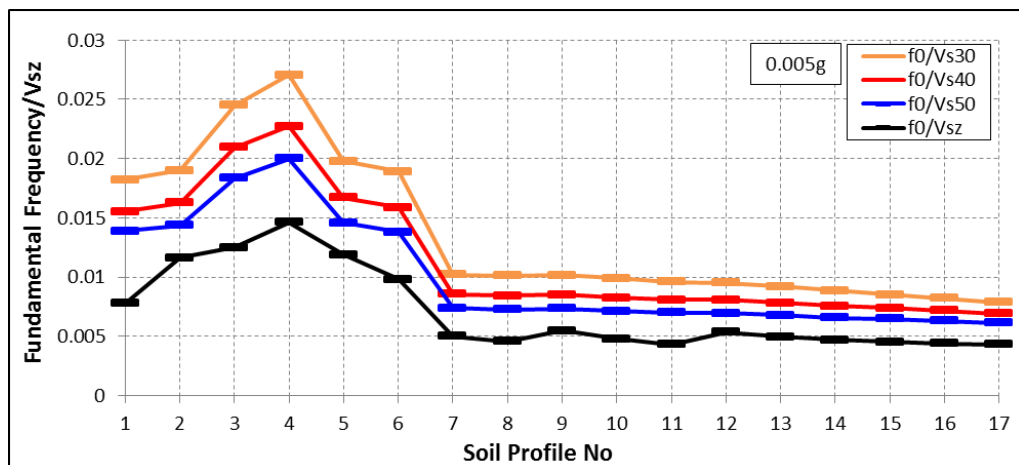


Figure 5.170. The correlation of f_0 with V_{sz} for 0.005g impulsive bedrock acceleration.

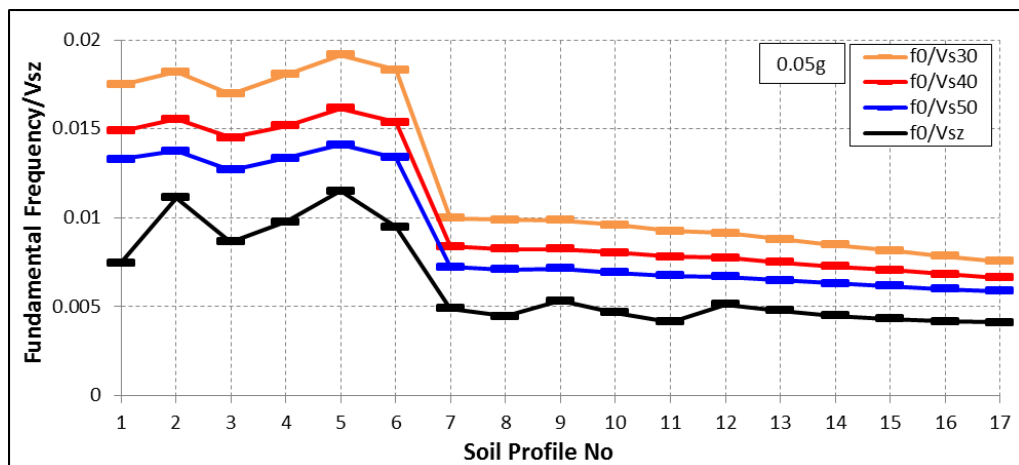


Figure 5.171. The correlation of f_0 with V_{sz} for 0.05g impulsive bedrock acceleration.

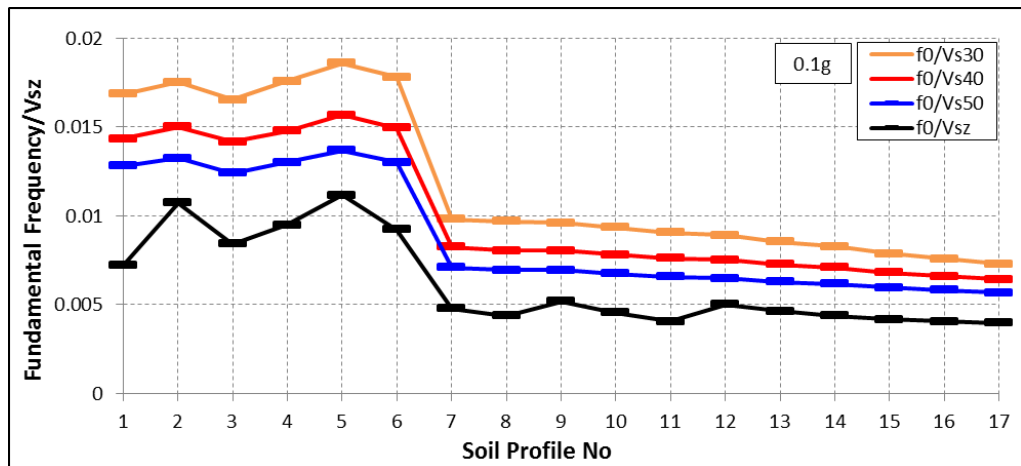


Figure 5.172. The correlation of f_0 with V_{sz} for 0.1g impulsive bedrock acceleration.

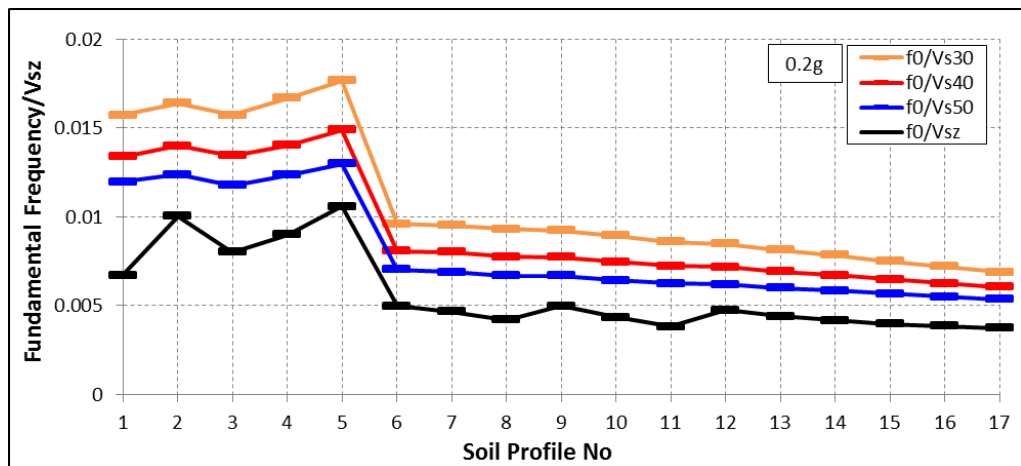


Figure 5.173. The correlation of f_0 with V_{sz} for 0.2g impulsive bedrock acceleration.

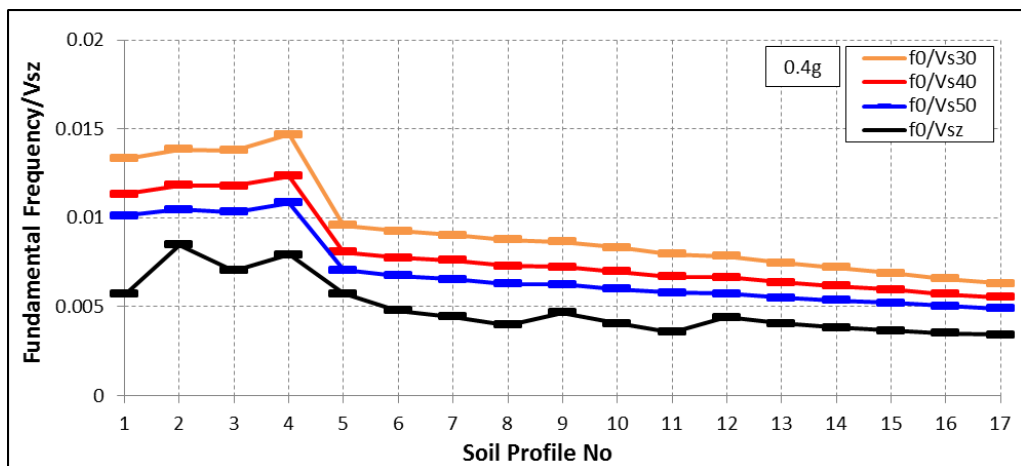


Figure 5.174. The correlation of f_0 with V_{sz} for 0.4g impulsive bedrock acceleration.

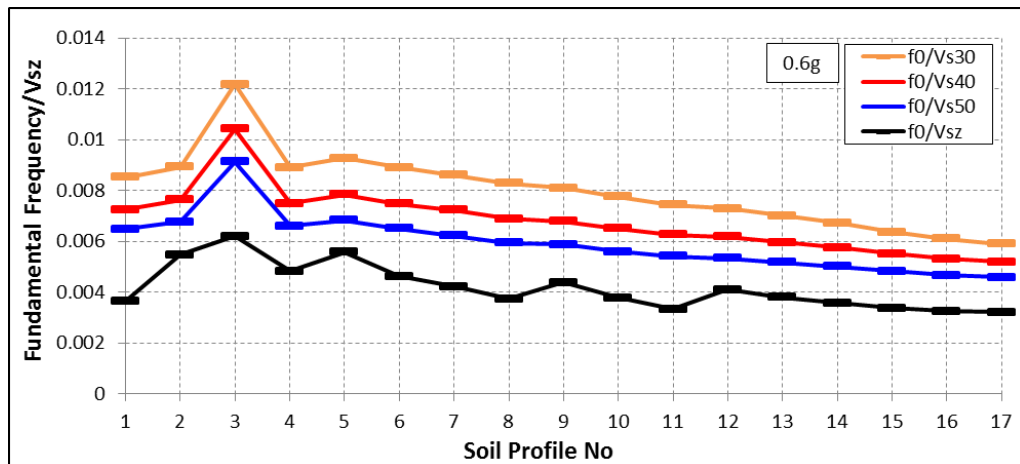


Figure 5.175. The correlation of f_0 with V_{sz} for 0.6g impulsive bedrock acceleration.

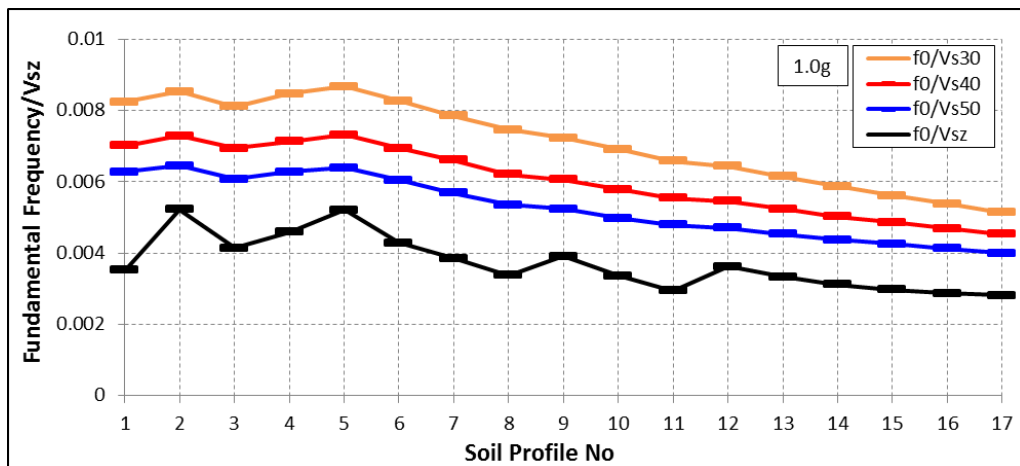


Figure 5.176. The correlation of f_0 with V_{sz} for 1.0g impulsive bedrock acceleration.

The correlations of f_0 with V_{sz} (i.e., the variations of AE) were presented for gradually increasing bedrock acceleration levels in Figure 5.177 and 5.178. For convex profiles, the AE variations were lower at 0.05g, 0.1g and 1.0g compared to other acceleration levels. For 0.05g acceleration level, the best performing parameters were V_{s50} for profiles no 1, 3, 5, 6; and V_{s30} for no 2 and 4. For 0.1g, the optimal parameters were V_{s50} for profiles no 1, 3, 4, 5, 6; and V_{s30} for no 2. For 1.0 g acceleration level, the best performing ones were V_{s50} for profiles no 1, 5; V_{s30} for no 2, 6; and V_{s40} for no 3, 4.

For linear/concave profiles, the AE variations were similar for all bedrock acceleration levels. The best performing parameters were V_{sz} and V_{s50} for all bedrock accelerations.

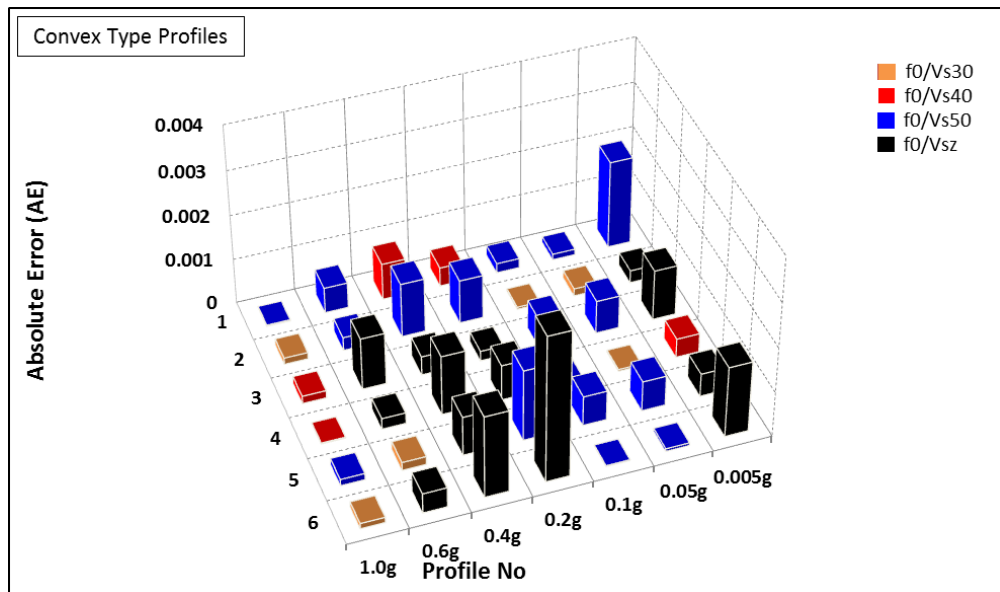


Figure 5.177. The variation of AE for f_0/V_{sz} with increasing impulsive bedrock accelerations for convex profiles.

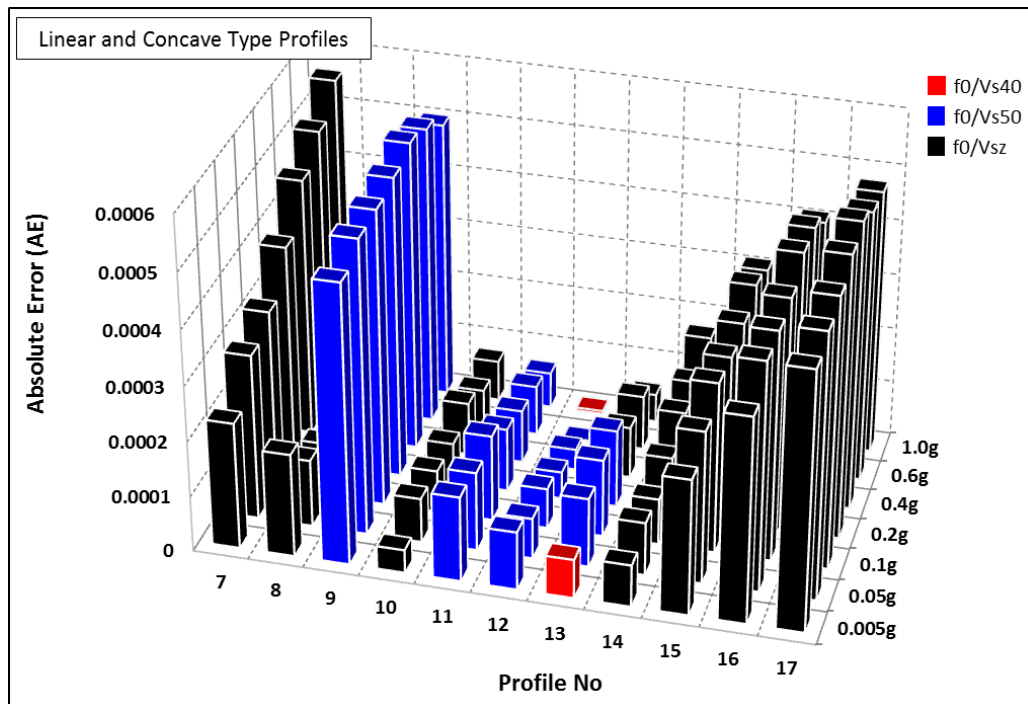


Figure 5.178. The variation of AE for f_0/V_{sz} with increasing impulsive bedrock accelerations for linear/concave profiles.

As a general statement, the optimal parameters were V_{s50} for convex profiles for 0.05g, 0.1g and 1.0g acceleration levels, and V_{sz} for linear/concave profiles for all acceleration levels.

5.2.3.6. Fundamental Frequency Characterization by T_{tz} . The correlation of fundamental soil frequency with T_{tz} at various depths was investigated for equal wave travel time model by gradually increasing bedrock accelerations, and shown in Figures 5.179-5.185. There is a distinct transition point between the correlations for convex and linear/concave profiles. For convex profiles, constant relations were observed just for 0.05g, 0.1g and 1.0g bedrock impulsive accelerations. For linear and concave profiles, the correlations were linear for all bedrock acceleration levels. The AE variations for $f_0 \times T_{tz}$ correlations were presented for gradually increasing impulsive bedrock accelerations in Figure 5.186 and 5.187.

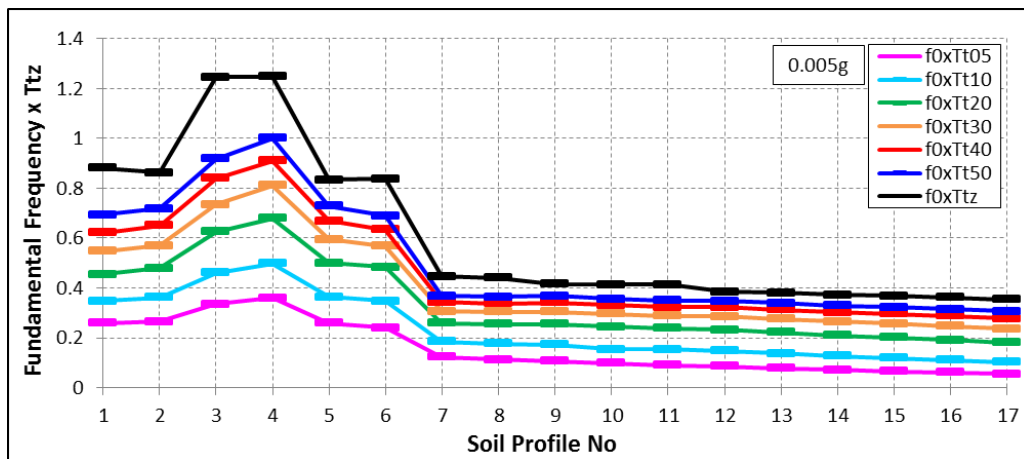


Figure 5.179. The correlation of f_0 with T_{tz} for 0.005g impulsive bedrock acceleration.

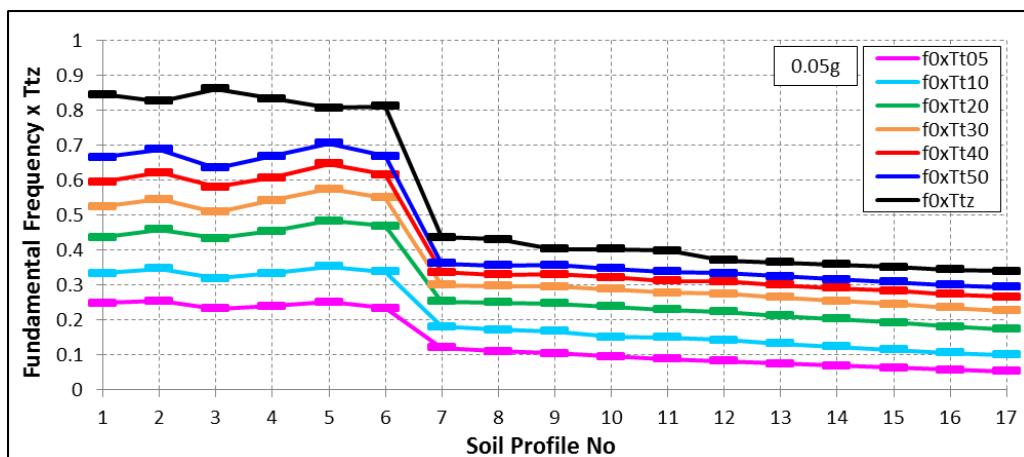


Figure 5.180. The correlation of f_0 with T_{tz} for 0.05g impulsive bedrock acceleration.

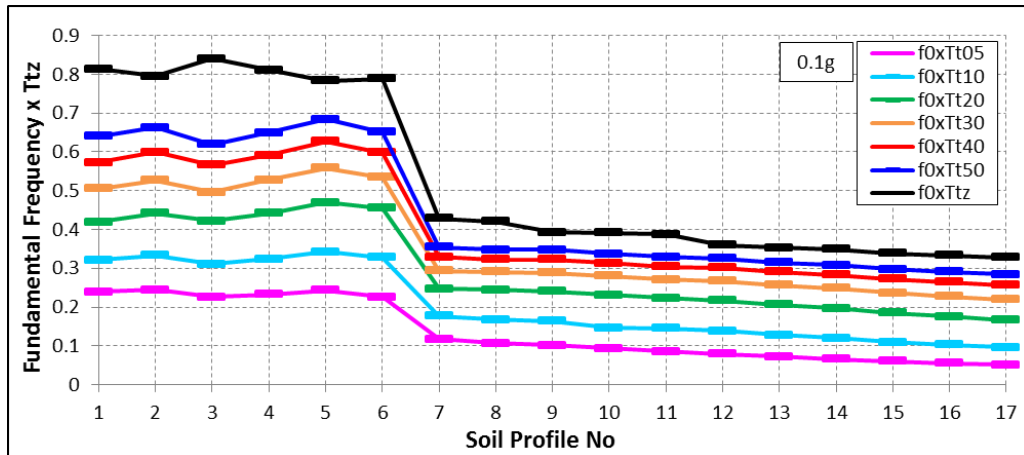


Figure 5.181. The correlation of f_0 with T_{tz} for 0.1g impulsive bedrock acceleration.

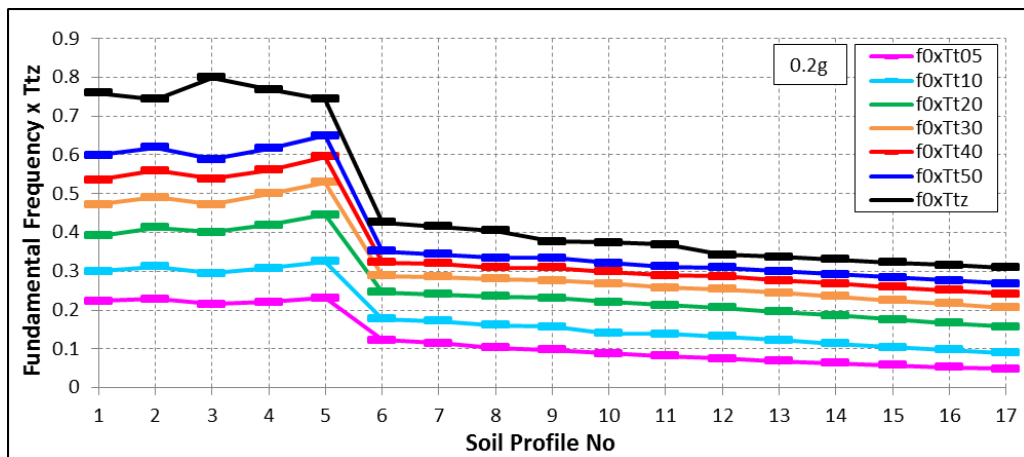


Figure 5.182. The correlation of f_0 with T_{tz} for 0.2g impulsive bedrock acceleration.

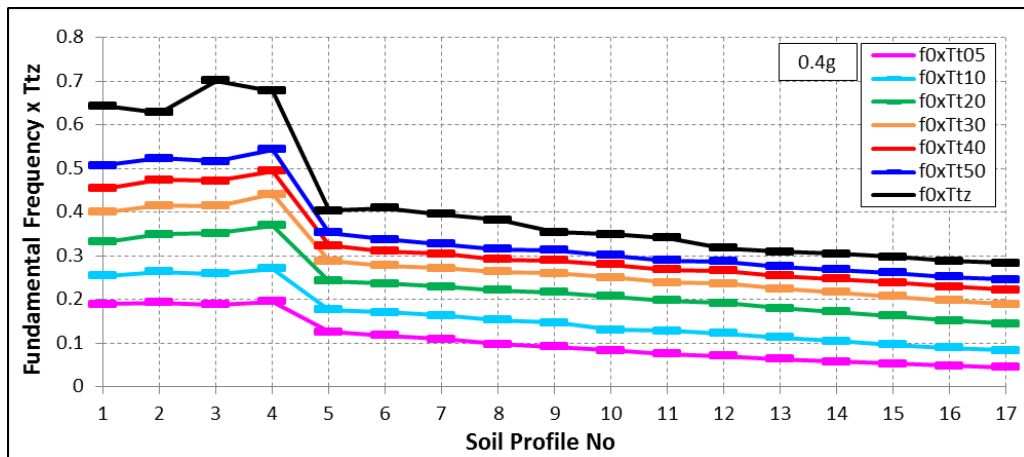


Figure 5.183. The correlation of f_0 with T_{tz} for 0.4g impulsive bedrock acceleration.

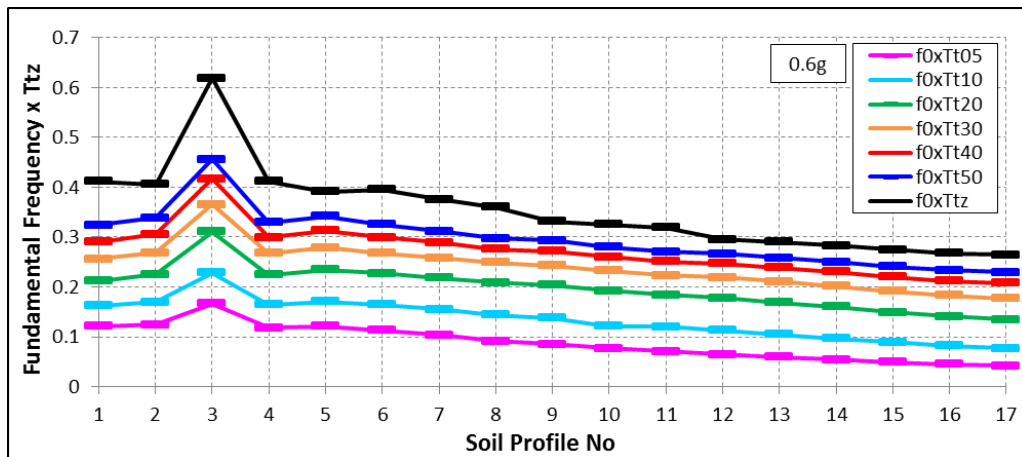


Figure 5.184. The correlation of f_0 with T_{tz} for 0.6g impulsive bedrock acceleration.

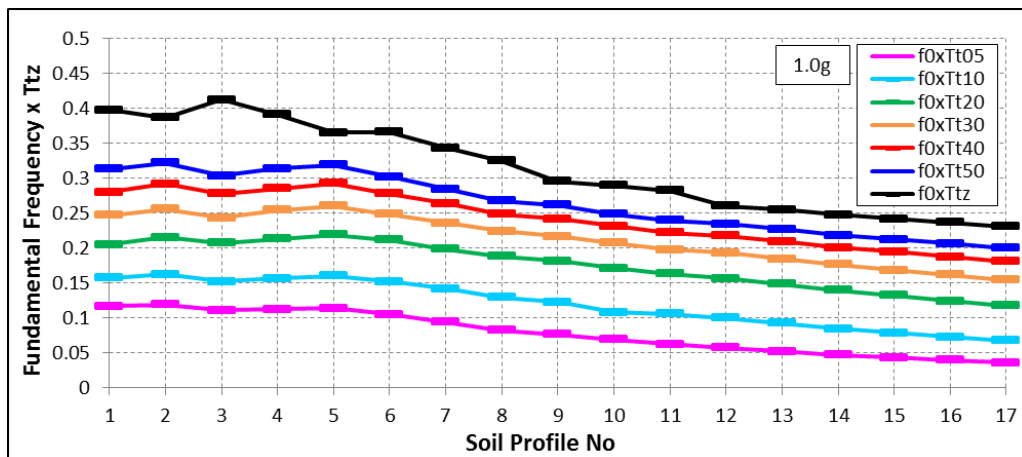


Figure 5.185. The correlation of f_0 with T_{tz} for 1.0g impulsive bedrock acceleration.

The AE levels were lower at 0.05g, 0.1g and 1.0g bedrock accelerations for convex profiles. For 0.05g acceleration level, the best performing parameters were T_{t10} for profiles no 1, 6; T_{t20} for no 2; T_{t05} for no 3, 5; and T_{t30} for no 4. For 0.1g, the optimal parameters were T_{t05} for no 1, 3, 5; T_{t20} for no 2, 4; and T_{t50} for no 6. For 1.0g bedrock acceleration level, the best performing one were T_{t10} for no 1, 4; T_{tz} for no 2; T_{t05} for no 3, 5; and T_{t20} for no 6.

For linear/concave profiles the AE levels were the same for all bedrock acceleration levels. The best performing parameters were T_{t50} and T_{t05} for 0.005g; and T_{t05} for the higher bedrock acceleration levels.

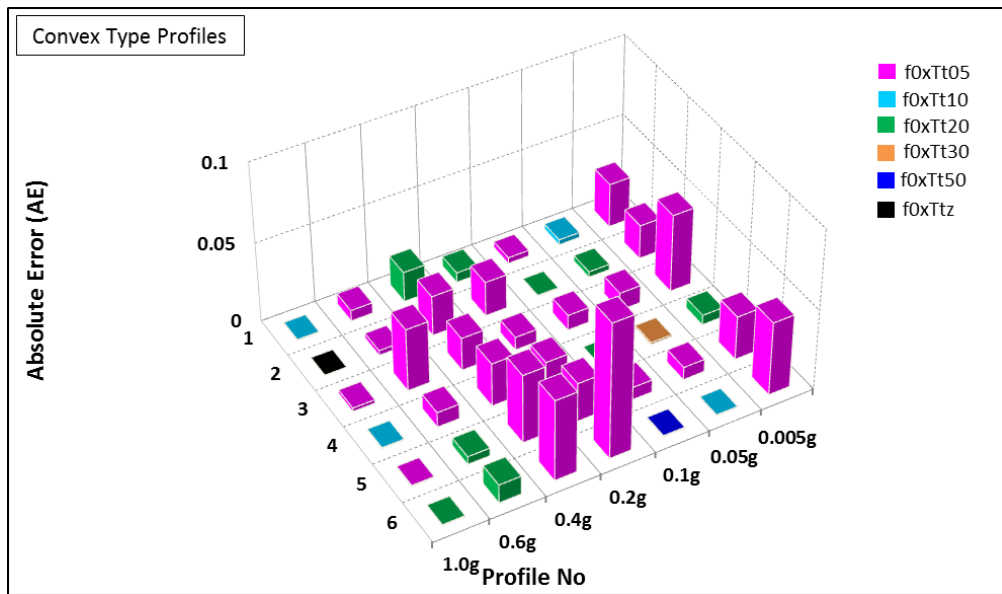


Figure 5.186. The variation of AE for f_0xT_{tz} with increasing impulsive bedrock accelerations for convex profiles.

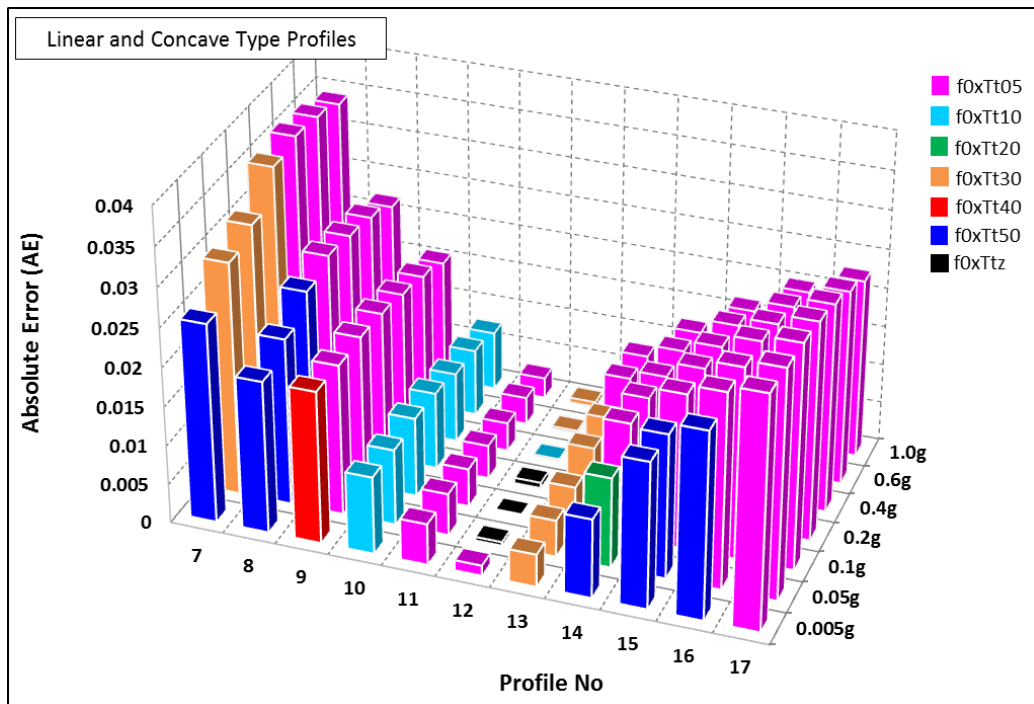


Figure 5.187. The variation of AE for f_0xT_{tz} with increasing impulsive bedrock accelerations for linear/concave profiles.

As a general statement, the optimal parameters were T_{t05} for 0.05g, T_{t05} and T_{t20} for 0.1g and T_{t05} and T_{t10} for 1.0g for convex type profiles. For linear and concave profiles,

T_{105} and T_{150} for 0.005g, and T_{105} were the optimal ones for the higher bedrock acceleration levels.

5.2.4. The Best Performing Parameters for Site Amplification and Fundamental Frequency Characterization

We have investigated the validity of V_{s30} and the performance of alternative averaged shear wave velocities, V_{sz} , and wave travel times, T_{tz} , at various depths to characterize soil amplification factor and fundamental frequency. The correlation of soil amplification factors with fundamental soil frequencies, surface PGAs and shear strains were studied as well. The performance of V_{s30} and alternative parameters were evaluated by using the AE parameter (i.e., the Absolute Error parameter; which gives a measure of scattering from a constant) for the equal thickness and equal wave travel time models, and impulsive and white-noise bedrock acceleration inputs. The best performing parameters were defined for each velocity profile by the lowest AEs for gradually increasing bedrock acceleration levels. We summarize the best performing parameters for each profile type (i.e., convex, linear and concave) and bedrock acceleration levels in this section. The performance of these parameters was investigated through the analysis of 3 cases as follows;

- (i) Equal layer thickness (i.e., $h=2$ m) model by impulsive accelerations.
- (ii) Equal layer thickness (i.e., $h=2$ m) model by white-noise accelerations.
- (iii) Equal wave travel time (i.e., $t=0.04$ sec) model by impulsive accelerations.

In the Tables below, the equal layer thickness and the equal wave travel time models are labelled as “ $h=2$ m” and “ $t=0.04$ sec”, whereas the impulsive and white-noise type bedrock accelerations are labelled as “I” and “W”, respectively. We should note that analyses of different layering models by impulsive bedrock accelerations presented nearly the same results, hence we analyzed the equal travel time model just for impulsive accelerations since we know that the analysis results by white-noise accelerations would be the same as those for impulsive accelerations.

According to the computed shear strains for each layering model and bedrock acceleration type, 0.005g acceleration level corresponds to linear elastic, 0.05g, 0.1g, 0.2g,

0.4g and 0.6g correspond to nonlinear elastic response, and $\text{Acc.} \geq 1.0\text{g}$ to elasto-plastic strain ranges in the velocity profiles (The definition of strain levels are based on the study of Vucetic, 1994).

We firstly present in Table 5.17, the correlation of soil amplification factors with surface PGAs for both groups of profiles. The symbol of “✓” means that it is possible to characterize soil amplification by surface PGA, and the symbol of “-” means that soil amplification cannot be characterized by surface PGA. The table shows that the surface PGA can characterize soil amplification only for convex profiles for $\text{Acc.} \geq 0.05\text{g}$.

Table 5.17. The characterization of soil amplification by surface PGAs.

AF/ Surface PGA						
Profile Type	Linear / Concave			Convex		
Bedrock PGA	h=2 m, I	h=2 m, W	t=0.04 sec, I	h=2 m, I	h=2 m, W	t=0.04 sec, I
0.005g	-	-	-	-	-	-
0.05g	-	-	-	✓	✓	-
0.1g	-	-	-	✓	✓	✓
0.2g	-	-	-	✓	✓	✓
0.4g	-	-	-	✓	✓	✓
0.6g	-	-	-	✓	✓	✓
1.0g	-	-	-	✓	✓	✓

Table 5.18 shows the correlation of soil amplification factors with fundamental frequency for each layering and bedrock acceleration types. f_0 performed well only for convex profiles for $\text{Acc.} \leq 0.4\text{g}$.

Table 5.18. The characterization of soil amplification by f_0 .

AF/ f_0						
Profile Type	Linear / Concave			Convex		
Bedrock PGA	h=2 m, I	h=2 m, W	t=0.04 sec, I	h=2 m, I	h=2 m, W	t=0.04 sec, I
0.005g	-	-	-	✓	✓	✓
0.05g	-	-	-	✓	✓	✓
0.1g	-	-	-	✓	✓	✓
0.2g	-	-	-	✓	-	✓
0.4g	-	-	-	✓	-	✓
0.6g	-	-	-	-	-	-
1.0g	-	-	-	-	-	-

Based on the minimum AEs, the optimal V_{sz} parameters for the characterization of soil amplification factors are presented in Table 5.19 for all layering and bedrock acceleration types.

According to the table, the optimal V_{sz} parameters are:

- For linear and concave profiles: V_{s10} or V_{s05} for impulsive Acc. $\geq 0.2g$ and white-noise Acc. $\geq 0.05g$.
- For convex profiles: V_{s100} or V_{s50} for impulsive Acc. $\leq 0.2g$ and for all white-noise accelerations.

Table 5.19. The best performing V_{sz} parameters for soil amplification characterization.

AF/ V_{sz}						
Profile Type	Linear / Concave			Convex		
Bedrock PGA	h=2 m, I	h=2 m, W	t=0.04 sec, I	h=2 m, I	h=2 m, W	t=0.04 sec, I
0.005g	-	-	-	V_{s100}	V_{s100}	V_{s50}
0.05g	-	V_{s05}	-	V_{s100}	V_{s100}	V_{s50}
0.1g	-	V_{s10}	-	V_{s100}	V_{s100}	V_{s50}
0.2g	V_{s05}	V_{s10}	V_{s05}	V_{s100}	V_{s100}	V_{s50} or V_{sz}
0.4g	V_{s10} or V_{s05}	V_{s10}	V_{s05}	-	V_{s100}	-
0.6g	V_{s10}	V_{s10}	V_{s10}	-	V_{s100}	-
1.0g	V_{s10}	V_{s10}	V_{s10}	-	V_{s100}	-

Alternatively, we have investigated the performance of wave travel times at various depths, T_{tz} , for all layering and bedrock acceleration types. The results are summarized in Table 5.20. The optimal parameters are identified as follows:

- For linear and concave profiles: T_{t20} or T_{t05} for impulsive Acc. $\leq 0.05g$ and T_{t100} for white-noise Acc. $\geq 0.2g$.
- For convex profiles: T_{t100} for impulsive Acc. $\geq 0.4g$ and for white-noise Acc. $\geq 0.2g$.

Table 5.20. The best performing T_{tz} parameters for soil amplification characterization.

AF/ T_{tz}						
Profile Type	Linear / Concave			Convex		
Bedrock PGA	h=2 m, I	h=2 m, W	t=0.04 sec, I	h=2 m, I	h=2 m, W	t=0.04 sec, I
0.005g	T_{t20}	T_{t10}	T_{t20}	-	-	-
0.05g	T_{t05}	-	T_{t05}	-	-	-
0.1g	-	-	-	-	-	-
0.2g	-	T_{t100}	-	-	T_{t100}	-
0.4g	-	T_{t100}	-	T_{t100}	T_{t100}	T_{tz}
0.6g	-	T_{t100}	-	T_{t100}	T_{t100}	T_{tz} or T_{t50}
1.0g	-	T_{t100}	-	T_{t100}	T_{t100}	T_{tz}

Figure 5.21 presents the best performing averaged velocities at various depths for fundamental soil frequency characterization. The optimal parameters are identified as follows:

- For linear and concave profiles: V_{s100} or V_{s50} for all acceleration types and levels.
- For convex profiles: V_{s50} for impulsive acceleration levels of 0.05g, 0.1g and 1.0g, and V_{s100} for white-noise Acc. $\geq 0.4g$. It can be generalized that V_{s100} or V_{s50} can be used for bedrock accelerations $\geq 0.05g$.

Table 5.21. The best performing V_{sz} parameters for f_0 characterization.

f_0/V_{sz}						
Profile Type	Linear / Concave			Convex		
Bedrock PGA	h=2 m, I	h=2 m, W	t=0.04 sec, I	h=2 m, I	h=2 m, W	t=0.04 sec, I
0.005g	V_{s100}	V_{s100}	V_{sz} or V_{s50}	-	-	-
0.05g	V_{s100}	V_{s100}	V_{sz} or V_{s50}	V_{s50}	-	V_{s50}
0.1g	V_{s100}	V_{s100}	V_{sz} or V_{s50}	V_{s50}	-	V_{s50}
0.2g	V_{s100}	V_{s100}	V_{sz} or V_{s50}	-	-	-
0.4g	V_{s100}	V_{s100}	V_{sz} or V_{s50}	-	V_{s100}	-
0.6g	V_{s100}	V_{s100}	V_{sz} or V_{s50}	-	V_{s100}	-
1.0g	V_{s100}	V_{s100}	V_{sz} or V_{s50}	V_{s30} or V_{s40}	V_{s100}	V_{s50} or V_{s40} or V_{s30}

Table 5.22 shows the performance of T_{tz} at various depths for the characterization of fundamental soil frequency. The best performing parameters are identified as:

- For linear and concave profiles: T_{t05} for all acceleration types and levels.

- For convex profiles: T_{t50} or T_{t05} for impulsive acceleration levels of 0.05g, 0.1g and 1.0g; and T_{t05} for white-noise Acc. $\geq 0.4g$. It can be generalized that T_{t05} can be used for bedrock accelerations $\geq 0.05g$.

Table 5.22. The best performing T_{tz} parameters for f_0 characterization.

$f_0 \times T_{tz}$						
Profile Type	Linear / Concave			Convex		
Bedrock PGA	h=2 m, I	h=2 m, W	t=0.04 sec, I	h=2 m, I	h=2 m, W	t=0.04 sec, I
0.005g	T_{t05}	T_{t05}	T_{t50} or T_{t05}	-	-	-
0.05g	T_{t05}	T_{t05}	T_{t05}	T_{t50}	-	T_{t05}
0.1g	T_{t05}	T_{t05}	T_{t05}	T_{t50}	-	T_{t05} or T_{t20}
0.2g	T_{t05}	T_{t05}	T_{t05}	-	-	-
0.4g	T_{t05}	T_{t05}	T_{t05}	-	T_{t20}	-
0.6g	T_{t05}	T_{t05}	T_{t05}	-	T_{t05}	-
1.0g	T_{t05}	T_{t05}	T_{t05}	T_{t20}	T_{t05}	T_{t05} or T_{t10}

5.2.5. Correlation of Linear and Nonlinear Site Amplification Factors and Fundamental Frequencies

We have studied the nonlinear soil response and its correlations with linear soil response for each layering type and increasing bedrock acceleration levels. The objective was to determine if we can estimate the nonlinear fundamental soil frequencies and soil amplification factors from the linear ones by simple means. Fundamental soil frequencies can easily be identified reliably from ambient noise measurements (i.e., by spectral analysis), but not the amplification factors (Lachet and Bard, 1994; Field and Jacob, 1995; Atakan, 1995, Safak, 1997 and Parolai, 2012). Other types of field measurements including reference site methods (e.g., SSR-Standard Spectral Ratio) should be used to identify site amplification. Since ground noise measurements (by microtremors, traffic noise, wind etc.) correspond to weak motions, hence low shear stresses, the calculated fundamental soil frequencies represent linear soil behavior.

In this study, the linear soil amplification factors and fundamental frequencies are assumed to correspond to those at 0.005g bedrock acceleration level. For increasingly higher bedrock acceleration levels, where the soil gradually becomes nonlinear, the correlation was investigated in terms of the ratio of the linear parameters to the nonlinear ones. Figure 5.188 to 5.193, show the linear/nonlinear ratios of fundamental soil

frequencies for each profile, layering scheme, bedrock input type, and bedrock acceleration levels. The ratios for linear/concave profiles increase linearly (i.e., increasing nonlinearity) with increasing bedrock PGAs in all three cases, besides an irregular increasing trend was seen for each convex profile. Both equal thickness and travel time models by impulse bedrock motion revealed so similar correlations even if the layering type is different. The degree of nonlinearity for white-noise type accelerations was observed higher than the impulsive type accelerations.

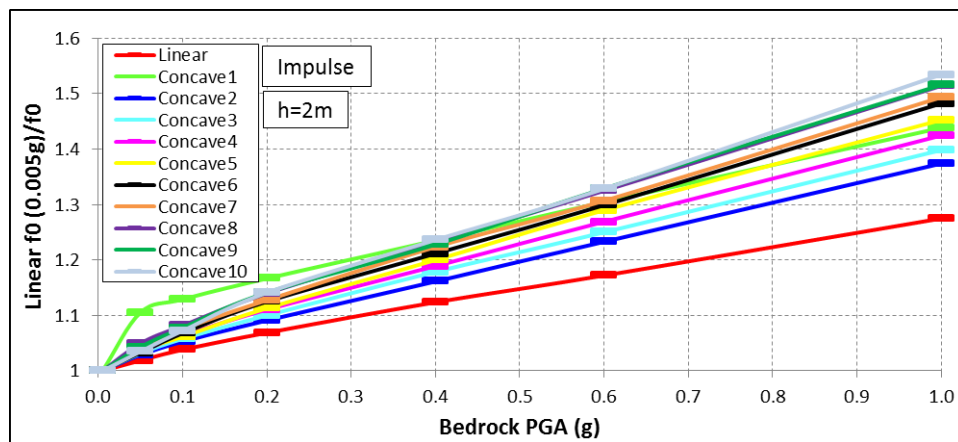


Figure 5.188. Relation between linear and nonlinear f_0 with increasing impulsive accelerations for linear and concave profiles of equal thickness model.

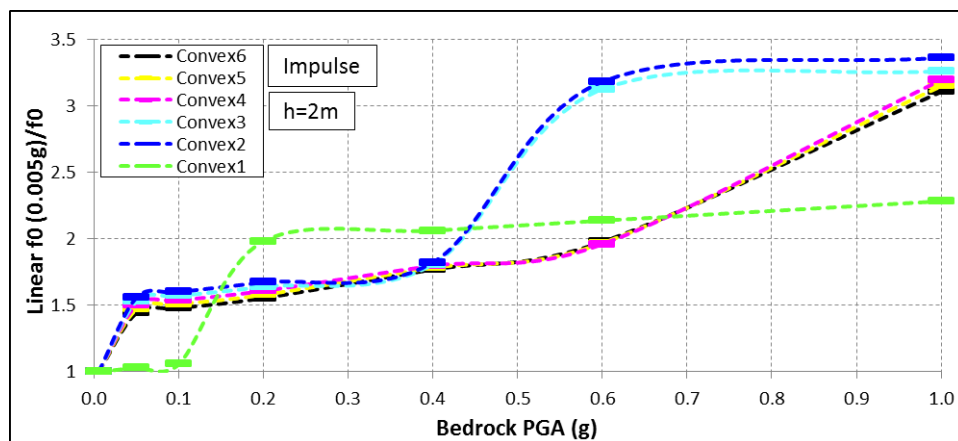


Figure 5.189. Relation between linear and nonlinear f_0 with increasing impulsive accelerations for convex profiles of equal thickness model.

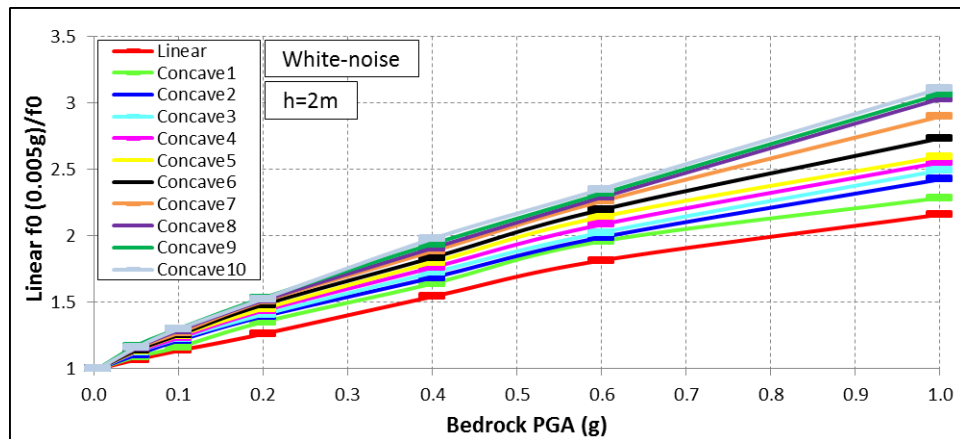


Figure 5.190. Relation between linear and nonlinear f_0 with increasing white-noise accelerations for linear and concave profiles of equal thickness model.

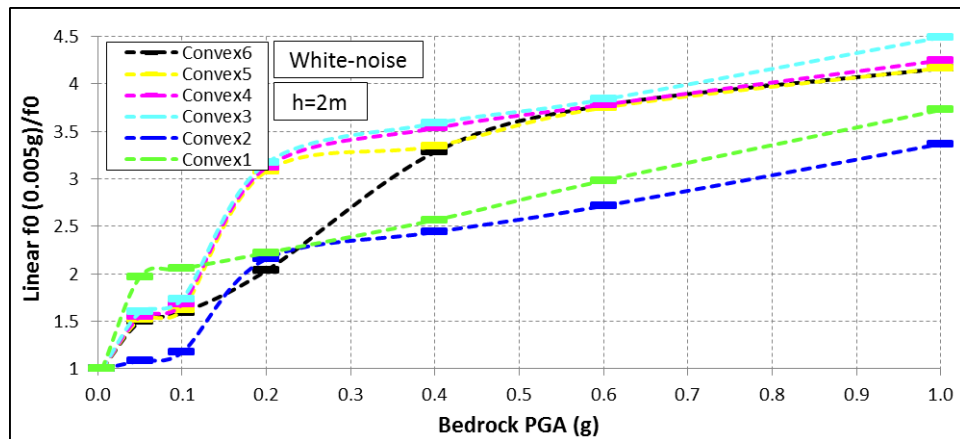


Figure 5.191. Relation between linear and nonlinear f_0 with increasing white-noise accelerations for convex profiles of equal thickness model.

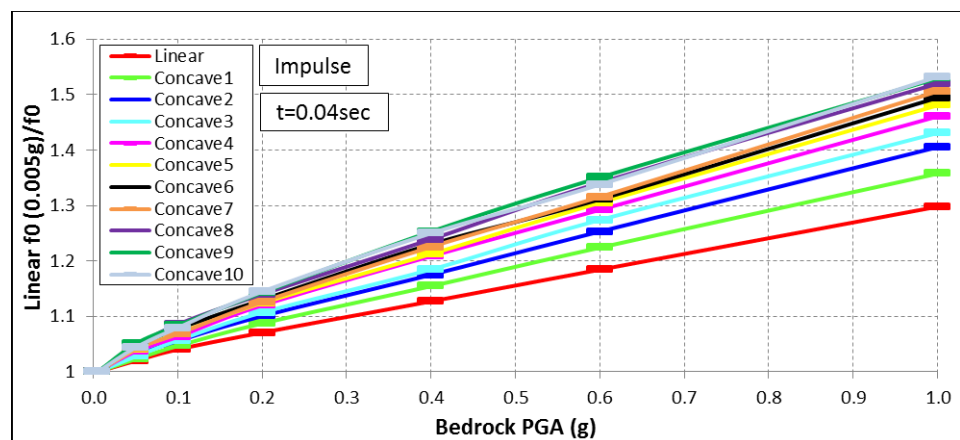


Figure 5.192. Relation between linear and nonlinear f_0 with increasing impulsive accelerations for linear and concave profiles of equal travel time model.

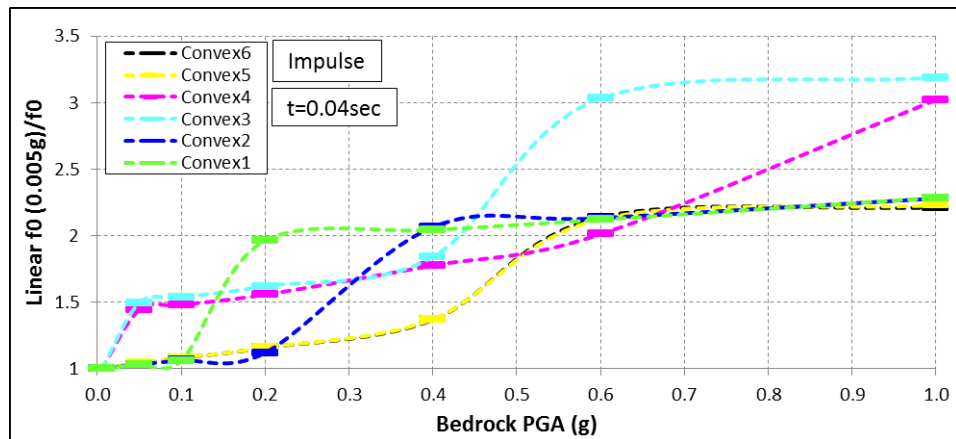


Figure 5.193. Relation between linear and nonlinear f_0 with increasing impulsive accelerations for convex profiles of equal travel time model.

We presented the correlation of linear soil amplification factors with the nonlinear ones for each layering and bedrock acceleration types (Figure 5.194-Figure 5.199). The correlations of amplification factors for equal thickness and equal travel time models under impulsive motion were very similar to those for the fundamental soil frequency. The degree of nonlinearity was higher for white-noise type bedrock accelerations. Considering that the linear amplification can easily be calculated from field measurements, these guidelines provide a useful tool to estimate nonlinear site amplification.

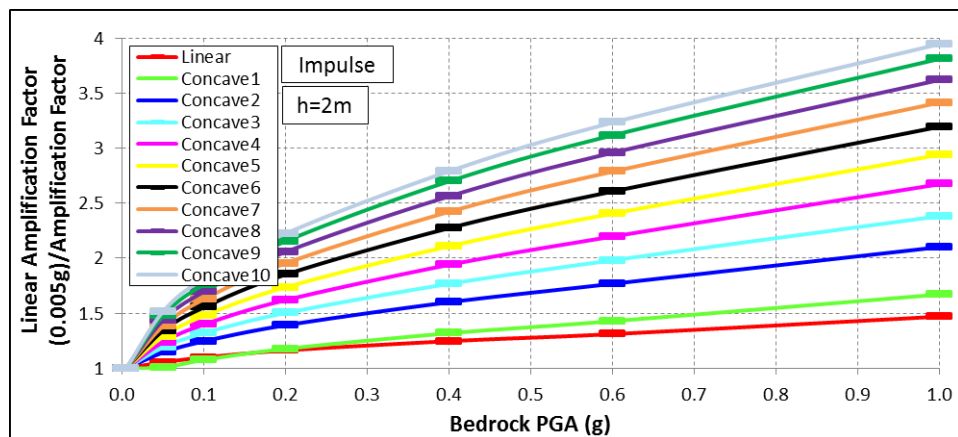


Figure 5.194. Relation between linear and nonlinear soil amplification with increasing impulsive accelerations for linear and concave profiles of equal thickness model.

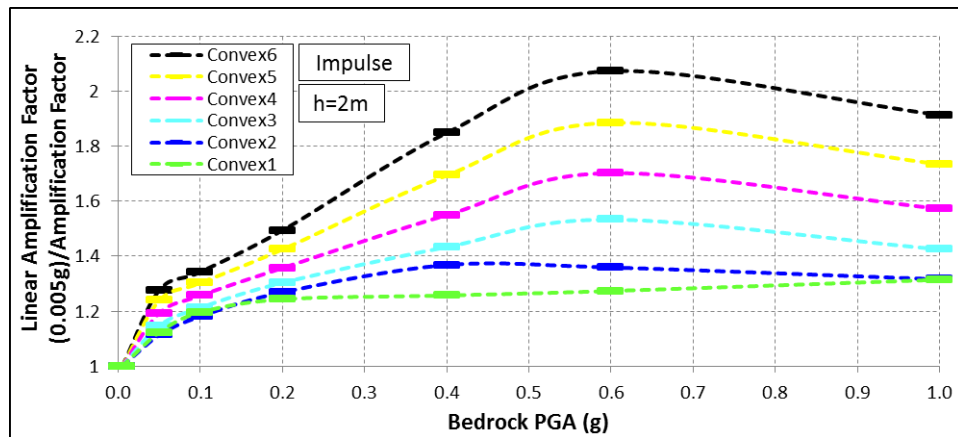


Figure 5.195. Relation between linear and nonlinear soil amplification with increasing impulsive accelerations for convex profiles of equal thickness model.

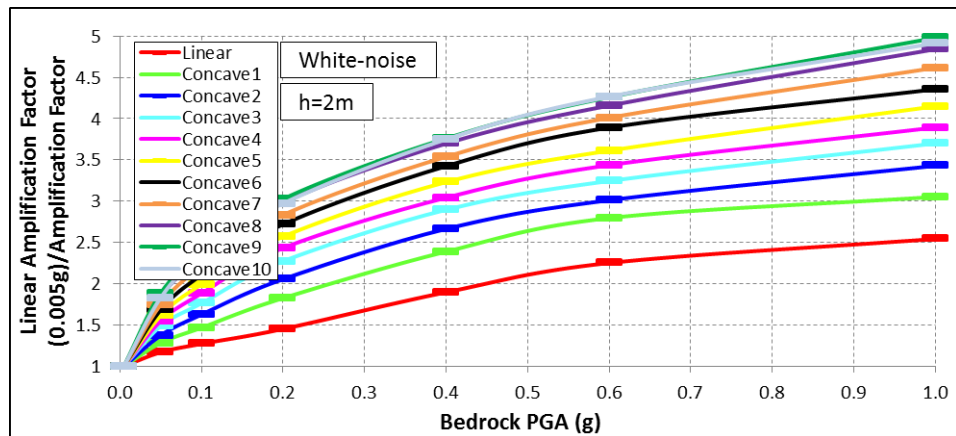


Figure 5.196. Relation between linear and nonlinear soil amplification with increasing white-noise accelerations for linear and concave profiles of equal thickness model.

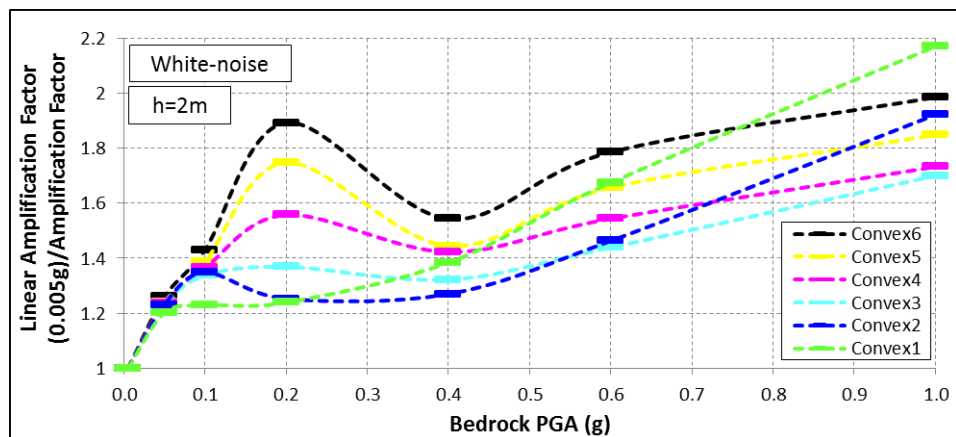


Figure 5.197. Relation between linear and nonlinear soil amplification with increasing white-noise accelerations for convex profiles of equal thickness model.

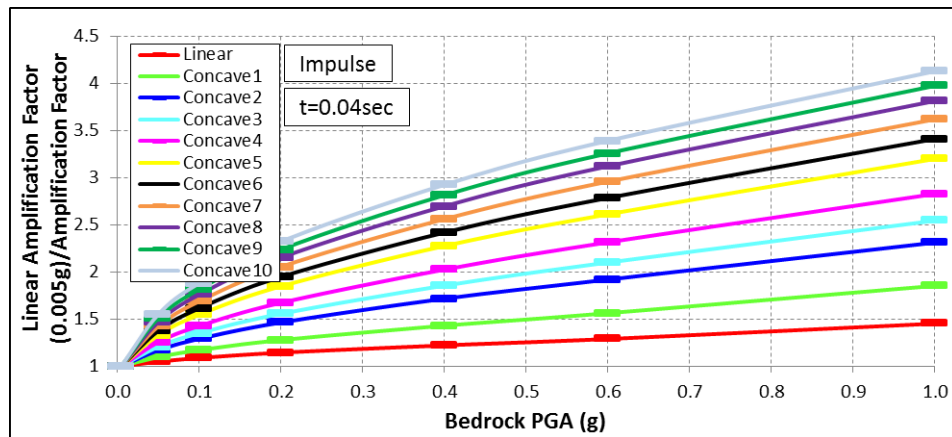


Figure 5.198. Relation between linear and nonlinear soil amplification with increasing impulsive accelerations for linear and concave profiles of equal travel time model.

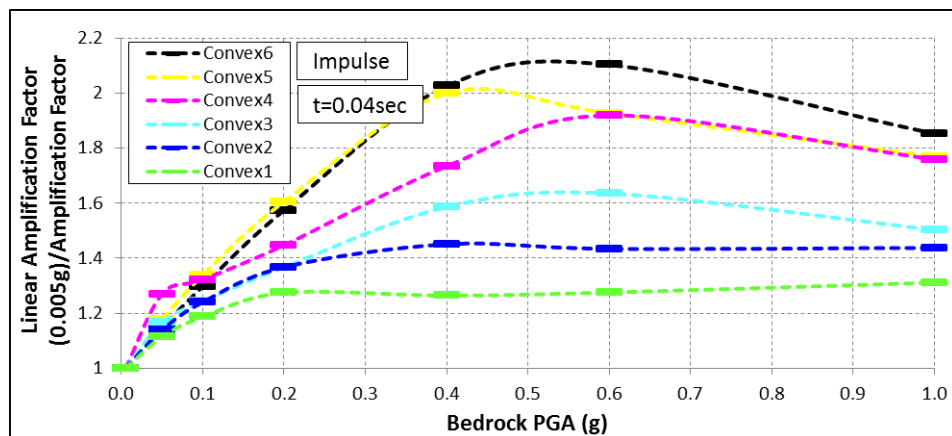


Figure 5.199. Relation between linear and nonlinear soil amplification with increasing impulsive accelerations for convex profiles of equal travel time model.

6. CONCLUSIONS

We carried out a parametric study to investigate the reliability of V_{s30} and some alternative parameters, including time-averaged shear wave velocities, V_{sz} , and wave travel times, T_{tz} , at various depths to characterize site amplification factor and fundamental frequency. For this purpose, we considered 17 shear wave velocity profiles changing from convex (i.e., the velocities changing faster near the surface and slower near the bedrock) to concave (i.e., the velocities changing slower near the surface and faster near the bedrock) for the same bedrock depth. The soil media was divided into layers first with equal thicknesses (i.e., $h=2$ m), and then with equal wave travel times (i.e., $t=0.04$ sec). We studied the correlations of calculated site amplification factors and fundamental soil frequencies for each layering and profile type for the impulsive and white-noise type bedrock accelerations for gradually increasing amplitudes. We also investigated the correlations of surface PGAs and shear strains with V_{sz} , T_{tz} . Moreover, we investigated the relationship between linear and nonlinear soil response, and proposed some practical methods to estimate nonlinear soil amplification factors and fundamental soil frequencies from the linear ones. This can have significant implications in practice, because linear soil response can be obtained from simple field measurements. The significant findings of this study are listed below:

1. Linear site response analysis is applicable for low bedrock accelerations ($\text{Acc.} \leq 0.005g$). For higher bedrock accelerations ($\text{Acc.} > 0.005g$), linear analysis overestimates the response, because it cannot account for the reduction in shear modulus and increase in damping ratio.
2. For bedrock accelerations $\leq 0.6g$ (i.e., linear elastic and nonlinear elastic strain ranges), convex profiles have higher fundamental soil frequencies, sometimes observed at the second and higher peaks of transfer function, than the ones for linear/concave profiles. They would amplify high frequency portion of ground motions more than the low frequency portions. For linear and concave profiles, f_0 values were observed at the first peaks of transfer functions for all bedrock acceleration levels.

3. The impedance ratios between the consecutive layers are the critical parameter influencing soil amplification.
4. The degradation of soil stiffness occurred more rapidly by white-noise type bedrock accelerations compared to impulsive type accelerations resulting in lower soil amplification factors, lower fundamental frequencies, higher shear strains and higher surface PGAs. Thus, the frequency content of bedrock motions is an important factor on nonlinear soil response.
5. There is a sharp change in the correlations with V_{sz} , T_{tz} , surface PGA and shear strains when switching from convex to concave profiles.
6. The correlations differ for each bedrock acceleration type (e.g., impulsive and white-noise) and differ by gradually increasing acceleration levels. However, for different layering schemes under the same bedrock acceleration type (i.e., impulsive), the correlations do not differ.
7. For convex profiles only, surface PGAs for all bedrock acceleration types $\geq 0.05g$, and fundamental soil frequencies for all bedrock acceleration types $\leq 0.4g$ can be used for the characterization of soil amplification.
8. Alternative V_{sz} and T_{tz} parameters performed better than V_{s30} to characterize soil amplification.
9. For linear/concave profiles, the optimal parameters to characterize soil amplification are V_{s05} or V_{s10} for all bedrock accelerations $\geq 0.2g$. For convex profiles, they are V_{s50} or V_{s100} for bedrock accelerations $\leq 0.2g$.
10. In terms of travel times, the optimal parameters to characterize soil amplification for linear/concave profiles are T_{t20} or T_{t05} for all bedrock accelerations $\leq 0.05g$. For convex profiles, the optimal parameter is T_{t100} for all bedrock accelerations $\geq 0.4g$.
11. For convex profiles, V_{s100} performed well for bedrock accelerations $\leq 0.2g$, while T_{t100} performed well for bedrock accelerations $> 0.2g$ to characterize soil amplification. For linear and concave profiles, V_{05} or V_{s10} can be used for bedrock accelerations $\geq 0.2g$, while T_{05} or T_{t20} can be used for bedrock accelerations $\leq 0.05g$.
12. For linear and concave profiles, fundamental soil frequency can be characterized by V_{s50} or V_{s100} and T_{05} for all bedrock accelerations. These parameters can also be used for convex profiles for bedrock accelerations $\geq 0.05g$.

13. The optimal parameters vary according to the profile type. There is a distinct difference between convex and linear/concave profiles for soil amplification and f_0 characterization.
14. For the profiles considered, nonlinear soil amplification factors and fundamental frequencies can be estimated from the linear ones. This has a practical significance, since the latter one can be identified from simple field measurements (e.g., ambient noise measurements).

REFERENCES

Atakan, K., 1995, "A review of the type of data and the techniques used in empirical estimation of local site response", *Proceedings of the Fifth International Conference on Seismic Zonation*, Nice, France, 17-19 Oct., Vol. II, pp. 1451-1460.

Bardet, J. P., K. Ichii, C. H. Lin, 2000, *EERA: A Computer Program for Equivalent-linear Earthquake Site Response Analyses of Layered Soil Deposits*, University of Southern California, Los Angeles.

Borcherdt, R. D., 1970, "Effects of local geology on ground motion near San Francisco Bay", *Bulletin of the Seismological Society of America*, Vol. 60, pp. 29-61.

Borcherdt, R. D., G. Glassmoyer, 1992, "On the characteristics of local geology and their influence on ground motions generated by the Loma Prieta earthquake in the San Francisco Bay region, California", *Bulletin of the Seismological Society of America*, Vol. 82, No. 2, pp. 603-641.

Borcherdt, R. D., 1994, "Estimates of site-dependent response spectra for design (methodology and justification)", *Earthquake Spectra*, Vol. 10, pp. 617-653.

Building Seismic Safety Council (BSSC), 1997, *NEHRP Recommended Provisions for Seismic Regulations for New Buildings and Other Structures*, Part 1: Provisions (FEMA 302), Washington, D.C.

Cadet, H., P. Y. Bard, A. M. Duval, 2008, "A new proposal for site classification based on ambient vibration measurements and the KiK-net strong motion data set", *Proceedings of the Fourteenth World Conference on Earthquake Engineering*, Beijing, China, 12-17 Oct, Paper no: 03-01-0036.

Cadet, H., P. Y. Bard, A. M. Duval, E. Bertrand, 2012, “Site effect assessment using KiK-net data: part 2-site amplification prediction equation based on f_0 and V_{sz} ”, *Bulletin of Earthquake Engineering*, Vol. 10, pp. 451-489, doi: 10.1007/s10518-011-9298-7.

Castellaro, S., F. Mulargia, P. L. Rossi, 2008, “ V_{s30} : Proxy for seismic amplification?”, *Seismological Research Letters*, Vol. 79, No. 4, pp. 540-543.

Derras, B., P. Y. Bard, F. Cotton, 2017, “ V_{s30} , slope, H_{800} and f_0 : performance of various site-condition proxies in reducing ground-motion aleatory variability and predicting nonlinear site response”, *Earth Planets and Space*, Vol. 69, No. 133, doi: 10.1186/s40623-017-0718-z.

Dobry, R., M. Vucetic, 1987, “State-of-the-art report: dynamic properties and seismic response of soft clay deposits”, *Proceedings of the International Symposium on Geotechnical Engineering of Soft Soils*, Mexico City, Vol. 2, pp. 51-87.

European Committee for Standardization (CEN), 1998, *Eurocode 8: Design of structures for earthquake resistance, part 1: general rules, seismic actions and rules for buildings*, EN 1998-1, <http://www.cen.eu/cenorm/homepage.htm>, accessed date: 27.05.2020.

Field, E. H., K. H. Jacob, 1995, “A comparison and test of various site response estimation techniques, including three that are non reference-site dependent”, *Bulletin of the Seismological Society of America*, Vol. 85, pp. 1127–1143.

Gallipoli, M. R., M. Mucciarelli, 2009, “Comparison of site classification from V_{s30} , V_{s10} , and HVSR in Italy”, *Bulletin of the Seismological Society of America*, Vol. 99, No. 1, pp. 340-351, doi: 10.1785/0120080083.

Hashash, Y. M. A., D. R. Groholski, C.A. Philips, D. Park, 2008, *DEEPSOIL v3.5beta: User Manual and Tutorial*.

Hassani, B., G. M. Atkinson, 2016, “Applicability of the site fundamental frequency as a V_{s30} proxy for Central and Eastern North America”, *Bulletin of the Seismological Society of America*, Vol. 106, No. 2, pp. 653-664, doi: 10.1785/0120150259.

Idriss, I. M., H. B. Seed, 1968, “Seismic response of horizontal soil layers”, *Journal of the Soil Mechanics and Foundation Division, ASCE*, Vol. 94, No. 4, pp. 1003-1031.

Idriss, I. M., J. I. Sun, 1992, *User's Manual for SHAKE91*, Center for Geotechnical Modeling, Dept. of Civil and Environmental Engineering, Univ. of California, Davis, California.

International Conference of Building Officials (ICBO), 1997, *Uniform Building Code*, Volume 1, California, U.S.A.

Kokusho, T., Y. Yoshida, Y. Esashi, 1982, “Dynamic properties of soft clay for wide strain range”, *Soils and Foundations*, Japanese Society of Soil Mechanics and Foundation Engineering, Vol. 22, No. 4, pp. 1-18, https://doi.org/10.3208/sandf1972.22.4_1.

Kokusho, T., K. Sato, 2008, “Surface-to-base amplification evaluated from KiK-net vertical array strong motion records”, *Soil Dynamics and Earthquake Engineering*, Vol. 28, No. 9, pp. 707-716, doi:10.1016/j.soildyn.2007.10.016.

Kramer, S. L., 1996, *Geotechnical Earthquake Engineering*, Prentice-Hall, New Jersey.

Lachet, C., P. Y. Bard, 1994, “Numerical and theoretical investigations on the possibilities and limitations of the Nakamura's technique”, *Journal of Physics of the Earth*, Vol. 42, pp. 377-397.

Laurendeau, A., F. Cotton, O. J. Ktenidou, L. F. Bonilla, F. Hollender, 2013, “Rock and stiff-soil site amplification: dependency on V_{s30} and Kappa (κ_0)”, *Bulletin of the Seismological Society of America*, Vol. 103, No. 6, pp. 3131-3148, doi: 10.1785/0120130020.

Lee, V. W., M. D. Trifunac, 2010, "Should average shear-wave velocity in the top 30 m of soil be used to describe seismic amplification?", *Soil Dynamics and Earthquake Engineering*, Vol. 30, No. 11, pp. 1250-1258, doi:10.1016/j.soildyn.2010.05.007.

Lermo, J. F., F. J. Chavez-Garcia, 1993, "Site effect evaluation using spectral ratios with only one station", *Bulletin of the Seismological Society of America*, Vol. 83, pp. 1574-1594.

Luzi, L., R. Puglia, F. Pacor, M. R. Gallipoli, D. Bindi, M. Mucciarelli, 2011, "Proposal for a soil classification based on parameters alternative or complementary to V_{s30} ", *Bulletin of Earthquake Engineering*, Vol. 9, No. 6, pp. 1877-1898.

Mucciarelli, M., M. R. Gallipoli, 2006, "Comparison between V_{s30} and other estimates of site amplification in Italy", *Proceedings of the First European Conference on Earthquake Engineering and Seismology*, Geneva, Switzerland, 3-8 Sept., CD-Rom Ed., Paper no: 270.

Nakamura, Y., 1989, "A method for dynamic characteristics estimation of subsurface using microtremor on the ground surface", *Quarterly Report of Railway Technical Research Institute*, Vol. 30, pp. 25-33.

Nogoshi, M., T. Igarashi, 1971, "On the amplitude characteristics of microtremor (part 2)", *Journal of the Seismological Society of Japan*, Vol. 24, pp. 26-40.

Ordóñez, G. A., 2011, *SHAKE2000: A Computer Program for the 1-D Analysis of Geotechnical Earthquake Engineering Problems, User's Manual*, July, Revision.

Park, D., Y. M. A. Hashash, 2004, "Probabilistic seismic hazard analysis with nonlinear site effects in the Mississippi embayment", *Proceedings of the Thirteenth World Conference on Earthquake Engineering*, Vancouver, Canada, 1-6 Aug., CD-Rom Ed., Paper no: 1549.

Parolai, S., 2012, *Investigation of site response in urban areas by using earthquake data and seismic noise*, In: Bormann, P. (Ed.), *New Manual of Seismological Observatory Practice 2 (NMSOP-2)*, Potsdam: Deutsches GeoForschungsZentrum GFZ, pp. 1-38.

Regnier, J., F. Bonilla, A. M. Duval, J. F., Semblat, E. Bertrand, 2011, “Revisiting V_{s30} as a proxy parameter for site effects: a case study using KiK-net data”, *Proceedings of the Fifth International Conference on Earthquake Geotechnical Engineering*, Santiago, Chile, 10-13 Jan.

Regnier, J., L. F. Bonilla, E. Bertrand, J. F., Semblat, 2014, “Influence of the V_s profiles beyond 30 m depth on linear site effects: assessment from the KiK-net data”, *Bulletin of the Seismological Society of America*, Vol. 104, No. 5, pp. 2337-2348, doi: 10.1785/0120140018.

Safak, E., 1997, “Models and methods to characterize site amplification from a pair of records”, *Earthquake Spectra*, EERI, Vol. 13, pp. 97-129.

Schnabel, P. B., J. Lysmer, H. B. Seed, 1972, *SHAKE: A Computer Program for Earthquake Response Analysis of Horizontally Layered Sites*, Report UCB/EERC-72/12, Earthquake Engineering Research Center, Univ. of California, Berkeley: Berkeley, California.

Seed, H. B., I. M. Idriss, 1970, *Soil moduli and damping factors for dynamic response analysis*, Report No. UCB/EERC-70/10, University of California, Berkeley, December.

Steidl, J. H., 2000, “Site response in Southern California for probabilistic seismic hazard analysis”, *Bulletin of the Seismological Society of America*, Vol. 90, No. 6B, pp. S149-S169.

Stewart, J. P., A. Liu, Y. Choi, 2003, “Amplification Factors for Spectral Acceleration in Tectonically Active Regions”, *Bulletin of the Seismological Society of America*, Vol. 93, pp. 332–352.

Sun, J. I., R. Golersorki, H. B. Seed, 1988, *Dynamic moduli and damping ratios for cohesive soils*, Ref. No. UCB/EERC-88/15. College of Engineering, University of California at Berkeley, USA.

Turkish Ministry of Public Works and Settlement, 1998, *Specification for Structures to be Built in Disaster Areas*, TEC-98, Ankara, Turkey.

Vucetic, M., 1992, "Soil properties and seismic response", *Proceedings of the Tenth World Conference on Earthquake Engineering*, Madrid, Spain, 19-24 Jul., Vol. 3, pp. 1199-1204.

Vucetic, M., 1994, "Cyclic threshold shear strains in soils", *Journal of Geotechnical Engineering*, ASCE, Vol. 120, No. 12, pp. 2208-2228.

Zen, K., Y. Umehara, K. Hamada, 1978, "Laboratory tests and in-situ seismic survey on vibratory shear modulus of clayey soils with various plasticities", *Proceedings of the Fifth Japan Earthquake Engineering Symposium*, Tokyo, Japan, 28-30 Nov., pp. 721-728.

Zhu, C., M. Pilz, F. Cotton, 2020, "Which is a better proxy, site period or depth to bedrock, in modelling linear site response in addition to the average shear-wave velocity?", *Bulletin of Earthquake Engineering*, Vol. 18, pp. 797-820, <https://doi.org/10.1007/s10518-019-00738-6>.